

**The Wear and Biological Activity of Antioxidant
UHMWPE for use in Total Hip Replacements**

Nicholas James Gowland

Submitted in accordance with the requirements for the degree of

Doctor of Philosophy

The University of Leeds

School of Biomedical Sciences

September 2014

The candidate confirms that the work submitted is his own and that appropriate credit has been given where reference has been made to the work of others.

This copy has been supplied on the understanding that it is copyright material and that no quotation from the thesis may be published without proper acknowledgement

© 2014 The University of Leeds and Nicholas James Gowland

Acknowledgements

Firstly, I would like to offer my huge thanks and gratitude to Professor Joanne Tipper. As my main supervisor, Professor Tipper has guided me through the journey of my PhD, offering constant guidance, unrelenting encouragement, and inspiration. From my first meeting with Joanne at the start of my final year of my undergraduate degree, she has been my professional mentor, and I shall be eternally grateful to her for everything I have achieved over the last five years.

I would also like to thank my co-supervisors; Dr Sophie Williams and Professor John Fisher. Their expertise in mechanical engineering and the wider field of joint replacements has been invaluable throughout my project, and their advice has been incredibly important. A project as multidisciplinary as this would have been so much more difficult without the breadth of knowledge available to me throughout, and I feel very lucky to have had such a strong team of individuals behind me.

I must thank Professor Eileen Ingham, for her advice at vital checkpoints throughout my PhD, and for the high standard of research she has implemented in her research group in Biomedical Sciences. With this, I would like to thank all the members of the Ingham group. You really are an inspiring group of scientists, from a range of disciplines and backgrounds, and I have had an amazing four years working with you. I must offer special thanks to the lab manager Dr Daniel Thomas. His expertise, patience and friendliness are unrivalled, and as with many PhD projects before, he has been essential to the smooth running of my project. I would also like to thank Dr Ai Qin Liu for her knowledge and expertise in cell culture, the single station wear simulator, and all round help throughout my PhD. Her incredibly well written thesis has been so helpful during the writing of my own thesis. I would like to thank Dr Iraklis Papageorgiou for his valuable advice on my biological experiments, in addition to Dr Catherine Bladen for her expertise in UHMWPE and the challenges that come with working with this material.

The mechanical engineering side to my project was completely new to me four years ago, and without the help of the excellent technical team in the mechanical engineering laboratory I would have struggled with this side of my project. I must thank Irvin Homan for his assistance during the six station and single station pin-on-

plate experiments, Adrian Eagles for his help in the measurements lab, Jane Cardie for keeping me well stocked with plates and pins, and the rest of the iMBE technical team. I want to also thank Sha Zhang for her help and constant advice with particle isolation and characterisation.

From a personal point of view, I must thank the group of friends who have kept me laughing throughout my PhD, and made this journey so enjoyable. Thanks to Carly, Caroline and Hazel, for all the fun we had in the skinny office and in Leeds in general. Also; Tony, Iraklis and Dan, for the fun times when a little bit more testosterone was required. I have amazing memories with you all, and I wish you continued success both professionally and personally.

I have to thank a few of my best friends outside of the laboratory also, who I have been lucky enough to live with throughout my PhD. Mike, Windass, Mark, Robbie and Witty; living with you guys has been so helpful during my PhD. To go home to your best friends every day for seven years is pretty amazing, and you guys really helped so much.

I would like to give my deepest thanks to my incredible, loving girlfriend Stephanie. Your support has been unwavering, and at times, you may not have even noticed the support you were giving me. But the happiness you bring, and the love you constantly show, allows me to conquer anything.

Finally, I want to express my eternal appreciation for everything my parents have done throughout my PhD and my life. My drive to succeed, my high standards, and passion for everything I do, is purely down to your influence, and I can never thank you enough for everything you have done. Dad, every day you inspire me to achieve as much success as you have in your career, and your stories and science questions throughout my childhood are what inspired me to be a scientist and to make a discovery. Mum, your support is incredible. Your discipline and incredibly high standards have allowed me to follow my dream and do something as demanding as a PhD. For all this and so much more, I'm eternally grateful. This thesis is dedicated to you both.

Abstract

Total hip replacements (THR) are considered one of the most successful surgical procedures in medicine; eliminating pain and restoring mobility following conditions such as osteoarthritis. The majority of THR implants have a metal femoral head articulating against an UHMWPE acetabular cup, however, UHMWPE wear debris is generated over time, and this wear debris stimulates an osteolytic immune response around the implant, leading to aseptic loosening and eventually failure of the prosthesis.

Highly crosslinked UHMWPE has been developed with excellent wear resistance, however the generation of free radicals following gamma irradiation can lead to oxidation of the UHMWPE material, reducing the mechanical properties of UHMWPE. In addition, oxidation through lipid absorption *in vivo* has been shown to occur, independent of irradiation-generated radical species. This led to the development of antioxidant UHMWPE, with vitamin E enhanced highly crosslinked UHMWPE introduced clinically in the hip in 2007, and hindered phenol enhanced highly crosslinked UHMWPE introduced clinically in the knee in 2012.

Using a six station pin-on-plate wear simulator under kinematics associated with the hip joint, it was shown that the introduction of a vitamin E or hindered phenol antioxidant to UHMWPE had no significant effect on the wear factor. The addition of moderate (5MRad) and high (10MRad) levels of crosslinking significantly reduced the wear factor of UHMWPE, both with and without vitamin E. Comparing both these highly crosslinked antioxidant UHMWPE materials to virgin UHMWPE, there was no significant difference in the wear particle size distribution observed, indicating the addition of high levels of crosslinking and antioxidant enhancement had no significant effect on the size distribution of UHMWPE wear debris.

A large volume of clinically relevant sterile wear debris was generated in 25% bovine serum (v/v) to then incubate with peripheral blood mononuclear cells (PBMNCs) isolated from healthy human donors. Testing both the vitamin E enhanced and hindered phenol enhanced UHMWPE, along with non-antioxidant highly crosslinked UHMWPE wear debris, it was shown that vitamin E enhanced highly crosslinked UHMWPE caused significantly lower levels of TNF- α release from PBMNCs compared to the non-antioxidant highly crosslinked UHMWPE. This

reduction in TNF- α release was also observed in hindered phenol enhanced highly crosslinked UHMWPE, indicating the presence of vitamin E or hindered phenol antioxidants caused a reduction in the release of the osteolytic cytokine TNF- α . Stimulation of significant levels of cytokine release from PBMNCs was only achieved in 3D culture at a wear debris concentration of $>200 \mu\text{m}^3$.

Vitamin E enhanced highly crosslinked UHMWPE wear debris was also shown to stimulate lower levels of reactive oxygen species production in PBMNCs, compared to highly crosslinked UHMWPE wear debris. This indicated that the presence of vitamin E in highly crosslinked UHMPWE wear debris led to intracellular antioxidant activity, reducing the oxidative stress following treatment with wear debris. These results showed clear evidence that enhancement of highly crosslinked UHMWPE with a vitamin E or hindered phenol antioxidant has no significant effect on the wear resistance of the material, however the antioxidant and anti-inflammatory properties of these materials lead to lower levels of TNF- α and reactive oxygen species production in macrophages, potentially reducing the levels of osteolysis around the implant.

Table of Contents

Acknowledgements	iii
Abstract	v
Table of Contents	vii
List of Tables	xiv
List of Figures	xvi
List of Abbreviations	xxii
Chapter 1 Introduction	1
1.1 Anatomy of the Hip Joint	1
1.2 Kinematics of the Natural Hip Joint	5
1.3 Arthritis and Total Hip Arthroplasty	6
1.4 History of Total Hip Arthroplasty	8
1.5 Bearing Materials for Total Hip Arthroplasty	10
1.5.1 Metal on Metal Hip Replacement	10
1.5.2 Ceramic on Ceramic Hip Replacement	16
1.5.3 PEEK, Carbon Fibre and Graphene Composite Materials	18
1.6 Ultra High Molecular Weight Polyethylene	20
1.7 Tribology of UHMWPE	21
1.8 Wear Testing and Isolation of UHMWPE Wear Particles	24
1.9 Failure of UHMWPE total hip replacements	28
1.10 Crosslinked UHMWPE	33
1.11 Incidence of UHMWPE oxidation	38
1.12 Vitamin E	41
1.13 Doping of UHMWPE with Vitamin E	45
1.14 Wear and Oxidative Stability of Vitamin E enhanced UHMWPE	47
1.15 Biological Response to Vitamin E Enhanced UHMWPE	51
1.16 Alternative Antioxidants for use in UHMWPE	55
1.17 Hindered Phenols	58
1.18 Aims	61
Chapter 2 Materials and Methods	64
2.1 Wear Testing	64
2.1.1 UHMWPE Materials	64
2.1.2 Methods	66
2.1.2.1 Machining and Preparation of UHMWPE Pins	66
2.1.2.2 Machining of CoCr Plates	67
2.1.2.3 Surface Measurement of CoCr Plates	67
2.1.2.4 Weighing of UHMWPE Pins	68

2.1.2.5 Preparation of 25% (v/v) Bovine Serum	69
2.1.2.6 Assembly of the Six Station Pin on Plate Simulator	69
2.1.2.6.1 Preparation of the Linear Bearing Trays	69
2.1.2.6.2 Preparation of the Pin Holders	72
2.1.2.6.3 Final Assembly of the Test Rig	73
2.1.2.7 Dismantling the Wear Test Rig	74
2.1.2.8 Cleaning the Components and Specimens	76
2.1.2.9 Calculating Wear Factor	76
2.2 Generation of Wear Particles under Aseptic Conditions for Cell Culture Studies	78
2.2.1 Machining and Preparation of UHMWPE pins	78
2.2.2 Machining and Preparation of CoCr plates	78
2.2.3 Surface Measurement of CoCr Plates	79
2.2.4 Weighing of UHMWPE Pins	79
2.2.5 Preparation of the UHMWPE Pins	79
2.2.6 Preparation of Lubricant	80
2.2.7 Assembly of the Single Station Pin-on-Plate Wear Simulator	80
2.2.7.1 Preparation and Sterilisation of the Components of the Single Station Pin-on-Plate Wear Simulator	80
2.2.7.2 Sterilisation of Wear Simulator Components and Class II Cabinet	81
2.2.7.3 Assembly of the Single Station Pin-on-Plate Wear Simulator	81
2.2.7.4 Setting up the Syringe Driver Mechanism	82
2.2.7.5 Bacterial Testing of the Lubricant	83
2.2.7.6 Disassembly of the Single Station Pin-on-Plate Wear Simulator	84
2.3 Isolation and Characterisation of UHMWPE Particles from Serum	85
2.3.1 Isolation of UHMWPE Particles from Serum	85
2.3.2 Filtration of Sample	87
2.3.3 Field Emission Gun Scanning Electron Microscope (FEGSEM) Analysis of Wear Particles	88
2.3.3.1 Preparation of Filters for Scanning Electron Microscopy	88
2.3.3.2 FEGSEM Analysis	89
2.3.4 Particle Image Analysis and Size Distribution Graphs	89
2.4 Culture of Human Peripheral Blood Mononuclear Cells (PBMNCs) with UHMWPE Particles to Determine the Biological Response to UHMWPEs	91
2.4.1 Stock Solutions	91

2.4.1.1 Transport Medium	91
2.4.1.2 Culture Medium	91
2.4.1.3 2% (w/v) Low Melting Point Agarose	92
2.4.2 Endotoxin testing of the serum lubricant using the Limulus Amebocyte Lysate (LAL) assay	92
2.4.2.1 Sample Details	92
2.4.2.2 Additional Reagents and Equipment	93
2.4.2.3 Preparation of Lubricant Samples	93
2.4.2.4 Preparation of Reagents	93
2.4.2.5 Performing the LAL Endotoxin Assay	94
2.4.2.6 LAL Results Interpretation	95
2.4.3 Preparation of UHMWPE particle suspensions in 2% (w/v) agarose gels	95
2.4.3.1 Calculation of the particle volume: cell ratio for cell culture experiments	97
2.4.3.2 Calculation of the Fluosphere® dosing volume required in cell culture experiments	98
2.4.3.3 Preparation of particle containing 0.4% (w/v) agarose gels	99
2.4.4 Isolation of human PBMNCs from the blood of healthy volunteers	99
2.4.4.1 Determination of viable PBMNCs using Trypan blue exclusion assay	100
2.4.5 Culture of PBMNCs with UHMWPE particles to determine the biological response to wear particles	101
2.4.5.1 Determining the cell viability using the ATP Lite™ Assay	102
2.4.5.2 Measurement of the TNF- α release from PBMNCs incubated with UHMWPE particles	103
2.4.5.2.1 Preparation of reagents for the TNF- α ELISA	104
2.4.5.2.2 Preparation of ELISA plate	104
2.4.5.2.3 Performing the ELISA	105
2.4.5.2.4 Analysis and Statistical Analysis of ELISA results	106
2.4.6 Culture of U937 Cell Line with UHMWPE Wear Debris to Determine the Cellular Response to Wear Particles	107
2.4.6.1 Resurrection and Splitting of U937 Cells	107
2.4.6.2 Differentiation of U937 Cells	108
2.4.6.3 Harvesting and Culture of U937 Cells with UHMWPE Wear Debris	108

2.4.7 Confocal Imaging of UHMWPE Particle Uptake by PBMNCs in 0.4% (v/v) Agarose Gel	109
2.4.7.1 Generation of Wear Particles under Aseptic Conditions for Particle Uptake Studies	109
2.4.7.2 Fractionation of UHMWPE Wear Debris using Filtration	110
2.4.7.3 Fluorescence Labelling of UHMWPE Wear Debris	110
2.4.7.4 Culture of Fluorescently Labelled UHMWPE Wear Particles with PBMNCs	111
2.4.7.5 Confocal Laser Scanning Microscopy Imaging of UHMWPE Particle Uptake by PBMNCs	113
Chapter 3 Pin on Plate Wear Testing and Particle Characterisation of Antioxidant UHMWPE Materials With and Without Crosslinking	114
3.1 Introduction	114
3.2 Materials and Methods	117
3.2.1 Materials	117
3.2.2 Determination of Wear Factor of Different UHMWPEs using the Six Station Pin-on-Plate Wear Simulator	118
3.2.3 Characterisation of UHMWPE Wear Debris from the Six Station Pin-on-Plate Wear Simulator	121
3.3 Results	122
3.3.1 Determining the Wear Factor of UHMWPE With and Without an Antioxidant and at Three Levels of Crosslinking	122
3.3.2 Isolation and Characterisation of Wear Particles Generated from UHMWPE With and Without Crosslinking and Antioxidant Addition	125
3.3.2.1 Isolation and Characterisation of Wear Particles Generated from GUR1050 Virgin UHMWPE and GUR1050 Vitamin E enhanced Highly Crosslinked UHMWPE	125
3.3.2.2 Comparison of the Frequency and Volume Size Distribution for GUR1050 Virgin and GUR1050 Vitamin E enhanced Highly Crosslinked UHMWPE	131
3.3.2.3 Isolation and Characterisation of Wear Particles Generated from GUR1020 Virgin UHMWPE and Hindered Phenol Enhanced Highly Crosslinked UHMWPE	134

3.3.2.4 Comparison of the Frequency and Volume Size Distribution for GUR1020 Virgin and GUR1020 Hindered Phenol enhanced Highly Crosslinked UHMWPE	141
3.4 Discussion	143
3.5 Conclusion	150
Chapter 4 The Biological Response of Peripheral Blood Mononuclear Cells to Antioxidant UHMWPE Wear Debris	151
4.1 Introduction	151
4.2 Materials and Methods	156
4.2.1 Materials	156
4.2.2 Methods	157
4.2.2.1 Generation of UHMWPE Wear Particles using the Aseptic Single Station Pin-on-Plate Wear Simulator	157
4.2.2.2 Endotoxin testing of the Serum Lubricant	157
4.2.2.3 Culture of PBMNCs with Fluorescein-Labelled UHMWPE Wear Particles for Analysis of Particle Uptake using Confocal Microscopy	157
4.2.2.4 Culture of PBMNCs with UHMWPE Wear Particles	158
4.2.2.5 Culture of U937 Cell Line with UHMWPE Wear Particles	159
4.2.2.5.1 Differentiation of U937 Cells	159
4.2.2.5.2 Harvesting and Culture of U937 Cells with UHMWPE Wear Debris	160
4.3 Results	161
4.3.1. Generation of Clinically Relevant UHMWPE Wear Particles using the Aseptic Single Station Pin-on-Plate Wear Simulator – Test A	161
4.3.1.1 Determination of the Endotoxin Levels in Serum Lubricants	164
4.3.2 Uptake of UHMWPE Wear Particles by PBMNCs in the Agarose Gel Cell Culture Technique	165
4.3.3. Development of the Method for Assessment of the Effects of UHMWPE Wear Particles on TNF- α Production in PBMNCs- Test A	172
4.3.3.1 TNF- α Release from PBMNCs Stimulated with Highly Crosslinked Vitamin E Enhanced UHMWPE Wear Debris under Initial Conditions	174

4.3.3.2 TNF- α Release from PBMNCs Stimulated with Highly Crosslinked Vitamin E Enhanced UHMWPE Wear Debris embedded in Different Concentrations of Agarose Gel	178
4.3.3.3 TNF- α Release from PBMNCs Stimulated with Highly Crosslinked Vitamin E Enhanced UHMWPE Wear Debris - Optimising the Cell Seeding Density	183
4.3.3.4 Cellular Response of U937 Cells to Vitamin E enhanced Highly Crosslinked UHMWPE Wear Debris	189
4.3.4. Development of the Method for Assessment of the Effects of High Volume Concentrations of UHMWPE Wear Particles on TNF- α Production in PBMNCs- Test B	195
4.3.4.1. Generation of Clinically Relevant UHMWPE Wear Particles using the Aseptic Single Station Pin-on-Plate Wear Simulator – Test B	195
4.3.4.2 Determination of the Endotoxin Levels in each Serum Lubricant Sample	197
4.3.4.3 Cellular Response to High Volume Concentrations of Highly Crosslinked UHMWPE Wear Debris	198
4.3.5 Investigating the Cellular Response to High Volume Concentrations of Vitamin E enhanced Highly Crosslinked UHMWPE and Highly Crosslinked UHMWPE Wear Debris	204
4.3.5.1 Cellular Response to High Volume Concentrations of Vitamin E enhanced Highly Crosslinked UHMWPE and Hindered Phenol enhanced Highly Crosslinked Wear Debris Using Optimised Conditions	
4.3.5.2 Cellular Response to Vitamin E enhanced Highly Crosslinked UHMWPE, Hindered Phenol enhanced Highly Crosslinked UHMWPE, and Highly Crosslinked UHMWPE Wear Debris	209
4.4. Discussion	212
4.5 Conclusions	219
Chapter 5 The Production of Reactive Oxygen Species in Peripheral Blood Mononuclear Cells in Response to UHMWPE Wear Particles	220
5.1 Introduction	220
5.2 Materials	223
5.3 Methods	223
5.3.1 Generation of UHMWPE Wear Particles using the Aseptic Single Station Pin-on-Plate Wear Simulator	223
5.3.2 Culture of PBMNCs with UHMWPE Wear Debris in	224

Chamber Slides	
5.3.3 Detection of Reactive Oxygen Species in PBMNCs using the Image-iT™ LIVE Detection Kit Following Incubation with UHMWPE Wear Debris	227
5.3.4 Imaging and Quantification of Oxidative Stress in PBMNCs Using Fluorescence Microscopy	227
5.4. Results	229
5.4.1 Generation of Sterile UHMWPE Wear Debris	229
5.4.2 Visualisation of Reactive Oxygen Species Following Treatment with UHMWPE Wear Debris	229
5.4.3 Quantification of ROS Intensity in PBMNCs Incubated with UHMWPE Wear Debris	236
5.5 Discussion	239
5.6 Conclusion	244
Chapter 6 Discussion	245
6.1. Pin on Plate Wear Testing of Antioxidant UHMWPE Materials With and Without Crosslinking	249
6.2 Particle Characterisation of Antioxidant UHMWPE Materials With and Without Crosslinking	252
6.3 Biological Response of Peripheral Blood Mononuclear Cells to Antioxidant UHMWPE Wear Debris	254
6.4 The Production of Reactive Oxygen Species in Peripheral Blood Mononuclear Cells in Response to UHMWPE Wear Particles	260
6.5 Future Work	261
6.6 Conclusion	265
References	267
Appendix 1	i
Appendix 2	vii

List of Tables

Table 2.1	UHMWPE's tested in this study, detailing the name, resin type, gamma irradiation dose applied, antioxidant added (if any), the supplier and the abbreviation used throughout the study	65
Table 2.2	UHMWPE materials from which sterile wear particles were generated using the aseptic single station pin-on-plate wear simulator.	79
Table 2.3	Additional reagents and equipment used in the LAL endotoxin assay	93
Table 2.4	Typical cell culture conditions for the culture of PBMNCs with UHMWPE particles in agarose gel	97
Table 2.5	The properties of the Fluospheres [®] used in this study. Fluospheres [®] have a density of $1.05 \times 10^{-6} \mu\text{g} \cdot \mu\text{m}^{-3}$.	98
Table 2.6	The reagents made up for use with the ELISA kit.	104
Table 2.7	The reagents provided with the ELISA kit and the preparation required	104
Table 3.1	UHMWPE materials tested in this chapter, including the resin, gamma irradiation dose, antioxidant, supplier and the abbreviation to be used for each material throughout the chapter.	117
Table 3.2	Mean surface roughness of each smooth high-carbon CoCr plate used in this study against GUR 1050 UHMWPE pins.	119
Table 3.3	Mean surface roughness of each smooth high-carbon CoCr plate used in this study against GUR 1020 UHMWPE pins.	120
Table 4.1	UHMWPE materials used in the cell culture experiments.	156
Table 4.2	The concentration of UHMWPE wear debris in serum lubricant samples collected from the aseptic single station pin-on-plate wear simulator during Test A.	164
Table 4.3	Levels of endotoxin present in the lubricant samples generated in 25% (v/v) bovine serum lubricants using the single station pin-on-plate simulator (Test A)	165
Table 4.4	Cell culture conditions for the initial experiments investigating the biological response to antioxidant UHMWPE.	174

Table 4.5	Cell culture conditions for experiments investigating the biological response to antioxidant UHMWPE using different agarose concentrations	180
Table 4.6	Cell culture conditions for experiments investigating the biological response to antioxidant UHMWPE using an increased cell seeding density of 2×10^5 cells per well	184
Table 4.7	Cell culture conditions for experiments investigating the biological response of U937 cells to antioxidant UHMWPE	190
Table 4.8	UHMWPE materials used in the cell culture experiments.	196
Table 4.9	The concentration of UHMWPE wear debris in serum lubricant samples collected from the aseptic single station pin-on-plate wear simulator during Test B.	196
Table 4.10	Levels of endotoxin present in the lubricant samples generated in 25% (v/v) bovine serum lubricants using the single station pin-on-plate simulator (Test B).	197
Table 4.11	Optimised cell culture conditions for experiments investigating the dose response PBMNCs to highly crosslinked UHMWPE	199
Table 4.12	Optimised cell culture conditions for experiments investigating the biological response of PBMNCs to antioxidant UHMWPE	204
Table 5.1	Additional materials and reagents used for the investigation of the production of reactive oxygen species in PBMNCs in response to UHMWPE wear debris.	223

List of Figures

Figure 1.1	An anterior view showing the pelvis and the position of the acetabulum.	1
Figure 1.2	An anterior view of the top half of a right femur	2
Figure 1.3	The ligamentum teres can be seen embedded in the femoral head and connected to either side of the acetabular notch, blending with the traverse ligament	3
Figure 1.4	The increase in wear as femoral head diameter increases.	10
Figure 1.5	The bearings used in total hip arthroplasty in the UK over a period of 9 years.	15
Figure 1.6	Ceramic-on-ceramic BIOLOX® delta from Ceramtec AG, manufactured by Biomet.	18
Figure 1.7	Schematic showing the microstructure of UHMWPE.	20
Figure 1.8	Schematic of the postulated mechanisms behind aseptic loosening.	31
Figure 1.9	The wear factors of UHMWPE gamma irradiated with different doses; non-crosslinked (0MRad), moderately crosslinked (5MRad) and highly crosslinked (10MRad).	34
Figure 1.10	The worn cup surfaces at different levels of irradiation.	35
Figure 1.11	Chemical structure of α -tocopherol, showing the chroman head and phytyl tail.	42
Figure 1.12	Schematic showing the different methods of vitamin E doping of UHMWPE.	46
Figure 1.13	The cumulative wear volume for virgin and vitamin E enhanced UHMWPE tibial components (n=3) in knee simulator testing.	49
Figure 1.14	Showing the cell viability of U937 human histiocytes incubated with different concentrations of vitamin E.	52
Figure 1.15	The structure of Chimassorb® 994, and the proposed mechanism of free radical scavenging.	57
Figure 1.16	A phenol molecule reacting with a free radical and example of the reactions that take place.	59
Figure 1.17	Molecular structure of Pentaerythritol Tetrakis (HPAO)	60
Figure 2.1	Diagram showing the dimensions of the pins used in the 6 station pin-on-plate wear tests and the aseptic single station pin-on-plate wear rig.	67

Figure 2.2	Schematic showing A) the tracks (blue arrows) measured by the Form Talysurf 120L to calculate the mean surface roughness of a B) standard CoCr plate.	68
Figure 2.3	Removable components of the six station pin-on-plate wear rig	71
Figure 2.4	A bird's eye view of the assembled linear bearing tray and bath with 50 ml of 25% (v/v) bovine serum.	72
Figure 2.5	Exploded and fully assembled view of the pin holder.	73
Figure 2.6	The fully assembled 6 station pin-on-plate wear rig.	75
Figure 2.7	Schematic showing the method for bacterial testing of serum lubricant using agar plates.	84
Figure 2.8	A schematic showing an exploded view of the glass filtration unit (left) and the fully assembled glass filtration unit (right).	88
Figure 2.9	Schematic showing the culture of UHMWPE particles with PBMNCs, both in solution (1) and in 0.4% (w/v) agarose (2).	96
Figure 2.10	Schematic showing the microscope slide – cell culture well assembly.	111
Figure 3.1	Mean wear factors for each UHMWPE material after 2 weeks testing (>500,000 cycles) against smooth CoCr plates in 25% (v/v) bovine serum.	124
Figure 3.2	FEGSEM images of UHMWPE wear particles isolated from serum lubricant used on the six station pin-on-plate wear rig.	126
Figure 3.3	A) The mean percentage frequency and B) the mean percentage volume size distribution of GUR 1050 Virgin UHMWPE particles generated on the six station pin-on-plate wear rig.	127
Figure 3.4	FEGSEM images of UHMWPE (1050 Vit E 10) wear particles isolated from serum lubricant used on the six station pin-on-plate wear rig.	129
Figure 3.5	The mean percentage frequency and mean percentage volume size distribution of GUR 1050 Vit E 10 UHMWPE particles generated on the six station pin-on-plate wear rig.	130
Figure 3.6	Comparison of 1050 Virgin and 1050 Vit E 10 wear particles generated on the six station pin-on-plate wear rig; A) the mean frequency size distribution; B) the mean volume size distribution	133
Figure 3.7	FEGSEM images of UHMWPE (1020 Virgin) wear particles isolated from serum lubricant used on the six station pin-on-plate wear rig.	136

Figure 3.8	A) The mean percentage frequency and B) the mean percentage volume size distribution of GUR 1020 Virgin UHMWPE particles generated on the six station pin-on-plate wear rig.	137
Figure 3.9	FEGSEM images of UHMWPE (1020 AOX 8) wear particles isolated from serum lubricant used on the six station pin-on-plate wear rig.	139
Figure 3.10	A) The mean percentage frequency and B) the mean percentage volume size distribution of GUR 1020 AOX 8 UHMWPE wear particles generated on the six station pin-on-plate wear rig.	140
Figure 3.11	Comparison of 1020 Virgin and 1050 AOX 8 UHMWPE wear particles generated on the six station pin-on-plate wear rig; A) the mean frequency size distribution; B) the mean volume size distribution.	142
Figure 4.1	Mean wear factors for 1050 Virgin UHMWPE against smooth ($R_a < 0.01 \mu\text{m}$) and rough ($R_a 0.07\text{-}0.09 \mu\text{m}$) CoCr alloy counterfaces.	162
Figure 4.2	A) The mean percentage number and B) the mean percentage volume size distribution of GUR1050 Virgin UHMWPE wear debris generated on the six station pin-on-plate simulator against either a smooth ($R_a < 0.01 \mu\text{m}$) CoCr alloy counterface, or a rough ($R_a 0.07\text{-}0.09 \mu\text{m}$) CoCr alloy counterface for 500,000 cycles.	163
Figure 4.3	Visualisation of $0.04 \mu\text{m}$ Fluospheres internalised by PBMNCs.	167
Figure 4.4	Visualisation micrometre sized 1050 HXL UHMWPE wear particles internalised by PBMNCs.	169
Figure 4.5	Visualisation of nanometre sized 1050 HXL UHMWPE wear particles internalised by PBMNCs.	171
Figure 4.6	A) Cell viability and B) TNF- α release from PBMNCs isolated from donor 2 incubated with 1050 HXL and 1050 Vit E 10 UHMWPE wear debris at a concentration of $100 \mu\text{m}^3$ debris per cell for 24 hours at 37°C in 5% (v/v) CO_2 in air.	175
Figure 4.7	A) Cell viability and B) TNF- α release from PBMNCs isolated from donor 12 incubated with 1050 HXL and 1050 Vit E 10 UHMWPE wear debris at a concentration of $100 \mu\text{m}^3$ debris per cell for 24 hours at 37°C in 5% (v/v) CO_2 in air.	176

Figure 4.8	A) Cell viability and B) TNF- α release from PBMNCs isolated from donor 13 incubated with 1050 HXL, 1050 Vit E 10 and 1050 Virgin UHMWPE wear debris at a concentration of 100 μm^3 debris per cell for 24 hours at 37°C in 5% (v/v) CO ₂ in air.	177
Figure 4.9	A) Cell viability and B) TNF- α release from PBMNCs isolated from donor 1 incubated with 1050 HXL, 1050 Vit E 10 and 1050 Virgin UHMWPE wear debris at a concentration of 100 μm^3 wear debris per cell for 24 hours at 37°C in 5% (v/v) CO ₂ in air.	180
Figure 4.10	A) Cell viability and B) TNF- α release from PBMNCs isolated from donor 2 incubated with 1050 HXL and 1050 Vit E 10 UHMWPE wear debris at a concentration of 100 μm^3 wear debris per cell for 24 hours at 37°C in 5% (v/v) CO ₂ in air.	182
Figure 4.11	A) Cell viability and B) TNF- α release from PBMNCs isolated from donor 7 incubated at with 1050 HXL and 1050 Vit E 10 UHMWPE wear debris at a concentration of 100 μm^3 wear debris for 24 hours at 37°C in 5% (v/v) CO ₂ in air.	185
Figure 4.12	A) Cell viability and B) TNF- α release from PBMNCs isolated from donor 3 incubated with 1050 HXL, and 1050 Vit E 10 UHMWPE wear debris at a concentration of 100 μm^3 wear debris for 24 hours at 37°C in 5% (v/v) CO ₂ in air.	186
Figure 4.13	A) Cell viability and B) TNF- α release from PBMNCs isolated from donor 15 incubated with 1050 HXL UHMWPE wear debris at a concentration of 100 μm^3 wear debris for 24 hours at 37°C in 5% (v/v) CO ₂ in air.	188
Figure 4.14	A) Cell viability and B) TNF- α release from U937 derived macrophages incubated with 1050 HXL, 1050 Vit E 10 and 1050 Virgin UHMWPE wear debris at a concentration of 100 μm^3 for 24 hours.	192
Figure 4.15	A) Cell viability and B) TNF- α release from PBMNCs isolated from donor 2 incubated with 1050 HXL UHMWPE wear debris at concentrations 100 μm^3 , 200 μm^3 and 600 μm^3 wear debris per cell for 24 hours at 37°C in 5% (v/v) CO ₂ in air.	200
Figure 4.16	A) Cell viability and B) TNF- α release from PBMNCs isolated from donor 8 incubated with 1050 HXL UHMWPE wear debris at concentrations 100 μm^3 , 200 μm^3 and 600 μm^3 wear debris per cell for 24 hours at 37°C in 5% (v/v) CO ₂ .	202

Figure 4.17	A) Cell viability and B) TNF- α release from PBMNCs isolated from donor 8 incubated with 1050 HXL and 1050 Vit E 10 UHMWPE wear debris at a concentration of 500 μm^3 wear debris per cell for 24 hours at 37°C in 5% (v/v) CO ₂ .	206
Figure 4.18	A) Cell viability and B) TNF- α release from PBMNCs isolated from donor 15 incubated with 1050 HXL and 1050 Vit E 10 UHMWPE wear debris at a concentration of 500 μm^3 wear debris per cell for 24 hours at 37°C in 5% CO ₂ (v/v) in air.	208
Figure 4.19	A) Cell viability and B) TNF- α release from PBMNCs isolated from Donor 8 incubated with 1050 HXL, 1050 Vit E 10 and 1020 AOX 8 UHMWPE wear debris at a concentration of 500 μm^3 wear debris per cell for 24 hours at 37°C in 5% (v/v) CO ₂ in air.	211
Figure 5.1	Visualisation of the presence of ROS in PBMNCs (cells only negative control) following incubation for 48 hours at 37°C in 5% (v/v) CO ₂ .	231
Figure 5.2	Visualisation of the presence of ROS in PBMNCs following incubation with 1050 HXL UHMWPE wear debris at a concentration of 100 μm^3 per cell, for 48 hours at 37°C in 5% (v/v) CO ₂ .	232
Figure 5.3	Visualisation of the presence of ROS in PBMNCs following incubation with 1050 Vit E 10 UHMWPE wear debris at a concentration of 100 μm^3 per cell, for 48 hours at 37°C in 5% (v/v) CO ₂ .	233
Figure 5.4	Visualisation of the presence of ROS in PBMNCs following incubation with 1050 HXL UHMWPE wear debris at a concentration of 100 μm^3 per cell, over 48 hours at 37°C in 5% (v/v) CO ₂ .	234
Figure 5.5	Visualisation of the presence of ROS in PBMNCs following incubation with 1050 Vit E 10 UHMWPE wear debris at a concentration of 100 μm^3 per cell, for 48 hours at 37°C in 5% (v/v) CO ₂ .	235
Figure 5.6	Mean intensity of ROS in PBMNCs isolated from donor 8 treated with 1050 HXL UHMWPE wear debris at a concentration of 100 μm^3 over 48 hours at 37°C in 5% (v/v) CO ₂ in air.	237

Figure 5.7 Mean intensity of ROS in PBMNCs isolated from donor 11 treated with 1050 Vit E 10 UHMWPE wear debris at a concentration of 100 μm^3 over 48 hours at 37°C in 5% (v/v) CO_2 in air.

238

Abbreviations

µg	Microgram
µl	Microlitre
µm	Micrometre
µm ³	Micrometre cubed
ANOVA	Analysis of variance
ASTM	American Standard for Testing and Materials
atm	Atmospheres pressure
ATP	Adenosine triphosphate
AVED	ataxia with isolated vitamin E deficiency
BMI	Body Mass Index
BSA	Bovine serum albumin
C-C	Carbon to carbon
C-H	Carbon to hydrogen
CFR- PEEK	Carbon fibre-reinforced polyetheretherketone
CMC	Carboxy methyl cellulose
CO ₂	Carbon Dioxide
COC	Ceramic-on-ceramic
CoCr	Cobalt Chrome
CPS	Counts per second
DG	Dodecyl galate
DNA	Deoxyribonucleic acid
EtO	Ethylene oxide
EU	endotoxin units
FBS	Foetal Bovine Serum
FDA	Food and Drug Administration
FEG-SEM	Field emission gun scanning electron microscopy
FS	Fluospheres

FTIR	Fourier transform infrared spectroscopy
g	Grams
GA	Gallic acid
g.mol ⁻¹	Grams per mole
GUR	Granular, UHMWPE and Ruhrchemie
h	Hour
HBA	Heated blood agar
HEPES	N-(2-hydroxyethyl) piperazine-N'-(2-ethanulfonic acid)
HNO ₃	Nitric Acid
HPAO	Hindered phenol antioxidant
HRP	Horseradish peroxidase
H ₂ SO ₄	Sulphuric Acid
Hz	Hertz
ICAM-1	Intercellular adhesion molecule-1
IL-1 β	Interleukin-1 β
IL-6	Interleukin-6
IL-8	Interleukin-8
LAL	Limulus amebocyte lysate
LDL	Low-density lipoprotein
LPS	Lipopolysaccharide
LRW	LAL reagent water
M	Molar
mM	Millimolar
MCSF	Macrophage colony stimulating factor
mg	Milligram
MHC	Major histocompatibility complex
MHRA	medical and healthcare products regulatory agency
min	Minute

ml	Millilitre
mm	millimetre
MOM	Metal-on-metal
MRad	Mega rads
mRNA	Messenger ribonucleic acid
MSD	Minimum significant difference
N	Newton
NA	Nutrient agar
NaCl	Sodium Chloride
NaOH	Sodium Hydroxide
ng	Nanogram
ng.ml ⁻¹	Nanogram per millilitre
kGy	Kilogray
NF-κB	Nuclear factor kappa-light-chain-enhancer of activated B cells
NHS	National Health Service
NJR	National Joint Registry
KOH	Potassium hydroxide
OA	Osteoarthritis
OH	Hydroxide group
PBMNCs	Peripheral blood mononuclear cells
PBS	Phosphate buffered saline
PDGF	Platelet derived growth factor
PE	Polyethylene
PEEK	Polyetheretherketone
pg	Picogram
PGE ₂	Prostaglandin E ₂
PPC	Positive product control
PPM	Parts per million

PTFE	Polytetrafluoroethylene
PVC	Polyvinyl chloride
R _a	Roughness
RANKL	Receptor activator of nuclear factor kappa-β ligand
RPMI	Rosslyn park memorial institute
SA	Streptavidin
SAB	Saboraud dextrose agar
TNF-α	Tumour necrosis factor alpha
THA	Total hip arthroplasty
THR	Total hip replacement
TJR	Total joint replacement
UHMWPE	Ultra high molecular weight polyethylene
UK	United Kingdom
UV	Ultraviolet
USA	United States of America
VE	Vitamin E
v/v	volume/volume
w/v	weight/volume

Chapter 1

Introduction

1.1 Anatomy of the Hip Joint

The hip joint is a multiaxial ball and socket joint located laterally and anteriorly to the buttocks, and provides the movement capability of the femur. The joint is comprised of the acetabulum and the femoral head. The acetabulum is a forward, outward, downward facing cavity formed by the convergence of the ilial, ischial and pubic ossification centres that join at the triradiate cartilage (Figure 1.1), which allows the articulation of the femoral head within the socket (Drake et al., 2005). The femoral head is an imperfect sphere made up of a lattice of cancellous bone that is covered in articular cartilage, and is located at the proximal end of the femur (Figure 1.2). The cancellous bone coupled with the articular cartilage provides an ideal weight bearing structure that distributes the applied stresses to the dense bone of the femoral neck and proximal femur (Koval and Zuckerman, 2000).

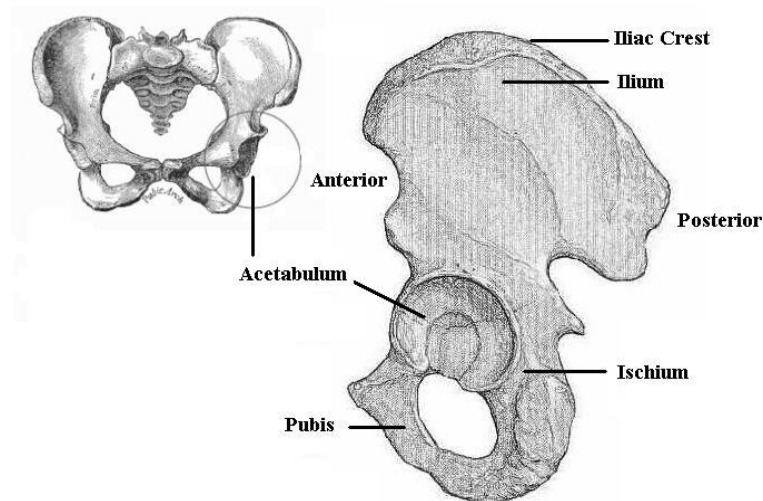


Figure 1.1 – An anterior view showing the pelvis and the position of the acetabulum (left image). The right image is the left acetabulum enlarged to show the physiology of the surrounding bone (Grays, 1918)

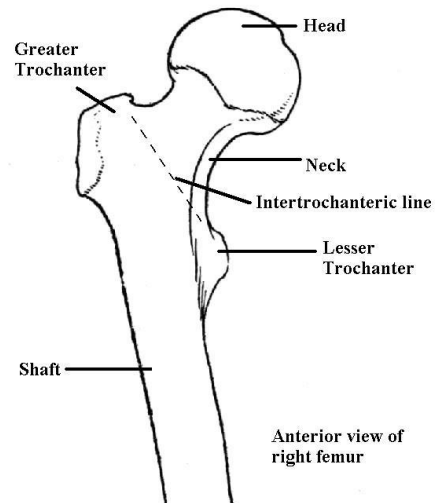


Figure 1.2 - An anterior view of the top half of a right femur.

(Reproduced from Grays, 1918).

Three main ligaments provide the stability of the hip joint. The iliofemoral ligament is attached to the ilium and extends down to the femur where it is attached at the anterior intertrochanteric line. The pubofemoral ligament attaches from the pelvis to the femur. The ischiofemoral ligament enhances the posterior stability attaching from the posterior ischium (behind the acetabulum) to the intertrochanteric line. All three of these ligaments blend with the hip capsule for attachment to the femur. Another important ligament is the ligamentum teres found in the fovea capitis femoris. It adds little stability beyond childhood but is more important as an arterial blood supply to the femoral head (Figure 1.3) (Gray, 1918).

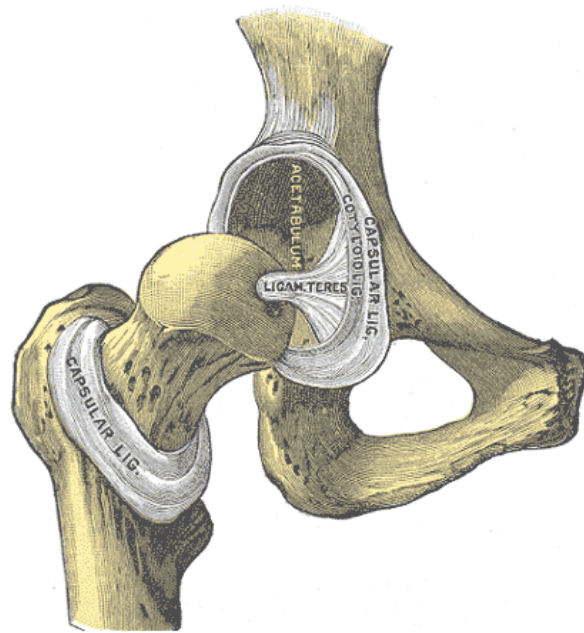


Figure 1.3 – The ligamentum teres can be seen embedded in the femoral head and connected to either side of the acetabular notch, blending with the transverse ligament (Gray, 1918)

The hip capsule is the connecting and supporting soft tissue structure that surrounds the hip joint. The capsule is attached to the labrum at the top and the femoral neck at the bottom (posteriorly) (Koval and Zuckerman, 2000). The acetabular labrum is a rim of fibrocartilage found on the edge of the acetabulum. The labrum acts to deepen and extend the socket, making it less likely that the femoral head will dislocate. The hip joint is a synovial joint designed for stability and weight bearing, capable of movements including flexion, extension, abduction, adduction and rotation (Drake et al., 2005). The capsule contains periarticular connective tissue, which is made up of fibroblasts, fibrous proteins, extracellular substance and water (Neumann, 1999). The fibroblasts synthesise collagen which is composed of several tropocollagen fibrils linked together at regular intervals to add strength. Many collagen fibres form fosciculi, producing a ‘rope’ like weave of fibres that adds strength and rigidity to the connective tissues of the joint. In addition to collagen, fibroblasts produce elastin; a protein that adds elasticity to the connective tissue. Elastin allows the hip capsule to stretch and elongate during movement. It is the combination of these molecules, in addition to glycosaminoglycans and water that make up the

characteristics of the connective tissue. The synovial membrane lines the internal capsule and tendon sheaths, and contains synoviocytes (Dupont, 1997). These cells secrete synovial fluid, which adds nutrition to the connective tissues and lubrication to the joint, which in combination with cartilage acts to lubricate the joint.

Articular cartilage found on the femoral head is around 4mm thick, reducing to 3mm at the periphery (Koval and Zuckerman, 2000). This tissue has excellent compression resistance properties and is therefore ideal to protect the underlying bone from the forces experienced in the hip joint. Articular cartilage is composed mainly of collagen, glycosaminoglycans, water and chondrocytes, with no blood vessels present (McDevitt, 1973). Chondrocytes are the only cell type found in articular cartilage and are responsible for maintaining the extracellular matrix of cartilage. Chondrocyte viability is essential for function of articular cartilage due to the need for the synthesis of the substances that make up articular cartilage (Ramakrishnan et al., 2010).

The weight bearing properties associated with articular cartilage are largely due to its biochemical structure. Glycosaminoglycans bind to the proteoglycan core of cartilage and branch out from this core in all directions, markedly increasing the surface area of the tissue (Buckwalter et al., 1985). The glycosaminoglycans are negatively charged and therefore attract water into the matrix of the substance, ensuring the cartilage remains hydrated (Bhosale and Richardson, 2008). As pressure is exerted on the joint, the cartilage is deformed as the water in the matrix moves away from the high pressure. This allows the articular cartilage to absorb and dissipate the stress on the joint, while returning to its hydrated state when the pressure is removed as water returns to fill the matrix (Neumann, 1999).

Articular cartilage, synovial fluid and the macrostructure of the hip joint ensure a super-lubricated joint capable of resisting compression and stress encountered in day to day activities. However, as a result of aging, disease or trauma, the normal balance of cartilage turnover can be disrupted, leading to irreversible cartilage damage. This can lead to complications in the hip joint, and these complications could ultimately result in arthritis and eventually the need for a total hip replacement.

1.2 Kinematics of the Natural Hip Joint

The main function of the hip joint is to allow the movement of the leg in space, and provide stability during weight bearing activities such as standing, walking or running. During standing (on two legs), the hip joint supports the head, trunk and upper limbs of the body, equating to around 62% of the body weight (Maquet, 1985). However during walking, the forces in the hip joint alter according to the progress through the walking cycle.

During walking, the hip undergoes two phases; the swing phase and the static phase. During the swing phase of walking, the hip joint undergoes flexion, followed by loading to begin the static phase. Simultaneously, the other hip is in the static phase undergoing extension, whereby the effective centre of gravity moves from the between the centre of the pelvis (during two leg standing) away from the supporting hip, due to the additional weight of the non-supporting leg. On the supporting hip joint, loads can reach 3-4 times body weight. Within this static phase, the hip undergoes two points of peak load, one at the heel strike and one at the toe-off. The heel strike occurs following flexion of the hip and describes the moment the heel of the foot impacts the ground, creating an instant large load at impact of around four times body weight, and ending the swing-phase of the walking cycle. The toe-off occurs following extension of the hip and begins the swing-phase of the walking cycle (Anderson and Blake, 1994). Between these two peaks the load of the hip joint is around two times body weight.

Looking closer at the articulating surface of the natural hip joint, the peak pressures experienced during the heel strike and toe-off are not evenly distributed across the contact surface. During walking, peak pressures exist at the superior-posterior aspect of the lateral roof of the acetabulum, with contact pressure spread across 80% of the contact surface. However during activities such as ascending stairs, peak pressures are significantly higher. When descending stairs, the peak pressure is across a more concentrated area, however the location of peak pressure also translocates to a more superior position. This variation in peak pressures and distribution patterns can lead to higher stress and deformation of the articular cartilage (Guilak, 1995, Yoshida et al., 2006). In a healthy hip joint, the horseshoe shape of the articular cartilage in the hip, in addition to the non-load bearing acetabular fossa, contributes to lower and

more homogenous distribution of contact stresses during activity (Daniel et al., 2005). In dysplastic hips, the peak stresses on the load bearing area of the contact surface is considerably and statistically significantly higher than in normal hips, leading to significantly higher cartilage deformation. The varying stresses and pressures present at the articulating surface of the natural hip are important when considering the range of morbidities that can develop in the hip. One of the main reasons for variations in the stresses at the hip is an individual's walking gait cycle.

The gait cycle describes the individual manner of performing the walking cycle, and involves a full stride of the walking cycle. During walking, the static phase occupies around 60% of the gait cycle, while the swing phase occupies 40% of the gait cycle. Variations in gait and differences in stress on the articulating surface of the hip joint can be due to body weight, femoral head/acetabulum size and morphology, and the position of the loading point during the peak load points (Abt et al., 1981).

1.3 Arthritis and Total Hip Arthroplasty

Arthritis is a degenerative disease of joints which can lead to pain and disability, and is caused by the degradation and loss of articular cartilage, leading to the inflammation of the synovial membrane. The loss of articular cartilage in arthritis subsequently leads to joint instability and severe pain in the affected area, to the point where the function of the joint is compromised. It is estimated that arthritis affects 10 million people in the UK, with around 1.2 million individuals consulting their GP with symptoms of osteoarthritis in 2006 (ArthritisResearchUK, 2011). It is also estimated that 1.6 million people in the UK have X-ray evidence of osteoarthritis (ArthritisUK., 2011-2012). One in five Americans were diagnosed with a form of arthritis in 2004/05 and osteoarthritis was the most prevalent form of the disease. Osteoarthritis accounted for \$128 billion spent annually and it has been estimated this number will rise considerably by 2030 (Hootman et al., 2006). These figures highlight the huge impact of arthritis worldwide.

Osteoarthritis is a rheumatic condition associated with wear of cartilage over time, caused by disintegration of cartilage and the formation of new bone under the cartilage, resulting in pain and lack of function (Dekker et al., 1992). It shows a

predisposition to patients with a high body mass index (BMI) (McCarthy et al., 2009), and patients with a high BMI are also at an increased risk of total hip replacement as a result of osteoarthritis (Buckwalter and Mankin, 1998, Karlson et al., 2003, Buckwalter et al., 2005). Osteoarthritis is thought to be caused by a combination of systemic and local factors. Systemic factors include age, sex, race, hormone levels and genetic disposition to the disease. The increase in incidence of osteoarthritis with age is thought to be partly due to the reduced levels of oestrogen in postmenopausal women, and the reduced biological response of the tissues, such as chondrocyte response to growth factors (Felson and Zhang, 1998). In addition to these biological factors, wear and tear is also responsible for damage to the cartilage protecting the hip joint. Stress induced damage to the matrix of the cartilage leads to the influx of water and fluids, and if this damage exceeds the ability of the chondrocytes to repair the matrix, cysts will eventually develop. These cysts are initially asymptomatic, however due to the loss of cartilage, eburnation of the exposed bone occurs, leading to microfractures and causing pain and disability in the joint (McCarthy et al., 2009).

Rheumatoid arthritis is a systemic inflammatory disease that mainly affects synovial joints, leading to a painful condition and loss of function. Rheumatoid arthritis has a prevalence of 1-3% in the population, and is the most common inflammatory joint disease in humans (McCarthy M, 2009). It is an autoimmune disease and is characterised by the action of host immune cells causing the pathogenicity that is associated with the disease (Fournier, 2005, Dhaouadi et al., 2007). The exact mechanisms behind rheumatoid arthritis are unknown, although a strong T cell response is believed to be crucial to the development of the disease. One hypothesis is that there is a genetic susceptibility to the disease whereby a highly immunogenic antigen is expressed on a major histocompatibility complex II (MHC II) molecule to CD4+ T cells. This then triggers a strong inflammatory response involving cytokines and immune cells that culminates in inflammation and the destruction of cartilage (Scheinecker et al., 2009).

Current treatments for arthritis concentrate on reducing pain and inflammation in an attempt to restore some function to the joint. Pharmacological treatments include acetaminophen and non-steroidal anti-inflammatory drugs to target the pain and inflammation respectively (Seed et al., 2009). Hip osteotomy is a surgical treatment

that involves realignment of the hip joint, altering the load bearing surface. (Pellicci et al., 1985, Rogers et al., 2009). Another surgical procedure for articular cartilage repair is debridement, which involves the removal of flaps of loose cartilage (Getgood et al., 2009). However, in terms of restoring mobility, both these procedures have mixed levels of success, and are short term treatments where symptoms often reoccur (Moseley et al., 2002).

In recent times, cutting edge tissue-engineered techniques have been researched in an attempt to regenerate the articular cartilage and therefore restore function to the joint. The use of natural and synthetic scaffolds in tissue engineered cartilage have been investigated, however, these scaffolds have so far failed to fulfil the necessary requirements of articular cartilage. Furthermore, while the use of stem cells to populate these scaffolds has been promising, the cartilage tissue produced from these cells has been shown to be inferior to that produced by chondrocytes (Johnstone et al., 2013). Despite these findings, the field of tissue engineering remains an exciting and promising area where the rapid progress being made could lead to successful treatments for arthritis in the hip joint.

Joint replacement surgery has been shown to be a suitable treatment for conditions in the hip joint where the pain and lack of mobility have come to impact heavily on the patient's quality of life. Total hip replacements have been considered one of the most successful surgical procedures in medicine, successfully eliminating pain, restoring mobility, and returning the high quality of life expected in today's society (American Academy of Orthopaedic Surgeons, 2013).

1.4 History of Total Hip Arthroplasty

In the 18th century, various methods of treating hip joint pain and disability existed, such as joint excision, hip osteotomy and interposition arthroplasty. Interpositional materials included pig bladder, muscle and silver plates. The first attempt at a hip implant was made in 1891 by the German scientist Professor Themistocles Glück. Glück developed an ivory ball and socket joint fixed to the bone with nickel-plated screws to restore function in hip replacements destroyed by tuberculosis. Around the year 1918, Sir Robert Jones covered a reconstructed femoral head with a strip of

gold foil and observed retention of motion after 21 years; the longest successful follow up at that time (Gomez and Morcuende, 2005). In the 1920's, Marius Smith-Petersen devised a hip mould arthroplasty using glass, Bakelite and plastics, although all failed. Smith-Petersen went on to revise the idea, using cups made from the metal Vitallium, with reported success rates of 82% (Toledo-Pereyra, 2004).

Sir John Charnley is credited with the innovation of the low friction arthroplasty as it is known today. His long journey to developing this type of implant and surgery began with a succession of friction experiments on animal and human joints (Kurtz, 2009b). Investigating the hydrodynamic principles of cartilage in the hip joint, he concluded that this was impossible to replicate in an artificial hip and therefore the most important attribute in an artificial joint was low friction. Charnley's material of choice was polytetrafluoroethylene (PTFE, Teflon) due to its low coefficient of friction (0.04-0.05). Sir John Charnley designed a 'double cup' prostheses, where the acetabulum was replaced with a PTFE shell, and a PTFE ball was secured on the femoral neck, replacing the natural femoral head, however both the shell and ball experienced severe wear leading to failure.

Charnley experimented with a metal femoral head and filled PTFE cups, but with no significant reduction in wear. The development of a wear testing rig, devised by Harry Craven, brought about the recognition and use of ultra high molecular weight polyethylene (UHMWPE) as a bearing material in arthroplasty. With Charnley initially unimpressed by the material, Craven demonstrated very low wear of the polymer compared with PTFE, and this led to development of the 'gold standard' arthroplasty; a stainless steel femoral head and stem secured with acrylic cement, articulating on an UHMWPE acetabular cup (Charnley, 1973, Kurtz, 2009b, Learmonth et al., 2007). Another revolutionary aspect of Charnley's design was the use of a small femoral head. Charnley designed a 22.25mm diameter stainless steel femoral head, much smaller than the previously designed metal-on-metal prostheses. Smaller femoral heads produce less wear compared to larger heads, and this is shown in Figure 1.4 (Donaldson et al., 2005). Almost all hip prostheses used today use the principle of the Charnley low friction arthroplasty, however different materials have been developed and different combinations produced in order to improve the long term performance of total hip replacements.

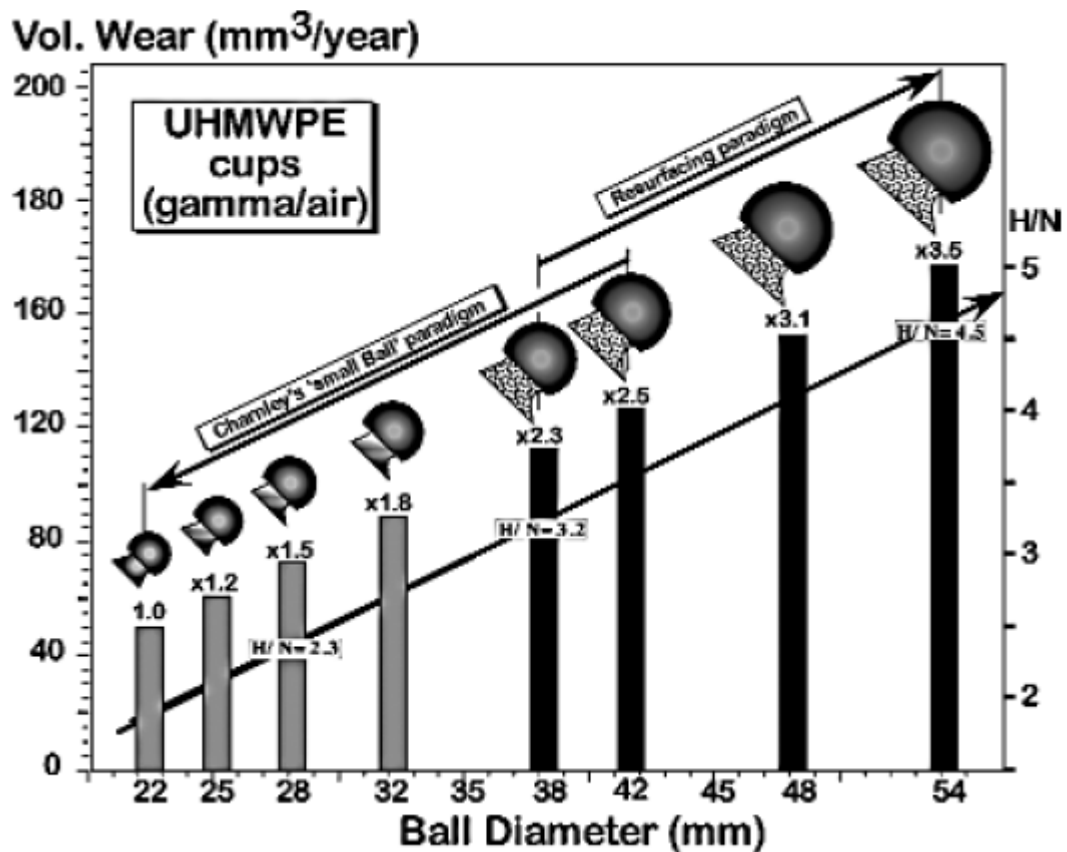


Figure 1.4– The increase in wear as femoral head diameter increases. Charnley’s small femoral heads displayed the lowest wear, while the larger heads showed the greatest levels of wear (Donaldson et al., 2005).

1.5 Bearing Materials for Total Hip Arthroplasty

1.5.1 Metal on Metal Hip Replacement

The first metal-on-metal (MOM) hip replacement was performed by Philip Wiles in 1938 and involved a stainless steel prosthesis fixed to the bone using screws (Wiles, 1957). These hip replacements were used to treat Stills disease, a type of juvenile rheumatoid arthritis.

McKee, a former colleague of Wiles, experimented with alternative materials for MOM bearings, leading to the development of cobalt-chromium (CoCr) prostheses.

McKee and Farrar found CoCr to have a lower friction coefficient than stainless steel, and at the time believed this material to be more biocompatible (McKee and Watson-Farrar, 1966). The first generation MOM prostheses consisted of CoCr as the bearing material, and a stem design seen in the Thompson prostheses that McKee considered to improve the femoral component. This hip replacement had a 7 year success rate of 57% and some prostheses lasted up to 16 years. The design was further developed when it was found that the main reason for failure was loosening. McKee incorporated acrylic cement into the design, which not only improved fixation when applied with a studded acetabular cup, but also acted to better distribute weight over the joint than the two screws used previously (McKee and Chen, 1973).

The use of acrylic cement and a CoCr femoral head eventually led to the second generation implant, which consisted of a cobalt-chromium (CoCr) articulating surface with an ultra-high molecular weight (UHMWPE) modular liner, and a CoCr acetabular shell, often described as a sandwich design. This implant allowed compatibility with existing acetabular shells, and allowed for fixation without the use of screws (Kurtz and Ong, 2009). However, the generation of UHMWPE wear particles became an issue, leading to osteolysis and loosening, limiting the life of the prostheses to about 20 years (Dorr et al., 2000).

This prompted the further development of MOM replacements, this time with improved clearance between the femoral head and the acetabular component. Increased clearance between the surfaced reduces wear to a certain level, until a distance too great negatively affects the film lubrication, therefore increasing wear. The Metasul[®] prosthesis was developed and introduced in 1988 by Sulzer and comprised a metal-on-metal bearing with a UHMWPE acetabular backing. This bearing showed very good survivorship rates, with one study showing only one revision in 90 implants due to aseptic loosening, with a 94.4% survivorship rate seen after 12.3 years follow up (Saito et al., 2010). The precision of these bearings resulted in low friction and low wear of around $5\mu\text{m}^3$ /per year (Weber, 1996) This bearing showed reduced wear compared to earlier MOM bearings (Dorr et al., 2000).

The use of MOM bearings gradually increased in popularity between 1999 and 2007, when at their peak MOM implants made up 37% of the total hip arthroplasties in the

USA (Mendenhall, 2008). Metal-on-metal implants showed much reduced wear rates compared to metal-on-polyethylene bearings, and were predicted to lead to an extended implant life and a lower rate of revision. The performance of MOM improved, with modern manufacturing and finishing techniques giving a super polished finish, therefore reducing the surface roughness of the bearing and moving the lubrication type closer to full fluid film (Tipper et al., 2005).

Hip resurfacing arthroplasty was thought to be a good alternative to THA for younger patients in need of a replacement. Hip resurfacing arthroplasty involves a prosthetic femoral head and acetabular cup that allows most of the femoral bone stock to be preserved. This makes hip resurfacing a viable option for patients who may require a total hip replacement later in life. Hip resurfacing arthroplasties showed excellent short term survival of 93-99% for 2-8 years follow up, with the Birmingham hip resurfacing (Smith and Nephew, Warwick, UK) having the lowest risk of revision (Macpherson and Breusch, 2010).

A concern regarding MOM implants and in particular MOM resurfacing arthroplasty is that despite the reduced wear rate and wear volume compared to UHMWPE bearings; the particles generated from MOM bearings have a mean size of around 50nm, considerably smaller than the mean size of UHMWPE particles. This means despite a smaller volume, the number of particles released from a MOM implant is higher for the same volume of UHMWPE, believed to be around 1-10 million particles per step, therefore raising concern about toxicity (Sieber et al., 1999, Tipper et al., 2005, Brown et al., 2007).

The biological consequences of the release of CoCr particles and ions include cytotoxicity, genotoxicity and hypersensitivity, and there is increasing evidence that the metal particles released during wear are highly toxic and cause pseudotumours (Pandit et al., 2008). Patient specific hypersensitivity is another aspect of cyst formation that can occur soon after implantation (Campbell et al., 2010). The nanometre sized particles generated during wear are released into the periprosthetic tissues and transported away from the implant site via the lymphatic system, leading to systemic distribution of metal particles (Jacobs et al., 1996). This claim was supported by analysis of metal ions in a number of different bodily fluids. Comparing eight patients implanted with MOM bearings over 20 years, and negative

control patients (no metallic implant), there was a 9-fold increase in chromium levels in serum, a 35-fold increase in chromium levels in urine and a 3-fold increase in serum cobalt levels in MOM patients compared to negative control patients. A short term study of implants of less than 2 years *in vivo* also showed significantly increased levels of serum cobalt and chromium ions. This study was supported by several other studies that highlighted an increase in systemic metallosis (Jacobs et al., 1996, Sieber et al., 1999, Hart et al., 2008, Figgitt et al., 2010)

Cobalt and chromium ions have been found to be genotoxic, with chromium (VI) ions entering cells through a sulphate ion transporter. Chromium is reduced from Cr(IV) to Cr(III) in the cytoplasm and leads to cross linking of DNA, resulting in DNA adducts and strand breaks. Damage to DNA, and the errors introduced to DNA as a result of this damage, is normally repaired by DNA repair mechanisms such as the *Ku* and DNA-dependent protein kinase. However, the saturation of these repair mechanisms as a result of the action of carcinogens such as Co and Cr ions can eventually lead to loss of function of certain parts of the DNA code. This can therefore result in loss of control of proliferation of the cell cycle, leading to carcinogenesis (Lodish et al., 2000). For this reason, chromium is a classified carcinogen (Figgitt et al., 2010). Cobalt and chromium ions, both alone and in combination, can cause chromosome aberrations *in vitro*. Chromium (IV) in combination with cobalt was found to be the most reactive. These metal ions are found in higher concentrations at various locations of the body in THA patients compared to people exposed to Co and Cr in industry (Figgitt et al., 2010)

Cobalt acts like an ‘assistant’ carcinogen, inhibiting the excision repair mechanism by inhibiting the incision and polymerisation enzymes. The combination of elevated levels of both these ions leads to DNA damage capable of causing cellular proliferation and tumour formation. In addition to the carcinogenic properties, these metal ions are also teratogenic and capable of crossing the placenta (Delaunay et al., 2010). Despite the classification of the ions as carcinogenic, there is currently no evidence to suggest the use of MOM implants increases the incidence of cancer. Two separate studies showed the incidence of cancer to be in line or below the incidence of the general population. It was also shown that when osteoarthritis was diagnosed in the patient, the incidence of cancer (stomach cancer and colorectal cancers) was reduced (Visuri et al., 1996, Visuri et al., 2006). Although these studies are

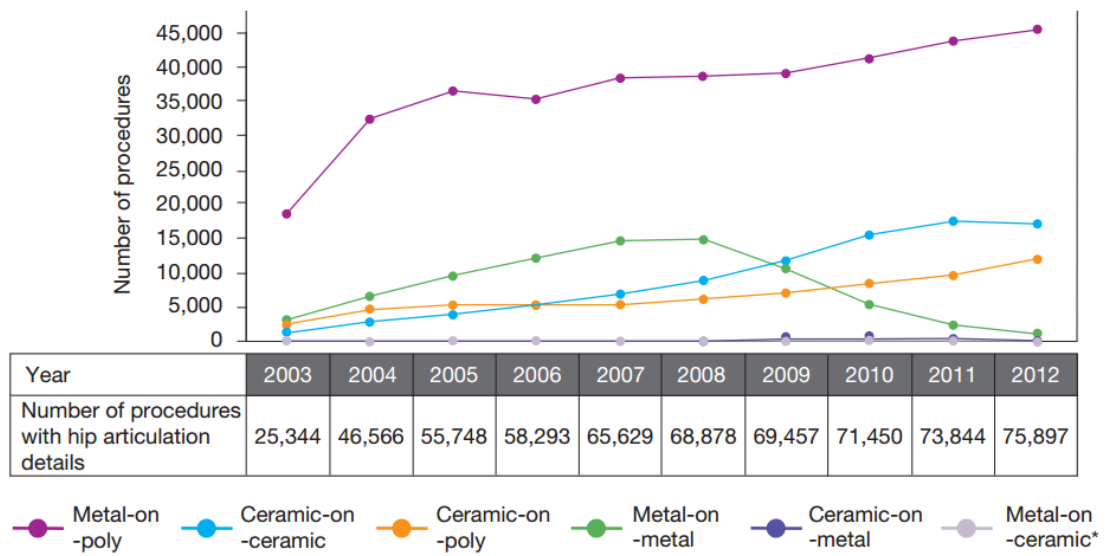
promising for MOM implants, it is after 20 and 30 year follow-ups that reliable data will be generated regarding the incidence of cancer as a result of metal ions from MOM implants.

Inflammatory soft-tissue masses, termed pseudotumours, have been found to occur after MOM hip resurfacing, and can be a cause of pain and reason for revision surgery. One study found that in a cohort of 1224 patients, after 8 years, failure due to pseudotumours was 4% (Glyn-Jones et al., 2009). A separate study found that wear of a MOM resurfacing implant was associated with pseudotumour formation, supporting the hypothesis that high levels of metal particles generated by wear can cause pseudotumours (Kwon et al., 2010).

While pseudotumours are associated with MOM hip resurfacings, atypical lymphocytic vasculitis-associated lesions (ALVAL) are commonly associated with MOM total hip replacements. These lesions are a result of a type IV hypersensitivity reaction to metal ions generated by wear, and cause pain and swelling around the joint. All these tumour-like lesions are complications associated with MOM replacements or resurfacings, and can result in revision surgery.

Despite the reduced wear of MOM bearings, and the strength of the prostheses making it ideal for younger, active patients, the issues surrounding toxicity of the particles have become increasingly worrying. In August 2010, DePuy™ recalled their ASR™ Articular Surface Replacement system due to a higher than expected revision rate of 8-9% after 3 years, and 12-13% after 5 years. This elevated revision rate was associated with the <50mm head diameters. The ASR™ Acetabular system was also experiencing higher revision rates of 13% over 5 years (MHRA, 2010). The reasons for revision were component loosening, malalignment, fracture of the bone, metal sensitivity and pain. This has caused concern regarding the use of metal-on-metal hip resurfacing, and combined with improvements in the performance of alternative bearings has led to a reduction in the use of metal-on-metal implants (Figure 1.5).

Hip articulation, trends 2003 to 2012.



© National Joint Registry 2013

Figure 1.5 – The bearings used in total hip arthroplasty in the UK over a period of 9 years. This shows the gradual increase in the total number of hip replacement procedures, along with the increase in the use of metal-on-UHMWPE and ceramic-on-ceramic. Metal-on-metal procedures have declined from 2007 onwards (National Joint Registry 2013 Report – www.njrcentre.org.uk)

1.5.2 Ceramic on Ceramic Hip Replacement

An increasingly common bearing material for use in total hip replacements is ceramic, with the most commonly used ceramic material being zirconia toughened alumina (Al_2O_3). The first reports of ceramic-on-ceramic (COC) hip replacements came from France in 1971, where Pierre Boutin used alumina-on-alumina. This design was developed by Shikata of Japan in 1977 to incorporate an UHMWPE acetabular cup which articulated against a ceramic femoral head (Kurtz and Ong, 2009). Early designs of COC hip replacements suffered complications, such as difficulty fixing the acetabular component, which led to tilting of the cup and subsequent edge loading and impingement (Winter et al., 1992). The materials and mechanisms used for ceramic components today contribute to a much improved material.

Ceramic materials used in orthopaedics have very low wear rates compared to metal-on-metal and metal-on-UHMWPE bearings (Campbell et al., 2004, Kurtz and Ong, 2009), with excellent biocompatibility, reducing the risk of particle-induced osteolysis. An *in vitro* simulator study comparing the wear rates of UHMWPE, CoCr and alumina showed a steady state wear rate of $0.004\text{mm}^3/10^6$ cycles for alumina. This was considerably lower than the Metasul mean wear rate of $0.119\text{mm}^3/10^6$ cycles and the UHMWPE mean wear rate of $13\text{mm}^3/10^6$ cycles (Clarke et al., 2000). The very low wear of alumina, in addition to its scratch resistance can be attributed to the hardness of the material (Willmann, 1996). Alumina is also more hydrophilic than CoCr (Kurtz and Ong, 2009), adding to the lower friction articulation of alumina against UHMWPE compared with CoCr on UHMWPE. A small grain size combined with a uniform distribution makes a good quality ceramic which is important to the long-term success of alumina bearings. Also crucial is good bone stock in the patient. This is demonstrated by a study that showed 100% survival of alumina-on-alumina bearings after 7 years in patients under 50 years old (Boutin et al., 1988).

Despite the ultra-low wear seen *in vitro*, wear rates *in vivo* were around $1\text{-}5\text{mm}^3/\text{annum}$. Due to the different wear rates, attempts were made to reproduce clinically relevant wear rates *in vitro* to further understand the performance of these materials. Clinical wear rates were not achieved *in vitro* using standard simulation conditions or by altering the lubricant or the acetabular cup angle. However, when

microseparation was applied to hip simulators the wear rate was 1.24mm^3 /per million cycles (Tipper et al., 2002). Microseparation is the separation of the femoral ball and acetabular socket, which can lead to rim contact and wear. Fluoroscopic video of patients with total hip replacements showed microseparation up to 2.8mm, with a mean separation of 1.2mm in 10 metal-on-polymer bearings (Lombardi et al., 2000). It was also observed that the femoral head separated from the acetabulum, yet maintained contact with the superior rim of the acetabulum. This microseparation motion is thought to be the cause of stripe wear seen in *ex vivo* alumina implants (Tipper et al., 2002).

Historically, a significant issue with ceramic components was the *in vivo* fracture risk, with fracture rates in the literature ranging from 0.5% to 0.06% (Tateiwa et al., 2008). This is due to the brittle nature of ceramics, where the grain size dictates the microscopic internal flaws of the material (Kurtz and Ong, 2009). Chipping fracture was more common than complete fracture, yet the multiple fragments generated through fracture caused catastrophic failure. However, the risk of fracture is still relatively low, and with its ultra-low wear, research has focused on further improving ceramic materials. A modern hybrid ceramic called BIOLOX delta has been developed, composed of 72.5% alumina, 25.5% zirconia and 2% mixed oxides (Figure 1.6). The addition of nano-sized yttria-stabilized zirconia particles to the alumina acts to reduce the initiation and propagation of cracks, also increasing the materials strength, fracture strength and toughness. However, BIOLOX delta is still susceptible to stripe wear and surface damage as a result of microseparation. In a hip simulator applying microseparation conditions, the 28mm BIOLOX® delta bearing generated low wear rates of 0.13mm^3 /million cycles. However, stripe wear was also generated on the femoral heads and acetabular cups, increasing the surface roughness from around 5nm to 20nm (Al-Hajjar et al., 2010).



Figure 1.6 – Ceramic-on-ceramic BIOLOX® delta from DePuy International. This shows the components used a ceramic-on-ceramic hip replacement. The femoral head component (right) has the ability to be connected to a variety of stems, depending on the physiology of the patients femur and the surgeons preference. The acetabular cup (top left) is shown. The coupling of the components is shown in the bottom left image.

1.5.3 PEEK, Carbon Fibre and Graphene Composite Materials

A promising modern alternative polymer material being used for joint replacement is polyetheretherketone (PEEK). This is a composite material that has shown promising wear results *in vitro*. This material has been coupled with carbon fibres to increase the strength of the material. One study showed wear of $1.16\text{mm}^3/10^6$ cycles for an alumina femoral head articulating against a PEEK acetabular component, compared to $38.6\text{mm}^3/10^6$ cycles generated from standard UHMWPE. This low wear rate was also sustained over longer-term testing, simulating 25 years of wear, demonstrating very promising survivorship (Scholes et al., 2008).

The biological response to PEEK and carbon fibre reinforced PEEK (CFR-PEEK) has only recently been investigated as interest in this material grows. Utzschneider et al., (2010) showed a comparable biological response between PEEK and UHMWPE particles, with both materials showing a similarly enhanced leukocyte-endothelial cell interaction compared to the negative control (PBS) (Utzschneider et al., 2010). These authors used histology to look at the synovial tissue of mouse knees after particles from both PEEK and UHMWPE were injected in. This method has the restriction of only looking at sections of the tissue and scoring the slides. An alternative method to better corroborate the biological response to particles would be to isolate clinically relevant PEEK particles and culture the particles generated with primary mouse or human monocytes. This would then allow for the comparison between the cytokine response between UHMWPE and PEEK.

Polyetheretherketone showed good biocompatibility, showing no significant adverse effects on cell viability, and no cytotoxicity or mutagenesis (Katzner et al., 2002). These results show PEEK and carbon fibre-PEEK to be promising biomaterials for possible use in prostheses. Considerable further *in vivo* research is required, but this material could be considered an acceptable alternative bearing material for the future. Another composite material being investigated for use as a bearing material in total hip replacements is a graphene-UHMWPE composite. This material is in its infancy, however this material has been shown to have significantly improved wear resistance compared to virgin UHMWPE (Tai et al., 2012).

Amongst the number of bearing materials currently available in total hip replacements, UHMWPE remains the gold standard bearing material. Metal-on-UHMWPE make up around 58% of all primary hip replacements in the UK, with UHMWPE the bearing material of choice in 65% of primary hip replacements (National Joint Registry, 2013). However, the success of UHMWPE has been due to the gradual evolution of the material from its inception by Charnley, to its modern equivalent today.

1.6 Ultra High Molecular Weight Polyethylene

UHMWPE is a linear homopolymer of ethylene, with the generic chemical formula - $(C_2H_4)_n$ - where n is the degree of polymerisation. Polyethylene is a commonly used polymer in industry and packaging. Clinical UHMWPE materials can have a degree of polymerisation of $n=200,000$, with a minimum degree of polymerisation of $n=36,000$, giving UHMWPE a minimum molecular weight of 1 million g/mol (Kurtz, 2009d, Sobieraj and Rimnac, 2009). UHMWPE is composed of a crystalline phase and an amorphous phase (Figure 1.7). The crystalline phase is arranged as a series of folds generating lamellae located randomly amongst the amorphous phase, and tie molecules link individual lamellae together, adding crystallinity (Kurtz, 2009d). The lamellae are 10-50nm thick and 10-50 μ m long, with an average space between lamellae of approximately 50nm.

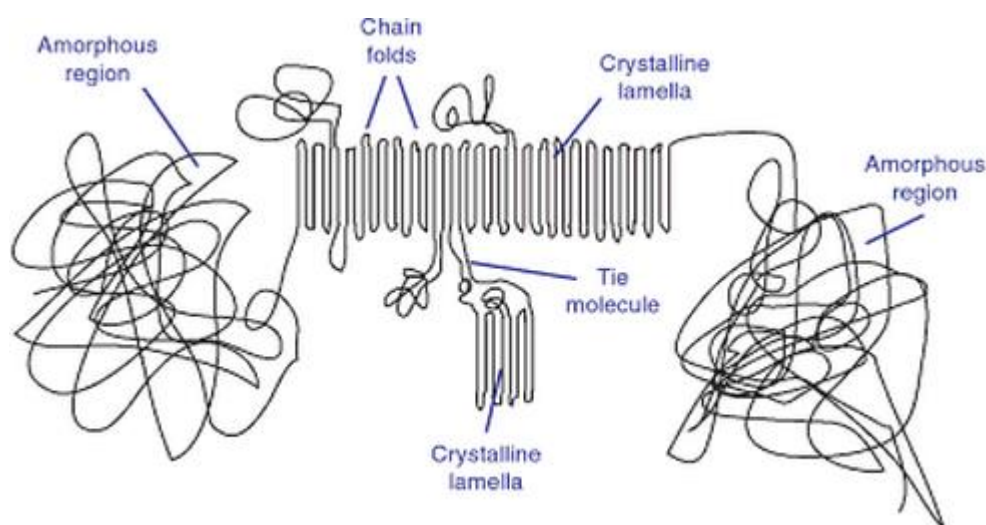


Figure 1.7– Schematic showing the microstructure of UHMWPE. This shows the amorphous and crystalline regions made up of long strands of polyethylene (Kurtz, 2009a).

The manufacture of UHMWPE for use as a bearing component in joint replacement begins with the ingredients ethylene and hydrogen, with titanium tetra chloride as the catalyst. This produces a powder which is then transformed into a liquid under high

temperatures ($>137^{\circ}\text{C}$) and pressures. Melted UHMWPE does not flow like other melted polymers and therefore the initial formation of the component is achieved either by both compression moulding or ram extrusion. The polymer is then finished at an accurate mix of temperature, pressure and time, to properly consolidate the component. Machining may then be carried out to finalise the form of the component. The UHMWPE component is then sterilised to prevent infection following implantation.

The use of UHMWPE as the bearing material in total joint replacements underwent steady growth following the publication of Charnley's experiences with UHMWPE. A follow up study by Charnley and Halley revealed that after an initial bedding in period, the average penetration rate of UHMWPE in total joint replacements during the first 5 years was 0.18 mm/year for the 72 patients included in the study. This was shown to subsequently drop to 0.1 mm/year during the 5-10 year period, showing the excellent performance of this material compared to previous prostheses (Charnley and Halley, 1975). Despite these promising results in terms of the low wear of UHMWPE *in vivo*, further research into failed Charnley explants showed wide variation in the wear rates of UHMWPE. From 82 retrieved UHMWPE cups, there was a very broad negative correlation to implantation time before failure and wear rate, however the spread was wide, and several cups had worn at a higher rate than presented by Charnley. This showed the importance of generating a greater understanding of the wear mechanisms of UHMWPE to allow for improvement to be made to the material.

1.7 Tribology of UHMWPE

Tribology is the study of friction, lubrication and wear, and these are important concepts for the development of UHMWPE as a bearing material in joint replacement. Wear of UHMWPE is the major cause of failure in joint replacements. It is the wear particles and debris generated that cause the problems associated with failure, such as inflammation, osteolysis and aseptic loosening (Green et al., 1998, Fisher and Ingham, 2004). The detailed immunological response to UHMWPE wear debris is discussed in more detail in section 1.8.

Since the introduction of the first *in vitro* wear tests for metal-on-UHMWPE by Charnley in 1960, *in vitro* wear tests have been conducted to better understand the wear and wear mechanisms that occur in UHMWPE *in vivo*. Early wear simulators were diverse in their method of motion, however these simulators only exerted unidirectional motion on the test components, yielding wear rates significantly lower than the rates observed *in vivo* (Barbour et al., 1999, Rose et al., 1982, Wang et al., 1997, Kurtz, 2009b). From these results transpired the importance of multidirectional motion in the wear of UHMWPE *in vivo*, with the addition of multidirectional motion to wear tests delivering wear rates comparable to those observed physiologically (Walker et al., 1996). The importance of multidirectional motion in the wear of UHMWPE is related to the cross shear and aspect ratio values of the wear track. When considering UHMWPE as a bearing material *in vivo*, it was proposed that differences in gait patterns of an individual could produce different wear factors as a result of the cross shear and aspect ratio values of the resulting wear track (Turell et al., 2003). While increasing aspect ratio has been shown to increase wear rates of virgin UHMWPE up to a critical value, a study by Korduba and Wang (2011) found the wear rate of highly crosslinked UHMWPE (90 kGy) to be unaffected by increasing aspect ratio (Korduba and Wang, 2011). The effect of crosslinking of UHMWPE is discussed in more detail in section 1.10.

The mechanism for wear of UHMWPE is believed to be the generation and break up of fibrils on the surface of the polymer, generated by the articulation of the femoral head against the UHMWPE acetabular cup. It is thought multidirectional articulation ruptures the surface of these submicron fibrils, generating particle debris (Muratoglu, 2009). It is important to point out that the generation of fibrils is the last step in a sequence of surface disruption, where folds, then ripples are produced, finally forming fibrils (Yamamoto et al., 2003). The formation of UHMWPE particles can occur due to cyclic mechanical loading at articulating interfaces, however particles can also be formed at the modular interfaces and non-articulating interfaces such as where the polyethylene acetabular cup is connected to the shell. This leads to the accumulation of particles in surrounding tissue (Hukkanen et al., 1997, Abu-Amer et al., 2007).

There are several types of wear that are important in hip replacements. Abrasive wear is due to hard protuberances forced to move against a softer surface. This type

of wear is caused by the asperities present on the harder surface causing damage to the softer surface, resulting in the loss of material from the softer surface. This type of wear can be present in metal-on-UHMWPE bearings due to the difference in hardness. Adhesive wear is the wear generated from the sliding of asperities, causing the rupture of the solid surface and progressive loss of the material. Adhesive wear describes the material transfer from any two sliding surfaces as asperities interact (Santavirta et al., 2003). Third-body wear is another type of wear that is clinically relevant. This type of wear is due to third body particles such as polymethylmethacrylate (PMMA) cement used in fixation, or bone, interacting with the articulating surfaces and causing scratches or imperfections. These scratches have asperities that interact and cause further wear. Finally, corrosive wear is a very important type of wear especially in metal-on-metal bearings. This is the wear generated by chemical reactions on the metal, therefore altering the performance of the material. Metals that have been oxidised have different mechanical properties therefore altering the mechanics of the bearing (Affatato et al., 2008). Corrosive wear has once again been mentioned as an important factor in the failure of modern metal-on-metal hip replacements, with the release of metal ions as a result of corrosion leading to adverse reactions in some patients (Langton et al., 2010).

Lubrication has a major influence on bearing wear. The ideal form of lubrication for any total hip replacement is full fluid film lubrication (Scholes et al., 2000). This is the type of lubrication that completely separates the two articulating surfaces so there is no contact between their asperities. This would mean almost no wear, however this concept is difficult to achieve (Hall et al., 1994). Boundary lubrication occurs when the lubrication between the surfaces is insufficient to fully separate the asperities. This causes the asperities to come in contact, and the motion causes wear. The lubrication mechanism of the bearing is dictated by several properties of the bearing itself. These include the surface roughness, material combination, thickness of the cup, clearance between the components and the size of the femoral head (Hall et al., 1994). These properties contribute towards the materials friction torque.

The parameters dictating wear include surface roughness, clearance between the bearings, coefficient of friction and sliding distance (Bhatt and Goswami, 2008). The surface roughness of the material articulating against UHMWPE is important in the wear behaviour of the polymer. The coefficient of friction of the material increases

as surface roughness increases, and wear rate correlates with this (Cho et al., 2004). Surface roughness has been found to be important in bearing survivorship, especially in hard-on-soft bearings, where abrasive wear is common. The lowest surface roughness is achieved on metal components. Ito et al., (2010) analysed 108 retrieved metal femoral components that were coupled with UHMWPE acetabular shells. The mean surface roughness of the femoral heads was $0.18 \pm 0.18\mu\text{m}$. The roughest femoral heads ($0.56\mu\text{m}$) increased UHMWPE wear, and there was positive correlation between increasing surface roughness of the metal head and increasing wear (Ito et al., 2010).

The understanding of the tribology of UHMWPE is important for the development of a low-wearing, longer lasting bearing material in total hip replacements. Crucial to evaluating the wear performance of UHMWPE prior to implantation is wear testing of the components *in vitro*, in addition to the analysis of wear debris generated under clinical conditions.

1.8 Wear Testing and Isolation of UHMWPE Wear Particles

The use of wear testing to compare different materials and their tribological attributes covers a vast range of prosthesis; therefore numerous simulators have been developed to simulate different joints in the body. Such machines include finger, spine, knee and hip simulators (Galvin et al., 2006, Joyce, 2010, Grupp et al., 2010). For hip simulation alone there are a number of different types of machines that have been developed to test different components and different materials under a range of tribological conditions. While joint simulators are effective at determining the overall performance of a prosthesis, simple configuration wear tests are also an important part of testing the materials' properties and wear performance, prior to simulator testing.

The improvement of wear test simulators for determining the wear performance of materials used in joint replacement has led to more accurate predictions of a materials performance *in vivo*, and therefore improvements in joint replacement as a whole. Early wear testers were comprised of unidirectional pin-on-disk, disk-on-plate, sphere-on-disk, or pin-on-plate wear rigs, however these early wear test

machines exerted unidirectional motion on the test components, yielding wear rates significantly lower than the rates observed *in vivo* (Barbour et al., 1999, Rose et al., 1982, Wang et al., 1997, Kurtz, 2009b). The introduction of multidirectional wear test rigs was a major development for determining *in vitro* the performance of potential materials for use *in vivo* (Baykal et al., 2014). Multidirectional pin-on-disk or pin-on-plate wear simulators have been shown to be reliable in determining the wear factor or wear rate of UHMWPE at different levels of crosslinking. Highly crosslinked UHMWPE has been shown to be differentiated from virgin UHMWPE based on wear testing using these simple configurations testers. Sliding distance was shown to be linearly related to wear rate, and therefore the introduction of a wear factor equation, to normalise the wear rate according to the total sliding distance per million cycles, has been shown to be beneficial for the comparison of different UHMWPE materials (Baykal et al., 2014). It was also determined that the comparison of pin-on-plate wear test results with wear test results in the literature may not be conclusive due to differences in load, contact area and stress yielding different active wear mechanisms, and therefore wear tests conducted within a single study would yield more reliable data for comparison of UHMWPE.

A commonly used method of wear testing, and the method adopted in the present study, is multidirectional pin-on-plate wear testing. While joint simulators are used to test the performance of a specific component or design, pin-on-plate wear simulators are used to test the wear performance of the material. Multidirectional pin-on-plate wear simulators use a plate that moves back and forth as the pin rotates, replicating the multidirectional motion of the femur against the acetabulum. The pin is attached to the machine and a force applied, simulating the forces of the hip joint, whilst the articulating surface is submerged in a lubricant (Tipper et al., 2000, Galvin et al., 2006). In a pin-on-plate wear test, Kang et al., (2008) used a compressive load of 80N on an UHMWPE pin with a contact surface of 10mm. These conditions were selected to simulate the compressive forces of the hip joint. The authors articulated the UHMWPE pin against a CoCr plate, which was polished to an average surface roughness of 0.01 μ m. A lubricant of 25% (v/v) bovine serum in sterile water was used, with 0.1% (w/v) sodium azide added to the lubricant to inhibit bacterial growth during testing. The lubricant was changed every 330,000 cycles and this enabled the authors to analyse the lubricant (Kang et al., 2008). This is one example of the

conditions commonly used during pin-on-plate wear testing in order to replicate wear accurately *in vitro*.

Joyce and Unsworth (2004) highlighted the importance of the type of lubricant and motion used in these rigs to generate wear particles. Distilled water as a lubricant yielded higher wear rates than bovine serum or ringers solution (Joyce and Unsworth, 2004). Scholes and Unsworth et al., (2006) investigated different protein concentrations of lubricants and the effect of these on the friction factor. The authors tested a combination of UHMWPE, CoCr and alumina ceramic bearings and generated different friction factors with the use of three different lubricants; human synovial fluid, bovine serum and carboxymethyl cellulose (CMC). When these lubricants were tested using the metal-on-metal bearing and the ceramic-on-ceramic bearing, the friction factors were significantly different for each lubricant. The authors hypothesised that the change in the friction factor may be due to the adsorption of the protein at the surface of the bearing. This forms a layer of protein covering the bearing and therefore reduces the contact between asperities, increasing the degree of fluid film lubrication and reducing friction (Scholes and Unsworth, 2006). Testing *in vitro* is important to determine the conditions and materials most suitable for clinical use; therefore it is vital the conditions reflect the ones found *in vivo*.

Another method of analysing the wear of a hip replacement is recovery of the prosthesis and periprosthetic tissue from failed implants. This provides the opportunity to analyse the wear of the implant, and characterise the wear particles generated *in vivo*. When the tissue samples are excised from the hip, tissue digestion is necessary to isolate and analyse wear particles. Baxter et al., (2009) evaluated different methods for tissue digestion to identify the most efficient and effective technique. The authors compared basic (KOH, NaOH), acidic (HNO₃) and enzymatic conditions (proteinase K, liberase blend 3). The digestion efficiency was calculated by cutting one gram of periprosthetic tissue specimens into 0.25 x 0.25cm cubes and exposing the cubes to the agent for 24hrs. The initial and final weights of the filters (1µm pore filters) and tissue were calculated to quantify the digestion. For digestion of porcine tissue, 5M NaOH was the most effective, with only minimal amounts of undigested tissue. Statistically, 5M NaOH, 5M KOH and 15M KOH all generated final tissue weights of less than 1% of the initial tissue weight. Enzymatic

digestion was not as effective as alkali or acid, with 15.8M HNO₃ showing very thorough tissue digestion (Baxter et al., 2009).

A method for isolating and characterising wear debris of UHMWPE from periprosthetic tissue was outlined by Tipper et al., (2000). In this method, 1g of periprosthetic tissue was digested with 12M KOH at 60°C for 2-5 days. Lipid extraction was performed using chloroform: methanol (2:1) incubation at room temperature for 2-3 days, followed by centrifugation at 2000g for 10 min. Following this, absolute ethanol was added with stirring at 4°C for 24hrs to precipitate any proteins, which were removed by centrifugation at 2000g (4°C) for 2hrs. To isolate the particles, the supernatant was sequentially filtered through preweighed 10µm and 0.1µm cyclopore filters. The filters were dried and then weighed to determine the mass of the particles, and sections of the dried filters were analysed using scanning electron microscopy (Tipper et al., 2000). This method was successful in removing the tissue and isolating the polyethylene particles from periprosthetic tissue, and additionally has been shown to be suitable for isolating polyethylene particles from serum lubricants used *in vitro* (Tipper et al., 2006).

Wear testing *in vitro* has generated a strong understanding of the mechanical performance of UHMWPE, however, an understanding of the biological response to UHMWPE wear debris, and the subsequent failure mechanisms of metal-on-UHMWPE implants has also been shown to be crucial in predicting the performance of a UHMWPE bearing *in vivo*, in order to ultimately produce a longer lasting hip replacement.

1.9 Failure of UHMWPE total hip replacements

While a total hip replacement consisting of a metal femoral head articulating against a UHMWPE acetabular cup is considered the gold standard for total hip arthroplasty, failure of this type of bearing occurs at a rate of around 1% per year, with 75% of these failures being caused by aseptic loosening as a result of the biological response to wear particles (Towheed and Hochberg, 1996, Crawford and Murray, 1997). The other 25% of failures are mainly due to infection, technical errors during surgery or recurrent dislocation (Malchau et al., 1993). With an increase in the number of younger patients requiring a total hip replacement, the demand for a longer lasting total hip replacement has driven research and development of alternative polyethylenes.

One of the major causes of failure in metal-on-UHMWPE total hip replacements is aseptic loosening. Aseptic loosening is the gradual release of the prostheses from the bone it is embedded or cemented into. One aspect of aseptic loosening is mechanical. For example, a lack of initial stability as a result of remodelling of the devitalised bone bed may lead to migration of the prostheses (Aspenberg and Herbertsson, 1996). This is due to the formation of a membrane between the acrylic cement and the bone that causes lubrication between the prostheses and the bone. Also, poor initial fixation or loss of mechanical fixation over time can cause aseptic loosening (Abu-Amer et al., 2007).

However, the most important cause of aseptic loosening is the biological response to UHMWPE wear debris, leading to an innate immune response that culminates in the loss of bone mass around the implant. Over the course of a year, as the patient uses their total hip replacement, billions of polyethylene wear particles are generated by wear of the UHMWPE bearing surface, with these wear particles ranging in size from nanometres to several millimetres (Fisher and Ingham, 2004). The size, morphology and volume of the particles have been shown to dictate the severity of the immune response. Histological studies investigating the phagocytosis of particles found that larger polyethylene particles ($>10\mu\text{m}$) stimulated macrophages to become multinucleated giant cells which can engulf these larger particles. These areas of giant cell formation and phagocytosis can also become surrounded by a fibrous

capsule which can increase the recruitment of macrophages and stimulate a sustained innate immune response (Pazzaglia et al., 1987, Murray and Rushton, 1990).

The primary role of macrophages is to recognise and neutralise infectious agents such as bacteria and fungi, which exist in the nanometre to micrometre size range. As a consequence, wear particles within this size range are phagocytosed by macrophages. The critical size range for macrophage activation by UHMWPE particles *in vitro* was determined to be 0.2-0.8 μm , at a concentration of 10-100 μm^3 per cell (Green et al., 1998, Ingham and Fisher, 2000, Liu, 2012). Macrophage activation by UHMWPE wear particles leads to the release of osteolytic cytokines and cell control molecules as part of the innate immune response. Cytokines and cell signalling molecules associated with the particle stimulated response include tumour necrosis factor- α (TNF- α), interleukin-1 α (IL-1 α), IL-1 β , IL-3, IL-6, macrophage colony stimulating factor- α (M-CSF), platelet-derived growth factor (PDGF), Receptor activator of nuclear factor κ -B (RANK)(and its ligand RANKL), the NF- κ B transcription factor pathway, and secretory products such as prostaglandin-E2 (PGE2) and adhesion molecules (Green et al., 1998, Schwarz et al., 1999, Ingham and Fisher, 2000, Abu-Amer et al., 2007) (Figure 1.8). These cytokines act on a number of different cell types, and specifically their interaction with osteoclasts, osteoblasts and fibroblasts leads to an increase in the population of osteoclasts around the implant. The type-1 membrane surface protein RANK is found on the surface of pre-osteoclasts, and its ligand; RANKL, is crucially found on the surface of T cells. With the increase in RANK and T cell levels following macrophage activation there is an increase in osteoclast activation, which is an important step in the osteolytic response caused by UHMWPE particles (Abu-Amer et al., 2007).

Interleukin-1 and IL-6 are also important cytokines in the inflammatory response to wear particles and the subsequent bone resorption. These inflammatory responses can lead to fluid around the prostheses and a membrane, causing loosening. The importance of these cytokines was demonstrated *in vivo* with analysis of the interface membranes that surrounded the femoral components of failed total hip replacements (Chiba et al., 1994). The authors compared total hip replacement patients with osteolysis and those without. Patients who were experiencing osteolysis showed a higher concentration of macrophages, as well as a higher concentration of smaller polyethylene particles in the periprosthetic tissue. Higher concentrations of TNF- α ,

IL-1 and IL-6 were observed in the interface membranes of hip replacements undergoing osteolysis compared to those without osteolysis (Chiba et al., 1994). This provided clinical evidence of the importance of these inflammatory cytokines in osteoclastogenesis, osteolysis and aseptic loosening. Another study found that macrophages taken directly from periprosthetic tissue had the ability to differentiate into osteoclast precursors (Sabokbar et al., 1997). This highlighted the link between the generation of wear particles and the subsequent immune response, to the activation of osteoclasts and osteolysis. It is the presence of osteoclasts that is vital to the demineralisation of bone, the loss of bone mass around the implant, and the loosening of the prosthesis.

The normal balance of osteoblasts and osteoclasts is unbalanced by this inflammatory response, leading to the resorption of bone and osteolysis, and the loosening of the prostheses. It is the recruitment, activation and increase in proliferation of osteoclasts, in addition to the reduction in osteoblast number and activity that causes increased bone resorption, osteolysis and eventually aseptic loosening causing failure of the prostheses. The exact interactions that take place between the osteolytic cytokines and osteocytes are unknown, although there is an important relationship between macrophages and osteoclasts, since they originate from the same hematopoietic stem cells. Macrophage colony stimulating factor and osteoclast colony stimulating factor play a role in the normal differentiation of hematopoietic stem cells into osteoclasts (Lorenzo et al., 1987, Hayase et al., 1997). In addition to this, particle stimulated macrophages have been found to have the ability to differentiate into osteoclast precursor cells directly, further disrupting the normal balance of osteoclasts and osteoblasts that maintains the healthy turnover of bone.

Early research implicated polymethylmethacrylate cement as the source of particles leading to osteolysis, although it was shown that cementless hip implants generated more wear particles than cement-fixed implants (Gallo et al., 2002). Some modern femoral components use a hydroxyapatite-coated stem as hydroxyapatite stimulates the synthesis of bone, therefore embedding the femoral stem into the femur. This method of fixation has yielded some excellent results *in vitro* and *in vivo* (Kress et al., 2010). While bone cement can induce osteolysis, polyethylene particles are considered to be more important in inducing bone resorption (Ingham et al., 2000).

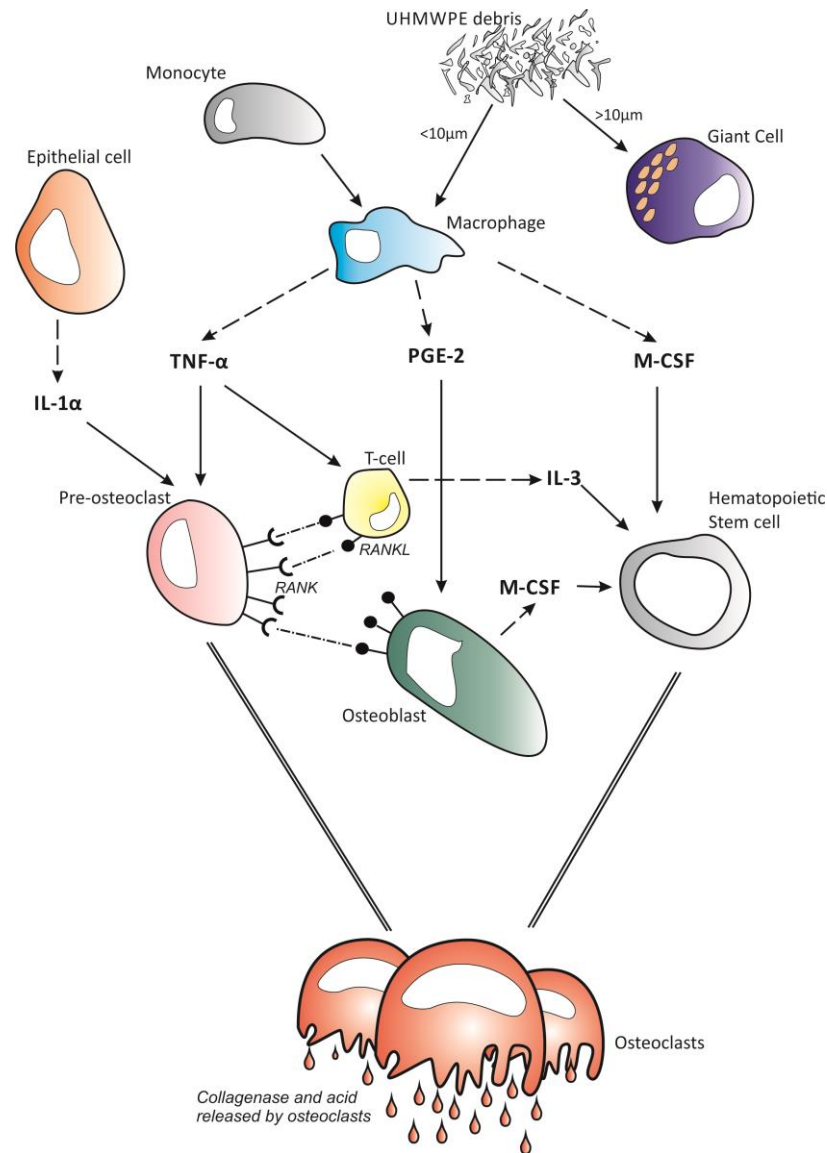


Figure 1.8 – Schematic of the postulated mechanisms behind aseptic loosening. Polyethylene wear particles larger than $10\mu\text{m}$ in diameter are phagocytosed by multinucleated giant cells. Particles smaller than $10\mu\text{m}$ are phagocytosed by macrophages, with particles between $0.2\text{-}0.8\mu\text{m}$ being considered the most biologically active particles. The dashed black arrows show a substance released from a cell, the solid black lines show that substance acting on a cell. The dashed gold lines show an interaction between ligand (RANKL) and receptor (RANK), and the double black lines show the cell changing as a result of the cytokines and interactions. This shows the importance of macrophages in releasing cytokines that increase the proliferation of osteoclasts. Also important are epithelial cells and T cells; both cells commonly seen in areas of inflammation. $\text{TNF-}\alpha$, $\text{IL-1}\alpha$ and the interaction between RANKL and RANK stimulate the activation of pre-osteoclasts to osteoclasts. Prostaglandin E-2 stimulated the expression of RANK ligand on osteoblasts, while hematopoietic stem cells are stimulated by M-CSF and IL-3 to differentiate into osteoclasts. This leads an overall increase in osteoclasts, with a decrease in osteoblasts, therefore concluding in bone resorption and aseptic loosening of the prosthesis.

Genetic susceptibility to osteolysis as a result of UHMWPE is becoming an increasingly important area of focus in increasing survivorship of implants. Mullins et al., (2007) investigated a series of 228 Charnley total hip replacements implanted into patients between 1972 and 1973 and found a 30 year survival rate of 73% (± 6.1). This demonstrated that some Charnley hip arthroplasties could last beyond 30 years, while some would fail before 10 years (10 year survivorship of 93%) (Mullins et al., 2007). It was hypothesised that the difference in success rate of the same bearings could be due to a patient specific reaction to wear debris, therefore inducing a different level of osteolysis. Zhang et al., (2008) investigated the inflammatory response and level of osteoclastogenesis of three different genetic groups of mice when implanted with UHMWPE particles under the skin of the calvarium (a portion of the skull). An immunological assay was conducted using an enzyme linked immunosorbent assay (ELISA) for TNF- α and IL-1 β . The authors found a difference in the levels of both cytokines between all three groups, although none were significantly different. The levels of osteoclastogenesis were measured using a leukocyte acid phosphatase staining kit, and counter stains, to identify osteolytic cells, termed TRAP+ cells. One type of mouse (C57BL/6J) showed significantly higher levels of osteoclastogenesis compared to the other two types of mouse (Balb/c, Kunming). This shows the variation in the immune response to polyethylene particles in a mouse model, therefore indicating such variation could occur in humans, potentially leading to a more aggressive cytokine response and subsequently an increased rate of osteolysis (Zhang et al., 2008). Heterogeneity in human donors has also been demonstrated in a previous study by Liu (2012). When investigating the cellular response to UHMWPE wear debris, some donors responded with a significantly elevated level of TNF- α release compared to the cells only, whereas some donors did not produce a cytokine response to the same treatment (Liu, 2012). The eventual aim in this area of research is to develop a test which can be carried out on a patient before a total hip replacement, and a patient 'more reactive' with UHMWPE wear debris can be detected and therefore given an alternative bearing.

1.10 Crosslinked UHMWPE

The importance of UHMWPE wear debris on stimulating osteolysis in patients has been well documented, and the wear mechanisms of UHMWPE are well understood. This understanding of the wear mechanisms, combined with importance of reducing the generation of UHMWPE wear debris from the bearing, lead to research into a more wear resistant UHMWPE material for use in total hip replacements.

A study by Bragdon et al., (1996) demonstrated how the motion of articulation changed the wear patterns of UHMWPE, in particular how multidirectional articulation increased wear (Bragdon et al., 1996). Research conducted into the mechanisms of wear led to the hypothesis that increasing the entanglement density of the polymer would reduce the surface deformation during multidirectional articulation. Entanglement is the structural twisting or entwining of strands in a polymer, leading to strength at the joins between the strands. A reduction in surface deformation and subsequent wear was first provided by melt-annealing, but later radiation crosslinking was added to the method.

Melt-annealing of UHMWPE with irradiation increased wear resistance *in vivo*, but this increase was found to be mainly due to an increase in crosslinking between the strands, not necessarily an increase in entanglement density. Crosslinking reduced the formation of surface fibrils and increased wear resistance, leading to the development of highly crosslinked UHMWPE. Conventional radiation doses of 25kGy, normally used to sterilise the polyethylene, conferred moderate levels of crosslinking in the polymer, although it was found that higher levels of radiation, for example 50kGy, significantly increased the amount of crosslinking and this material was termed highly crosslinked UHMWPE (Kurtz et al., 1999).

A significant increase in wear resistance has been demonstrated in UHMWPE treated with high levels of gamma irradiation, with a positive correlation between irradiation dose and wear resistance (Endo et al., 2001, Galvin et al., 2006) . This relationship between increasing irradiation dose and the reduction in wear of UHMWPE is demonstrated in Figure 1.9.

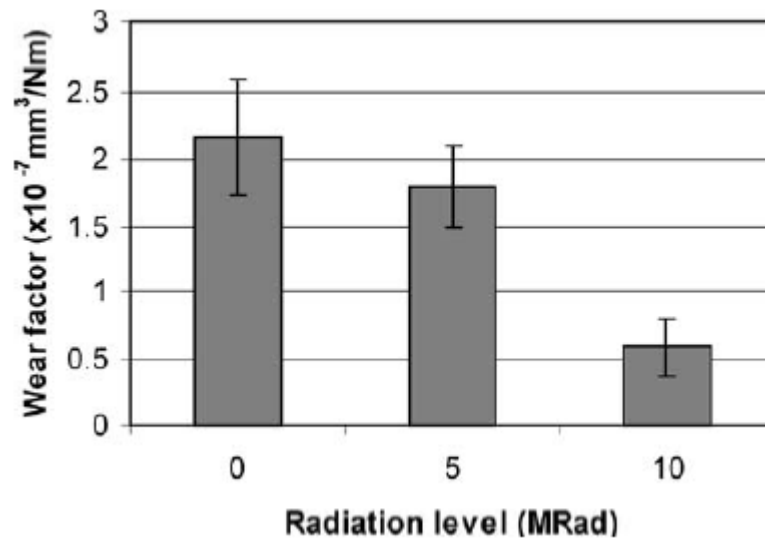


Figure 1.9 – The wear factors of UHMWPE gamma irradiated with different doses; non-crosslinked (0MRad), moderately crosslinked (5MRad) and highly crosslinked (10MRad). The graph shows the reduction in the wear factor as radiation dose increases (Galvin et al., 2006).

The effect of irradiation on the surface of the polymer was studied *in vitro* via the investigation of the disruption and appearance of surface fibrils after wear of irradiated and non-irradiated UHMWPE. The simulator ran for 6 million cycles, to simulate 6 years of wear. Compared to the surface disruption and fibrils on the non-irradiated component, the 2.5-Mrad irradiated component surface was less disrupted and fibrils were less frequent and smaller (1-5 μ m) in length. The fibrils of the irradiated polymer also had a 24-fold reduced aspect ratio, and in general the surface disruption was greatly reduced with increased irradiation (Figure 1.10); (Yamamoto et al., 2001).

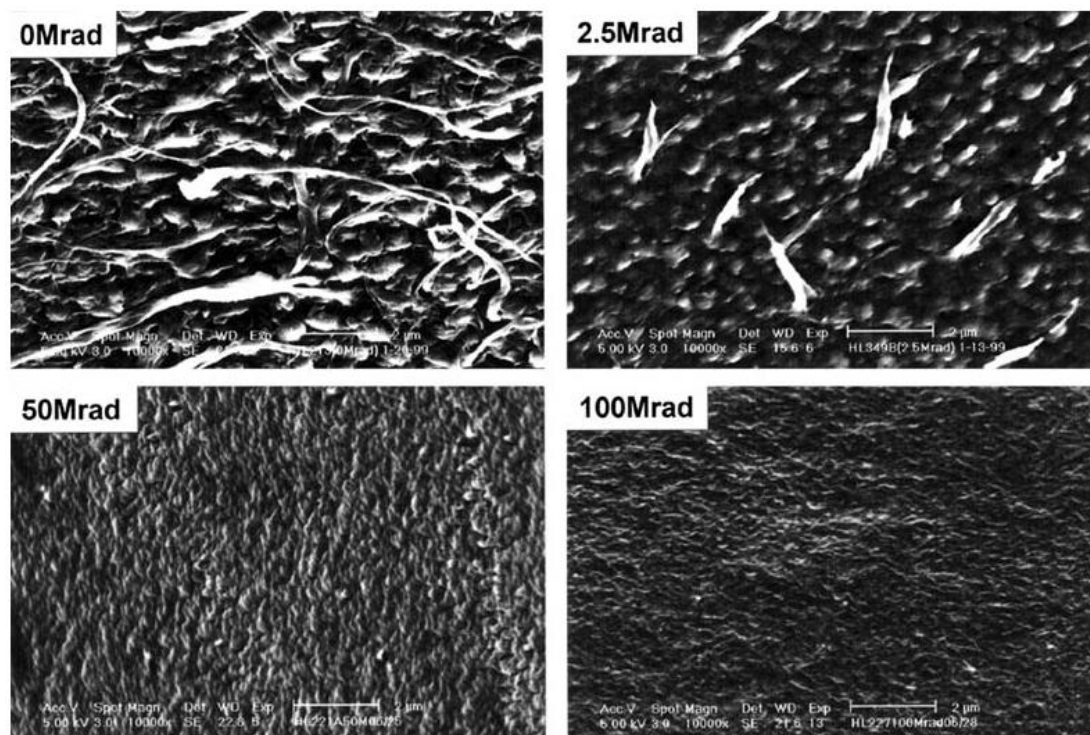


Figure 1.10 - The worn cup surfaces at different levels of irradiation. The reduction in surface disruption can be seen as radiation dose increases. The non-crosslinked surface (0Mrad) shows the most disruption, while the very highly crosslinked surface (100Mrad) shows little surface disruption with no fibrils forming (Koval KJ, 2000, Yamamoto et al., 2001).

Ionising radiation leads to the generation of free radicals through the cleaving of C-H and C-C bonds in the polymer. The cleavage of C-C bonds is termed chain scission, and it is this scission that allows the recombination and crosslinking of neighbouring strands. However, following gamma irradiation, most of the free radicals generated do not reform but stay embedded in the polymer with the ability to cause oxidation during either storage or *in vivo* (Al-Ma'adeed et al., 2006). The free radicals generated can react with oxygen during storage or *in vivo* to produce peroxyradicals. Peroxyradicals remove a hydrogen from polyethylene chains and can themselves react with oxygen, therefore generating a chain reaction of radicals. Peroxyradicals react with hydrogen to form hydroperoxides, which then degrade into oxidation products such as ketones, esters and acids. These oxidation products cause further chain scission leading to embrittlement of the polymer.

The presence of free radicals can be significantly reduced by post-irradiation melting. Heating highly crosslinked UHMWPE to above its melting point provides sufficient energy to release free radicals from the amorphous region of the polymer,

and for the free radicals to recombine, reducing the residual free radical burden (Oral et al., 2005, Muratoglu, 2009). However, it has been demonstrated that post-irradiation melting reduces fatigue strength and reduces crystallinity of the polymer, producing a less favourable bearing material (Wang, 2006, Al-Ma'adeed et al., 2006).

Durasul, manufactured by Zimmer, is a clinically available highly crosslinked UHMWPE. This type of UHMWPE is irradiated with 95kGy gamma irradiation at 125°C and post-irradiation melted (Muratoglu, 2009). In a study comparing the *in vivo* wear of Durasul polyethylene acetabulum liner and a virgin UHMWPE liner after 5 years, the annual linear wear rate of Durasul was 55% lower than the virgin UHMWPE liner (Dorr et al., 2005). This is one example of a clinically available highly crosslinked and melted UHMWPE performing better than standard UHMWPE clinically.

An alternative mechanism for reducing residual free radicals in highly crosslinked UHMWPE is post irradiation annealing. That is the process of heating the polymer to below its melting point in order to release free radicals yet still preserve the favourable mechanical properties of highly crosslinked UHMWPE. However, this process was shown to be less effective at reducing the free radical burden in UHMWPE compared to post-irradiation melting (Currier et al., 2010).

Despite the low wear rates observed with highly crosslinked UHMWPE, some explant studies have highlighted the mechanical disadvantages of highly crosslinked UHMWPE. While crosslinking may increase the wear resistance of UHMWPE, the negative effects on the mechanical properties have been shown to be a problem with modern components. Bradford et al., (2004) investigated the wear of 21 highly crosslinked and annealed UHMWPE acetabular components explanted from patients. All of these components showed surface cracking, abrasion, pitting or scratches on the articulating surface. Surface damage was visible to the naked eye and damage to all the components was found to be much more severe than that seen from most hip simulators. The surface cracks and other major surface disruptions were attributed to the decreased ductility and fatigue resistance as a result of the extensive crosslinking (Bradford et al., 2004).

Tower et al., (2007) investigated four highly crosslinked Longevity[®] UHMWPE acetabular cups retrieved from two patients. All of these cups showed severe cracking at the rim, and this was seen to be the area of most damage. These two studies are examples of clinically relevant failures of highly crosslinked UHMWPE. It seems any disruption to either the amorphous or crystalline phase in UHMWPE can affect the mechanical behaviour of the material. When compared to virgin materials, studies have found a reduction in the mechanical properties such as ductility, fatigue resistance and crystallinity (Sobieraj and Rimnac, 2009). The overall opinion on highly crosslinked UHMWPE is positive, due to the improvements in wear resistance and the subsequent reduction in incidences of osteolysis. However, the incidence of oxidation as a result of the free radicals generated during gamma irradiation was considered a fundamental problem in UHMWPE that needed addressing.

1.11 Incidence of UHMWPE oxidation

Gamma sterilisation of UHMWPE in air was a commonly used method of sterilisation for early UHMWPE components, but it was found to significantly increase the levels of oxidation of the polymer compared with non-sterilised UHMWPE (Rockwood and Wirth, 2002). Retrieved hip and knee replacements from failed arthroplasties that had undergone gamma in air sterilisation showed a subsurface white band as a result of oxidation; a property not seen in non-sterilised or ethylene oxide-sterilised components. The white band, a concentrated area of oxidation, demonstrated reduced mechanical properties that occurred as a result of oxidation. The UHMWPE within this band was found to have significantly reduced elongation and ultimate tensile strength, leading to an increased brittleness. These properties of oxidised UHMWPE compromise the performance of the polyethylene in a joint and can lead to increased wear (Al-Ma'adeed et al., 2006).

Ethylene oxide is a highly toxic gas that neutralises bacteria, viruses and spores, and had been adopted as a mechanism of sterilisation of prostheses by several companies, including Smith and Nephew, Inc (Kurtz et al., 1999). Ethylene oxide sterilisation was deemed a dangerous method of sterilisation by Charnley due to its residual toxicity; although modern evidence has shown UHMWPE has no binding to the gas therefore toxicity is not an issue. Ethylene oxide gas (EtO) has been found to be an effective method of sterilisation that does not generate free radicals and therefore does not compromise the mechanical properties of the polymer (Costa et al., 1998). One of the few drawbacks of using such a poisonous chemical is the infrastructure required to use the gas in this way.

The ultimate risks of gamma radiation in air were not fully realised until the 1990's, when it was recognised that a common cause of failure of implants was due to the generation of wear particles as a result of oxidative damage to the UHMWPE. This research recognised that gamma sterilisation in the presence of oxygen caused a cascade of chemical reactions involving and culminating in the generation of free radicals. Modern sterilisation techniques involve gamma sterilisation in an inert atmosphere, preventing the diffusion of oxygen during irradiation. In order to maintain an oxygen-free environment, barrier packaging is used, such as a foil and film packaging. The concept is simply to remove oxygen from the packaging using

vacuum packaging, however sometimes an inert gas, such as Argon or Nitrogen can be used in the packaging (Kurtz, 2009c).

While sterilisation in an inert atmosphere was shown to reduce oxidation, the introduction of high levels of gamma irradiation of the polymer as a method to increase crosslinking renewed concerns towards the incidence of oxidation of highly crosslinked UHMWPE. Oxidation of UHMWPE commonly occurs after gamma irradiation (Sutula et al., 1995), leading to a reduction in mechanical strength, reduced ductility, embrittlement and component rim cracking (Kinov et al., 2010). In one study, gamma irradiated UHMWPE bars were found to contain subsurface allyl radicals, and upon exposure to oxygen, a surface layer of peroxy radicals formed. Over 3 years this peroxy radical band increased in size (Alam et al., 2004). The source of oxygen in this mechanism of oxidation was thought to be dissolved oxygen and reactive oxygen species in body fluids around the prosthesis. The synovial fluid of the hip and knee joints contain dissolved oxygen, and patients with osteoarthritis have been shown to have elevated dissolved oxygen levels around the joint, indicating a possible increased incidence of *in vivo* oxidation (Treuhaft and McCarty, 1971, Kurtz, 2009a).

As previously mentioned in section 1.6.2, post irradiation heat treatments were introduced to reduce the free radical burden following high levels of gamma irradiation. Clinical performance has supported the hypothesis that post irradiation treated UHMWPE components have increased oxidative stability, with remelted UHMWPE components showing reduced oxidation compared to annealed components, suggesting the reduction in free radicals was crucial to the reduction in oxidation (Rowell et al., 2010, Atwood et al., 2010).

While the presence of free radicals was found to be vital to oxidation *in vivo*, Oral et al., (2010) demonstrated an alternative method of oxidation occurring in components without the presence of free radicals. There have been several incidences of highly-irradiated and remelted UHMWPE components showing unexplained areas of oxidation and reduced crosslink densities after explantation. These components showed a correlation between time implanted and oxidation, indicating a novel pathway for the generation of free radicals. This hypothesis was based on research by Costa et al., (2001) which demonstrated the diffusion of products from the

surrounding synovial fluid into UHMWPE component of hip replacements (Costa et al., 2001). Organic compounds were extracted from slices of the retrieved UHMWPE component using boiling cyclohexane, and analysed using Fourier transform infra-red spectroscopy (FTIR) and gas chromatography-mass spectrometry. The extracts from UHMWPE showed a similar composition to the synovial fluid from the donor, with compounds such as squalene, cholesterol, esters of cholesterol and fatty acids present. While this study did not look at remelted components, it was noted that increased crosslinking did not affect the diffusion of these apolar compounds.

Oral et al., (2012) developed an *in vitro* model of squalene and cholesterol stearate absorption in highly irradiated (100kGy) remelted UHMWPE, followed by accelerated aging to determine if lipid absorption could affect oxidation in UHMWPE (Oral et al., 2012). These authors showed a significant increase in the oxidation index of UHMWPE exposed to squalene for 14 days compared to the non-lipid exposed control. The depth of oxidation increased over time. Cholesterol stearate-doping caused no measurable oxidation. It was hypothesised that squalene initiates oxidation by reacting with oxygen and generating lipid peroxy radicals which attack polyethylene chains. It was also proposed that the initial reaction with oxygen is dependent on reactive oxygen species present in the synovial fluid, therefore the reactivity of the lipid may affect the rate of oxidation. This method of oxidation is independent of free radicals, indicating a change in the understanding of UHMWPE oxidation *in vivo*.

While remelted UHMWPE relies on the high temperatures to quench the free radicals generated during gamma irradiation, this new method of oxidation provides a mechanism that could occur independent of irradiation generated radicals. This oxidation mechanism is a hypothesis that has not been shown to occur *in vivo*. However it is clear that oxidation can occur *in vivo* independent of the presence of free radicals prior to implantation, and is therefore immune to the post-irradiation heat treatments currently employed. This has therefore strengthened the appeal of introducing an antioxidant compound into UHMWPE which will be present throughout the life of the material and active *in vivo*. This subsequently led to the introduction of vitamin E as the first antioxidant compound incorporated into clinically available UHMWPE for use in joint replacements.

1.12 Vitamin E

With concerns regarding the mechanical properties of UHMWPE after annealing or melting, there has been increased research into compounds that reduce the free radical burden of the polymer whilst protecting the favourable mechanical properties of UHMWPE. The appeal was to be able to reduce *in vivo* oxidation, while not reducing the fatigue resistance or fracture resistance properties that make UHMWPE an excellent bearing material (Gomez-Barrena et al., 2008). Vitamin E was considered an ideal antioxidant for use in this way, and in 2007, highly crosslinked vitamin E enhanced UHMWPE for use in total hip replacements became clinically available.

In 1936, Evans et al., (1936) isolated an ‘alcohol resembling alpha tocopherol’ from the unsaponifiable constituent of wheat germ oil (Emerson et al., 1936). The same compound was also isolated from cotton seed oil. This was the first description of α -tocopherol (Drummond and Hoover, 1937).

The chemical formula of α -tocopherol is $C_{29}H_{50}O_2$ and the structure is shown in Figure 1.11. It is described as 5,7,8-trimethyltolcol and is a lipophilic compound, therefore providing good interactions with polyethylene (Oral et al., 2004). The chroman head serves as a reducing agent, donating a hydrogen atom to the oxidising agent and therefore stopping any further reactions with that radical. When the chroman head of α -tocopherol donates a hydrogen atom it becomes a tocopheryl free radical with the ability to combine with another free radical. This means one α -tocopherol molecule can remove two free radicals. The long carbon-rich phytyl tail is what makes the molecule lipophilic, enabling it to interact with membranes, which is an area where vitamin E is biologically crucial.

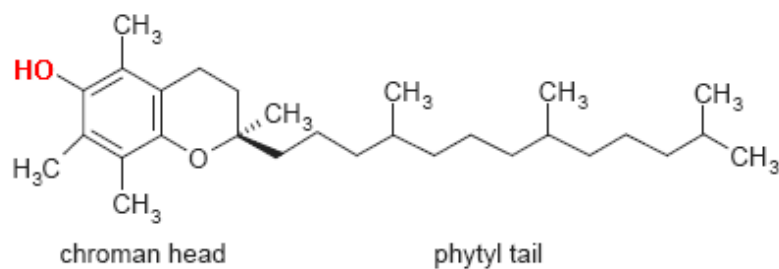


Figure 1.11 - Chemical structure of α -tocopherol, showing the chroman head and phytyl tail. It is the OH group (red) that donates the hydrogen atom in order to receive the radical species from a free radical.

Schneider (2005) described an antioxidant reaction as ‘the interception of the auto-oxidation radical chain process’, and α -tocopherol (referred to as vitamin E from this point) does this by reacting with fatty acid peroxy radicals, therefore preventing lipid peroxidation (Schneider, 2005). Lipid peroxidation is the gradual oxidative degradation of the lipids, and in cells this leads to damage of the cytoplasmic membrane, eventually leading to necrosis. Vitamin E is considered to be a lipid antioxidant, scavenging free radical intermediates generated throughout the peroxidation of unsaturated fatty acids (Diplock, 1983). Vitamin E is positioned in the membrane, perpendicular to the plane of the bilayer with the hydroxyl group pointing to the lipid-water interface (Quinn, 2004). This is the basis of the antioxidant properties of α -tocopherol in cells, although α -tocopherol is also recognised as an anti-inflammatory molecule, broadening its range of medical applications to treat conditions where inflammation is important (Reiter et al., 2007).

The importance of vitamin E in animals can be demonstrated in vitamin E-deficient experimental animals. Muscular dystrophy and encephalomalacia (softening of the brain tissue due to inflammation and or hemorrhage) were observed in vitamin E deficient chickens (Shih et al., 1977), and the importance of vitamin E in maintaining the redox state of sulphur-containing amino acids has been demonstrated. In vitamin E deficient rats, neuromuscular lesions developed, as well as normocytic anaemia and skin ulcers (Machlin et al., 1977).

Deficiency of vitamin E is extremely rare in humans with the only known cases being due to fat malabsorption conditions. Where vitamin E deficiency does occur in

humans, spinocerebellar lesions develop in addition to other disfunctions (Schneider, 2005). This deficiency can be seen in patients with autosomal neurodegenerative disease; ataxia with isolated vitamin E deficiency (AVED). This is the inability to incorporate vitamin E into very low density lipoproteins (VLDL) in the liver, an important step in the metabolism of vitamin E.

Two studies by Hill et al., (2001; 2003) revealed the synergy of vitamin E with vitamin C and selenium. In animal models, a vitamin E and C deficient diet resulted in paralysis of all the limbs and difficulty breathing, culminating in mortality in 8 of the 21 guinea pigs just 9 days after starting the diet. In a separate study investigating a vitamin E and selenium deficiency, myopathy occurred and 7 of the 13 mice were euthanised after 30-35 days. This fatal myopathy was associated with lipid peroxidation in the affected muscle, a condition where absence of the antioxidant properties of vitamin E is apparent (Hill et al., 2001, Hill et al., 2003).

In addition to the antioxidant properties of vitamin E, it has also been found to inhibit protein kinase C in smooth muscle cells. This inhibition is thought to be indirect, as vitamin E was seen to activate protein phosphatase type 2A *in vitro*, which could lead to the dephosphorylation and deactivation of protein kinase C (Ricciarelli et al., 1998). This is thought to be an important part of the anti-inflammatory properties of vitamin E.

Due to its anti-inflammatory properties, vitamin E has also been strongly linked as a protective compound against atherosclerosis. Atherosclerosis is a vascular disease characterised by the thickening of the artery wall due to the build-up of fatty residues. An important stage in early atherosclerosis is the deposition of oxidised low-density lipoprotein (LDL) in the arterial wall (Schneider, 2005). Specific receptors on macrophages recognise the LDL and phagocytose the mass, leading to lipid-filled foam cells and fatty streaks on the artery wall.

Vitamin E acts in many ways to protect against the initiation of atherosclerosis. Firstly, vitamin E significantly reduces the monocyte-endothelial cell adhesion that is normally important in atherogenesis. This is achieved through the downregulation of the adhesion molecule ICAM-1. Vitamin E also reduces platelet adhesion and accumulation, an important step in the initiation of atherosclerosis (Osterud and Bjorklid, 2003). Vitamin E has also been found to inhibit uptake of oxidised LDL by

monocyte-derived macrophages (Ricciarelli et al., 2000). The scavenger receptor CD36 is found on smooth muscle cells and is important in uptake of oxidised LDL. Vitamin E applied to smooth muscle cells results in the downregulation of CD36 mRNA, and therefore reduced expression. These examples indicate the multiple effects that vitamin E has on one disease.

The range of applications of vitamin E is vast. From causing a significant reduction in interleukin-1 β expression and therefore blocking joint inflammation and destruction seen in rheumatoid arthritis, to inhibiting interleukin-4 gene expression and therefore reducing the levels of a cytokine crucial to atopic diseases (De Bandt et al., 2002, Li-Weber et al., 2002). The use of vitamin E has also been implicated in the treatment of some forms of cancer. Multiple studies have highlighted the possible protective effect of vitamin E combined with selenium against radiogenic and chemical transformation of cells, therefore possibly resulting in cancer-protection of the tissue (Borek et al., 1986, Noaman et al., 2002). Cells pre-treated with vitamin E and selenium showed increased levels of glutathione and reduced transformation. The increased levels of glutathione (a natural antioxidant) indicate an alternative antioxidant is present, therefore allowing for the levels of glutathione to increase as it is not used in the reaction. However, a study on the effect of these compounds on prostate cancer showed no reduction in the incidence of prostate cancer, putting doubt on the possible application of vitamin E in this way (Hatfield and Gladyshev, 2009).

Research has also shown the anti-inflammatory properties of vitamin E, both *in vivo* and *in vitro*. In some studies the antioxidant properties have been found to be related to the anti-inflammatory actions. In a study by Devaraj et al., (1996), it was shown that the supplementation of monocytes relevant to atherosclerosis with vitamin E resulted in a reduction in lipid peroxidation, and a reduction in the release of reactive oxygen species and IL-1 β . This was once again related to the inhibition of protein kinase C, but the action was recognised as anti-inflammatory nonetheless. The anti-inflammatory properties of vitamin E have also been implicated in the prevention of cardiovascular disease through the inhibition of oxidation of low-density lipoproteins (Devaraj et al., 1996, Reiter et al., 2007).

Nonetheless, what is clear is the crucial role that vitamin E plays in the human body, from the cellular level right through to the function and protection of organs and organisms. It is the antioxidant and free radical scavenging properties of vitamin E, in addition to its biocompatibility, that brought about the use of vitamin E enhanced UHMWPE in an attempt to incorporate a highly crosslinked polymer with an antioxidant compound to confer oxidative stability to the material.

1.13 Doping of UHMWPE with Vitamin E

In order to generate a material where the presence of vitamin E can protect against oxidation, vitamin E must be evenly distributed throughout the polymer. There are two ways of preparing vitamin E enhanced UHMWPE; diffusion and blending (Figure 1.12). Diffusion involves submerging the manufactured component in a vitamin E solution and allowing vitamin E to diffuse into the polymer. The benefit of using vitamin E diffusion is that vitamin E is not present during the irradiation and crosslinking stage to interfere with free radicals during crosslinking; therefore the beneficial effects of crosslinking are not affected (Oral et al., 2007).

The alternative method for doping of UHMWPE with vitamin E is blending. This involves mixing the UHMWPE resin powder with vitamin E powder prior to irradiation and machining into the components (Oral et al., 2005). This method showed reduced oxidation of the polymer *in vitro* compared with conventional gamma-sterilised UHMWPE, however it was shown that 0.1wt% and 0.3wt% blended vitamin E reduced the crosslink density by 17% and 47% respectively. This supports the hypothesis put forward by Oral et al., (2005) that vitamin E blending before irradiation reduced the primary free-radicals available for crosslinking, and therefore effectively reduced the crosslinking of UHMWPE, leading to reduced wear resistance compared to diffused vitamin E in highly crosslinked UHMWPE (Oral et al., 2005).

Clinically, vitamin E enhanced UHMWPE is available in both blended and diffused materials. The clinical materials Vivacit-E[®] (Zimmer, Warsaw, Indiana, USA) and eCiMa[™] (Corin, Gloucestershire, UK) are both vitamin E blended highly crosslinked UHMWPE, while the E1[®] (Biomet, Warsaw, Indiana, USA) bearing materials is a

vitamin E diffused highly crosslinked UHMWPE. One of the disadvantages of diffused vitamin E is the difficulty in accurately controlling the even distribution of the vitamin E solution through the polymer. Vitamin E distribution is very well distributed in blended vitamin E UHMWPE due to the ability to thoroughly mix the polymer and vitamin E powder prior to consolidation.

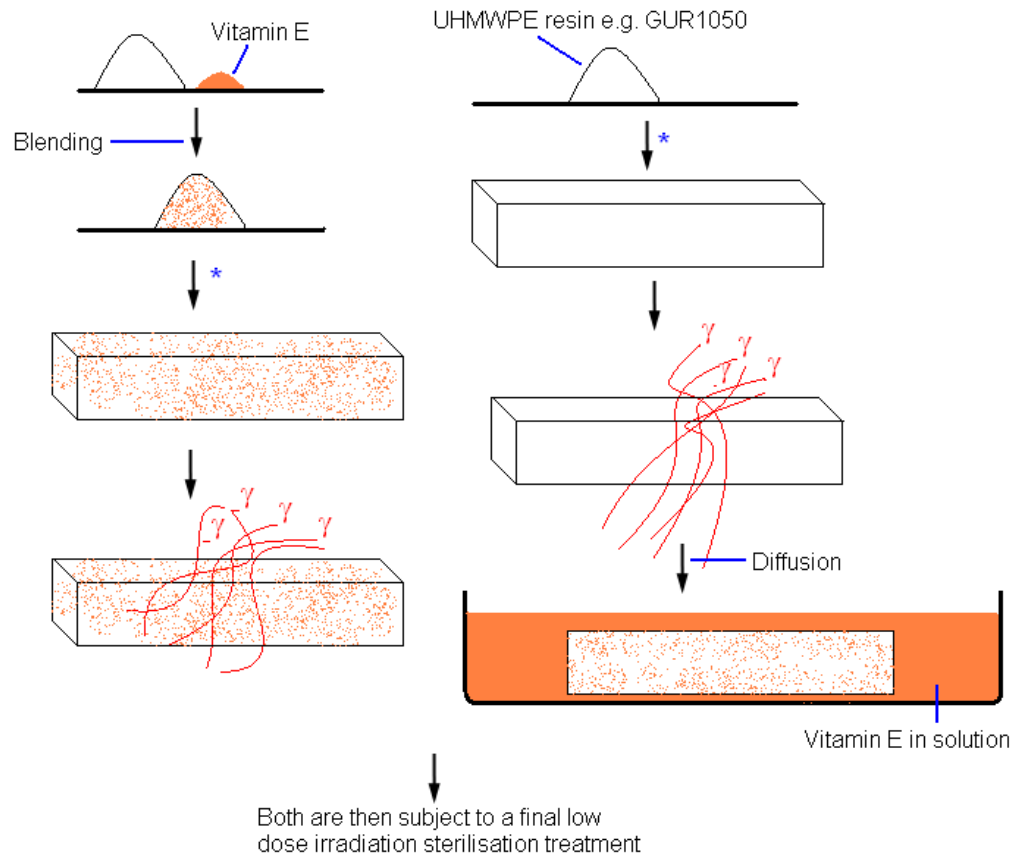


Figure 1.12 - Schematic showing the different methods of vitamin E doping of UHMWPE. The left side shows the blending method, where the vitamin E is added to the UHMWPE before the material is manufactured (*) – compression moulded or ram extrusion moulded), followed by crosslinking by high dose gamma irradiation. The right hand side shows the diffusion method, where the crosslinked material is then soaked in vitamin E solution for 2 hours at 120°C.

1.14 Wear and Oxidative Stability of Vitamin E enhanced UHMWPE

Several studies have been performed to compare the wear of virgin-UHMWPE (non-doped) and vitamin E enhanced UHMWPE. Wannomae et al., (2010) compared the wear rate of vitamin E enhanced UHMWPE and virgin UHMWPE. The doped polymer was a compression moulded GUR1050 puck (Ticona), vacuum packed and electron beam irradiated to 100kGy. It was then vitamin E doped by diffusion by immersing in α -tocopherol solution for 7 hours at 120°C to a 1.1% wt vitamin E content. The vitamin E enhanced pucks were then vacuum packaged and gamma sterilised (25-40 kGy). The negative control pucks were compression moulded GUR1050 (Ticona) pucks gamma sterilised at 25-40kGy.

Wear was generated on a multidirectional pin-on-plate rig with 100% (v/v) bovine serum as a lubricant. The wear test ran for 2 million cycles and the wear rates were calculated every 0.5 million cycles through gravimetric analysis. Vitamin E enhanced GUR1050 UHMWPE showed a significantly reduced wear rate compared to virgin GUR1050 UHMWPE. Some samples were also age accelerated to investigate the potential antioxidant protection vitamin E might offer. Accelerated aging was carried out at 1 atm of air at 80°C for 5 weeks (oven-aged). This treatment generated increased wear rates for oven-aged virgin UHMWPE compared to non oven-aged. Vitamin E enhanced UHMWPE that was oven-aged showed a significantly reduced wear rate compared to oven-aged virgin UHMWPE, once again indicating that vitamin E doping conferred wear resistance (Wannomae et al., 2010).

The methods used by Wannomae et al., (2010) did have limitations. The study compared a highly crosslinked (100 kGy electron beam irradiation) vitamin E enhanced UHMWPE material against a virgin UHMWPE material. With the presence of two variables between the materials (crosslinking, vitamin E enhancement), it is impossible to draw conclusions about the cause of the reduction in wear. Previous studies have shown the introduction of high levels of crosslinking to UHMWPE significantly reduce the wear rate (Galvin et al., 2006), therefore it more likely the 100 kGy irradiation dose was the factor which led to the reduction in wear for the vitamin E enhanced highly crosslinked UHMWPE.

In a separate study, Teramura et al., (2008) used 0.3% wt and 3.0% wt vitamin E enhanced UHMWPE knee components to determine the delamination and wear resistance of vitamin E. The vitamin E enhanced components were made from UHMWPE GUR1050 blended with α -tocopherol where the powder was then direct compression moulded at 220°C. The test components were not sterilised and the experiments were conducted in air using a knee joint simulator. The particles were isolated from the bovine calf serum lubricant at 0.5 million cycle intervals up to 5 million cycles and the wear volume was calculated using gravimetric wear. The wear particles were isolated by sequential filtration using cyclopore filters and imaged by scanning electron microscopy of the filters. The authors showed a reduced wear volume for vitamin E enhanced UHMWPE compared to virgin UHMWPE, with a significant difference after 5 million cycles of knee simulation (Figure 1.13). In addition to a reduced wear volume, the wear debris from the vitamin E enhanced components exhibited a 5% reduction in submicron sized particles compared to virgin UHMWPE, although this difference was not statistically significant (Teramura et al., 2008). It was important to note that the study by Teramura et al., (2008) used a vitamin E concentration higher than used clinically in the EU and USA. This should be addressed in future research by in addition to using higher doses of vitamin E, clinically relevant vitamin E enhanced UHMWPE (0.1% w/w) should also be included in the study in order to generate data that is clinically relevant to all parts of the world.

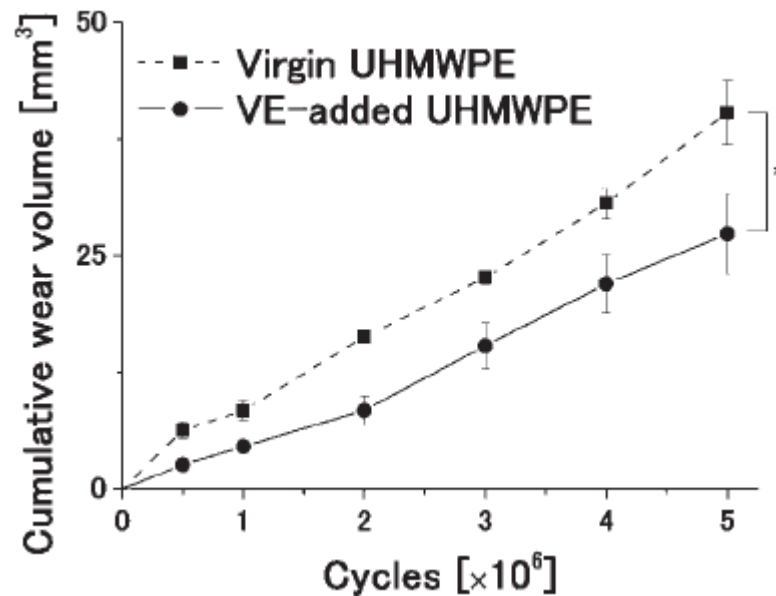


Figure 1.13 - The cumulative wear volume for virgin and vitamin E enhanced UHMWPE tibial components (n=3) in knee simulator testing. After 5 million cycles there is a significant difference in cumulative wear volume compared to virgin UHMWPE (Teramura et al., 2008).

A study by Oral et al., (2006) investigated the effect of vitamin E doping on the wear rate of UHMWPE. The non-vitamin E enhanced components were made from isostatically moulded GUR1050 (Ticona), packaged in argon gas and gamma sterilised (dose not outlined). The vitamin E enhanced components were also isostatically moulded GUR1050 components, annealed, packaged under argon gas and gamma irradiated at 85kGy to generate a highly crosslinked polymer. The components were then doped with vitamin E by immersion at 120°C (duration not outlined). The components were then packaged under argon and sterilised (dose not outlined). Using a hip simulator, the authors investigated how vitamin E affected the adhesive and third-body wear of UHMWPE. The average wear rate of conventional UHMWPE was 9.54 ± 0.73 mg/million cycles, and the vitamin E enhanced UHMWPE had an average wear rate of 0.78 ± 0.28 mg/million cycles. With the addition of third body bone cement particles, the 28mm diameter virgin UHMWPE component yielded a wear rate of 20.55 ± 0.50 mg/million cycles, while the 28mm diameter vitamin E enhanced, irradiated UHMWPE component gave a wear rate of 5.76 ± 0.82 mg/million cycles. With the addition of third body wear particles vitamin

E gave a 72% reduction in the wear rate compared to the virgin material (Oral et al., 2006). These results are comparable to data generated for the wear rate of gamma irradiated and melted UHMWPE (Muratoglu et al., 2001, Oral et al., 2006). However, the advantage of vitamin E doping is that the melting stage can be omitted from the manufacture process, therefore preserving the mechanical properties of the polymer. Once again however, this study compared a highly crosslinked vitamin E enhanced UHMWPE component to a virgin UHMWPE material.

A separate study showed a wear rate of highly crosslinked vitamin E enhanced UHMWPE to be comparable to that of a highly crosslinked remelted UHMWPE component, indicating the presence of vitamin E to highly crosslinked UHMWPE had no negative effect on the wear of the component. The aforementioned study also demonstrated reduced oxidation in vitamin E enhanced highly crosslinked UHMWPE compared to the non-vitamin E highly crosslinked UHMWPE following five weeks of accelerated aging (Oral et al., 2004). While the study showed the potential for vitamin E to protect against oxidation following irradiation, a separate study also showed that vitamin E in UHMWPE had the potential to protect against the alternative mechanism of oxidation mentioned previously, lipid initiated oxidation.

Oral et al., (2012) showed vitamin E doping (blended) at a minimum dose of 0.3% (wt) protected against squalene initiated oxidation *in vitro*. However, the clinical antioxidant concentration of 0.1% (wt) vitamin E did not protect against squalene initiated oxidation. The study hypothesised that due to the irradiation following vitamin E doping, the antioxidant activity of vitamin E was adversely affected, as a result of the free radicals generated in the presence of vitamin E (Oral et al., 2012). While the higher dose of 0.3% (wt) may seem an attractive alternative to protect against this form of oxidation, it has been shown that higher doses of vitamin E (blended) adversely affect the crosslinking efficiency of UHMWPE. This therefore shows the importance of developing an optimised antioxidant UHMWPE, whereby the oxidative stability and crosslinking level of UHMWPE are at the optimum level for longevity and performance.

1.15 Biological Response to Vitamin E Enhanced UHMWPE

Vitamin E is considered to be a biocompatible compound, and is required by animals as part of a healthy diet and for the normal function of cells. The recommended daily intake of vitamin E is 15 mg and this is commonly taken orally (Institute of Medicine, 2000). Naturally, vitamin E can be found in foods such as whole grains, leafy green vegetables and vegetable oils (Sheppard et al., 1993).

The biocompatibility of vitamin E in the synovial joint of the knee and hip has been demonstrated by vitamin E injections in animal models, where no inflammation or sterile puss was observed. These experiments showed that even the high doses of 10mg of vitamin E injected into a joint had no adverse effects. This may indicate that vitamin E levels released *in vivo* from total hip replacement components would not cause pathology or a toxicological response.

In order to investigate the cellular response to vitamin E, Tipper et al., (2011) incubated peripheral blood mononuclear cells and U937 human histiocytes with vitamin E at a seeding density of 1×10^4 cells per well. An ATP-Lite assay was used to determine the cell viability after 24 hrs in an atmosphere of 5% (v/v) CO₂ in air (Figure 1.14). The authors determined that vitamin E was well tolerated by cells, only significantly affecting cell viability of U397 cells at 4mM concentration or greater, and peripheral blood mononuclear cells at 3mM (Tipper et al., 2011). This demonstrated the very low toxicity of vitamin E to human cells, as high concentrations were required to induce a reduction in cell viability.

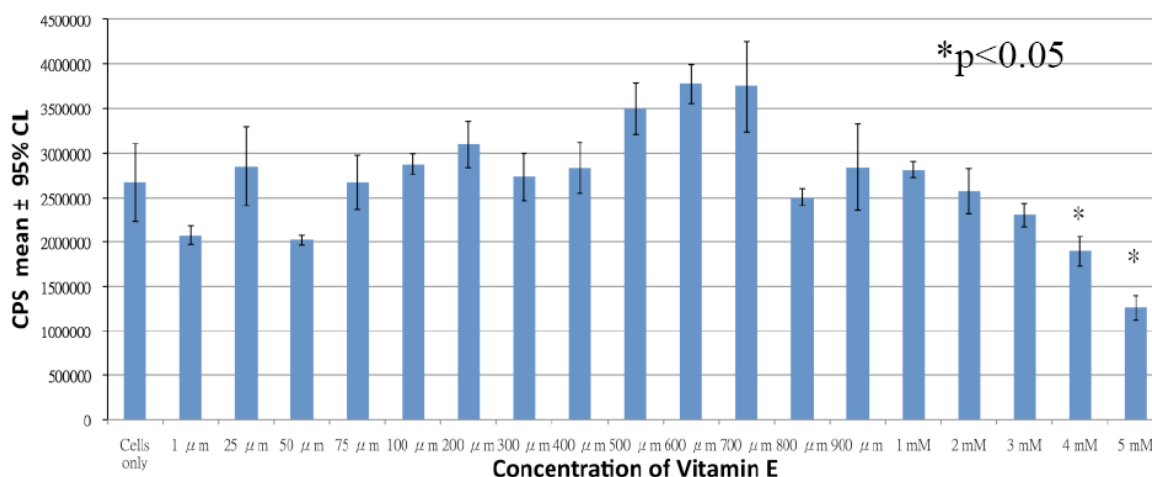


Figure 1.14 - Showing the cell viability of U937 human histiocytes incubated with different concentrations of vitamin E. Significant loss in cell viability is shown by asterisk (Tipper et al., 2011). Compared to cells only, there is no significant effect on cell viability with the addition of vitamin E up to a concentration of 3mM. At concentrations greater than 4mM cell viability is significantly affected.

In addition to understanding the biological response to vitamin E, it is important to understand the biological response to UHMWPE; the material that the antioxidant compound is being added to. One aspect of the biological response to UHMWPE to consider is the biological response to wear particles generated from the polymer. The biological response to UHMWPE wear debris was previously described in section 1.9, and the importance of wear debris in stimulating osteolysis around UHMWPE-containing implants has been detailed. While UHMWPE is a bioinert material; the particles generated during wear are able to stimulate the activation of macrophages which then leads to an innate immune response. Previous studies have shown that the particle size, morphology and volume dose are crucial to the severity of the osteolytic response to the wear particles, with the critical particle size range for macrophage activation found to be 0.1 μm - 1.0 μm at a ratio of 100 μm³ of wear debris per cell (Green et al., 1998, Ingham and Fisher, 2000). The volume of particles generated within this critical size range has been shown to dictate the strength of the immune response; therefore the overall wear particle volume does not necessarily command the immune response. The morphology of particles has also been shown to affect the critical size range for biologically active particles, with

rounder, more even particles possessing a slightly higher critical size range for macrophage stimulation (Green et al., 1998).

In terms of the overall biological response to virgin UHMWPE particles, this has been demonstrated in several cell types, including primary human macrophages, U937 histiocytic cell line, fibroblasts, chondrocytes and synoviocytes; with an increase in osteolytic cytokine release and inflammatory cell mediators the most common response to particle stimulation (Park et al., 2013, Bladen et al., 2013a). However, the biological response to different types of UHMWPE is also an important area of research, especially with the introduction of novel UHMWPE materials clinically, such as vitamin E enhanced highly crosslinked UHMWPEs.

A study by Teramura et al., (2009) investigated the biological response to vitamin E enhanced UHMWPE particles (non crosslinked) in comparison to the biological response to virgin UHMWPE particles. Particles generated by a pin-on-plate wear simulator were cultured with human peripheral blood mononuclear cells (PBMNCs) at a particle volume of $100 \mu\text{m}^3$ using the agarose technique, whereby particles and cells are suspended in contact in agarose. Vitamin E enhanced UHMWPE at 3% (w/w) and 0.3% (w/w) was compared to virgin UHMWPE in terms of the cell viability of cells and the cytokine release. While neither UHMWPE treatment had a significant effect on the cell viability of PBMNCs, virgin UHMWPE wear particles stimulated a significantly higher level of TNF- α release from mononuclear cells compared with vitamin E enhanced UHMWPE, which gave a TNF- α release comparable to the cell only negative control. This trend was also seen for the release of other cytokines important to osteolysis, such as IL-1 β , IL-6 and IL-8 (Teramura et al., 2009). This indicated that vitamin E had a significant anti-inflammatory effect and significantly reduced the levels of osteolytic cytokines released from monocyte cells in response to wear particles. However, the clinical relevance of this study to the EU and USA is questionable, due to the higher dose of vitamin E enhancement used (0.3-3% wt) compared to the clinically relevant dose used in vitamin E enhanced highly crosslinked UHMWPE in the EU and USA (0.1% wt).

A separate study by Bladen et al., (2013) investigated the osteolytic cytokine response of PBMNCs to vitamin E enhanced (0.1% wt) UHMWPE wear debris at a dose of $100 \mu\text{m}^3$ per cell. The authors observed a significant reduction in the TNF- α

release from PBMNCs incubated with vitamin E enhanced UHMWPE compared to virgin UHMWPE (Bladen et al., 2013a). There were no significant differences in the wear and wear particle size distributions of these materials, therefore the results indicated the presence of vitamin E in UHMWPE wear particles exerted an anti-inflammatory effect on the cells. Despite the promising results in the two studies mentioned, the vitamin E enhanced UHMWPE materials used in the studies were non-crosslinked. The non-crosslinked material is not a clinically relevant antioxidant material, with the clinically available vitamin E enhanced UHMWPE material being treated with high levels of crosslinking. In addition, there is some debate as to the ability of vitamin E to leach from non-crosslinked and crosslinked UHMWPE, therefore potentially affecting the availability of vitamin E to cells.

A separate study by Wolf et al., (2007) investigated the biocompatibility of vitamin E enhanced UHMWPE in terms of its cytotoxicity to mouse L929 fibroblasts and HF-SAR (human skin fibroblasts) compared to virgin UHMWPE. When culturing these cell types on surfaces composed of either the virgin or vitamin E enhanced UHMWPE, the authors observed no difference in cell proliferation rates. In addition, there was no difference in mitochondrial activity between cells grown on either material, with results comparable to cells cultured on the polystyrene negative control (Wolf et al., 2007). This study showed that both these UHMWPE materials had no adverse effect on cell proliferation, however, crucially there was no positive control included in the study, the inclusion of which would have added confidence to the conclusion that both these UHMWPE had no significant effect on cell proliferation.

Animal studies have been performed to investigate the bone remodelling response to UHMWPE particles. An animal study performed by Bichara et al., (2013) used UHMWPE particles implanted under the skin of the calvarium of mice. Comparing a vitamin E enhanced highly crosslinked UHMWPE to virgin UHMWPE particles, the vitamin E enhanced highly crosslinked UHMWPE particles showed a significant reduction in osteolysis compared to virgin UHMWPE particles (Bichara et al., 2013). While this indicated vitamin E could offer some protection against osteolysis, the material tested was a post-irradiation vitamin E *diffused* material; therefore the vitamin E may be more readily available than the vitamin E blended materials such as Vivacit-E® and ECiMa™, which are irradiated after addition of vitamin E.

Despite the excellent biocompatibility demonstrated for vitamin E, along with the anti-inflammatory properties which have been indicated to be beneficial to reducing osteolysis *in vivo*, one study has demonstrated the ability for vitamin E to have a negative effect on bone mass. The study by Fujita et al (2012) compared the bone mass of healthy mice to mice deficient in alpha-tocopherol transfer protein; a key protein for the transfer of alpha tocopherol (a form of vitamin E) from the liver to lipoprotein. While alpha-tocopherol deficient mice displayed negative effects such as infertility and ataxia due to the reduced levels of serum alpha-tocopherol, they showed an increased bone mass due to lower bone resorption compared to the healthy mice. Bone formation was not affected by the vitamin E deficiency, and the authors concluded that alpha-tocopherol increased bone resorption by stimulating the fusion of osteoclasts (Fujita et al., 2012). This study presented a contrasting conclusion to the studies mentioned previously in terms of the potential role of vitamin E in osteolysis. However, the study by Fujita et al., used a mouse model, and while this can be a reliable model, further work is needed to investigate the effect of vitamin E on human bone mass. In addition, the doses of vitamin E used in the previous study seemed very high for the size of the animal, and the equivalent doses of vitamin E would not be expected to elute from a vitamin E enhanced UHMWPE component.

While vitamin E enhanced highly crosslinked UHMWPEs have been shown to have many positive attributes, such as its oxidative resistance and potential anti-osteolytic properties, alternative antioxidants for use in UHMWPE are being investigated, with the aim to find a more suitable antioxidant to further improve this ever evolving bearing material.

1.16 Alternative Antioxidants for use in UHMWPE

Despite the well documented mechanical and chemical benefits of enhancing UHMWPE with vitamin E, there are certain drawbacks associated with both methods of vitamin E doping. While the negative impact of pre-irradiation blending has been mentioned in terms of the reduction in crosslinking efficiency caused by vitamin E, there are also disadvantages of post-irradiation diffusion, for example the time consuming nature of the process and the lack of accuracy in creating a homogenous

distribution of vitamin E throughout the polymer. Also, the aesthetics of the yellow-brown material could be considered a negative attribute to a manufacturer as patient research and choice of replacement increases. Research into alternative antioxidants to vitamin E is continuing in order to improve the antioxidant properties of the stabilised polymer.

Hindered amine light stabilisers have been proposed as an alternative free radical scavenger for use in UHMWPE in joint replacements. Chimassorb[®] 994 is a hindered amine light stabiliser that has been FDA approved for use (0.3 wt%) in polyethylene that is intended to come in contact with food, so this type of compound is currently being used as a biomaterial stabiliser. The mechanism of free radical scavenging believed to occur with Chimassorb[®] involves the conversion of an amine group to a nitroxide group. One hypothesis is that the formed nitroxide can react with an alkyl radical, forming an aminoether, and the formed aminoether can react with a peroxy radical once again forming an aminoether capable of reacting again. This and other mechanisms for scavenging by hindered amine light stabiliser therefore propose that the nitroxide molecule is not consumed, but recycled to continue its scavenging (Figure 1.15); (Yub and Denisov, 1974).

Gijsman et al., (2010) investigated the mechanical and oxidative effects of UHMWPE enhanced with three different hindered amine light stabilisers, in addition to a vitamin E enhanced UHMWPE. Although vitamin E enhanced UHMWPE was superior in terms of mechanical strength and protection against oxidation, the hindered amine light stabilisers were shown to protect against oxidation, and therefore warrant further research into these compounds (Gijsman et al., 2010).

Lanthanides are found in the table of elements from atomic number 57 to 71, and some of these elements have been investigated as possible antioxidant compounds for the protection of UHMWPE *in vivo*. Europium (III) stearate was used in a study by Laurent et al., (2010), and was blended with GUR1050 UHMWPE powder. The powder was then compression moulded and gamma irradiated at 3.5kGy. The lanthanide-doped UHMWPE and the non-doped UHMWPE were subjected to accelerated aging and the oxidation index was compared. The addition of europium (III) stearate reduced the oxidation index, demonstrating the oxidation resistance invoked by the addition of this chemical. Also, the two doses of lanthanide used

(750ppm and 7500ppm) showed little difference in protection, an observation which the authors implied indicated the presence of a renewable antioxidant (Laurent et al., 2010). In addition to antioxidant properties, europium (III) stearate has well documented anti-inflammatory properties in combination with a low cytotoxicity. These results show the potential for another antioxidant in UHMWPE although comparison studies with vitamin E are required to evaluate the effectiveness of lanthanides in the current landscape of hip arthroplasty biomaterials (Laurent et al., 2010).

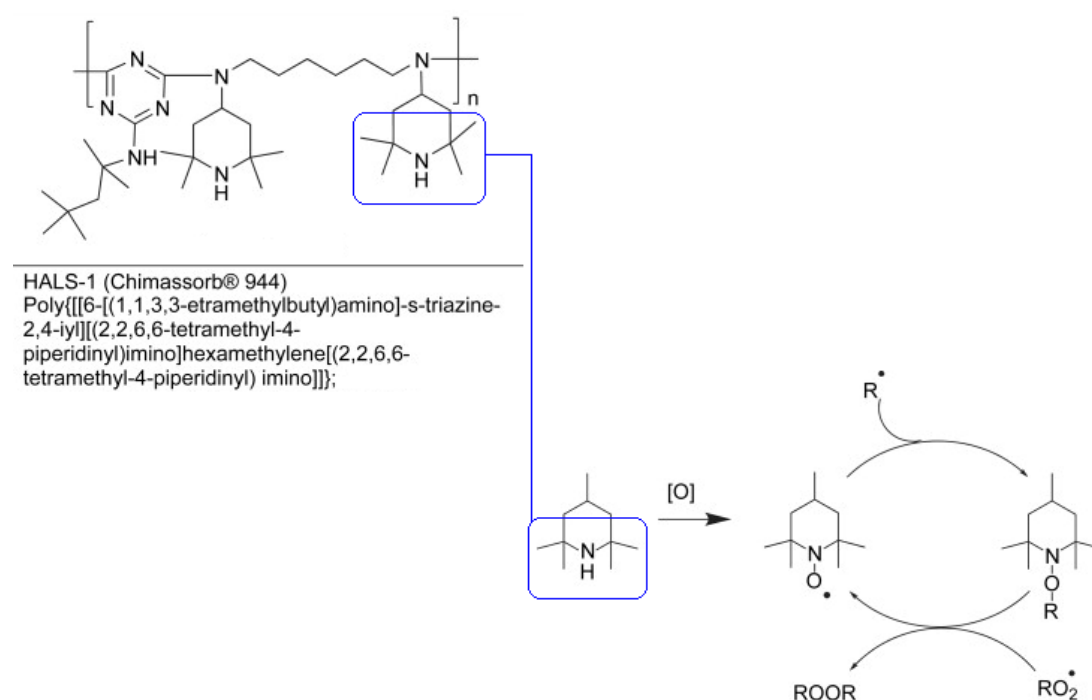


Figure 1.15 - The structure of Chimassorb® 994, and the proposed mechanism of free radical scavenging. This shows the way the nitroxide is recycled while consuming two radical groups. The $R\cdot$ group represents the radical species with an unpaired electron (Gijsman et al., 2010).

The naturally occurring polyphenols gallic acid (GA) and dodecyl gallate (DG) have also been investigated as potential antioxidants for their use in UHMWPE. A previous study investigating the oxidative stability of these novel antioxidant UHMWPE incorporated both GA and DG into UHMWPE at a range of doses (0.5%-1.0%wt) and irradiation doses (50kGy, 100kGy, 150kGy). The GA and DG

enhanced UHMWPEs showed comparable oxidative stability to vitamin E enhanced UHMWPE following accelerated aging. However, while the presence of vitamin E was shown to hinder crosslinking following irradiation, the polyphenol compounds had no negative effect on crosslinking. It was believed this preservation of crosslinking was due to the increased stability in GA and DG compared to alpha tocopherol following gamma irradiation. Also, it was understood that the ability of alpha tocopherol to become a tocopheryl radical contributed to the reduction in crosslink density of the polymer following irradiation, compared to the polyphenol enhanced materials. The findings of the previous study suggests polyphenols could increase the efficiency of crosslinking of UHMWPE while still maintaining the oxidative stability found with vitamin E enhanced UHMWPE. Research into new and improved antioxidant compounds has continued, with the aim to develop an oxidative resistant, wear resistant UHMWPE. Following the introduction of vitamin E enhanced highly crosslinked UHMWPE; the first alternative antioxidant UHMWPE for use clinically was developed, incorporating a hindered phenol antioxidant into UHMWPE for use in the knee.

1.17 Hindered Phenols

Hindered phenols are phenolic stabilisers, and are recognised as effective antioxidant compounds. They have the ability to block chain reactions of free radicals due to their ability to donate hydrogen atoms. In addition, due to the ability of their electrons to be in several places they can produce several mesomeric forms and therefore remain stable (Figure 1.16).

The phenol group is the crucial part of the molecule, as highlighted in Figure 1.16. Pentaerythritol Tetrakis (3-)3,5-di-tert-butyl-4-hydroxyphenyl) propionate) (referred to as hindered phenol antioxidant; HPAO) is an example of a hindered phenol compound being used in UHMWPE for total joint replacement components, with the chemical structure of HPAO shown in Figure 1.17. There are four phenol groups on each molecule of HPAO, indicating the antioxidant potential of the chemical. This hindered phenol compound has recently been incorporated into the first non-vitamin E antioxidant UHMWPE material; AOXTM (Green et al., 2013).

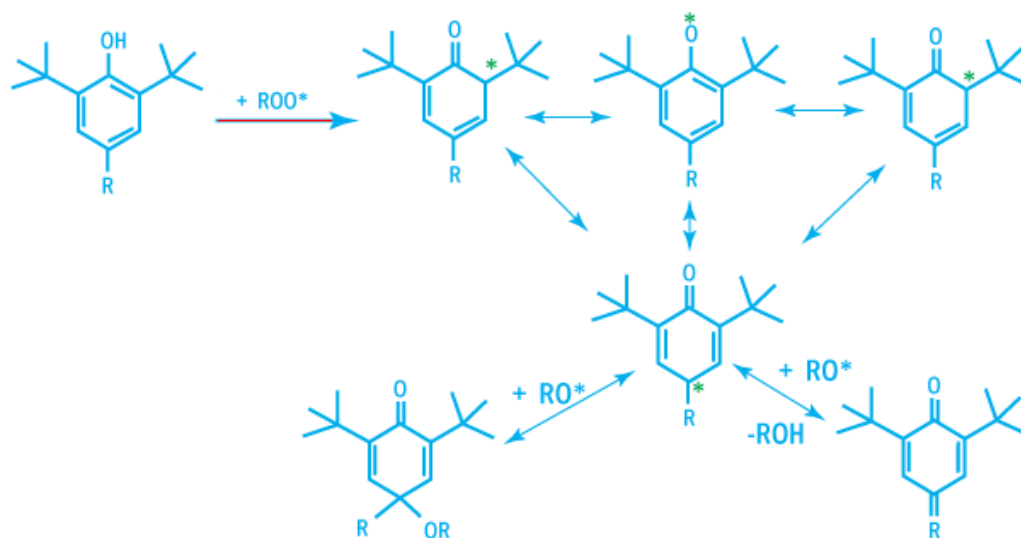


Figure 1.16 - A phenol molecule reacting with a free radical and example of the reactions that take place. The diagram on the right hand side of the red-highlighted arrow shows the different positions the radical species can reside.

<http://www.specialchem4adhesives.com/tc/antioxidants/index.aspx?id=hinderedphenols>

Some hindered phenol compounds have been used in orthopaedic implant devices for decades (Wroblewski et al., 2005). Studies have recently been conducted on the mechanical properties of hindered phenol doped UHMWPE. Narayan et al., (2010) investigated UHMWPE doped with three different hindered phenols; Pentaerythritol Tetrakis (HPAO; Figure 1.17), Octadecyl-3,5-di-tert-butyl-4-hydroxycinnamate (HPAO2) and Isooctyl-3,5-di-tert-butyl-4-hydroxycinnamate (HPAO3), and a non-enhanced UHMWPE was used as a negative control. All the specimens were prepared from GUR1020 (Ticona) powder compression moulded (0.3% w/w) and gamma irradiated at 10 MRad.

To investigate the oxidation index, carbonyl absorption was carried out as an indicator of the oxidation potential of a material. Due to the hindered phenol ester linkages, carbonyl absorption was initially higher in the hindered phenol-doped

UHMWPE than in the non-doped UHMWPE, although over 10 weeks the antioxidant UHMWPE remained almost constant, while the non-doped UHMWPE demonstrated an increasing oxidation index. These studies demonstrated that hindered phenols provided effective antioxidant compounds when they were added to UHMWPE (Narayan et al., 2010).

Narayan et al., (2010) also showed inefficient crosslinking and differing levels of carbonyl absorption between the different hindered phenols. This was thought to be due to the large molecules affecting the efficiency of forming crosslinks. The HPAO enhanced UHMWPE, the largest molecular antioxidant of the three materials, gave the lowest incidence of crosslinking of UHMWPE, supporting this that the size of the antioxidant molecule can affect the crosslinking efficiency. Overall this study showed that the use of hindered phenols in UHMWPE was advantageous for the protection of UHMWPE from oxidation (Narayan et al., 2010).

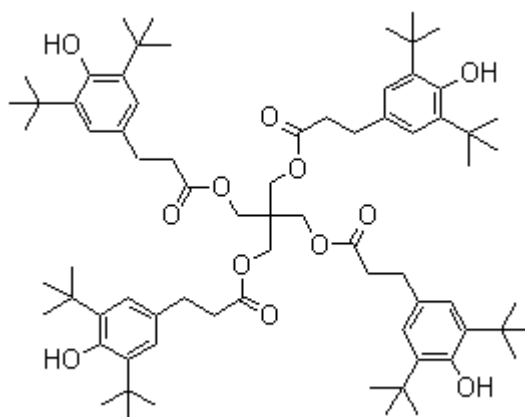


Figure 1.17 - Molecular structure of Pentaerythritol Tetrakis (HPAO)

<http://www.chemblink.com/products/6683-19-8.htm>

Certain hindered phenols have been found to provide excellent oxidation stability and therefore eliminate the need for post-irradiation melting. Irradiated hindered phenol-enhanced UHMWPE show better tensile strength and fatigue resistance compared to post-irradiation melted UHMWPE (King, 2010).

A study by Bladen et al., (2013) investigated the cytotoxicity of HPAO by incubating U937 human histiocytes and human peripheral blood mononuclear cells with HPAO at a seeding density of 2×10^4 cells per well, in 5% (v/v) CO₂ in air. It was found that HPAO was toxic to U937 cells at a concentration of 50µM, and toxic to peripheral blood mononuclear cells at 156µM. This demonstrated the high toxicity of HPAO, and compared to vitamin E (4mM toxic to U937 cells), HPAO was significantly more toxic to U937 cells *in vitro*. Interestingly, the authors found that HPAO conferred some protection to cells against solvents such as ethanol and dimethyl sulfoxide. This is an area where more research is required in order to further understand the biocompatibility of hindered phenols in UHMWPE components (Bladen et al., 2013b). The toxicity of hindered phenols and other antioxidants should be thoroughly investigated when considering these compounds as antioxidant additives for orthopaedic implants.

1.18 Aims

The development of UHMWPE as a bearing material in total hip replacements has led to the current highly crosslinked UHMWPE material used clinically today. This low wearing material has performed well *in vivo*, however the generation of free radicals and oxidative instability have been seen as concerns with this material, with previous attempts to reduce the free radical burden having negative effects on the mechanical properties of UHMWPE.

This has led to the introduction of antioxidant UHMWPE in total hip replacements, to maintain the oxidative stability of UHMWPE, and remove the need for post-irradiation heat treatments which have been shown to have a negative effect on the mechanical performance of the material. In 2007, a vitamin E enhanced highly crosslinked UHMWPE became available clinically for use in total hip replacements, with hindered phenol enhanced highly crosslinked UHMWPE available in 2012 for use in the knee. Despite these materials being clinically available, not much is known in terms of the biological response to wear debris generated from these highly crosslinked antioxidant materials. Wear debris generated from UHMWPE has been shown to be critical to the biological response *in vivo*, leading to the osteolytic immune response that results in aseptic loosening of the prosthesis and failure. With

the introduction of vitamin E to UHMWPE, it was hypothesised that alongside its antioxidant properties, the well documented anti-inflammatory properties of vitamin E could have an effect on the immune response to UHMWPE wear debris, potentially reducing the process of aseptic loosening.

Previous studies have investigated the biological response to vitamin E enhanced UHMWPE (non crosslinked), however those studies have not used the clinically relevant highly crosslinked materials, both in terms of the antioxidant materials and the non-antioxidant control materials. This study aims to use both these highly crosslinked UHMWPEs to determine the effect of vitamin E addition to highly crosslinked UHMWPE. Alongside the immune response to this wear debris, not much is understood in terms of the deeper mechanisms that occur in the cell in response to antioxidant UHMWPE, for example the oxidative stress in response to wear debris.

In addition to vitamin E, the hindered phenol enhanced highly crosslinked UHMWPE has recently been introduced clinically in knee replacements. This is a relatively untested material in terms of the biological response to wear debris, however this is an important aspect of predicting the performance of a novel UHMWPE material.

The primary aims of this study were to investigate the wear performance, wear particle size distributions and biological activity, in terms of the osteolytic cytokine release and production of reactive oxygen species, of two novel antioxidant UHMWPEs; vitamin E enhanced highly crosslinked UHMWPE, and hindered phenol enhanced highly crosslinked UHMWPE.

The main objectives of this study were:

1. To determine the effect of crosslinking and antioxidant enhancement on the wear factor of UHMWPE
2. To investigate the wear particle size distributions for the antioxidant UHMWPE materials, to determine the effect, if any, of antioxidant enhancement and crosslinking on the particle size and volume distribution.

3. To determine the biological response to clinically-relevant wear debris from both antioxidant UHMWPE materials using *in vitro* cell culture in terms of TNF- α release from PBMNCs.
4. To investigate the production of reactive oxygen species in PBMNCs in response to UHMWPE wear debris from vitamin E enhanced highly crosslinked UHMWPE wear debris

Chapter 2

Materials and Methods

All the materials used in this study are shown in Appendix A. The chemicals and reagents used in this study, along with their manufacturer, are shown in Table A-1. The equipment used in this study, along with their manufacturer, is shown in Table A-2. Consumables and plastic ware used in this study are shown in Table A-3.

2.1 Wear Testing

2.1.1 UHMWPE Materials

The following polyethylene materials were tested; GUR1050 virgin UHMWPE, GUR1050 vitamin E enhanced UHMWPE, GUR1050 vitamin E enhanced UHMWPE (5 MRad gamma irradiation), GUR1050 vitamin E enhanced UHMWPE (10 MRad gamma irradiation), GUR1050 Marathon[®] UHMWPE (5 MRad gamma irradiation), GUR1050 highly crosslinked UHMWPE (10MRad gamma irradiation), GUR1020 virgin UHMWPE, GUR1020 hindered phenol antioxidant (HPAO) enhanced UHMWPE and GUR1020 HPAO enhanced highly crosslinked UHMWPE (8 MRad gamma irradiation). All antioxidant compounds were blended with UHMWPE prior to manufacture unless stated otherwise. The vitamin E enhancement dose was 1000ppm while the HPAO was added at a dose of 700ppm. The hindered phenol antioxidant material used in this study was called AOX[™] by the manufacturer and will be referred to as AOX[™] from this point. The UHMWPE materials and their abbreviations are shown in Table 2.1.

Table 2.1 - UHMWPE's tested in this study, detailing the name, resin type, gamma irradiation dose applied, antioxidant added (if any), the supplier and the abbreviation used throughout the study

Material	Resin	Gamma Irradiation Dose	Antioxidant	Supplier	Abbreviation
1050 Virgin	GUR 1050	0 MRad	none	DePuy Synthes®	1050 Virgin
1050 Marathon®	GUR1050	5 MRad	none	DePuy Synthes®	1050 Marathon
1050 Highly Crosslinked UHMWPE	GUR1050	10 MRad	none	DePuy Synthes®	1050 HXL
1050 Vitamin E enhanced UHMWPE	GUR1050E	0 MRad	Vitamin E 1000 ppm	MediTech® Medical Polymers	1050 Vit E
1050 Vitamin E enhanced UHMWPE + 5 MRad Irradiation	GUR1050E	5 MRad	Vitamin E 1000 ppm	MediTech® Medical Polymers	1050 Vit E 5
1050 Vitamin E enhanced UHMWPE + 10 MRad Irradiation	GUR1050E	10 MRad	Vitamin E 1000 ppm	MediTech® Medical Polymers	1050 Vit E 10
1020 Virgin	GUR1020	0 MRad	none	DePuy Synthes	1020 Virgin
1020 Hindered Phenol enhanced UHMWPE	GUR1020	0 MRad	Hindered Phenol	DePuy Synthes	1020 AOX
1020 Hindered Phenol enhanced UHMWPE + 8 MRad	GUR1020	8 MRad	Hindered Phenol	DePuy Synthes	1020 AOX 8

2.1.2 Methods

In order to determine the wear factor of each material, four pins of each UHMWPE material were tested using a simple configuration six station pin-on-plate articulating wear simulator against smooth high-carbon content (0.27% w/w) cobalt-chromium (CoCr) plates to simulate the conditions of a metal-on-polyethylene hip arthroplasty. By measuring the wear from each pin gravimetrically over approximately 500,000 cycles, the wear factor for each UHMWPE was calculated ($n = 4$).

2.1.2.1 Machining and Preparation of UHMWPE Pins

The polyethylene pins for 1050 Vit E, 1050 Vit E 5 and 1050 Vit E 10 were machined in house from bar stock supplied as a gift by MediTech[®] Medical Polymers. The 1050 Virgin, 1050 Marathon, 1050 HXL, 1020 Virgin, 1020 AOX and 1020 AOX 8 pins were machined in house from bar stock supplied by DePuy Synthes. All pins were machined to specific dimensions. Pins had a 10mm contact face, with a pin diameter of 11.95mm and a depth of 12mm, as shown in Figure 2.1.

All pins were engraved with a number on the non-contact face of the cylinder to allow for identification and continuity of orientation in the test rig. All pins were soaked for at least 14 days in deionised water at room temperature to ensure that the mass change due to moisture absorption had reached a stable point. Pins were handled using tweezers and/or clean gloves from this point to prevent grease and debris coming into contact with the pins.

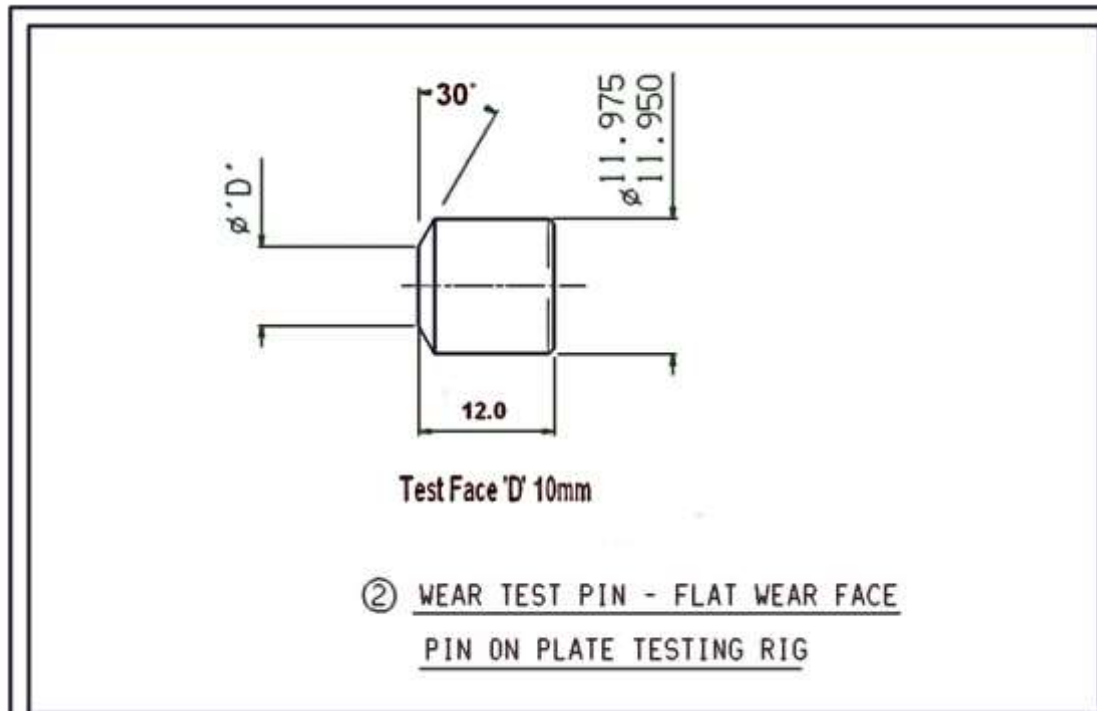


Figure 2.1 – Diagram showing the dimensions of the pins used in the 6 station pin-on-plate wear tests and the aseptic single station pin-on-plate wear rig. The measurement 'D' refers to the 10 mm diameter of the contact face.

2.1.2.2 Machining of CoCr Plates

Plates were manufactured in house from wrought cobalt-28chromium-6molybdenum high carbon-content alloy (0.27% w/w) (ASTM: F 1537 – 08) used for surgical implants. The dimensions of the plates are shown in Figure 2.2. For wear testing using the six station pin-on-plate wear simulator, plates were manufactured to have a smooth contact face to a mean R_a value of $\leq 0.01 \mu\text{m}$. For the single station wear simulator plates were manufactured to have a rough contact face to a mean R_a 0.7-0.9 μm .

2.1.2.3 Surface Measurement of CoCr Plates

The CoCr plate surface roughness was measured using the Form Talysurf 120L contacting surface profilometer which is housed in a temperature controlled laboratory. The measurement tracks taken are shown in Figure 2.2A. Several tracks were taken on the plate; two along the x axis ($p1$, $p2$) over a 10mm distance, 10mm

from the edge of the plate and 5mm apart, and an additional two tracks perpendicular to these ($p3$, $p4$). To calculate the surface roughness of each plate, a mean was taken of the four measurements. This was repeated for each plate that was tested in the six station pin-on-plate wear simulator and the single station aseptic wear simulator.

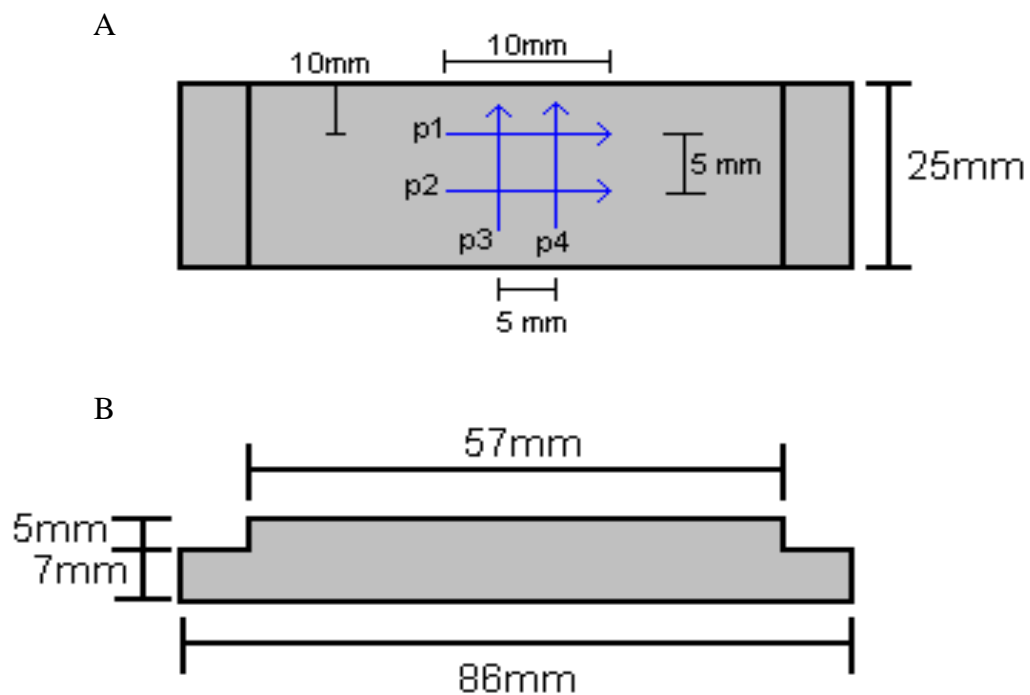


Figure 2.2 – Schematic showing A) the tracks (blue arrows) measured by the Form Talysurf 120L to calculate the mean surface roughness of a B) standard CoCr plate. A mean of the four measurements was taken to determine the representative surface roughness. Plates had standard dimensions of 86 mm length with a raised surface 57 mm in length, 25 mm width and a 13 mm total height (5 mm step) . Measurement tracks were 10 mm long traces and were taken 10 mm from the edge of the plate and then 5 mm apart. Tracks 10 mm in length were then taken perpendicular to these tracks, also 5 mm apart.

2.1.2.4 Weighing of UHMWPE Pins

Prior to weighing, UHMWPE pins were cleaned using household detergent, rinsed in distilled water, then sonicated in 70% (v/v) iso-propanol for 10 min, and dabbed dry

using medical wipes. Pins were stored at $21^{\circ}\text{C} \pm 2^{\circ}\text{C}$ for 72 hours before weighing. Immediately prior to weighing, pins were placed beneath an ion streamer for 10 min to remove any static build up. Pins were weighed using an AT21 Comparator digital microbalance (accurate to $1\ \mu\text{g}$) to give five measurements ($\pm 5\ \mu\text{g}$) with a mean weight being calculated for each pin. Tweezers were used to handle the pins to avoid contamination with dust or grease.

2.1.2.5 Preparation of 25% (v/v) Bovine Serum

Bovine serum was defrosted in a water bath at 37°C for 30 min. A volume of 500 ml of serum was mixed with 1500 ml of 0.3% (w/v) sodium azide into a container. This solution was aliquoted into 500 ml containers and stored at -20°C until required for wear testing.

2.1.2.6 Assembly of the Six Station Pin on Plate Simulator

2.1.2.6.1 Preparation of the Linear Bearing Trays

A six station pin-on-plate reciprocating wear test simulator was used to determine the wear factor of the UHMWPE pins against the CoCr plates. The stroke length was set at 28 mm with a rotation of $\pm 30^{\circ}$, and a load of 160 N at a reciprocating speed of 1 Hz. The tests were performed in 25% (v/v) bovine serum which was prepared as described in section 2.1.2.5. The calibration of the stroke length and reciprocating speed was performed by a lab technician.

The components of the wear test rig consisted of:

- 12 stainless steel screws (large)
- 12 stainless steel screws (small, short)
- 12 stainless steel screws (small, long)
- 6 stainless steel wells
- 6 stainless steel bath inserts
- 6 polymer baffles
- 6 stainless steel toothed racks
- 6 polymer gear wheels

- 4 bridge sections (covering 6 stations (2 double, 2 single))
- 6 ball bearing assemblies
- 6 collets (pin holders)
- 6 pin holder outer sleeves
- 6 threaded nuts
- 6 spacer pins
- 6 connecting rods
- 6 cantilever arms
- 6 weights
- 6 pivot pins
- 6 split pins
- 6 plastic sheets

The removable components of the 6 station pin-on-plate wear rig are shown in Figure 2.3. Additional equipment for the assembly of the wear rig was as follows:

- PVC tape
- Scalpel
- Four Allen keys to fit the appropriate screws
- Spirit level
- Adjustable wrench

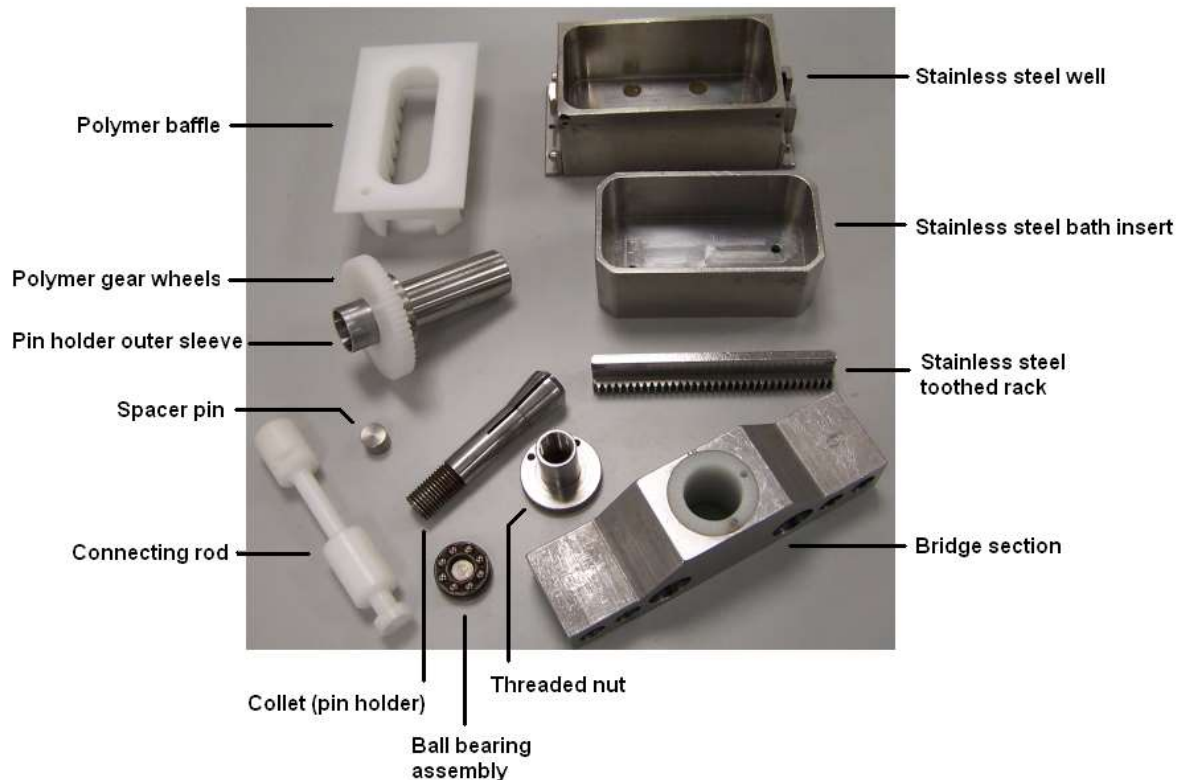


Figure 2.3 – Removable components of the six station pin-on-plate wear rig.

The appropriately numbered bath insert was placed in the correspondingly numbered stainless steel well. The appropriately numbered plate was then screwed into the bath insert using the large screws. The number on the plate was used to ensure correct orientation of the plate in the bath, and the plate-station pairing was noted.

The correct baffle was then placed into the bath, secured and sealed with two layers of PVC tape to prevent serum leaking from around the baffle. The screw holes on the side of the well were exposed by cutting the PVC tape away from these sections using a scalpel. The toothed rack was then secured onto the side of the well using two small screws. The assembled bearing tray is shown in Figure 2.4. The bearing tray was then placed onto the linear bearing platform with the plastic sheet underneath, and secured using four of the small-long screws. This was repeated for each bearing tray, and the plate-tray-station number allocation was noted.



Figure 2.4 – A bird’s eye view of the assembled linear bearing tray and bath with 50 ml of 25% (v/v) bovine serum. The bottom of the image shows the front of the linear tray, where the connecting rods slot in to attach to the tray. The toothed rack is shown on the left hand side of the image. The black PVC tape used to seal the bath is also shown.

2.1.2.6.2 Preparation of the Pin Holders

A stainless steel spacer was placed in the collet, followed by the test pin to ensure that at least 5mm of the test pin was protruding from the holder. The collet was then placed in an outer sleeve, correctly aligning the key and the taper. The pin holder was threaded through the hole in the bridge and a threaded nut screwed onto the end (top) of the pin holder, therefore securing the pin in the collet.

The gear wheel was attached to the pin holder below the bridge. The fully assembled pin holder is shown in Figure 2.5. With the pin holder now complete, the bridge-pin holder complex was slotted into the support brackets spanning the trays. The pin-station-holder number allocation was noted. The bridge was secured using the clamps, and the gear wheel was slotted neatly into the toothed rack. The pins were checked to ensure contact with the plates, and that the threaded nut was not in contact with the bridge. This was repeated for each station.



Figure 2.5 – The left hand image shows an exploded view of the components that make up the pin holder. The right image shows the fully assembled pin holder, showing the pin protruding from the bottom and the cog positioned above the pin. The pin holder was composed of the following components; **A** – Threaded nut; **B** – Bridge section; **C** – Pin holder outer sleeve with polymer gear wheel attached; **D** – Collet (pin holder); **E** – Spacer pin. The fully assembled image shows a 1050 Vit E 10 UHMWPE pin in place, protruding from the bottom of the pinholder.

2.1.2.6.3 Final Assembly of the Test Rig

Using a syringe, approx 50ml of 25% (v/v) bovine serum was added to each bath, ensuring the level of serum was approximately 2-3mm above the surface of the plate. The connecting rods were screwed into place, connecting the scotch yolk mechanism to the trays. The appropriately numbered cantilever arms were installed into the appropriate stations, and the bearing assemblies were installed. The pivot pin on the cantilever arm was secured using a split pin, and the cantilever arms were levelled using a spirit level. The ball bearing assemblies were placed on top of the threaded nut to provide a point for the load to be smoothly applied through.

The counter was reset, and the motor turned on. The speed was adjusted so the rig performed 60 cycles per minute (cpm), and the weights were placed in the correct position on the cantilever arm to give a load of 160 N. Alongside the pins being tested were also soak control pins of the same material, providing a control value for the mass change during soaking. These pins were prepared according to section 2.1.2.4 and submerged in 25% (v/v) bovine serum in a 50 ml container open to the

air. The control pins were placed near to the centre of the rig to ensure the same conditions as the test specimens. The Perspex lid was then replaced on top of the rig. The fully assembled wear rig is shown in Figure 2.6.

The rig was checked at least twice daily to ensure all components were running correctly and that the lubricant level was maintained. When the lubricant needed replenishing, 0.03% (w/v) sodium azide was added using a syringe.

2.1.2.7 Dismantling the Wear Test Rig

After approximately 250,000 cycles, which normally took approximately four days, the wear rig was stopped by first removing the weights from each station, followed by turning down the speed until the wear rig stopped, and the motor was turned off. The number of cycles was noted in order to calculate the sliding distance of the pins. The cantilever arms were removed and put back on their appropriate rack.

The connecting rods were unscrewed, disconnecting the trays from the scotch yolk mechanism. The ball bearing assemblies were removed and each bridge was released by unscrewing the clamps. The threaded nut was carefully unscrewed, allowing for the pin holder and polymer gear assembly to be removed from the bridge. The pin and spacer were removed from the collet onto medical wipes to protect the pin from grease and debris, and the collet was removed from the pin holder.

Each bearing tray was removed from the linear bearing platform, and the toothed racks, PVC tape, baffles and bath inserts removed from the well. The serum was then extracted from the bath inserts by carefully decanting into a suitably sized container. Using a syringe, the remaining particles were collected by washing out the bath with approximately 15 ml 0.03% (w/v) sodium azide. This method of serum extraction was used to prevent cross-contamination of samples. Serum was stored in a labelled container at -20°C until required for particle analysis. The plates were removed from the bath, taking care not to damage the surface when unscrewing.

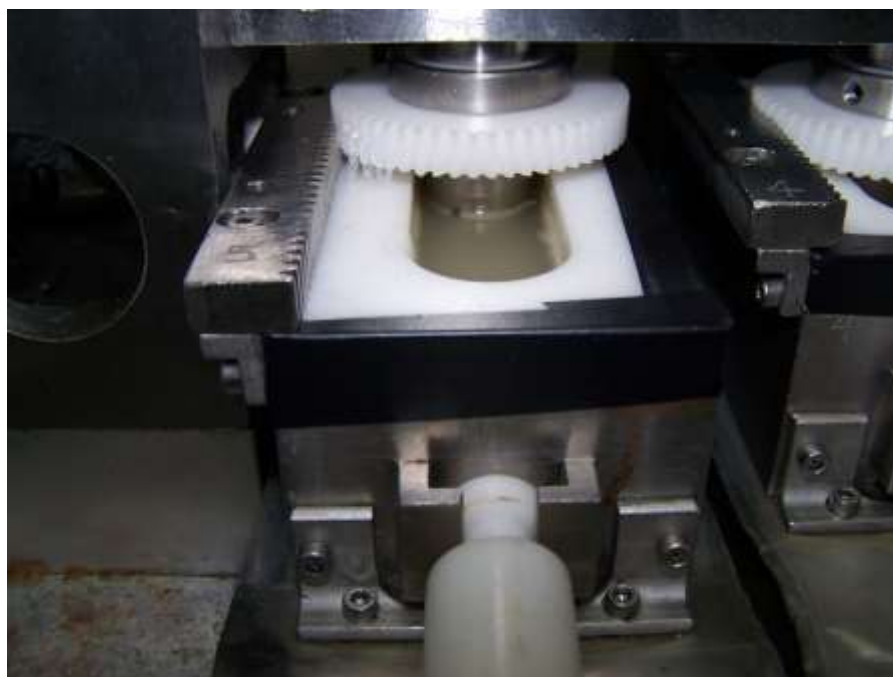


Figure 2.6 – The fully assembled 6 station pin-on-plate wear rig. The top image shows one individual station with the pin submersed in 25% (v/v) bovine serum. The bottom image shows the six stations, each with a cantilever arm and a weight situated to apply 160N of force.

2.1.2.8 Cleaning the Components and Specimens

After a week of wear testing, all the components and test specimens were washed thoroughly to remove any traces of serum. Immediately after the test, all the removable wear rig components and test specimens (pins, plates) were washed in household detergent solution. A hard bristled brush was used to scrub all the metal parts. After thorough cleaning, all the parts were rinsed with distilled water to remove the detergent.

Following this stage, all the components and specimens were then washed in 1% (v/v) Trigene solution for 20 min and then rinsed with distilled water. The wear rig components were then dried in air, while the pins, plates and plate-screws were placed in a sonicating water bath in 70% (v/v) iso-propanol solution for 10 min. The test specimens were then dabbed dry using medical wipes. The plates were wrapped in medical wipes ready for the following wear test, while the pins were stored in a petri dish for at least 48 hrs in the temperature controlled measurements laboratory. The pins were then weighed as described in section 2.1.2.4. The mass of each pin after two weeks of wear testing (approx 500,000 cycles) was subtracted from the starting weight of each pin to calculate the mass loss, and a mean mass loss was taken for the four pins. A mean volume loss and wear factor for each material was then determined.

2.1.2.9 Calculating the Wear Factor

The 6 station pin-on-plate wear rig was used to simulate the motion and forces experienced in the hip joint. This experiment was designed to run for a minimum of 500,000 cycles. The mass loss of each pin was calculated gravimetrically using an AT21 comparator microbalance. A mean of five measurements (within 0.00001g of each other) before and after testing were obtained and the soak control mass gain subtracted from the final mass.

In order to calculate the wear factor, the following equation was used:

Equation 1

$$\text{Wear Factor} = \frac{\text{Volumetric Loss}}{\text{Force} \times \text{Sliding Distance}}$$

This calculation was used to normalise the wear volume obtained from a wear test by including the force applied and the total sliding distance travelled by the UHMWPE pin component. The equation can be adjusted to allow for the input of results obtained in this report:

Equation 2

$$K = \frac{\left(\text{Mass Loss (g)} / \text{UHMWPE Density (kgm}^{-3}\text{)} \times 10^{-6} \right)}{\text{Force(N)} \times (2 \times \text{Stroke Length(mm)} \times 10^{-3} \times \text{cycles})}$$

This equation was then adjusted for the parameters in the 6 station pin-on-plate wear test so that only the mean mass loss and number of cycles were required. This simplified equation is shown below, with the input variables highlighted in red:

Equation 3

$$K = \frac{\text{Mass Loss (g)} / 0.934 \times 10^{-3}}{160N \times (2 \times 28mm \times 10^{-3} \times \text{cycles})}$$

Calculating the wear factor for each material allowed for comparison of the wear performance of each material. This equation yielded a wear factor for each pin, and a mean wear factor was taken for each material (n=4). The mean wear factors for all the UHMWPE tested were plotted onto a graph, with error bars showing $\pm 95\%$ confidence level. Mean wear factors were compared and any significant changes in the wear factor were determined using the student tukey method.

2.2 Generation of Wear Particles under Aseptic Conditions for Cell Culture Studies

In order to replicate the interaction between macrophages and UHMWPE particles that occurs during osteolysis, and to then determine the cytokine response to these particles, sterile endotoxin-free wear particles were required for culture with primary macrophages. In order to generate these wear particles, a single station pin-on-plate wear simulator was used under aseptic conditions and housed in a class II safety cabinet. This involved the sterilisation of all the simulator components, including the pin, plate, and 25% (v/v) bovine serum lubricant, and the use of aseptic technique, to generate a volume of sterile, endotoxin free wear particles for culture with PBMNCs.

2.2.1 Machining and Preparation of UHMWPE pins

The pins tested on the single station aseptic wear simulator were machined and prepared as described in section 2.2.1.1. The UHMWPE materials from which sterile particles were generated from are outlined in Table 2.2.

2.2.2 Machining and Preparation of CoCr plates

Plates were manufactured in house from wrought Cobalt-28Chromium-6Molybdenum high carbon-content alloy used for surgical implant (carbon content was 0.27% (w/w) and therefore can be specified as high-carbon according to ASTM: F 1537 – 08). Plates were scratched to produce a ‘rough’ surface, with a target R_a of 0.07-0.09 μm .

Table 2.2 - UHMWPE materials from which sterile wear particles were generated using the aseptic single station pin-on-plate wear simulator.

Name	Resin	Gamma Irradiation Dose	Antioxidant	Supplier
<i>Virgin 1050</i>	GUR 1050	0 MRad	none	DePuy Synthes
<i>Highly Crosslinked 1050 UHMWPE</i>	GUR1050	10 Mrad	none	DePuy Synthes
<i>Vitamin E enhanced UHMWPE + 10 MRad</i>	GUR1050	10 MRad	Vitamin E 1000 ppm	MediTech® Medical Polymers
<i>Virgin 1020</i>	GUR1020	0 MRad	none	DePuy Synthes
<i>AOX™ enhanced UHMWPE + 8 Mrad</i>	GUR1020	8 MRad	AOX™ (Pentaerythritol Tetrakis)	DePuy Synthes

2.2.3 Surface Measurement of CoCr Plates

The surface roughness of the CoCr plates was measured as outlined in section 2.2.1.3. The plate dimensions and measurement tracks are shown in Figure 2.2.

2.2.4 Weighing of UHMWPE Pins

To ensure there were no delays during assembly of the wear simulator, two pins for each material were prepared. Pins were weighed as outlined in section 2.1.2.4 and following a wear test, mean wear factors were calculated from n=4 measurements.

2.2.5 Preparation of the UHMWPE Pins

After weighing, the pins were rinsed in warm water, scrubbed using a soft toothbrush and household detergent and rinsed in deionised water three times. After rinsing, the pins were submersed in 4% (v/v) sodium hypochlorite in a universal tube and placed on a shaker at 120 rpm for 10 min. Using aseptic technique with a Bunsen burner; the pin was transferred to 10 ml nutrient broth and was incubated at 37°C for 48

hours with shaking to test for bacterial contamination. The broth was checked for bacterial contamination (clouding of the medium indicated contamination) and if there was none, the pins were transferred to 70% (v/v) ethanol using aseptic technique. The pins were stored in ethanol for a maximum of two weeks but usually used in the wear simulator within four days of preparation.

2.2.6 Preparation of Lubricant

The serum lubricant was made up either the day before or on the first day of the experiment. Particles for cell culture were generated in a lubricant that consisted of RPMI 1640 medium containing 25% (v/v) foetal bovine serum. This was prepared in a class II safety cabinet to ensure sterility. Five 50 ml aliquots of sterile, pyrogen free ultrapure water were also prepared in the class II laminar flow cabinet to be used in the syringe driver system during the experiment.

2.2.7 Assembly of the Single Station Pin-on-Plate Wear Simulator

2.2.7.1 Preparation and Sterilisation of the Components of the Single Station Pin-on-Plate Wear Simulator

A single station pin-on-plate reciprocating wear test simulator was used to generate particles from the UHMWPE pins under aseptic conditions. The stroke length was set at 28mm with a rotation of $\pm 30^\circ$, and a load of 160N at a reciprocating speed of 1Hz. The tests were performed in RPMI 1640 medium with 25% (v/v) bovine serum, which was prepared as described in section 2.1.2.5. The calibration of the stroke length and reciprocating angle was performed before testing by a lab technician.

The components of the wear test rig consisted of:

- 1 bath with toothed rack attached
- 1 rough CoCr plate (R_a 0.07-0.09 μm)
- 1 medium spacer
- 1 bridge
- 1 pin holder with cog attached
- 1 pin holder fastener

- 1 collet
- 2 long screws
- 2 short screws
- 1 tweezers
- 2 Allen keys

2.2.7.2 Sterilisation of Wear Simulator Components and Class II Cabinet

Prior to the day of set up of the simulator, all the removable rig components described above were cleaned thoroughly using household detergent and a toothbrush, and then soaked in 1% (v/v) Virkon for 20 min. Finally the components were sonicated in 70% (v/v) iso-propanol for 10 min. The components were dried at room temperature for 20 min. The bath, plate and screws were loosely assembled and wrapped in aluminium foil, and all other components (excluding the bridge) were individually wrapped in aluminium foil. These components were then sterilised by heating at 190°C for 3 hours in a hot air oven. The bridge section contained a plastic insert so could not be sterilised in the oven. This component was therefore thoroughly cleaned as described above and cleaned by spraying with 1% (v/v) Virkon followed by 70% (v/v) ethanol immediately before placing in the class II safety cabinet. The day before the experiment commenced, the class II safety cabinet was thoroughly cleaned using 1% (v/v) Virkon and then 70% (v/v) ethanol. The UV light was then turned on for 30 min after cleaning to ensure sterility.

2.2.7.3 Assembly of the Single Station Pin-on-Plate Wear Simulator

The class II safety cabinet was run on fan level two throughout setting up and running of the simulator. The operator wore a clean, howie style lab coat at all times. The class II safety cabinet was once again thoroughly cleaned using 1% (v/v) Virkon followed by 70% (v/v) ethanol prior setting up the simulator. Aseptic technique was followed whereby gloves and all equipment that was put into the cabinet were sprayed thoroughly with 70% (v/v) ethanol. Once all components were in the cabinet, sterile gloves were worn throughout the set up.

Each component was unwrapped inside the cabinet, removing the aluminium foil as each piece was required. The screws to fasten the plate securely to the bath were tightened, taking care not to touch the end of the Allen key that was in contact with the screws. Care was also taken to use the Allen key to hold the screws in order to avoid touching them and thus reducing the risk of contamination. The toothed rack component was then tightly screwed against the rear of the bath using the smaller diameter Allen key. The bath and plate were then placed into the rig, aligning the dowels. The bath itself was then fastened to the rig using the correct screws and Allen key. A small amount of anti-fretting lubricant was applied to the serrated edge of the toothed rack. The spacer was inserted into the collet using tweezers. Tweezers were then used to remove the pin from the ethanol, and the pin was carefully inserted in the correct orientation into the collet. The collet was then inserted into the pin holder, and the pin holder inserted through the bridge, which allowed for the pin to be tightened into the collet by tightening the pin holder fastener. A small amount of anti-fretting lubricant was applied to the cog, and the bridge was then placed into the rig and screwed into place. Checks were then performed to ensure the cog was in intimate contact with the serrated edge of the toothed rack, and that the pin holder was free to lift up and rotate in the bridge.

Approximately 35-40mls of RPMI 1640 medium with 25% (v/v) foetal bovine serum lubricant was added to the bath, ensuring a gap of 1-2mm to the top of the bath. The pin was lifted to allow the medium to lubricate all surfaces. The counter was reset, and the rig was then turned on without the load in place and the correct speed was selected (1Hz). Anti-fretting lubricant was applied to the washers and bearings before they were placed on top of the pin holder. The arm was then lowered, levelled using a spirit level, and then the load applied at 160N.

2.2.7.4 Setting up the Syringe Driver Mechanism

The syringe drive mechanism was composed of a syringe containing sterile water in a machine that slowly pushed the plunger of the syringe. A sterile tube delivered the water from the syringe (outside the safety cabinet) to the bath of the single station pin-on-plate wear simulator.

Prior to setting up, the connecting tube was sterilised using an autoclave at 121°C for 20 min, at 103 kPa, and 50 ml aliquots of sterile water were prepared as outlined in section 2.1.2.6.

The syringe driver delivery mechanism comprised a stainless steel delivery pipe, a screw and an Allen key. The components of the syringe driver delivery mechanism were prepared in the same way as the other metal components, as outlined in section 2.1.2.7.2. To assemble the syringe driver, the grub screw on the drive shaft was loosened, and the drive shaft rewound until all the exposed thread had disappeared. The drive shaft was connected to the threaded shaft by tightening the grub screw, ensuring correct alignment. In the cabinet, the delivery pipe was screwed onto the bridge ensuring the end of the pipe would be over the bath throughout the test. A 50 ml syringe was filled with 50ml of sterile pyrogen-free water. The connecting tube was unwrapped and one end firmly fitted around the non-dispensing end of the driver pipe. At this point the syringe was placed in one of the slots on the syringe holder, and the other end of the connecting tube was fitted to the syringe. The syringe holder-connecting tube assembly was then taken out of the cabinet and fitted onto the syringe driver. The nuts securing the syringe holder were secured, and the drive shaft was adjusted to ensure the driver mechanism was in contact with the syringe plunger. The syringe driver was switched on and adjusted accordingly for the test. Typically, approximately 40 ml of sterile water was dispensed over 24 hrs. Finally, the front exposed section of the cabinet surface was sprayed with 70% (v/v) ethanol to ensure sterility. The simulator was checked at least twice daily. The syringe within the syringe driver mechanism was changed daily using the method outlined above. Sterile technique was observed throughout.

2.2.7.5 Bacterial Testing of the Lubricant

Once a day throughout the running of the simulator, a 2 ml sample of lubricant was taken directly from the bath using a sterile syringe. This was aliquoted into a small sterile bijoux bottle. Before bacterial testing, heated-blood agar (HBA), nutrient agar (NA) and Sabouraud (SAB) plates were prepared by placing them inverted in the plate drying room for 30 mins at 37°C.

Using sterile technique with a Bunsen burner, a sample of the serum lubricant was plated out onto each plate i.e. flaming the platinum loop and flaming the top of the bijoux each time the loop was dipped into the serum. The serum was spread over the plates in a series of lines, shown in Figure 2.7, flaming the platinum loop between spreading each line. The NA and HBA plates were incubated at 37°C and the SAB plate at 30°C. The plates were checked over a 3 day period for bacterial growth. A small sample of lubricant was taken every day to ensure the test remained sterile.

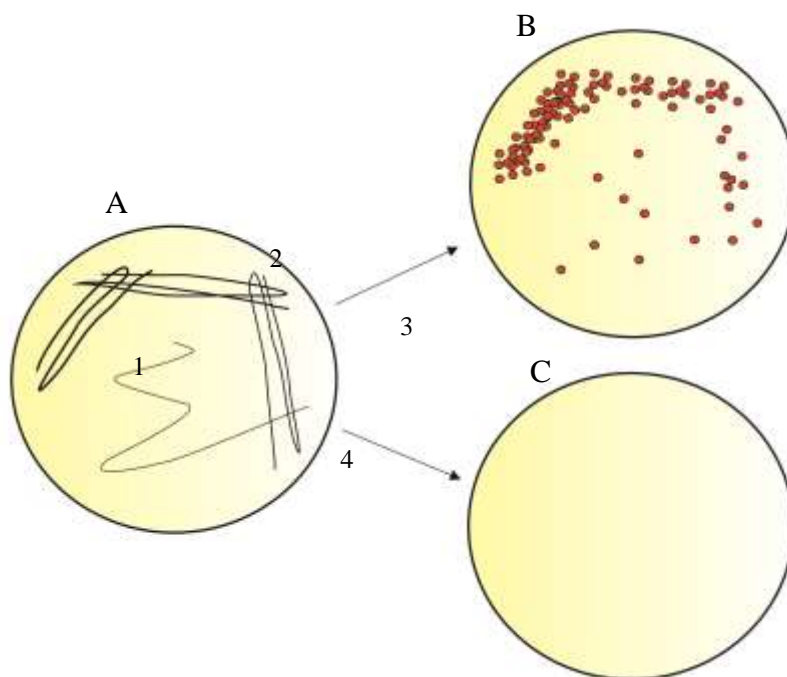


Figure 2.7 – Schematic showing the method for bacterial testing of serum lubricant using agar plates. Image A shows the series of lines used to spread the sample, with the platinum loop flamed after each line is spread. Image B shows the result of a contaminated sample, with bacteria colonies present where the sample has been spread on the agar. Image C shows the result of a non-contaminated sample, with no bacterial colonies present on the agar plate.

2.2.7.6 Disassembly of the Single Station Pin-on-Plate Wear Simulator

At the end of the test, the counter-weight was removed, and the speed controller was turned down until the rig stopped. The rig motor was then switched off, followed by the syringe driver motor. The number of cycles was noted.

The lubricant was removed from the bath using a sterile syringe and transferred to a sterile 60 ml container. The bath was tilted in order to collect all the lubricant, and the bath was washed with 10 ml sterile water to ensure efficient collection of wear particles. The final lubricant sample was tested for bacterial contamination as outlined in section 2.1.2.7.5. The components of the rig including the pin and plate were then disassembled and removed from the cabinet. All the components were cleaned in household detergent, and the pin was then placed in 70% (v/v) isopropanol in a sonicating water bath for 10 min. The pin was then dried and placed in the temperature controlled measurements laboratory to dry for 48 hrs. The pin was then weighed 5 times to obtain measurements with an accuracy of $\pm 5\mu\text{g}$. The other components were cleaned as outlined in section 2.1.2.7.2. The class II safety cabinet was cleaned with 1% (v/v) Virkon, followed by 70% (v/v) ethanol and the UV light was switched on for 30 min to ensure sterility.

2.3 Isolation and Characterisation of UHMWPE Particles from Serum

2.3.1 Isolation of UHMWPE Particles from Serum

The serum lubricant samples collected from the six station pin-on-plate wear tests were collected in order to isolate the wear particles present and determine the particle size distribution for each material. The methods previously used by Richards (Richards, 2008) for particle isolation was used in this study.

The serum samples were defrosted at 37°C in a water bath for 60 min before being processed. The serum samples were then gently agitated to resuspend particles and placed in a sonicating water bath for 30 min. Potassium hydroxide (KOH) pellets at a concentration of 12 M were weighed into a clean glass bottle at a concentration of 6.72 g for every 10 ml of serum being processed. The appropriate volume of serum (to provide approx. 1mm^3 wear debris) was then added to the glass bottle containing the KOH pellets, swirled to mix, and placed in a water bath at 60°C for approx 3-5 days, until the serum was completely digested. This was assessed visibly as the serum cleared when it was digested. Throughout the 60°C incubation, the serum was regularly swirled to mix in order to increase the efficiency of the digestion.

Following digestion, the serum was cooled to 4°C for 30 min, after which the digested serum was pipetted into sterile universal tubes in 10 ml volumes. An equal volume of 2:1 chloroform: methanol was then pipetted into the universal, and swirled to mix. The bottle was kept upright throughout as polyethylene will adhere to the plastic of the tube lids and could affect the outcome of the particle isolation. The samples were then incubated in a fume hood for 48 hrs at room temperature. Following this incubation, the serum was centrifuged at 2000 g for 20 min at room temperature to remove the proteins and lipids from the sample. The top layer was then pipetted into a clean universal, whilst being careful not to remove any of the bottom layer or the interface. Once again, an equal volume of 2:1 chloroform: methanol was added to the sample and this was incubated at room temperature for 48 hrs in a fume cupboard. This was repeated until the top layer was completely clear; indicating all the lipids and proteins had been removed.

Prior to the next step of the isolation, 500 ml absolute ethanol (99.7% (v/v)) was placed at -20°C for 30min in a clean, glass bottle. The top layer of the serum/cholorform/methanol solution was pipetted off for the final time, and placed in a clean Sorvall 250ml Dry Spin centrifuge bottle. An equal volume of ice-cold ethanol was added to the centrifuge bottle, and for multiple bottles the mass of each bottle was checked to be within 1g to ensure balancing of the centrifuge. When processing an odd number of samples, a Sorvall tube with the same volume of water was used to balance the centrifuge. The sample was then centrifuged at 2000 g for 20 min at 4°C to pellet the salt precipitate. After this, the supernatant was carefully decanted into a clean glass bottle taking care to not disrupt the pellet, and an equal volume of ultrapure water was added. A stirrer bar was added to the sample and it was incubated at 4°C on a stirrer platform overnight to precipitate any remaining proteins. The supernatant was then decanted into a clean sterile Sorvall 250 ml Dry Spin centrifuge bottle, and centrifuged at 10,000g for 2 hours at 4°C using a Sorvall high speed Evolution RC centrifuge (Sorvall SLA 1500 rotor). The supernatant was carefully decanted into a clean 500 ml bottle.

2.3.2 Filtration of Sample

All of the glass filtration apparatus was vigorously cleaned prior to use. Household detergent was used with a hard bristled brush, followed by three washes with de-ionised water. The apparatus was then rinsed with ultrapure water and sterilised in a hot air oven at 190°C for 4 hours. The filter tray was washed in the same way, but sterilised in an autoclave at 121°C for 20 min, at 103 kPa. The filtration unit was assembled as shown in Figure 2.8 in a class I laminar flow hood. All filtration was performed in a class 1 laminar flow hood to reduce airborne contamination of the filters. The supernatant was sequentially filtered through 10µm, 1µm and 0.015µm filters, as shown in Figure 2.8. The filters were handled with tweezers at the edges of the filter to prevent damage. Prior to the supernatant passing through the filter, 10 ml 70% (v/v) ethanol followed by 10 ml ultrapure water was passed through each filter to clean the filter and to check for any leaks in the apparatus. After filtering the supernatant, 10 ml ultrapure water was again used to wash the filter. After use, the filters were immediately placed in a sterile petri dish and dried under a red lamp for 4 hours in the class I hood. The filters were stored in an air tight box with silica gel to avoid an increase in moisture content prior to FEGSEM analysis.

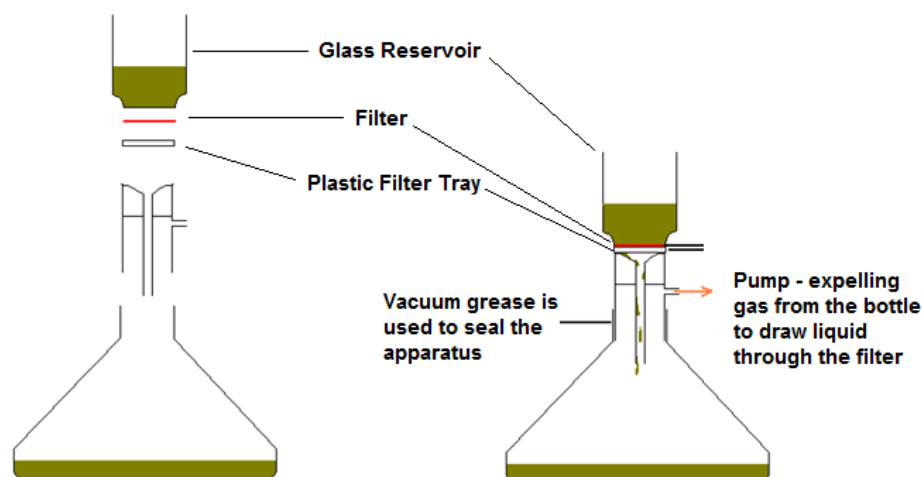


Figure 2.8 – A schematic showing an exploded view of the glass filtration unit (left) and the fully assembled glass filtration unit (right). The unit was comprised of 3 pieces of glass ware and one plastic filter tray. The apparatus was assembled as shown in the exploded view, building upwards. The glass reservoir (top) and the middle unit were clamped together, while the middle unit fits tightly into the neck of the bottle as vacuum grease was applied to the neck of the bottle before assembly. The filter was carefully placed in the centre of the filter tray and dampened with 70% (v/v) ethanol to remove any air bubbles. The pump was used to pull the liquid through the filter.

2.3.3 Field Emission Gun Scanning Electron Microscope (FEGSEM) Analysis of Wear Particles

2.3.3.1 Preparation of Filters for Scanning Electron Microscopy

A small section of each filter was cut and mounted onto an aluminium stub using a double sided adhesive carbon tab. The edge of the filter was painted with carbon paste and the filter was sputter coated with platinum to a thickness of 5nm. The coated samples were stored in an air tight box with silica gel, to provide a moisture free environment. Samples were imaged within five days to avoid microbial contamination on the filters.

2.3.3.2 FEGSEM Analysis

Each sample was observed using a LEO 1530 FEGSEM with SmartSEM Interface software. Images of particles on each filter were viewed using a voltage of 3kV and a working distance of 3mm. For each sample, 3 random fields of view per magnification were captured. A total of 60 images were captured per sample. The magnifications used to view each filter are listed below;

10 μ m filter stub

x400 x700 x1.5K x3K x8K x12K x15K

1 μ m filter stub

x1.5K x5K x10K x20K x30K x40K x65K

0.015 μ m filter stub

x10K x20K x30K x60K x75K x90K

2.3.4 Particle Image Analysis and Size Distribution Graphs

Scanning electron microscopy images were analysed in order to size the UHMWPE wear particles and compile frequency and volume size distribution graphs. Images were analysed using Image Pro Plus image analysis software. The whole area of each image was measured and recorded as (A). Each particle was then sized manually, measuring the particle area, perimeter, aspect, roundness, width and height. A minimum of 100 particles were analysed for each material. The data was exported to an Excel spreadsheet and sorted to generate a frequency and volume size distribution graph. Values for the percentage number of particles per area (N/A) in each size range, and the average percentage area of particles (P/N) in each size range were calculated. The size ranges analysed in this study were <0.1 μ m, 0.1-1.0 μ m, 1.0-10 μ m and >10 μ m. The results for the size distribution of wear particles was presented

as a percentage, and therefore not normally distributed. As a result, the raw data was transformed using arc-sin in order for descriptive statistics to be generated and a one-way ANOVA to be performed. The data was then back transformed to be presented as percentages.

2.4 Culture of Human Peripheral Blood Mononuclear Cells (PBMNCs) with UHMWPE Particles to Determine the Biological Response to UHMWPEs

In order to determine the biological response to UHMWPE wear debris *in vitro*, PBMNCs were isolated from the blood of healthy human donors and incubated for 24 hours with UHMWPE particles. Due to the density of UHMWPE causing particles to float in solution, a suspension medium was required to hold the particles and allow the cells to come into contact with them. This is outlined in section 2.4.3. Following incubation, cell viability was determined using an ATP Lite assay, and the supernatant was carefully collected to determine the cytokine response from the cells using an ELISA.

2.4.1 Stock Solutions

2.4.1.1 Transport Medium

Transport medium was used in this study for the temporary storage and transfer of cells during isolation of PBMNCs. Transport medium consisted of RPMI 1640 medium with 20 mM HEPES (N-(2-hydroxyethyl) piperazine-N'-(2-ethanulfonic acid)) and 100 $\mu\text{g}\cdot\text{ml}^{-1}$ penicillin/streptomycin. Transport medium was stored at 4°C for a maximum of four weeks.

2.4.1.2 Culture Medium

Culture medium was used for the final culture of PBMNCs and was intended to provide all the nutrients required for cell growth. Culture medium consisted of RPMI 1640 medium supplemented with 10% (v/v) foetal bovine serum (FBS), 2 mM L-glutamine and 100 $\mu\text{g}\cdot\text{ml}^{-1}$ penicillin/streptomycin. Culture medium was stored at 4°C for a maximum of four weeks.

2.4.1.3 2% (w/v) Low Melting Point Agarose

The 2% (w/v) low melting point agarose gel was made up with RPMI 1640 transport medium and 2% (w/v) low melting point agarose. The 2% (w/v) agarose gel was mixed thoroughly and heated until the powder had fully dissolved and the agarose medium was clear. The agarose medium was sterilised by autoclaving at 121°C for 20 min, at 103 kPa. The medium was then stored at 4°C until required for a maximum of four weeks.

2.4.2 Endotoxin testing of the serum lubricant using the Limulus Amebocyte Lysate (LAL) assay

Prior to incubation with PBMNCs, lubricant samples containing UHMWPE particles were tested to ensure there was no endotoxin present which would stimulate TNF- α release from PBMNCs in culture. The Limulus Amebocyte Lysate (LAL) assay is used to detect and quantify gram-negative bacterial endotoxin, or lipopolysaccharide (LPS), in human and animal products. In the presence of endotoxin, the LAL is activated, resulting in the release of p-Nitroalinine (pNa) which produces a yellow colour. This yellow colour is detected at an absorbance of 405nm, and the time taken for the absorbance to reach an onset value of 0.5OD is inversely proportional to the amount of endotoxin present. The absorbance of this colour is determined spectrophotometrically at 405 nm, and compared to a standard curve where endotoxin concentrations in the samples can be determined. In addition, positive product controls are used, where test samples are spiked with a known concentration of endotoxin. This is to determine the percentage recovery of the known concentration of endotoxin, in order to validate the results of the assay on the sample type used.

2.4.2.1 Sample Details

The aseptic single station pin-on-plate wear simulator was used to generate sterile lubricant samples containing UHMWPE wear particles. The LAL assay was therefore used to determine the endotoxin concentration in the lubricant samples. The lubricant was tested daily during the running of the test for the presence of microbes; however the presence of endotoxin was also determined.

2.4.2.2 Additional Reagents and Equipment

The additional reagents and equipment used in the LAL assay are shown in Table 2.3.

Table 2.3 – Additional reagents and equipment used in the LAL endotoxin assay.

Material	Supplier
Pyrychrome	Associates of Cape Cod Inc.
Pyrochrome reconstitution buffer	Associates of Cape Cod Inc.
Control Standard Endotoxin	Associates of Cape Cod Inc.
LAL reagent water (LRW)	Associates of Cape Cod Inc.
Pyroplate 96 well microplate	Associates of Cape Cod Inc.
Pyrotube test tubes	Associates of Cape Cod Inc.
Precision pipette tips	Associates of Cape Cod Inc.

2.4.2.3 Preparation of Lubricant Samples

Serum lubricant samples were prepared according to the method used in a previous study (Richards, 2008). Lubricant samples from the single station pin-on-plate wear simulator had previously been stored at -20°C; therefore prior to performing the assay, samples were incubated at room temperature for 30 min until the sample had completely defrosted. Samples were then incubated in a sonicating water bath for 40 min at 37°C. Samples were then diluted 1:100 using LAL reagent water prior to conducting the test.

2.4.2.4 Preparation of Reagents

1) Pyrochrome Reconstitution

The Pyrochrome reagent contained an aqueous extract of amebocytes of the horseshoe crab *Limulus polyphemus*, in addition to the chromogenic substrate. The pyrochrome was reconstituted using 3.2 ml of Pyrochrome reconstitution buffer per vial, at least 5 min prior to use. This vial was gently agitated to fully resuspend the pyrochrome pellet, avoiding vigorous mixing to prevent excessive foaming which

would affect the sensitivity of the pyrochrome. The vial of reconstituted Pyrochrome was covered with Parafilm[®] (VWR International, UK) and stored at 2-8°C in the dark when not being used. The reconstituted Pyrochrome was stored for no longer than 8 hours.

2) Control Standard Endotoxin Preparation

The control standard endotoxin was reconstituted using LAL reagent water according to the volume specified on each vial, to give a concentration of 100 EU.ml⁻¹. The reconstituted control standard was then vortexed for 30-60 seconds until complete dissolution occurred. A series of dilutions were then performed to achieve the desired series of four endotoxin standards (5 EU.ml⁻¹, 0.5 EU.ml⁻¹, 0.05 EU.ml⁻¹, and 0.005 EU.ml⁻¹). The standard solutions were vortexed in between each dilution and immediately prior to use to avoid the endotoxin adhering to the glass. Reconstituted endotoxin stock (100 EU.ml⁻¹) was stable for one week and stored at 2-8°C.

2.4.2.5 Performing the LAL Endotoxin Assay

The LAL endotoxin assay was performed using SkanIt[™] Software 3.2, and using a Multiskan[™] GO microplate spectrophotometer. A volume of 50 µl of each diluted sample and standard was dispensed into a Pyroplate 96 well plate in duplicate. A volume of 50 µl LAL reagent water was used as the negative control. The positive product controls were composed of 45 µl sample, with 5 µl 5 EU.ml⁻¹ standard positive control, providing a final endotoxin concentration of 0.5 EU.ml⁻¹ in each positive product control well. The positive product controls were loaded in duplicate.

A volume of 50 µl reconstituted Pyrochrome was then added to the negative control, endotoxin standards, samples and positive product controls to give a ratio of 1:1 (v/v). Immediately after dispensing the Pyrochrome, the 96 well plate was placed in an incubating plate reader. The plate was shaken for 10 seconds in the plate reader, after which a reading was performed using a kinetic reading type with a measurement filter of 405 nm at 37°C.

2.4.2.6 LAL Results Interpretation

Using the data generated in SkanIt™ software, a standard curve was produced, by regression analysis of the reaction time (onset time to reach 0.5OD) against the log endotoxin concentration of standards. The correlation coefficient obtained from the standard curve was required to be greater than 0.980 for a valid curve. The endotoxin concentration of the samples was calculated by the regression equation and adjusted according to the dilution of the samples. The endotoxin level of the negative controls was required to be significantly less than the lowest concentration of control sample used. Samples which exceeded the range of endotoxin level provided by the standard endotoxin concentrations were reported as either < the lowest standard concentration or > the highest standard concentration. The endotoxin concentration recovered from the positive product control was required to be within 50-200% of the known concentration of added endotoxin in the positive product control.

2.4.3 Preparation of UHMWPE particle suspensions in 2% (w/v) agarose gels

Due to the low density and high buoyancy of UHMWPE (0.945 g/cm³), particles cultured in culture medium will float to the surface, whereas cells will adhere to the bottom of the well. This creates a problem due to the lack of contact between the cells and particles, and therefore lack of stimulation of the cells. This problem has been avoided through the use of low melting point agarose as a medium within which to suspend the particles, while the cells can gradually penetrate the porous agarose gel and come into contact with particles. A schematic depicting this is shown in Figure 2.9.

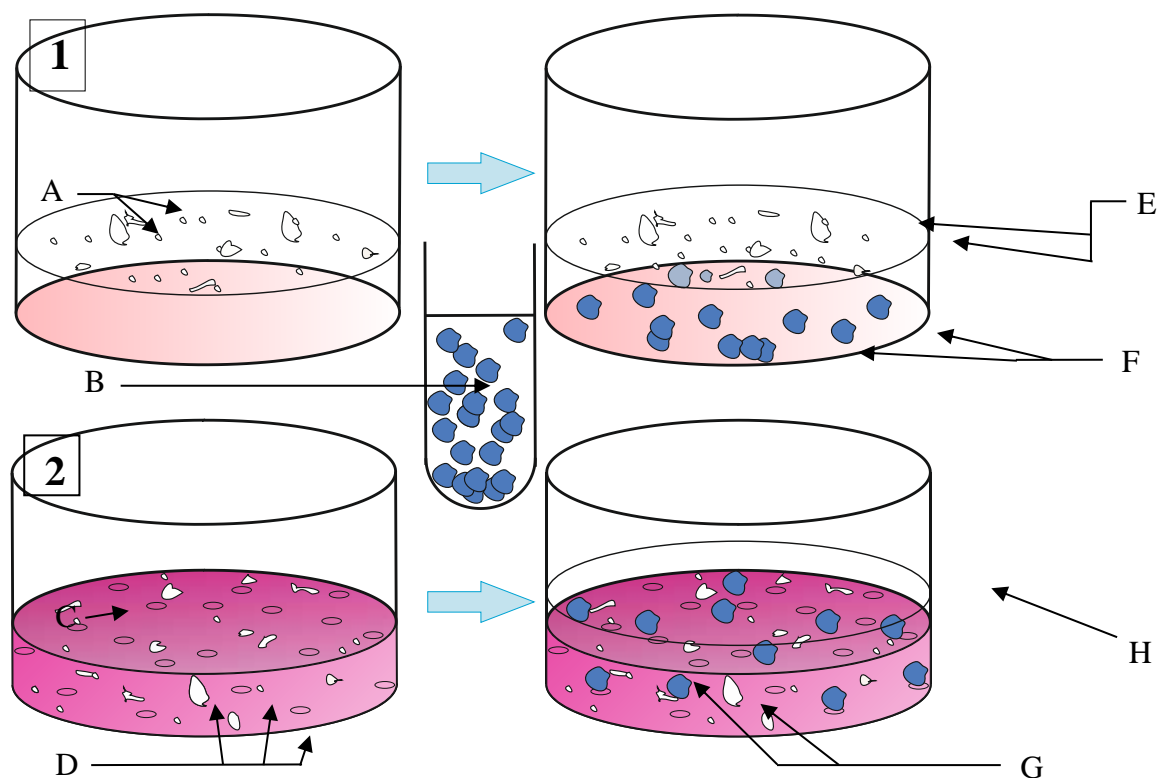


Figure 2.9 – Schematic showing the culture of UHMWPE particles with PBMNCs, both in solution (1) and in 0.4% (w/v) agarose (2). The agarose is necessary to act as a suspension medium for the particles and therefore allows the cells to come into contact with the particles. **A** – UHMWPE particles floating in media due to their high buoyancy; **B** – PBMNCs isolated from blood from a human donor; **C** – 0.4% (w/v) low melting point agarose plug; **D** – UHMWPE particles suspended in 0.4% (w/v) agarose gel; **E** – UHMWPE particles floating in culture media and therefore not in contact with cells; **F** – PBMNCs adhered to the bottom of the well; **G** – In agarose, the UHMWPE particles are held in suspension while the PBMNCs are able to contact the particles. The porous agarose gel allows for the penetration of cells deep into the agarose and the stimulation of macrophages by the particles; **H** – Following particle stimulation, the supernatant was harvested and cytokine release was measured using an ELISA. The cell viability was also determined using the ATP Lite assay.

2.4.3.1 Calculation of the particle volume: cell ratio for cell culture experiments

The conditions for the culture of PBMCs with UHMWPE are shown in Table 2.4. These values show the typical cell seeding density and particle concentration; however these values were altered during the project to determine the optimal conditions.

Table 2.4 – Typical cell culture conditions for the culture of PBMCs with UHMWPE particles in agarose gel.

Cell number	2 x 10 ⁵ per well
Particle Concentration	100 μm ³ per cell
Agarose Gel Concentration	0.4 % (w/v)
Agarose Gel Volume	300 μl
Plate	48 well plate

For this project, lubricants containing UHMWPE wear particles were used in cell culture studies as they were generated, with no fractionation of specific size ranges. This provided a clinically relevant representation of the full size range of wear particles that would be produced *in vivo*. The volume of lubricant required in each well was determined using the calculations shown below.

In order to provide a particle concentration of 100 μm³ per cell, and with a cell seeding density of 2 x 10⁵ per well, a particle volume of 2 x 10⁷ μm³ was required per well. The density of UHMWPE was determined to be as 1 x 10⁻⁶ μg.μm³ according to a previous study by Richards *et al* (2008). With this in mind, the following calculation was applied to determine the mass of particles required:

Equation 4

Mass of particles = Volume of particles x Density

$$= 2 \times 10^7 \mu\text{m}^3 \times 1 \times 10^{-6} \mu\text{g} \cdot \mu\text{m}^3$$

$$= 20 \mu\text{g}$$

Using this calculation, and taking a lubricant containing a particle concentration of $500 \mu\text{g}\cdot\text{ml}^{-1}$, a volume of $40 \mu\text{l}$ of lubricant would be required per well. This test was run in quadruplicate; therefore the total volume for four wells was calculated as $160 \mu\text{l}$. The agarose gel volume per well was $300 \mu\text{l}$, therefore a total volume of $1200 \mu\text{l}$ was required.

In order to have a final agarose concentration of 0.4% (w/v), the 2% (w/v) agarose stock solution required diluting 1:5 in the final gel. A volume of $60 \mu\text{l}$ of 2% (w/v) agarose was therefore required per well ($240 \mu\text{l}$ for four wells). Therefore, in order to make up four 0.4% (w/v) agarose gels containing $100 \mu\text{m}^3$ per cell, a volume of $160 \mu\text{l}$ of $500 \mu\text{g}\cdot\text{ml}^{-1}$ particle suspension ($40 \mu\text{l}$ per well) was added to $240 \mu\text{l}$ of agarose gel ($60 \mu\text{l}$ per well) and $800 \mu\text{l}$ RPMI Transport Medium ($200 \mu\text{l}$ per well), to give a final particle concentration of 2×10^7 per well, and final agarose concentration of 0.4% (w/v) in a $300 \mu\text{l}$ agarose gel.

2.4.3.2 Calculation of the Fluosphere[®] dosing volume required in cell culture experiments

In order to provide a positive control for particle stimulation, 200 nm and 40 nm polystyrene Fluospheres[®] were used. Fluospheres[®] have a uniform size distribution and therefore consistently stimulate PBMNCs to release $\text{TNF-}\alpha$. The Fluospheres[®] were provided at the concentrations shown in Table 2.5.

Table 2.5 – The properties of the Fluospheres[®] used in this study. Fluospheres[®] have a density of $1.05 \times 10^{-6} \mu\text{g}\cdot\mu\text{m}^{-3}$.

Diameter (μm)	Number of FS/ml	Volume of FS/ml (μm^3)
0.2	2.274×10^{12}	9.52×10^9
0.04	2.824×10^{14}	9.52×10^9

Cells were seeded at a density of 2×10^5 cells per well, therefore $2 \times 10^7 \mu\text{m}^3$ of Fluospheres[®] were required for a particle: cell ratio of $100 \mu\text{m}^3$ particles per cell. Fluospheres[®] were provided at a volume of $9.52 \times 10^9 \mu\text{m}^3$ per ml, giving a dilution factor of 476 to get the desired $2 \times 10^7 \mu\text{m}^3$. Using this dilution factor and applying it

to the volume, it was calculated that 2.1 μl of stock Fluospheres[®] was required per well.

2.4.3.3 Preparation of particle containing 0.4% (w/v) agarose gels

Prior to making the particle-gel suspensions, UHMWPE particles were defrosted in a 37°C water bath for 30 min. Fluospheres[®] and the defrosted UHMWPE particles were then placed in a sonicating water bath for a further 30 min. The 2% (w/v) low melting point (LMP) agarose was melted using a microwave at high power for 10 second intervals. The gel was gently mixed in between each 10 second heating period to ensure the gel was fully melted and no air bubbles remaining in the gel. The gel was then allowed to cool to a temperature considered 'hand hot' (35-40°C), when a gloved hand could comfortably hold the bottle of gel yet the gel was still warm.

The gels for each treatment were prepared in sterile bijoux, with the 2% (w/v) agarose the last component added to ensure the gel had as low a viscosity as possible. The particle-agarose suspension was mixed by gently pipetting up and down, and then pipetted into the relevant wells of the 48 well plate. The negative control (cells only) and positive control (lipopolysaccharide) wells were prepared from transport medium and agarose alone, e.g. in a 300 μl gel; 240 μl RPMI transport medium and 60 μl 2% (w/v) agarose.

2.4.4 Isolation of human PBMNCs from the blood of healthy volunteers

This study used 10 healthy donors aged between 24-60 years. All blood was collected in accordance with Faculty of Biological Sciences Ethics Committee approval (BIOSCI 10-018) and informed consent was obtained from the donor prior to venepuncture. The procedure for using blood was recorded and tracked using the Achiever tissue tracking system (Leeds Teaching Hospital NHS Trust and University of Leeds). From each donor, approximately 28 ml of blood was taken using a 21G needle and added to sodium heparinised collection tubes. The blood was collected on the morning of the cell seeding procedure to ensure cells were fresh for seeding.

Isolation of PBMNCs from blood was performed in a class II safety cabinet. Prior to isolation, RPMI 1640 transport medium and RPMI 1640 culture medium (section 2.2.1.1 and 2.2.1.2) were placed in a 37°C water bath for one hour to bring the medium to a suitable temperature for cells.

The blood was mixed gently by inverting the collection tubes and all the blood was pooled in a sterile 150 ml container and immediately diluted 1:1 with RPMI 1640 transport medium. This blood: transport medium mixture was then very carefully layered over 3 ml lymphoprep in sterile test tubes (7 ml blood: transport medium mixture per 3 ml lymphoprep). This was achieved by tilting the test tube, and angling the pipette against the side of the tube so the diluted blood streamed down the wall of the test tube, layering over the lymphoprep without mixing. The tubes were then centrifuged at 800 rcf for 30 min. A band of mononuclear cells was visible at the interface between the lymphoprep and blood plasma. Keeping the contents of each test tube separate, the mononuclear cell band was carefully removed and transferred to a clean sterile test tube using a sterile Pasteur pipette. The volume in each test tube was then made up to 10 ml with RPMI 1640 transport medium. These test tubes were centrifuged at 600 rcf for 30 min to form a pellet of cells at the bottom of each tube. The supernatant was discarded and the pellet resuspended in 10 ml RPMI 1640 transport medium, and centrifuged at 600 rcf for 30 min. This step was repeated if the medium remained cloudy. At this stage a white pellet was formed at the bottom of each test tube. The supernatant was discarded and each pellet was resuspended in 500 µl RPMI 1640 culture medium. These cell suspensions were then pooled to give a total cell suspension volume of 4 ml.

2.4.4.1 Determination of viable PBMNCs using Trypan blue exclusion assay

The Trypan blue exclusion assay is a quick way of determining the number of viable cells in a sample. The cell suspension was gently mixed by inverting to ensure an even concentration of cells throughout, and a 90 µl sample was taken and transferred to a sterile bijou. A volume of 10 µl of Trypan blue was added to the cell suspension sample and mixed by pipetting up and down. A 10 µl Trypan-cell sample was then added to the chamber of a clean haemocytometer. The haemocytometer was then

observed under an inverted light microscope to count the cells. The Trypan blue dye permeated any non-viable cells due to the loss of membrane potential after cell death, but was excluded from live cells, therefore these cells appeared colourless amongst the blue dye. A minimum of 100 cells were then counted from the 5 x 5 square grid in the centre of the haemocytometer. During this study, counting the cells in six randomly selected squares was often sufficient to count over 100 cells. This was then later compensated in the final equation to calculate the cell number. The equation is shown below.

$$\text{Number of cells in 1 ml} = \text{viable cells counted} \times (25/6) \times (10/9) \times 1 \times 10^4$$

Where 25/6 was the correction factor for counting 6 of 25 squares in a known area; 10/9 was the dilution factor for diluting 10 μ l trypan blue with the cell suspension; 1×10^4 was the dilution factor per ml. A working example of this equation is shown below where a typical cell count was 180.

$$= 180 \times (25/6) \times (10/9) \times 1 \times 10^4$$

$$= 8.3 \times 10^6 \text{ in 1 ml}$$

$$= 3.33 \times 10^7 \text{ total cells (in 4 ml)}$$

Data shown in a previous study (Liu, 2012) showed isolated PBMNCs to have a phagocytic fraction of 3-10%, with the author using a final phagocytic fraction of 6%. For this reason, the present study also used a 6% phagocytic fraction, and at this stage in the cell count the number of phagocytic monocytes was calculated using this percentage.

$$= 3.33 \times 10^7 \times 0.06$$

$$= \underline{2 \times 10^6 \text{ total phagocyte count in 4 ml}}$$

2.4.5 Culture of PBMNCs with UHMWPE particles to determine the biological response to wear particles

Following cell isolation and the solidification of the 0.4% (w/v) agarose gel, 2×10^5 cells were added to each well in 1 ml RPMI 1640 culture medium. Lipopolysaccharide (LPS) was added to the positive control wells at a concentration

of 200 ng.ml⁻¹ after seeding the cells. Negative control wells were seeded in the same way but with no particles or treatment. The positive control wells were seeded in a separate 48 well plate to ensure no cross-contamination of LPS. To reduce the rate of evaporation from the wells, 500 µl RPMI 1640 culture medium was added to surrounding wells. Plates were then covered and incubated in an atmosphere of 5% (v/v) CO₂ in air at 100% humidity at 37°C for 24 hours.

Cell viability was determined at the 24 hour time point using the ATP Lite™ assay. Cytokine release was also determined through the harvesting of the supernatant to be used in an ELISA. The supernatant was collected in a 900 µl volume (to account for some evaporation during incubation) and aliquoted into 3 x 96 well plates. A volume of 150 µl was aliquoted into each well, in duplicate, and into three plates to prevent the repeated freeze-thaw of samples ((150 µl x 2) x 3). These plates were wrapped in Parafilm and stored at -20°C until an ELISA was performed.

2.4.5.1 Determining the cell viability using the ATP Lite™ Assay

Adenosine triphosphate (ATP) is a nucleoside triphosphate molecule essential in all metabolically active cells as a source of energy. Its presence in all metabolically active cells makes it an excellent marker for viable cells, while ATP levels rapidly decline in cells undergoing necrosis or apoptosis. This study used a Luminescence ATP Detection Assay System (ATP Lite™) to determine the cell viability of PBMNCs following incubation.

This assay is based on the production of light caused by the reaction between cellular ATP with the added luciferase and D- Luciferin. This reaction is illustrated below.



The emitted light from this reaction is proportional to the ATP concentration with some limitations. The strengths of this assay for determining cell viability include its high sensitivity, linearity, speed and the lack of separation techniques. The assay has a signal half-life of 5 hours.

Prior to use, the reagents were removed from the cold room and incubated at room temperature for 20 min to allow the reagents to warm to room temperature. The culture supernatant in each well was harvested as described in section 2.2.5. A volume of 150 μ l mammalian cell lysis solution was added to each well, the plate was covered and placed on an orbital shaker at 700 rpm for 5 min. The lyophilized luciferase/D-luciferin substrate solution was reconstituted by adding 25 ml substrate buffer solution and gently shaken to dissolve. Following the lysis of the cells, 150 μ l substrate solution was added to each well, covered and wrapped in foil to protect the substrate from light. The plate was shaken on an orbital shaker at 700 rpm for 5 min. A volume of 100 μ l cell lysis solution from each well was transferred to a well in a white 96-well opti-plate in duplicate. This procedure was carried out in the dark to protect the substrate from light, and care was taken during pipetting due to the increase in viscosity of the solution following substrate addition. Following transfer of each sample to the opti-plate in duplicate, an adhesive sealing film was placed on the plate to prevent contamination, and the plate was placed in the black box of Top Count luminometer. After a dark-adapt period of 10 min, the light emission was read in counts per second (cps) of luminescence.

2.4.5.2 Measurement of the TNF- α release from PBMNCs incubated with UHMWPE particles

A solid-phase sandwich enzyme-linked immunosorbent assay (ELISA) was used to determine the concentration of cytokine release from PBMNCs after culture with UHMWPE particles. During this study ELISAs were primarily used to detect TNF- α release; an important cytokine involved in osteolysis (Ingham and Fisher, 2000). The principle behind this assay is the specific binding of the cytokine antigen to antibodies bound to the plate, which in turn leads to the binding of an enzyme which catalyses a substrate added during the process resulting in a colour change. In the presence of the antigen and the downstream binding of the enzyme, the intensity of the final colour change can be used to determine the concentration of the cytokine in the sample.

2.4.5.2.1 Preparation of reagents for the TNF- α ELISA

The reagents used in the ELISA are shown in Table 2.6 and 2.7. Prior to preparing reagents, two litres of phosphate buffered saline (PBS) solution was prepared and autoclaved at 121°C for 20 min, at 103 kPa, and stored at room temperature. Reagents were stored for a maximum of four weeks. The reagents provided with the ELISA kit are shown in Table 2.7.

Table 2.6 –The reagents made up for use with the ELISA kit.

Reagent (Stored at 2-8°C)	Composition
Coating Buffer	PBS (pH 7.2-7.4)
Wash Buffer	PBS with 0.05% (v/v) Tween20
Blocking Buffer	PBS with 5% (w/v) Bovine serum albumin (BSA)
Standard and Secondary Antibody Diluent Buffer	PBS with 1% (w/v) BSA
Streptavidin-HRP Diluent Buffer	PBS with 1% (w/v) BSA, 0.1% (v/v) Tween20

Table 2.7 – The reagents provided with the ELISA kit and the preparation required

Reagent (Stored at 2-8°C)	Preparation
TNF- α Standard; 800 pg/ml	Reconstituted with 1.25 ml diluent buffer
Capture Antibody	Sterile and diluted prior to use
Biotinylated anti-TNF- α Detection Antibody	Reconstituted with 550 μ l of distilled water
Streptavidin-HRP	Diluted prior to use
TMB Substrate	Ready to use

2.4.5.2.2 Preparation of ELISA plate

The ELISA was carried out using Eli-pair ELISA kits (Diacclone, France). For a typical TNF- α ELISA, 100 μ l TNF- α capture antibody was added to 10 ml coating buffer. This was enough to coat a full 96-well Maxisorp plate. A volume of 100 μ l of diluted capture antibody was then added to each well using an automated pipette. The plate was incubated at 4°C overnight. The diluted capture antibody was then

discarded and washed with 350 μ l wash buffer per well. The wash buffer was aspirated with a firm tap over absorbent paper to remove the wash buffer. This was repeated once. A volume of 250 μ l blocking buffer was then added to each well, the plate was covered and incubated at room temperature (18-25°C) for two hours. The plate was then washed with wash buffer a further three times and allowed to dry at room temperature for 24 hours. The plate was then covered, wrapped in Parafilm within an airtight container (with desiccant), and stored at 2-8°C for up to 1 month.

2.4.5.2.3 Performing the ELISA

Prior to performing the ELISA, cell: particle culture supernatant samples were thawed at room temperature for 60 min and all reagents shown in Table 2.6 were prepared. The TNF- α standard was reconstituted with diluent buffer as shown in Table 2.7, giving an 800 pg/ml sample. Serial dilutions were then produced to give 500 μ l of each concentration in sterile bijoux bottles (800 pg/ml, 400 pg/ml, 200 pg/ml, 100 pg/ml, 50 pg/ml, 25 pg/ml). Each dilution was swirled gently during preparation to ensure a homologous solution prior to further dilution. The standards and samples were then dispensed in duplicate at a volume of 100 μ l in each well. Where LPS was used as a positive control the sample was diluted 1:2 due to the anticipated high level of TNF- α release. This was important to ensure the TNF- α level did not exceed the maximum standard concentration. Diluent buffer was added as the blank standard.

The biotinylated anti-TNF- α detection antibody was reconstituted with 550 μ l distilled water prior to use. For one full plate, 100 μ l of reconstituted detection antibody was diluted in 5 ml antibody dilution buffer. A volume of 50 μ l was then dispensed in each well, the plate was covered and then incubated for three hours at room temperature (18 to 25°C). Following this incubation, the liquid was aspirated from the plate and 350 μ l wash buffer was dispensed in each well. The wash buffer was then aspirated and the plate tapped firmly against absorbent paper to remove any liquid. This wash step was repeated three times.

The HRP diluent buffer was prepared as shown in Table 2.6. Streptavidin-HRP was provided in a small volume in a vial, and this vial was centrifuged for 5 seconds prior to use to collect all the volume of the solution at the bottom. A volume of 5 μ l

of streptavidin-HRP was diluted in 500 μ l HRP diluent buffer immediately before use. For a full plate, 150 μ l of diluted streptavidin-HRP was diluted in 10 ml HRP diluent buffer, and 100 μ l of this dilution was added to each well. The plate was covered and incubated at room temperature for 20 min.

The streptavidin-HRP dilution was aspirated from the wells and washed three times with wash buffer, ensuring no liquid remained in the wells following the final wash. A volume of 100 μ l ready-to-use TMB (3,3',5,5'-Tetramethylbenzidine) was added to each well and the plate was covered and immediately wrapped in aluminium foil to incubate in the dark for 15 min at room temperature. A volume of 100 μ l 1M sulphuric acid (H_2SO_4) was added to each well to stop the reaction. During incubation the with TMB the solution turned blue in the presence of TNF- α , and the addition of sulphuric acid then turned the solution yellow. The absorbance value of each well was then read on a multiscan spectrum micro-plate spectrophotometer using a 450 nm primary wavelength and a 630 nm reference wavelength.

2.4.5.2.4 Analysis and Statistical Analysis of ELISA results

A linear standard curve for optical density against TNF- α concentration was generated using the average value for each concentration. From this standard curve, the average optical density for each sample was used to determine the TNF- α concentration in $pg.ml^{-1}$. Where samples were diluted (e.g. LPS), the values were multiplied by their dilution factor.

Final TNF- α values were plotted on a graph, using separate y-axis where there was a considerable difference in value, e.g. LPS on a different y-axis to cells only. Values are shown as means \pm 95% confidence level and analysed using a one-way ANOVA. Differences between the treatment groups and the negative control were determined by calculating the minimum significant difference (MSD) value ($p < 0.05$) using the Tukey-method (Sokal and Rohlf, 1981).

2.4.6 Culture of U937 Cell Line with UHMWPE Wear Debris to Determine the Cellular Response to Wear Particles

Cells derived from the U937 cell line were used in this study as a cell type that would remove the factor of donor variation from the cellular response. The U937 cell line is a human cell type established from a histiocytic lymphoma, displaying monocytic characteristics. Following stimulation it differentiates into macrophage cells, making it an ideal cell type to use as an alternative to PBMNCs isolated from human blood.

2.4.6.1 Resurrection and Splitting of U937 Cells

A vial containing U937 cells was carefully removed from liquid nitrogen and immediately thawed by incubating in a water bath at 37°C until the 1 ml of cell suspension in the vial was completely defrosted. All cell culture using U937 cells was carried out in a class II safety cabinet using aseptic technique. Prior to processing the cells, RPMI 1640 cell culture medium was made up, as described in section 2.4.1.2, and incubated in a water bath for 37°C for 1 hour to bring the medium to a suitable temperature for the cells.

In the class II safety cabinet, the 1 ml cell suspension was pipetted dropwise into 10 ml RPMI 1640 culture medium in a sterile universal. The universal containing cells was centrifuged at 150 rpm for 10 min to pellet the cells. Following this, the supernatant was disposed of, and the pellet was resuspended in 10ml RPMI culture medium. This cell suspension was pipetted into a T25 cell culture flask. The cells were then cultured at 37°C for 24 hours in an incubator. The U937 cell line is a suspension cell line and for that reason, cell culture flasks were incubated at a 45°angle to provide sufficient depth to the culture medium while maintaining a large surface area for gas diffusion.

Cells were viewed daily using a upright microscope to determine confluency. When cells appeared to be 80% confluent, the cell suspension was once again centrifuged at 150 rpm to pellet the cells. The cells were then resuspended in 10 ml RPMI 1640 culture medium, and the cell suspension was pipetted into two T25 cell culture flasks; 5 ml into each. A further 5 ml RPMI 1640 cell culture medium was then

added to each flask to provide a final volume of 10 ml per flask. Cells were incubated and split in this way until a sufficient density of cells was available.

2.4.6.2 Differentiation of U937 Cells

In order to stimulate the U937 cell line to become macrophages, cells were incubated in RPMI 1640 culture medium as described in section 2.4.1.2, with the addition of 10 ng.ml^{-1} phorbol 12-myristate 13-acetate (PMA). The PMA in the culture medium acts as a stimuli for macrophage differentiation. Cells were cultured in this PMA-enhanced culture medium for 24 hours with the flask laid flat to allow cells to settle. Cells were viewed under an upright light microscope, and differentiated cells could be seen attaching to the bottom of the flask. Following differentiation, the PMA-enhanced medium was removed from the flask, the cells were washed with 10 ml Dulbeccos Phosphate Buffered Saline (DPBS), followed by the addition of 10 ml fresh RPMI 1640 culture medium to be incubated with for 24 hours with the flask laid flat.

2.4.6.3 Harvesting and Culture of U937 Cells with UHMWPE Wear Debris

Prior to harvesting of differentiated U937 cells, trypsin/EDTA was warmed to 37°C in a water bath for 15 min. Trypsin/EDTA is used to detach cells from cell culture flasks in order to then isolate cells for cell culture. Flasks were viewed under the light microscope to ensure cell attachment. The cell culture medium was aspirated from the flask and 3 ml trypsin/EDTA was added to each flask. The cells were incubated with the trypsin/EDTA for 3 min at 37°C , after which the cells were gently tapped on the side to assist with cells detachment. The flasks were incubated for a maximum of 7 min (10 min total trypsin/EDTA incubation) depending on the process of cell detachment as seen using the light microscope.

The cell suspension was then aspirated from the flask and transferred to a sterile universal. A volume of 10 ml RPMI cell culture medium was added to the cell suspension to inhibit the trypsin/EDTA. Universals containing cells were centrifuged at 150 rpm for 10 min to pellet the cells. Following centrifugation, the supernatant

was disposed of, and the pellet of cells was resuspended in a known volume of RPMI 1640 culture medium.

Following the isolation of differentiated U937 cells, the number of viable cells was determined using the Trypan blue exclusion assay, as outlined in section 2.4.4.1. Cells were then seeded onto the agarose gels and incubated for 24 hours at 37°C, after which the cell viability was determined and the supernatant collected for TNF- α analysis, using the methods described in section 2.4.5.

2.4.7 Confocal Imaging of UHMWPE Particle Uptake by PBMNCs in 0.4% (w/v) Agarose Gel

In order to determine the uptake of UHMWPE wear debris by PBMNCs incubated using the agarose gel technique, fluorescently-labelled UHMWPE wear particles were embedded in the agarose gel, where PBMNCs were then seeded onto the gel, using the same culture method outlined in section 2.4.4. The main differences with this protocol is that the particle: cell culture is performed on a smaller scale using wells on a microscope slide, in addition to the use of fluorescent UHMWPE wear particles.

2.4.7.1 Generation of Wear Particles under Aseptic Conditions for Particle Uptake Studies

For the generation of sterile wear debris from the UHMWPE material, the aseptic single station wear simulator was used, as described in section 2.2. The preparation of the pin and simulator, and running of the simulator was performed as described in section 2.2. The only change was the use of 100% RPMI 1640 Transport Medium as the lubricant throughout the test. This was in order to provide a protein free environment which was necessary for fluorescein labelling of particles. Following the wear test, the particle lubricant suspension was collected and stored at -20°C until required.

2.4.7.2 Fractionation of UHMWPE Wear Debris using Filtration

In order to investigate the uptake of UHMWPE wear debris in two size ranges, UHMWPE wear debris was fractionated to produce a micrometre sample and a nanometre-sized sample. Fractionation of UHMWPE wear debris involved filtering the stock particle suspension onto a series of filters, after which the filters could be sonicated to disperse the particles into solution.

The filtration and labelling method was performed in a class I laminar flow cabinet to ensure the particle suspension remained sterile. Prior to filtration, 10 μm , 1 μm and 0.015 μm pore sized filters were washed with 70% (v/v) ethanol and dried under an infrared light for four hours. The filters were then weighed using an AT21 balance, accurate to 1 μg . All filtration glassware was sterilised in the oven at 190°C for 3 hours, while all polymer equipment was sterilised in the autoclave at 121°C for 20 min, at 103 kPa. The laminar flow cabinet was cleaned thoroughly with 70% (v/v) prior to use, and all equipment was sprayed with 70% (v/v) ethanol when being moved into the cabinet.

The stock particle suspension was then sequentially filtered through the filters, using the method outlined in section 2.3.2, with the only change being the use of sterile equipment and the use of aseptic technique in terms of spraying 70% (v/v) ethanol on gloves and equipment. Each filter was dried under an infrared light for four hours in the laminar flow cabinet, after which the filter was weighed to determine the mass of UHMWPE wear debris collected on each filter.

The 0.015 μm and 1 μm filters were cut into small pieces and separately added to a universal containing 5 ml RPMI Transport Medium to ensure each piece of filter paper was submerged. The universals were then sonicated for 30 min to disperse the wear particles into the solution, and then stored at 4°C until required for labelling.

2.4.7.3 Fluorescent Labelling of UHMWPE Wear Particles

In order to visualise the wear particles in the presence of cells under a confocal microscope, the wear particles were labelled with sodium fluorescein according the method described previously by Liu (2012).

The staining process was performed in a class I laminar flow cabinet to ensure sterility of particle suspensions. Micrometre and nanometre article suspensions prepared in section 2.4.7.2 were placed in a sonicating water bath for 30 min at 37°C to disperse the wear particles throughout the solution. A correct volume to provide 200 µg wear particles was taken from each particle suspension, and placed in separate sterile universals. A mass of 10 mg fluorescein sodium powder was dissolved in 10 ml sterile water to provide a sodium fluorescein dye solution at a concentration of 1 mg.ml⁻¹. A volume of 2 ml sodium fluorescein dye solution was added to each universal containing the particle suspensions, followed by 2 ml sterile bicarbonate buffered saline solution. The wear particles were incubated with the sodium fluorescein bicarbonate buffer overnight at 4°C.

Prior to filtration, two 25mm diameter 0.015 µm pore-sized filters were washed with 70% (v/v) ethanol and dried under an infrared lamp for four hours in a class I laminar flow cabinet. Following the particle-fluorescein dye incubation, the micrometre and nanometre particle suspensions were filtered separately through the 0.015 µm filter. This was followed by 15 ml RPMI 1640 Transport Medium to wash through any unbound sodium fluorescein. The filters were then separately placed in clean sterile universals, where 1 ml RPMI 1640 Transport Medium was added to each universal. The universals were then sonicated to disperse the labelled UHMWPE wear particles, ready to use in cell culture.

2.4.7.4 Culture of Fluorescently Labelled UHMWPE Wear Particles with PBMNCs

In order to image the agarose gel in which the UHMWPE wear particles were suspended, a thinner well was required to eventually fit under a confocal microscope lens. The author could not find a suitable cell-culture apparatus to provide this, and therefore constructed a custom cell culture-microscope slide. This involved a standard 75 x 26 mm microscope slide, with several layers of vinyl tape built up on one side of the slide to produce a stage. In this stage, a 10 x 10 square well was cut out using a scalpel blade. This well was deep enough to hold approx. 400 µl solution. An additional adjustment was the addition of an extra-long piece of tape for the sixth piece. This allowed for a tab to peel off the majority of the strips of tape prior to

imaging under the confocal microscope, leaving the well six-strips deep to hold the agarose gel for imaging. Prior to use, the wells of the apparatus were washed with 70% (v/v) ethanol and dried at room temperature for 2 hours. The apparatus was then sterilised in an autoclave at 121°C for 20 min, at 103 kPa. A schematic of the microscope-cell culture well construction is shown in Figure 2.10.

Following optimisation, it was determined that an agarose gel volume of 100 μl , with a total cell suspension volume of 280 μl , was the optimum cell culture condition. Particles were dosed at a concentration of 100 μm^3 per cell in 0.4% (w/v) agarose. Cell isolation and seeding of PBMNCs was carried out as described in section 2.4. Cells were incubated with UHMWPE wear debris over a period of 48 hours at 37°C in 5% (v/v) CO_2 in air. Fresh RPMI 1640 Culture Medium was added to the well at regular intervals to maintain the level of culture medium. Throughout the incubation, every effort was taken to protect the fluorescent particles from direct light.

Prior to imaging using the confocal microscope, cell culture medium was carefully extracted from the well. Cells were washed twice in DPBS, followed by the addition of 100 μl Hoechst 33342 ($5\mu\text{g}\cdot\text{ml}^{-1}$) to each well. Cells were incubated for 10 min in the dark, after which the Hoechst 33342 was aspirated from each well. The top layers of tape were removed, leaving the agarose gel in a smaller well. A volume of 100 μl RPMI 1640 Transport medium was added to each well, and a sterile cover slip was applied over each well. The slides were now ready for imaging.

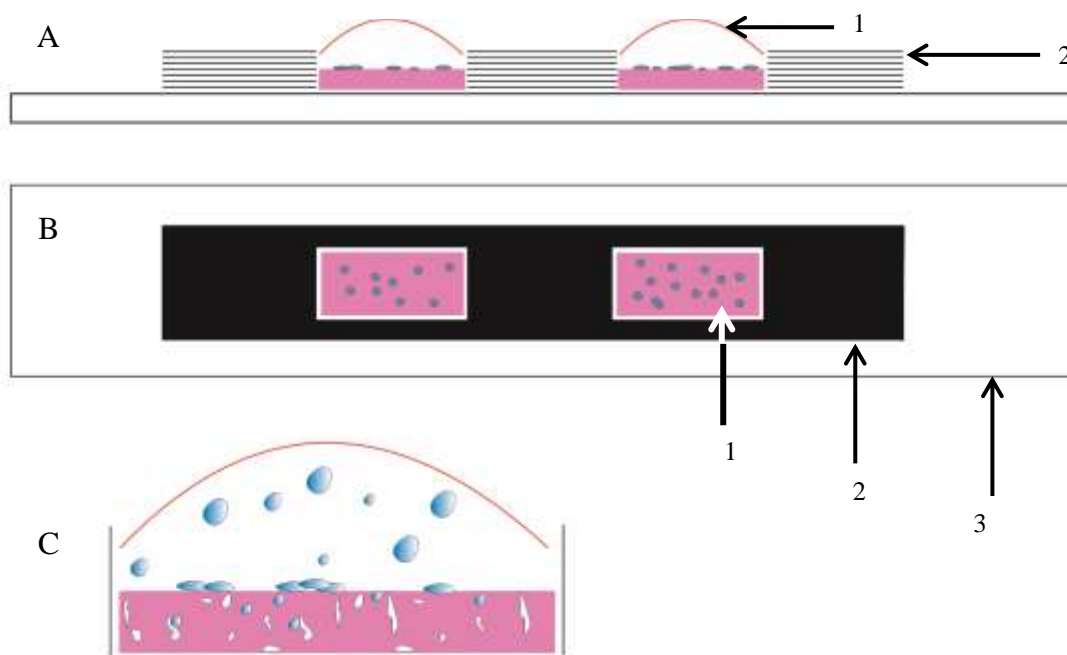


Figure 2.10 – Schematic showing the microscope slide – cell culture well assembly. Image A shows a side view of the apparatus, where layers of vinyl tape (2) were built up on a microscope slide (3) to create a solid stage. In this stage, two 10 x 10 mm wells were cut using a scalpel. In each well, 100 μ l agarose gel- particle suspension was added (1); followed by 280 μ l RPMI 1640 Culture Medium containing PBMNCs. Image B shows a birds-eye view of the apparatus. Image C shows a close up of an individual well. The agarose gel can be seen with UHMWPE particles embedded in it. PBMNCs are seeded on top of the gel (blue cell), while the red curved line indicated the meniscus of the Culture medium.

2.4.7.5 Confocal Laser Scanning Microscopy Imaging of UHMWPE Particle Uptake by PBMNCs

A Zeiss LSM510 Confocal laser scanning upright microscope was used to demonstrate the uptake of UHMWPE wear particles by PBMNCs in agarose gel culture. The images were taken using a 63 X oil lens with helium and argon lasers switched on. Channels for DAPI and FITC were used to image the blue nucleus and green fluorescent labelled particles respectively, in addition to bright field microscopy. Images were extracted and overlays were processed using ZEN 2009 software (Carl Zeiss Microscopy Ltd.). Throughout imaging, any bubbles under the cover slip were removed by reapplying to cover slip over fresh transport medium.

Chapter 3

Pin on Plate Wear Testing and Particle Characterisation of Antioxidant UHMWPE Materials With and Without Crosslinking

3.1 Introduction

In order to determine the wear performance of total hip replacements, wear simulators with varying degrees of sophistication have been used. Physiologically relevant joint simulators allow for the performance of the joint replacement to be analysed in detail, identifying the effects of design or changes in the motion of the walking cycle. A pin-on-plate wear simulator is a simpler simulator that enables the reproduction of some of the wear mechanisms observed *in vivo*, and thus allows the wear performance of the materials to be compared and evaluated, in addition to producing clinically relevant wear particles (Lancaster et al., 1997, Endo et al., 2001, Ingram et al., 2004, Galvin et al., 2006, Affatato et al., 2008). A six station multidirectional pin-on-plate wear simulator has been shown to be a suitable for determining the wear rate of UHMWPE due its ability to run six stations concurrently under the same conditions. Using kinematics shown to replicate the conditions in the hip during normal gait, clinically relevant wear debris has been produced and characterised (Galvin et al., 2006).

The wear performance of UHMWPE is critical to the survivorship of joint replacements that use UHMWPE as the bearing material. Osteolysis caused by UHMWPE wear particles is considered to be one of the most important modes of failure of metal-on-UHMWPE primary total hip replacements, accounting for around 75% of all failures (National Joint Registry, 2013). Particles generated from UHMWPE stimulate the activation of macrophages around the prosthesis, leading to an innate immune response that culminates in an increase in activity of osteoclasts (Bertolini et al., 1986). This causes an increase in bone resorption around the prosthesis, loosening the implant, which leads to pain and the need for revision surgery. The developments of UHMWPE over the last 20 years have focused on

increasing the wear resistance of the material in order to reduce osteolysis. The improvements in UHMWPE can largely be attributed to the introduction of gamma sterilisation in a vacuum or inert environment, barrier packaging, and the resultant high levels of crosslinking.

Highly crosslinked UHMWPE has been shown to produce significantly lower wear rates compared to virgin UHMWPE (Chiesa et al., 2000, Galvin et al., 2006). However, free radicals are generated during gamma irradiation through chain scission of the polymer, and these radical species have the potential to cause oxidation of the polymer. While some free radicals recombine to form beneficial crosslinks, most remain in the crystalline domain of the material and do not recombine, and it is these free radicals that are able to cause oxidation which can reduce the mechanical properties of UHMWPE (Wannomae et al., 2006). While thermal treatments were introduced in order to reduce the free radical burden, the challenge was to find a compromise between preserving the mechanical properties of UHMWPE whilst effectively removing the free radicals (Baker et al., 2003). Vitamin E was added to highly crosslinked UHMWPE in order to protect against oxidation whilst removing the need for heat treatment, therefore preserving the mechanical properties of UHMWPE. While studies have shown a reduction in the wear rate for vitamin E enhanced highly crosslinked UHMWPE compared to virgin UHMWPE (Haider et al., 2012, Micheli et al., 2012), no studies have clearly outlined the effect of each separate treatment (crosslinking and vitamin E enhancement) on the wear rate of UHMWPE. Alternative antioxidants to vitamin E are also being researched, with the aim of developing a more oxidative resistant material. Hindered phenols are antioxidants commonly used in industry, and one form of hindered phenol has recently been used in UHMWPE clinically under the name of AOX™ UHMWPE for use in knee replacements. The same material is also being investigated for use in hip replacements. Despite this, few studies have directly compared the wear performance of this new hindered phenol UHMWPE to other clinical highly crosslinked and antioxidant UHMWPE materials.

In addition to the wear rate of UHMWPE, particle size distribution has been shown to play an important role in osteolysis. A critical size range for macrophage activation has been shown to be 0.2-0.8µm (Ingham and Fisher, 2000). It is therefore important to focus on the wear rate *and* particle size distribution when evaluating

UHMWPE materials in terms of their clinical performance and potential to reduce osteolysis.

The aim of this section of the study was to investigate the wear of current clinical and experimental antioxidant UHMWPE materials. Specifically, this involved the wear testing of GUR1050 UHMWPE with three different levels of crosslinking, both with and without 1000 ppm vitamin E enhancement. This study also investigated the wear of GUR1020 UHMWPE at two different levels of crosslinking, both with and without the addition of a hindered phenol antioxidant (AOXTM UHMWPE). The wear particle morphology and size distribution of these UHMWPE materials was determined in order to investigate whether crosslinking and/or antioxidant enhancement had any effect on the wear factor or wear particle size distribution, and hence potentially on clinical performances of these materials.

A six station pin-on-plate wear rig was used to determine the wear of UHMWPE pins of each material. The wear rig incorporated multidirectional motion to replicate the kinematics found in the natural hip joint. Wear tests were performed against counterfaces comprised of smooth high-carbon cobalt chromium (CoCr) plates which simulated the smooth CoCr femoral head of the total hip replacement that would be used clinically. The wear test serum lubricant samples were collected and the particles isolated from the serum to determine the size distribution and particle characteristics produced by each material.

3.2 Materials and Methods

3.2.1 Materials

The UHMWPE materials tested in this chapter are shown in Table 3.1. The UHMWPE materials were kindly provided by DePuy Synthes Joint Reconstruction (Leeds, UK; Warsaw, USA) and MediTech Medical Polymers (Pennsylvania, USA). Additional gamma irradiation treatments were required for some experimental materials, and these were provided by DePuy Synthes Joint Reconstruction. Additional general materials used in this chapter are described in Tables A-1,-2 and-3 in Appendix A.

Table 3.1 – UHMWPE materials tested in this chapter, including the resin, gamma irradiation dose, antioxidant, supplier and the abbreviation to be used for each material throughout the chapter. *The exact dosage of hindered phenol in the AOX™ UHMWPE was disclosed by the manufacturer to be 700 ppm. The comparison of two separate doses of antioxidant (vitamin E – 1000 ppm; hindered phenol – 700 ppm) was not considered significant to the study, due to the difference in the chemical structure of the compounds in terms of the number of groups capable of neutralising radical species.

Name	Resin	Gamma Irradiation Dose	Antioxidant	Abbreviation
1050 Virgin	GUR1050	0 MRad	none	1050 Virgin
1050 Marathon®	GUR1050	5 MRad	none	1050 Marathon
1050 Highly Crosslinked UHMWPE	GUR1050	10 MRad	none	1050 HXL
1050 Vitamin E enhanced UHMWPE	GUR1050E	0 MRad	Vitamin E 1000 ppm	1050 Vit E
1050 Vitamin E enhanced UHMWPE + 5 MRad irradiation	GUR1050E	5 MRad	Vitamin E 1000 ppm	1050 Vit E 5
1050 Vitamin E enhanced UHMWPE + 10 MRad irradiation	GUR1050E	10 MRad	Vitamin E 1000 ppm	1050 Vit E 10
1020 Virgin UHMWPE	GUR1020	0 MRad	none	1020 Virgin
1020 Hindered Phenol enhanced UHMWPE	GUR1020	0 MRad	Hindered Phenol 700 ppm*	1020 AOX
1020 Hindered Phenol enhanced UHMWPE + 8 MRad irradiation	GUR1020	8 MRad	Hindered Phenol 700 ppm*	1020 AOX 8

The GUR1050 vitamin E enhanced UHMWPE material supplied by Meditech Medical Polymers (0 MRad, 5 MRad and 10 MRad) used GUR1050 UHMWPE as the raw material, with 1000 ppm vitamin E blended with the UHMWPE resin prior to consolidation.

Pins of each material were machined in-house to have a 10 mm wear face, and were soaked in deionised water for two weeks prior to weighing to ensure moisture uptake was stabilised prior to the wear test. High-carbon (0.27% w/v) cobalt chromium smooth ($R_a < 0.01$) plates were used as the counterface surface, and the mean R_a was determined prior to each test, as outlined in section 2.1.2.3.

3.2.2 Determination of Wear Factor of Different UHMWPEs using the Six Station Pin-on-Plate Wear Simulator

The wear tests were carried out using a multidirectional six station pin on plate simulator which is described in detail in Chapter 2.1. The purpose of the tests was to gravimetrically measure the mass loss from each pin over the course of two weeks (approximately 500,000 cycles), and then to calculate the wear factor for each UHMWPE material using equation 3 shown in section 2.1.2.9. During testing, at least two pins of each material were tested at the same time, depending on the allocation of the six stations, to give a final test sample of $n = 4$ for each material. During these wear tests, the six station pin-on-plate wear simulator was operated using a 28 mm stroke length with a rotation of $\pm 30^\circ$, under a load of 160 N, at a frequency of 1 Hz, as described in section 2.1.2.6.1. The wear tests used a serum lubricant comprised of 25% (v/v) bovine serum with 0.03% (w/v) sodium azide.

Pin on plate tests were performed using smooth high-carbon CoCr counterfaces, to replicate the smooth CoCr femoral heads articulating against the UHMWPE bearing *in vivo* (Eberhardt et al., 2009). To ensure plates had a mean surface roughness of $R_a \leq 0.01 \mu\text{m}$, each plate was measured using a Form Talysurf Contacting Profilometer. A total of four measurements were taken for each plate (Figure 2.2A, section 2.1.2.3) to give a mean value for each of the four plates tested against four pins. The mean surface roughness of each plate tested against GUR 1050 UHMWPE pins are shown

in Table 3.2. The mean surface roughness for plates tested against GUR 1020 UHMWPE pins are shown in Table 3.3. All plates used in the wear test had a surface roughness of $R_a \leq 0.01\mu\text{m}$ (two decimal places).

Table 3.2 – Mean surface roughness of each smooth high-carbon CoCr plate used in this study against GUR 1050 UHMWPE pins. Plates with a mean $R_a \leq 0.01\mu\text{m}$ (2 decimal places) were considered smooth. The table shows the mean value (\pm 95% confidence level, $n=4$). The measurement tracks to determine the mean roughness are shown in section 2.1.2.3. Four plates were measured to test against the four pins tested for each material.

UHMWPE Material	Mean R_a of CoCr Counterface (μm)			
	Plate 1	Plate 2	Plate 3	Plate 4
1050 Virgin	0.00603 (± 0.0009)	0.00638 (± 0.0028)	0.0074 (± 0.0018)	0.00743 (± 0.003)
1050 Vit E	0.00903 (± 0.0005)	0.00795 (± 0.0022)	0.00673 (± 0.0035)	0.00705 (± 0.0026)
1050 Vit E 5	0.00638 (± 0.0009)	0.0077 (± 0.0006)	0.00508 (± 0.0004)	0.00868 (± 0.0044)
1050 Marathon	0.01063 (± 0.0008)	0.00515 (± 0.0011)	0.00735 (± 0.0031)	0.0077 (± 0.0004)
1050 Vit E 10	0.00508 (± 0.0051)	0.00868 (± 0.0022)	0.01063 (± 0.0033)	0.00478 (± 0.0003)
1050 HXL	0.00735 (± 0.0014)	0.00618 (± 0.0006)	0.00853 (± 0.0019)	0.00605 (± 0.0007)

Table 3.3 – Mean surface roughness of each smooth high-carbon CoCr plate used in this study against GUR 1020 UHMWPE pins. Plates with a mean $R_a < 0.01\mu\text{m}$ (2 decimal places) were considered smooth. The table shows the mean value (\pm 95% confidence level, $n=4$). The measurement tracks to determine the mean roughness are shown in section 2.1.2.3. Four plates were measured to test against the four pins tested for each material.

UHMWPE Material	Mean R_a of CoCr Counterface (μm)			
	Plate 1	Plate 2	Plate 3	Plate 4
1020 Virgin	0.00758 (± 0.0009)	0.00595 (± 0.0003)	0.00738 (± 0.00068)	0.00995 (± 0.0002)
1020 AOX	0.00938 (± 0.0015)	0.0063 (± 0.0008)	0.0057 (± 0.0004)	0.0057 (± 0.0008)
1020 AOX 8	0.00668 (± 0.0016)	0.00918 (± 0.0071)	0.00668 (± 0.0006)	0.00653 (± 0.009)

The pin-on-plate wear simulator was assembled as described in section 2.1.2.6. A control pin of each material was soaked in 25% (v/v) bovine serum lubricant for the duration of the wear test to determine the uptake of lubricant throughout the test. The only variable in the test was the UHMWPE material used. Prior to and after a wear test, the pin was cleaned and weighed as described in section 2.1.2.4 to determine the mass loss during the wear test. The wear factor was then calculated for each pin using the equation outlined in section 2.1.2.9, after which the mean wear factor for each material was calculated to compare the wear performance of the different UHMWPE materials.

The two resins used in this study; GUR 1050 and GUR1020 are UHMWPE resins produced by Ticona. The major difference between these resins is their average molecular weight, with the GUR 1050 having an average molecular weight of 3.5×10^6 g/mol, and GUR 1020 having an average molecular weight of 5.5×10^6 g/mol. These resins did not contain added calcium stearate unlike some historical resins (such as GUR 1150 and 1120).

3.2.3 Characterisation of UHMWPE Wear Debris from the Six Station

Pin-on-Plate Wear Simulator

The aim of this part of the study was to characterise the size distribution of wear particles generated from each material during simple configuration wear simulation using the six station pin-on-plate wear simulator. The importance of particle size and volume distribution in the biological response to these particles has been shown in several studies (Green et al., 1998, Ingham and Fisher, 2000). A critical size range of 0.1-1.0 μm at a dose of 100 μm^3 per cell has been shown to stimulate a response in macrophages, showing the importance of the particle size distribution to the subsequent biological response. It is therefore important to determine the size and volume distribution of the particles from each material to examine these aspects of the materials' potential to stimulate a biological response.

The method for particle isolation and characterisation has been previously outlined by Richards et al., (2008). The principle behind this method was to remove proteins, lipids and salts, which may appear as contamination on the filters and will affect the SEM imaging, making particle characterisation difficult. Following the culmination of each wear test, the serum lubricant was collected from each station for isolation and characterisation of the wear debris for each UHMWPE material. Serum proteins were digested in alkali solution, followed by the removal of lipids using multiple 2:1 chloroform: methanol incubations. The methods used for particles isolation are described in detail in section 2.3.1. Lubricant samples were then filtered through a series of filters to collect the wear particles on the filter surface for SEM imaging. The filters used were 10 μm , 1 μm and 0.015 μm pore sized filters, and the filtration method is described in section 2.3.2. The particles present on these filters were imaged using a high resolution FEGSEM, as described in section 2.3.3. The particles in these images were then sized using Image Pro Plus image analysis software to generate a frequency and volume size distribution graphs for each material. The method used to generate these distribution graphs is described in section 2.3.4 (Richards, 2008).

3.3 Results

3.3.1 Determining the Wear Factor of UHMWPE With and Without an Antioxidant and at Three Levels of Crosslinking

The mean wear factors for the GUR 1050 UHMWPE and GUR 1020 UHMWPE pins tested in multidirectional pin on plate tests against smooth CoCr counterfaces are shown in Figure 3.1. With both GUR1050 and GUR1020 UHMWPE materials, there was a significantly lower wear factor as the levels of crosslinking increased. The mean wear factor of the 1050 HXL (10 MRad) UHMWPE material was 52% lower than the wear rate of the 1050 Virgin UHMWPE, and this difference was statistically significant (ANOVA, $p < 0.05$). The mean wear factor of Marathon UHMWPE (5 MRad) was 32% lower than that the wear rate of 1050 Virgin, with this difference also statistically significant (ANOVA, $p < 0.05$). This demonstrated a clear correlation for a decreased wear factor as the crosslinking level increased in non-antioxidant GUR1050 UHMWPE.

The mean wear factors for the vitamin E enhanced materials showed a similar trend to the non-antioxidant GUR1050 materials. The mean wear factor for 1050 Vit E 10 (10 MRad) UHMWPE was 65% lower than the mean wear factor of 1050 Vit E (non crosslinked) UHMWPE, and this was a statistically significant difference (ANOVA, $p < 0.05$). Furthermore, a significantly lower wear factor was observed in 1050 Vit E 5 (5 MRad) compared to the non-crosslinked 1050 Vit E UHMWPE material.

In order to determine any interaction between the GUR 1050 UHMWPE irradiation dose and additive level, a two-way analysis of variance was carried out (Irradiation dose vs additive). This showed no significant interaction between the two variables, supporting the observation that the addition of vitamin E to GUR 1050 UHMWPE had no effect on the wear factor.

Comparing the GUR1020 materials in a separate sub-group analysis of variance, there was no significant difference in the mean wear factors of each material, despite the addition of the hindered phenol antioxidant to UHMWPE, or with increasing the level of crosslinking (8 MRad)(ANOVA, $p > 0.05$). The mean wear factor of 1020 AOX UHMWPE was 18% lower than 1020 Virgin UHMWPE, with the mean wear factor of 1020 AOX 8 35% lower than the wear factor of 1020 Virgin UHMWPE.

These results demonstrated that increasing the levels of irradiation of UHMWPE increased the wear resistance of the material through beneficial crosslinking. To determine the effects of the addition of an antioxidant on the wear factor, comparisons were made between groups of materials.

When comparing the two GUR1050 materials without any crosslinking (1050 Virgin/ 1050 Vit E), there was no significant difference in their mean wear factors. This lack of a significant difference in the wear factor was observed in all the GUR1050 UHMWPE materials that possessed the same levels of crosslinking, such as the 5 MRad crosslinked materials 1050 Marathon and 1050 Vit E 5 ; and with the 10 MRad crosslinked materials 1050 HXL and 1050 Vit E 10 (ANOVA, $p>0.05$). These results indicated that the addition of vitamin E at 1000 ppm to GUR1050 UHMWPE had no significant effect on the wear factor under normal wear conditions. With the addition of the AOX antioxidant to GUR1020, there was no significant effect on the mean wear factor (comparing 1020 Virgin with 1020 AOX).

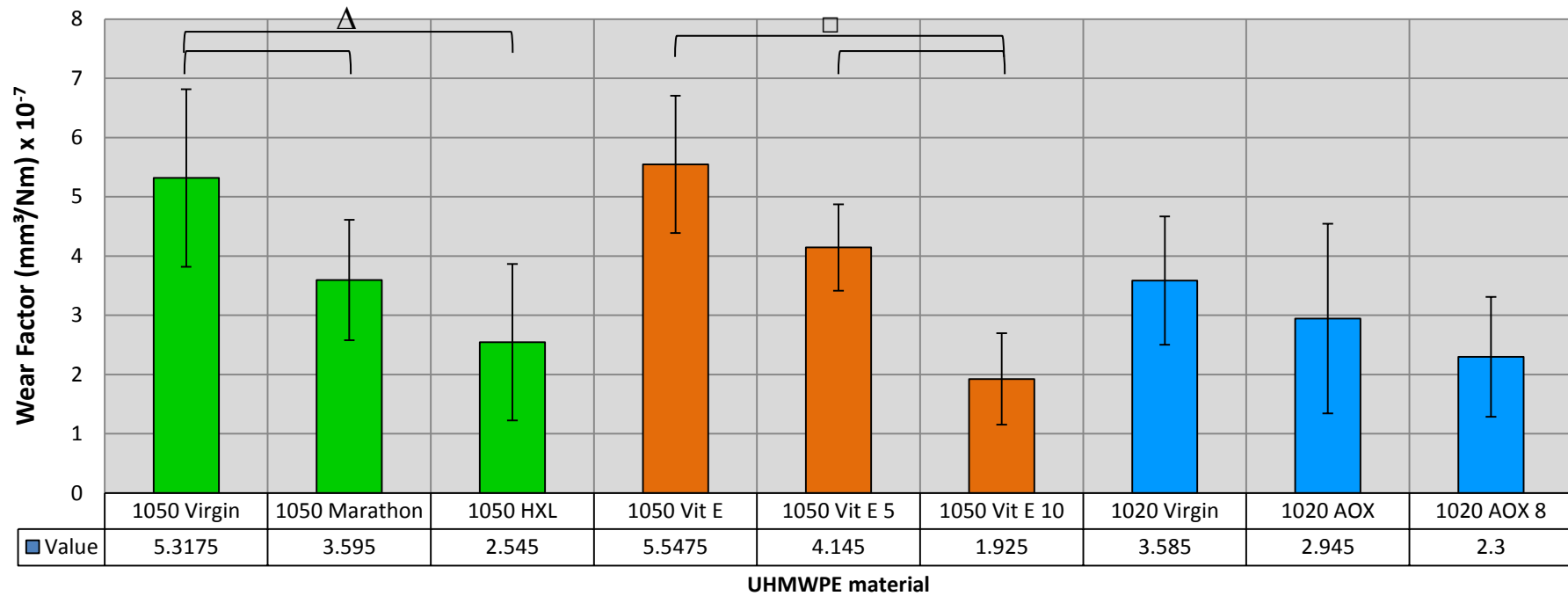


Figure 3.1 – Mean wear factors for each UHMWPE material after 2 weeks testing (>500,000 cycles) against smooth CoCr plates in 25% (v/v) bovine serum. Error bars show the 95% confidence level; n=4. Green bars show the wear factors of the non-enhanced GUR 1050; Orange bars show vitamin E enhanced GUR 1050; Blue bars show GUR 1020. Δ - depicts the significantly higher mean wear factor of 1050 Virgin and 1050 Marathon compared to 1050 HXL UHMWPE; \square – shows a significant higher mean wear factor of 1050 Vit E and 1050 Vit E 5 compared to 1050 Vit E 10 (ANOVA, $p < 0.05$).

3.3.2 Isolation and Characterisation of Wear Particles Generated from UHMWPE With and Without Crosslinking and Antioxidant Addition

For the GUR 1050 UHMWPE materials, the particles from 1050 Virgin, 1050 HXL and 1050 Vit E 10 were characterised. It was thought these materials would provide a good indication of the effect, if any, that crosslinking and/or vitamin E doping has on the size distribution of the wear particles compared to 1050 Virgin UHMWPE. Comparing the clinically relevant highly crosslinked UHMWPE and vitamin E enhanced clinically relevant UHMWPE materials to the virgin material allowed any significant difference in particle size distribution to be evident

From the six station pin-on-plate wear simulator tests, the serum lubricant from three of the four stations was processed and isolated, as described section 2.3. Samples from separate stations were kept separate throughout the whole process to allow for an n=3 value.

3.3.2.1 Isolation and Characterisation of Wear Particles Generated from GUR1050 Virgin UHMWPE and GUR1050 Vitamin E enhanced Highly Crosslinked UHMWPE

The SEM images showing wear particles from 1050 Virgin UHMWPE are shown in Figure 3.2, highlighting some of the different particle morphologies. Particles observed on the 10 μm filter were typically large, flake-like particles, as highlighted by the black arrow in image A. The yellow arrow in image A highlights a cluster of smaller, granular particles. The black arrow in image B shows a globular-shaped particle. A long, fibril shaped particle is shown in image D, highlighted by the black arrow. A globular particle of around 1 μm in length can also be seen alongside the fibril shaped particle.

The mean percentage frequency and volume size distribution graphs for the 1050 Virgin particles are shown in Figure 3.3. The mode of the frequency size distribution was within the 0.1-1.0 μm size range, however a large number of nanoscale particles were also isolated, with around 45% particles in this <0.1 μm size range. Around 5% of the total number of particles were in the 1.0-10 μm size range, with even fewer particles in the larger >10 μm size range.

The volume size distribution graph shows the importance of analysing volume in addition to frequency distribution, as a clear difference can be seen. The mode of the volume size distribution of 1050 Virgin wear particles was in the 1.0-10 μm size range, with around 56% of the volume of particles in this size range. Around 26% of the volume of particles was in the 0.1-1.0 μm , with less than 20% of the volume of particles in the larger >10 μm size range. As expected, despite nanoscale particles contributing a significant portion of the number of particles, these particles make up a very small percentage of the total volume of particles.

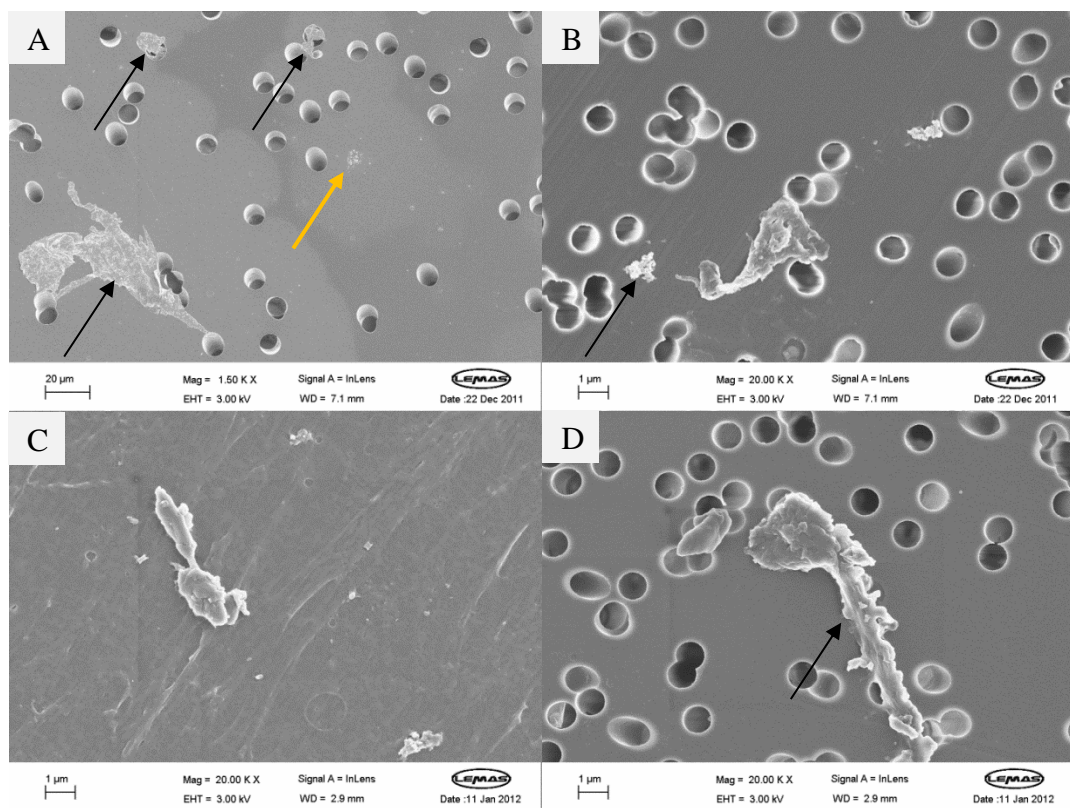


Figure 3.2 – FEGSEM images of UHMWPE wear particles isolated from serum lubricant used on the six station pin-on-plate wear rig. These particles were generated from GUR 1050 Virgin UHMWPE pins articulating against a smooth CoCr counterface. Image A shows a 10 μm filter imaged at a magnification of 1500x. The black arrows show flake like particles, while the orange arrow shows a cluster of smaller particles; Image B shows a 1 μm filter imaged at a magnification of 20,000x. The black arrow shows a globular-shaped particle; Image C shows a 0.015 μm filter imaged at a magnification of 20,000x. Image D is an additional image of a 1 μm filter imaged at a magnification of 20,000x. The black arrow shows a fibril shaped particle.

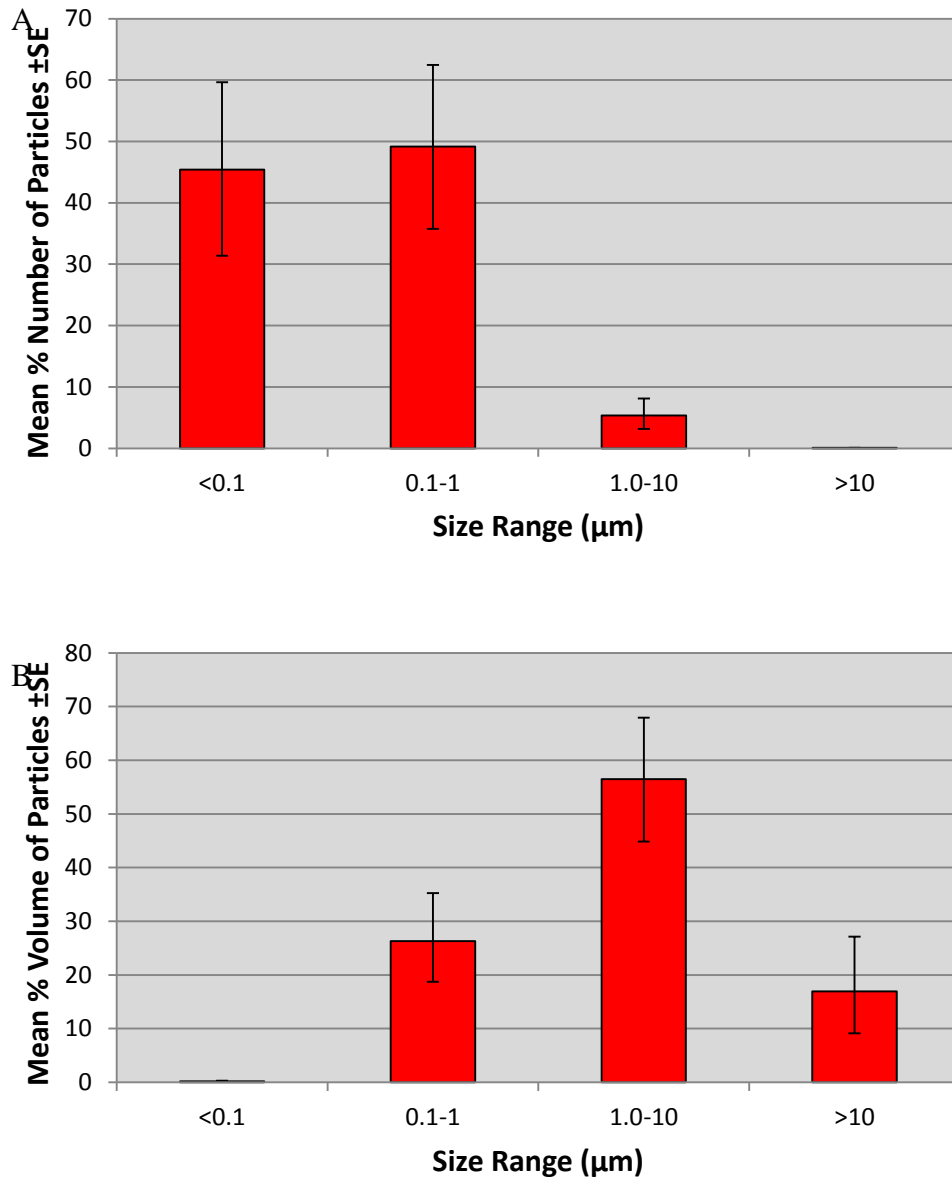


Figure 3.3 – A) The mean percentage frequency and B) the mean percentage volume size distribution of GUR 1050 Virgin UHMWPE particles generated on the six station pin-on-plate wear rig. The error bars represent \pm standard error of the mean.

The SEM images showing wear particles from 1050 Vit E 10 UHMWPE are shown in Figure 3.4. Large flake-like particles were seen on the 10 μm pore-size filter in image A, showing the complex shapes of wear particles generated under clinically relevant hip kinematics. A fibril-shaped particle with a length of approximately 25

μm is shown in image B, as highlighted by the black arrow. The black arrows in image C highlight four sub-micron particles on the 0.015 pore-size filter.

The mean percentage number and volume size distribution graph for particles generated from 1050 Vit E 10 are shown in Figure 3.5A and B. The mode of the frequency distribution was in the nanoscale range of $<0.1 \mu\text{m}$ (Figure 3.5A). Around a third of particles were in the 0.1-1.0 μm size range, while less than 5% particles were in the 1.0-10 μm size range. The volume distribution (Figure 3.5B) shows the mode size range to be in the 1.0-10 μm size range, making up around 55% of the total volume of wear particles for 1050 Vit E 10. Once again despite contributing a large number of particles to the overall sample, the nanoscale particles contribute only a very small percentage of the overall volume of particles.

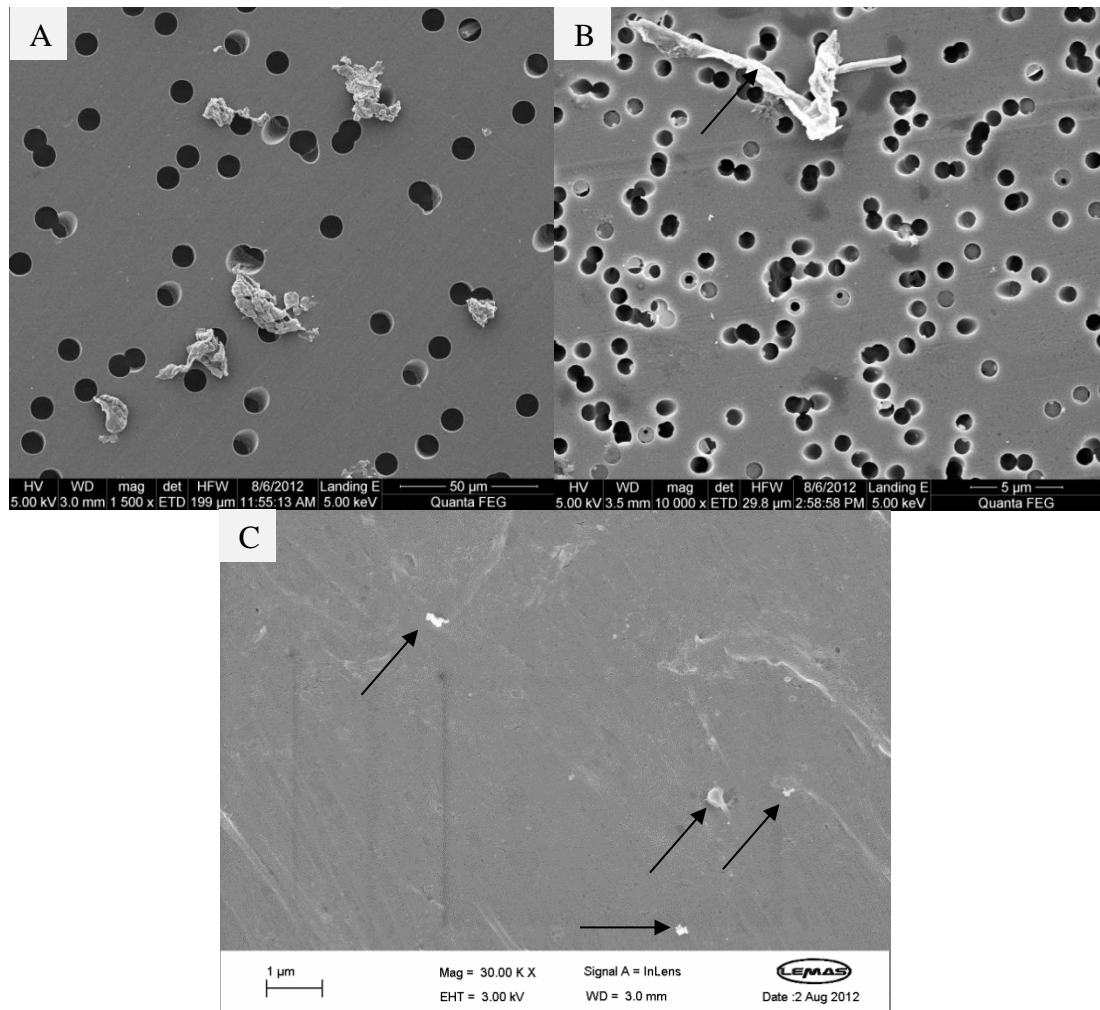


Figure 3.4 - FEGSEM images of UHMWPE wear particles isolated from serum lubricant used on the six station pin-on-plate wear rig. These particles were generated from GUR 1050 vitamin E enhanced 10 MRad irradiated UHMWPE pins articulating against a smooth CoCr counterface. Image A shows a 10 µm filter imaged at a magnification of 1,500x. Several flake-like particles are visible in this image. Image B shows a 1 µm filter imaged at a magnification of 10,000x. The black arrow shows a fibril shaped particle with an approximate length of 15 µm. Image C shows a 0.015 µm filter imaged at a magnification of 30,000x. Black arrows show the sub-micron particles present on the filter.

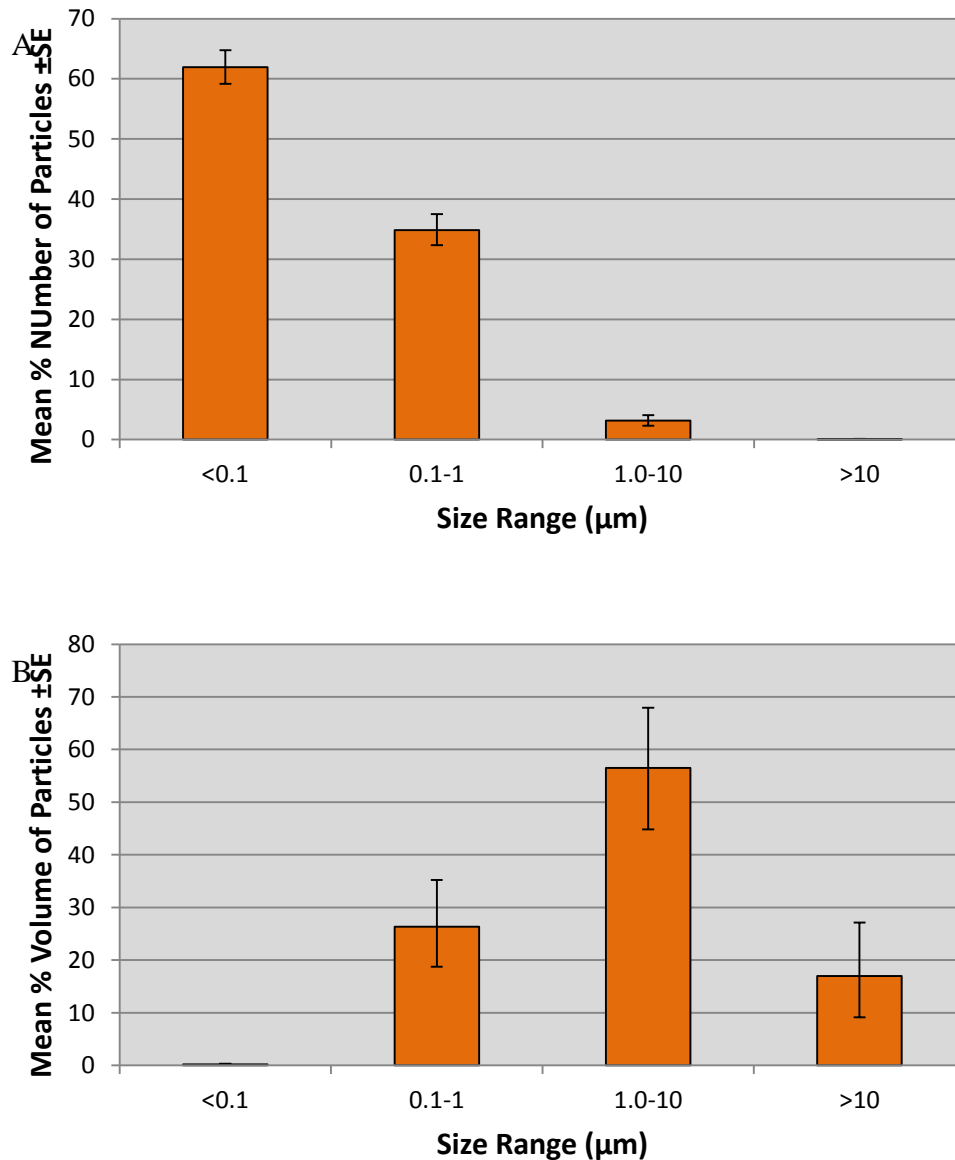


Figure 3.5 - A) The mean percentage frequency and B) the mean percentage volume size distribution of GUR 1050 Vit E 10 UHMWPE particles generated on the six station pin-on-plate wear rig. The error bars represent \pm standard error of the mean.

During imaging of the 1050 HXL UHMWPE wear debris using the FEGSEM, problems were experienced. On two occasions, the 1.0 μm filters were very badly contaminated with what appeared to be salts and proteins. This level of contamination was not observed in any of the other samples, and it was therefore determined that the serum sample being processed was contaminated. The lubricant sample collected from the second week of the wear test was therefore used to provide a different sample. Unfortunately, during imaging of these new samples,

there were technical problems when using the FEGSEM. For example, during one session, the level of static generated by the filter was making capturing a high resolution image almost impossible. A second layer of platinum coating was applied to try to reduce this static, however this did not improve the sample. A second technical fault occurred during a later session which results in several weeks of downtime for the FEGSEM.

Due to the limited volume of lubricant available from the six station pin-on-plate wear rig, and because the 1050 HXL sample required a large volume of lubricant to be processed in order to provide an adequate particle sample (due to the low wearing 1050 HXL material), these problems resulted in the loss of the 1050 HXL UHMWPE wear debris to analyse. This was a disappointing outcome; however this was an example of the limitations and difficulties experienced during research. As a result of the exclusion of this material, the study compared the particle size distribution of 1050 Virgin and 1050 Vit E 10 UHMWPE, to determine if there were any significant differences between these materials in terms of wear debris.

3.3.2.2 Comparison of the Frequency and Volume Size Distribution for GUR1050 Virgin and GUR1050 Vitamin E enhanced Highly Crosslinked UHMWPE

A comparison of the mean frequency and volume size distributions for the 1050 Virgin and 1050 Vit E 10 wear particles was performed. No significant differences were observed for either the frequency or volume size distribution of these materials (ANOVA $p > 0.05$). The mean frequency size distribution comparison graph is shown in Figure 3.6A, and indicated the majority of the particles generated were in the sub micrometre size ranges ($< 0.1 \mu\text{m}$, $0.1\text{-}1.0 \mu\text{m}$) for both 1050 Virgin and 1050 Vit E 10 UHMWPE. While the 1050 Virgin material generated a higher percentage number of particles in the nanoscale range, this was not significantly higher. Both materials had a small number of particles in $1.0\text{-}10 \mu\text{m}$ and $> 10 \mu\text{m}$ size range.

The mean volume distribution comparison graph is shown in Figure 3.6B. This graph shows a very similar mean volume size distribution for both materials. Both materials showed a mode volume distribution in the $1.0\text{-}10 \mu\text{m}$ size range, with both

materials generating over 50% of the volume of particles in this size range. A smaller proportion of the volume of particles was in the 0.1-1.0 μm (<30%) and <10 μm (<20%) size ranges. Nanoparticles, despite contributing a large majority of the number of particles, make up a very small percentage of the total volume of particles, with both materials generating less than 1% of the total wear volume in this size range.

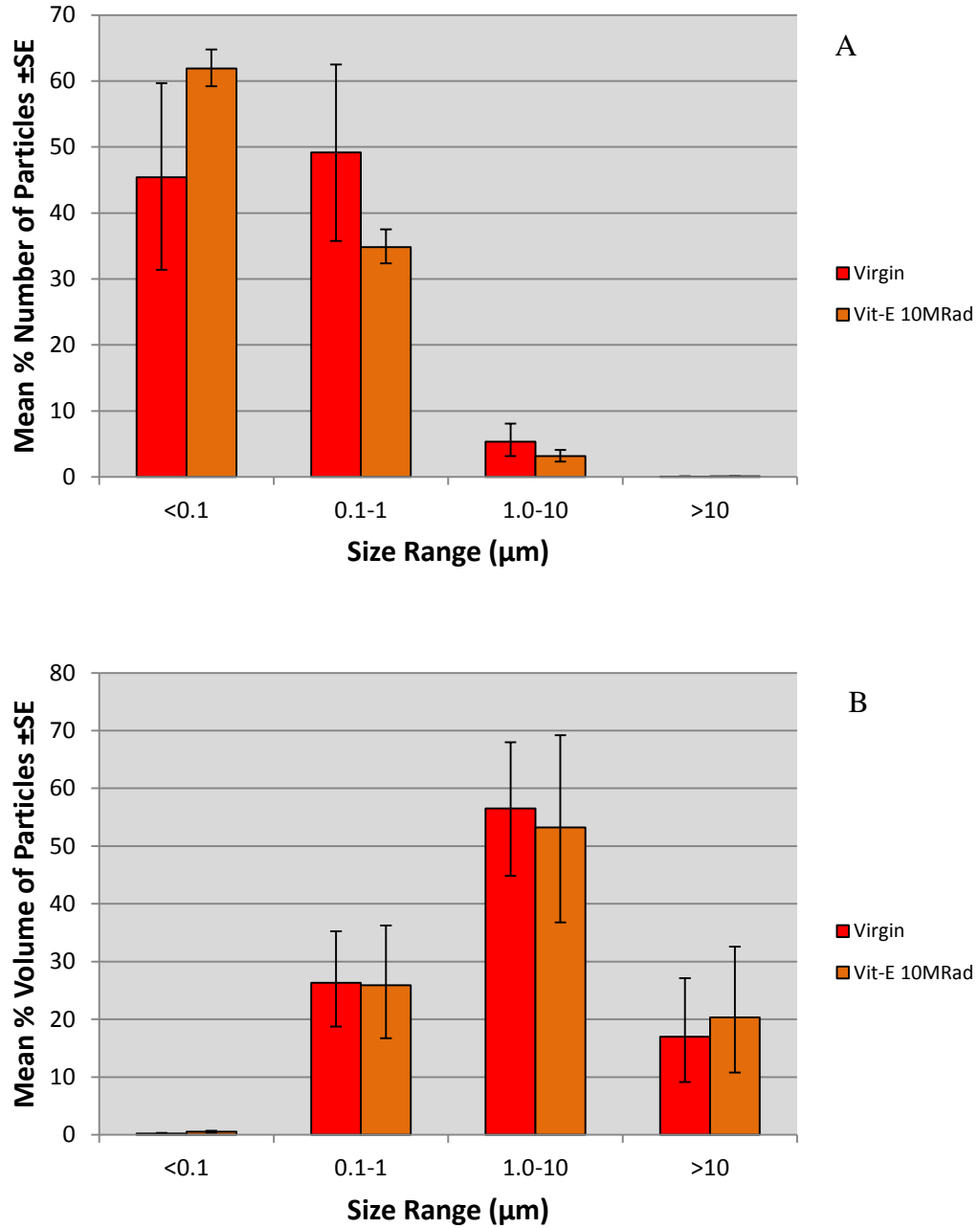


Figure 3.6 – Comparison of 1050 Virgin and 1050 Vit E 10 wear particles generated on the six station pin-on-plate wear rig; A) the mean frequency size distribution; B) the mean volume size distribution. The error bars show \pm standard error (SE) of the mean.

3.3.2.3 Isolation and Characterisation of Wear Particles Generated from GUR1020 Virgin UHMWPE and Hindered Phenol Enhanced Highly Crosslinked UHMWPE

Wear debris from GUR1020 Virgin UHMWPE and GUR1020 AOX 8 UHMWPE were isolated from the serum lubricant collected following the wear test of these materials to determine the wear factor. It was intended to also isolate and characterise the wear debris from a GUR1020 crosslinked but non-AOX UHMWPE material to provide a complete set of materials from this resin. However, this study was unable to source a GUR1020 UHMWPE material irradiated to 8 MRad for comparison with the AOX™ highly crosslinked UHMWPE. For this reason, 1020 Virgin and 1020 AOX 8 UHMWPE were compared in this section of the study.

The serum lubricant from three of the four stations was processed and particles isolated, as described in section 2.3. Samples were kept separate throughout the whole process to allow for an n=3 value. These materials were chosen as a good representation of the virgin GUR1020 material and the highly crosslinked antioxidant GUR1020 material. If crosslinking and AOX™ addition had a significant effect on the particle size distribution compared to 1020 virgin, this would be evident when comparing these two materials. .

The SEM images showing wear particles from 1050 Virgin UHMWPE are shown in Figure 3.2. Particles observed on a 10 µm filter were typically large, flake-like particles, as highlighted by the black arrows in image A. A single, flake-like particle was observed on a 1.0 µm filter in image B, captured at a magnification of 10,000x. A 0.015 µm filter captured at a magnification of 60,000x is shown in Image C. A micron-sized globular shaped particle was captured on this filter, with a submicron particle beside this larger particle, highlighted by the black arrow. Finally, an additional image of a 10 µm filter showed (image D) showed a flake-like particle surrounded by submicron wear debris. This is a very clear image of wear debris generated from 1020 Virgin UHMWPE.

The mean percentage frequency and volume size distribution graphs for 1020 Virgin wear particles are shown in Figure 3.8A and B respectively. The mode of the frequency size distribution was within the 0.1-1.0 µm size range, as shown in Figure 3.8A. The second most frequent size range of particles was the <0.1 µm size range,

with around 20% of particles falling in this size range. Around 10% particles were within the 1.0-10 μm size range, however, from the volume distribution, it was clear that this size range contributed over 70% of the total volume of the wear debris (Figure 3.8B). Only 20% of the volume of wear debris was within the 0.1-1.0 μm size range, with a lower percentage of the volume of particles in the $>10 \mu\text{m}$ and $<0.1 \mu\text{m}$ size range. This once again shows the importance of determining the percentage volume size distribution alongside the percentage number distribution.

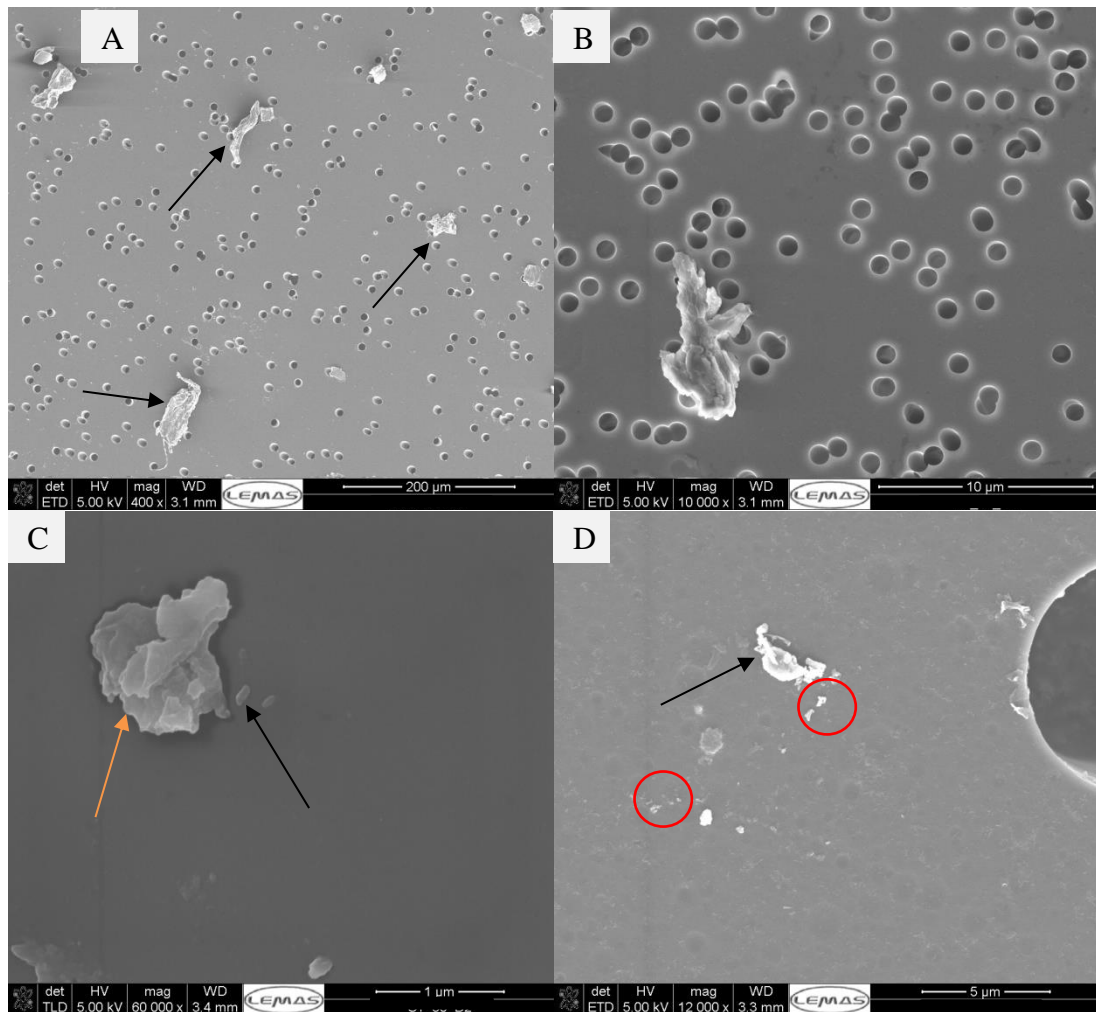


Figure 3.7 – FEGSEM images of UHMWPE wear particles isolated from serum lubricant used on the six station pin-on-plate wear rig. These particles were generated from GUR 1020 Virgin UHMWPE pins articulating against a smooth CoCr counterface. Image A shows a 10 μm filter imaged at a magnification of 400x. The black arrows show flake like particles; Image B shows a 1 μm filter imaged at a magnification of 10,000x; Image C shows a 0.015 μm filter imaged at a magnification of 60,000x. The orange arrow shows a globular shaped particle with a width of around 1 μm . The black arrow shows a submicron particle close to the larger particle. Image D is an additional image of a 10 μm filter imaged at a magnification of 12,000x. The black arrow shows a flake-like particle, surrounded by submicron wear debris highlighted in the red circles.

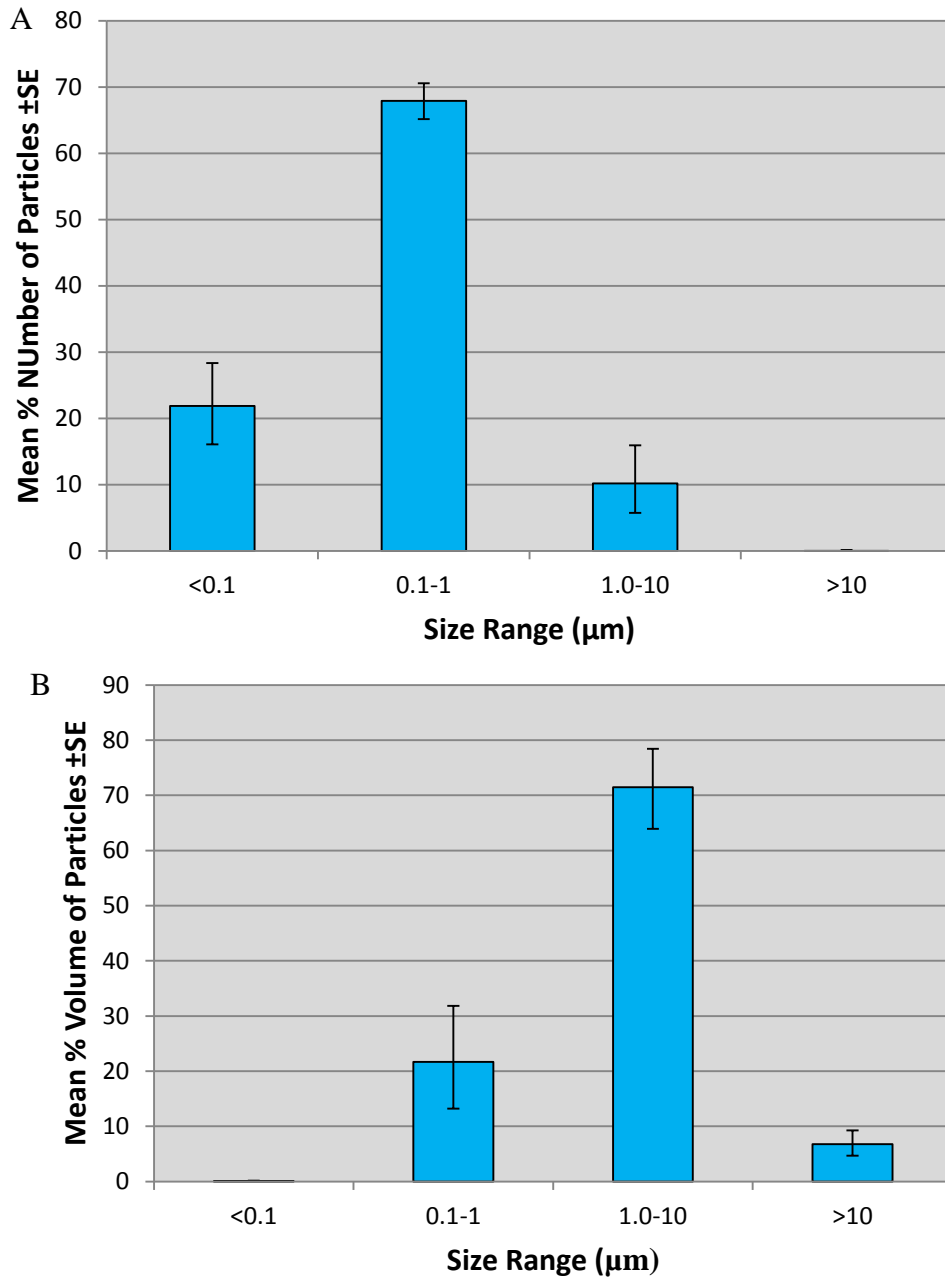


Figure 3.8 - A) The mean percentage frequency and B) the mean percentage volume size distribution of GUR 1020 Virgin UHMWPE particles generated on the six station pin-on-plate wear rig. The error bars represent \pm standard error of the mean.

Wear debris generated from GUR1020 AOX 8 was also isolated and characterised. Images of 1020 AOX 8 wear debris were obtained using high resolution SEM, and these images are shown in Figure 3.9. Some of the different particle morphologies are highlighted in these images. Particles observed on a 10 μm filter were typically large, flake-like particles, as highlighted by the black arrows in image A. Long, fibril-like extensions were often seen on these particles, as highlighted by the orange arrow. While these extensions do not hugely increase the volume of the particle, the perimeter and surface area of these particles were increased due to these thin extensions.

The 1.0 μm filter is shown in image B, captured at a magnification of 60,000x. A flake-like particle was observed on this filter, highlighted by the black arrow, along with a smaller globular-shaped particle. The 0.015 μm filter, imaged at a magnification of 10,000x, is shown in image C. This image showed clusters of sub-micron UHMWPE wear particles, as highlighted by the red circles. These smaller particles tended to be more globular and round in morphology. Finally, an additional image of a 10 μm filter (image D) showed two flake like particles imaged at a magnification of 1,500x. The detail in these flake-like particles was clear in these images. Once again, fibril extensions from the flake-like shapes were observed.

The mean percentage frequency and volume size distribution graphs for 1020 AOX 8 wear particles are shown in Figure 3.10A and B respectively. The mode of the frequency size distribution was within the 0.1-1.0 μm size range. The second most frequent size range of particles was the 1.0-10 μm size range followed closely by the <0.1 μm size range. A very small percentage of the number of the particles was in the >10 μm size range. This size range did however contribute the second highest percentage of the volume of particles generated. The mode size range for the volume distribution of the particles was the 1.0-10 μm size range. Despite contributing the largest percentage of the number of particles, the 0.1-1.0 μm size range contributed less than 10% of the total volume of wear particles.

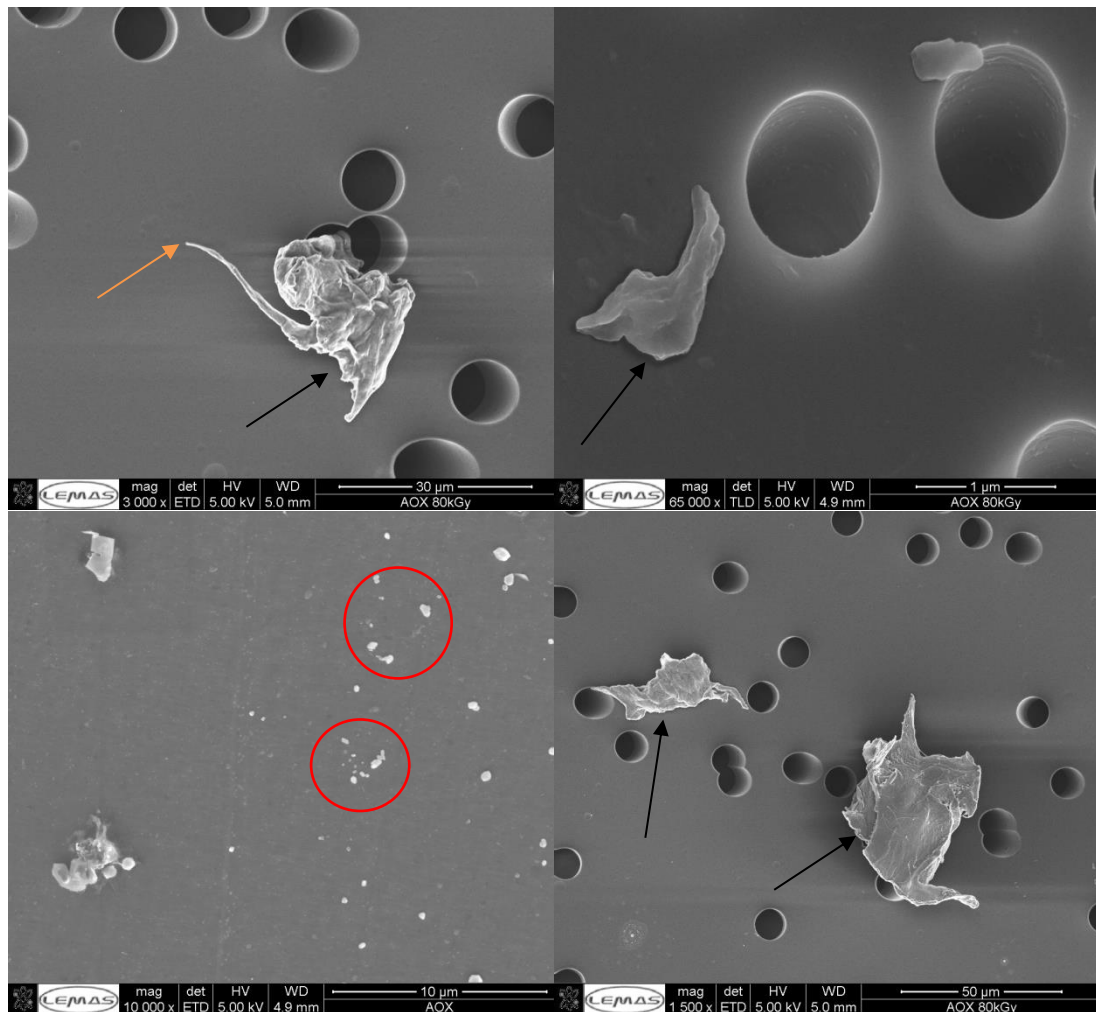


Figure 3.9 – FEGSEM images of UHMWPE wear particles isolated from serum lubricant used on the six station pin-on-plate wear rig. These particles were generated from GUR 1020 AOX 8 UHMWPE pins articulating against a smooth CoCr counterface. Image A shows a 10 μm filter imaged at a magnification of 300x. The black arrows shows a flake like particle with a fibril extension (orange arrow) around 25 μm in length; Image B shows a 1 μm filter imaged at a magnification of 60,000x. The black arrow shows a micron-sized particle; Image C shows a 0.015 μm filter imaged at a magnification of 10,000x. This image shows several particles smaller than a micron, with some of these particles highlighted by the red circle; Image D is an additional image of a 10 μm filter imaged at a magnification of 1,500x. The black arrows show two flake-like particles, also with fibril extensions.

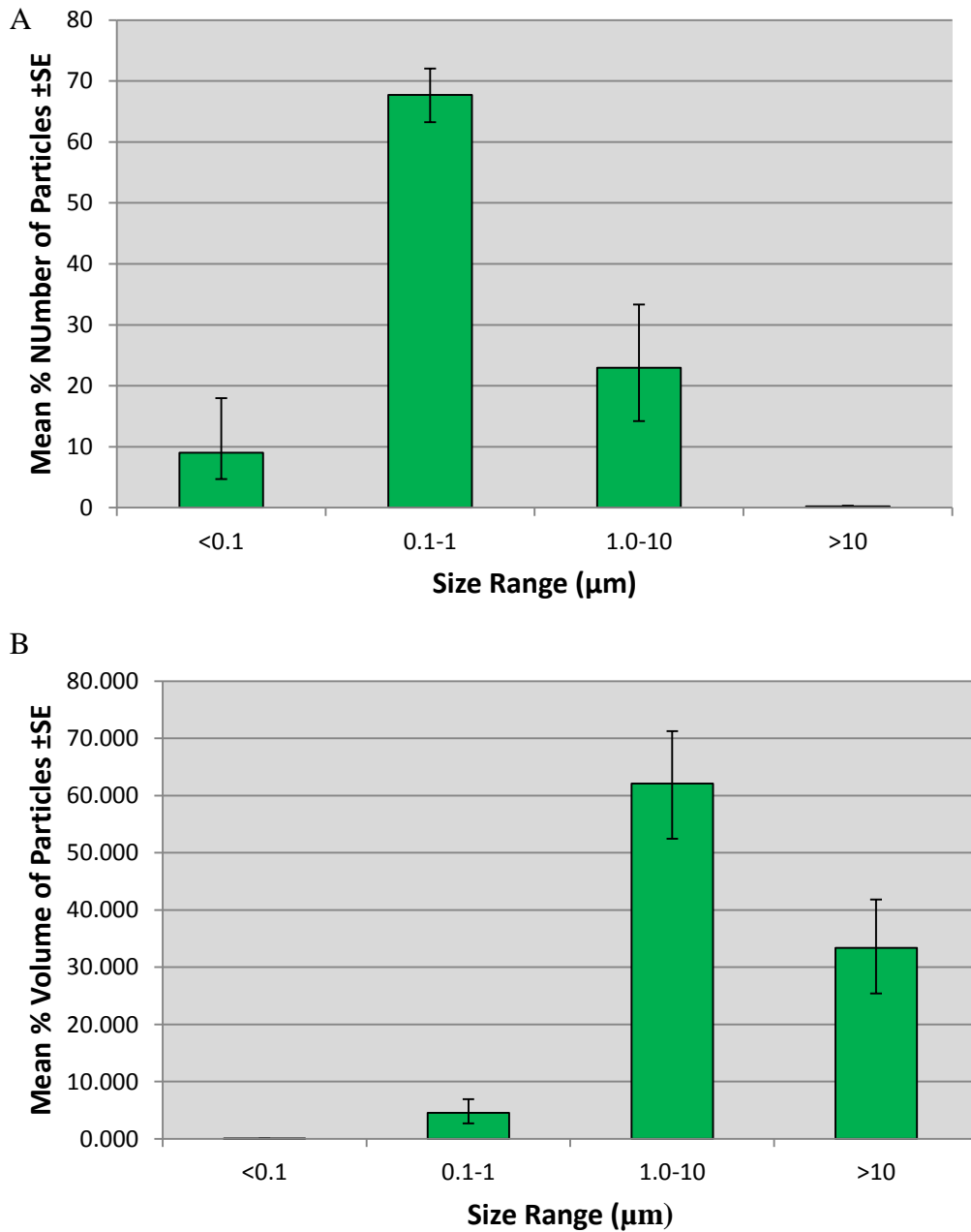


Figure 3.10 - A) The mean percentage frequency and B) the mean percentage volume size distribution of GUR 1020 AOX 8 UHMWPE wear particles generated on the six station pin-on-plate wear rig. The error bars represent \pm standard error of the mean.

3.3.2.4 Comparison of the Frequency and Volume Size Distribution for GUR1020 Virgin and GUR1020 Hindered Phenol enhanced Highly Crosslinked UHMWPE

A comparison of the mean frequency and volume size distribution of 1020 Virgin and 1020 AOX 8 UHMWPE wear debris was performed. No significant differences were observed between the two samples for either the frequency or volume distributions (ANOVA, $p > 0.05$). The mean frequency size distribution graph is shown in Figure 3.11A, and indicates that both 1020 Virgin and 1020 AOX 8 had a mode size range for the number of particles in the 0.1-1.0 μm size range. The size ranges $< 0.1 \mu\text{m}$ and 1.0-10 μm made up the majority of remainder of the particles characterised for both materials. Both materials generated a very low percentage of the number of particles in the size range greater than 10 μm .

The mean volume size distribution graph is shown in Figure 3.11B and also shows that both materials had a similar distribution of the volume of particles. Both materials had the mode percentage volume of particles in the 1.0-10 μm size range. A third of the wear debris from 1020 Virgin UHMWPE was in the $> 10 \mu\text{m}$ size range, whereas only a small percentage of the volume of wear debris from 1020 AOX 8 was in this large size range, although these differences were not statistically significant. Both materials had a low percentage volume of wear debris in the 0.1-1.0 μm size range; with this size range being thought be crucial to biological response to wear debris.

In conclusion, these results showed that there was no significant difference in the particle size distribution in terms of frequency and volume between 1020 Virgin and 1020 AOX 8 UHMWPE.

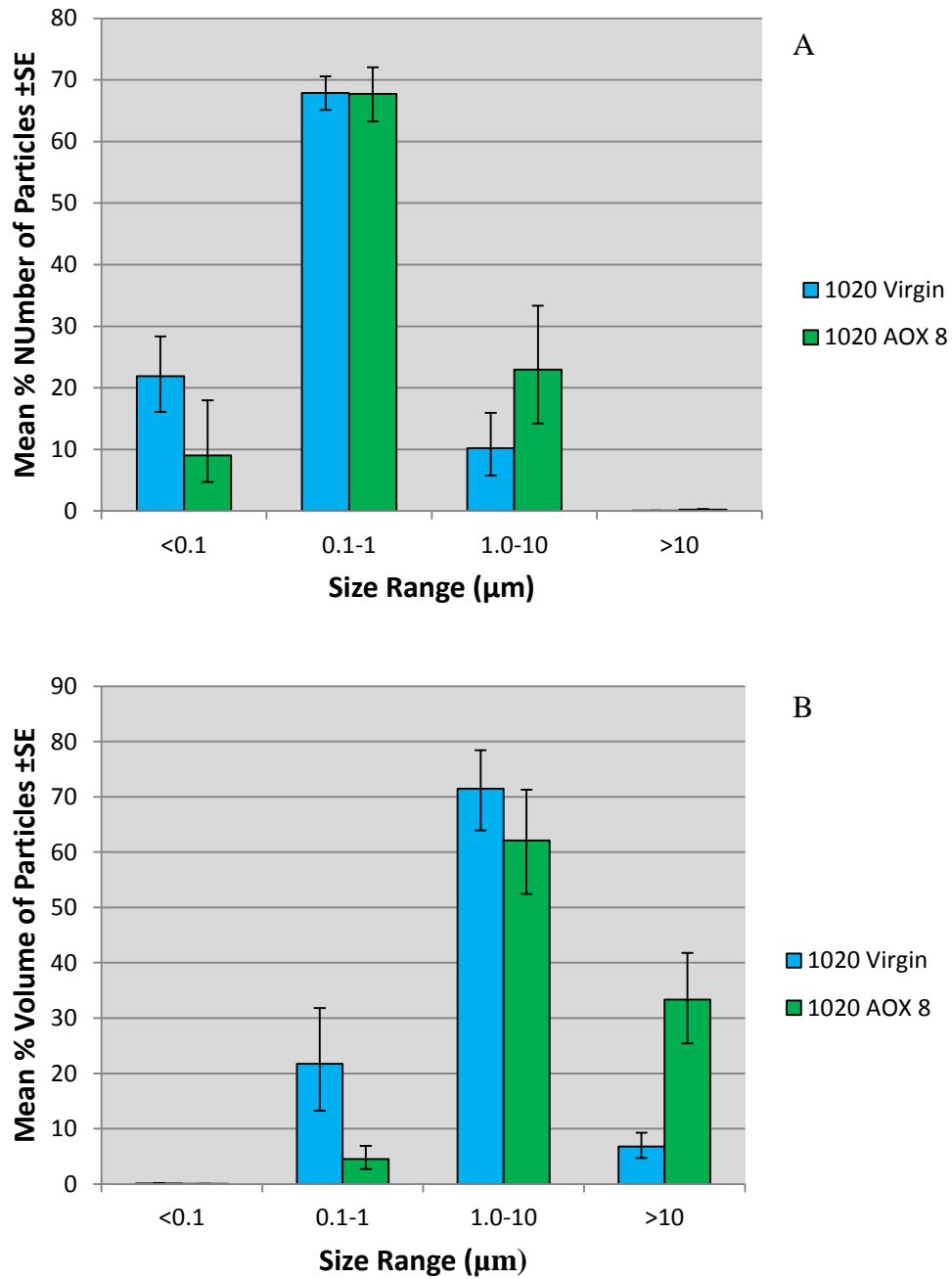


Figure 3.11 – Comparison of 1020 Virgin and 1050 AOX 8 UHMWPE wear particles generated on the six station pin-on-plate wear rig; A) the mean frequency size distribution; B) the mean volume size distribution. The error bars show \pm standard error (SE) of the mean.

3.4 Discussion

Wear Testing

In this chapter, the six station multidirectional pin-on-plate wear simulator was used to determine the wear factor of nine different UHMWPE materials. Wear tests were performed against smooth ($R_a < 0.01 \mu\text{m}$) high carbon CoCr counterfaces in a lubricant of 0.03% (w/v) sodium azide supplemented with 25% (v/v) bovine serum. This group of UHMWPE materials was comprised of experimental and clinically relevant materials, providing a strong matrix of materials that allowed for the comparison of the effect of crosslinking and/or antioxidant addition on the wear performance.

Each wear test used four pins per material and was operated over a two week period to allow for a minimum of 500,000 cycles at a rate of 1Hz. A load of 160N was applied throughout the test, with a stroke length of 28 mm, and a contact face on the UHMWPE material of 10 mm. Pins were weighed before and after the wear test to determine the wear of the pin gravimetrically. From this, the mean wear factor was determined for each material.

The results from the six station pin-on-plate wear simulator indicated that an increase in the level of crosslinking of UHMWPE produced a significantly lower wear factor compared to non-crosslinked UHMWPE. For each of the two GUR1050 categories of material; non-antioxidant (1050 Virgin, 1050 Marathon, 1050 HXL) and vitamin E enhanced (1050 Vit E, 1050 Vit E 5, 1050 Vit E 10), a significantly lower mean wear factor was demonstrated as crosslinking increased. A significantly lower wear factor was observed between 1050 Virgin and 1050 HXL, along with a significantly lower wear factor between 1050 Vit E and 1050 Vit E 10 (ANOVA; $p < 0.05$). There was no significant change in the wear factor observed between the GUR1020 materials, however a lower wear factor was still observed in 1020 AOX 8 compared to 1020 Virgin UHMWPE.

There was no significant difference in the wear factor between 1050 Virgin and 1050 Vit E, or between 1050 HXL and 1050 Vit E 10, indicating that the addition of vitamin E had no significant effect on the wear factor of these UHMWPE materials. A two-way analysis of variance also determined that there was no significant

interaction between the level of crosslinking and the addition of vitamin E enhancement (2-way ANOVA, $p < 0.05$). A previous study had concluded vitamin E reduced the wear of UHMWPE compared to conventional UHMWPE, however the aforementioned study tested vitamin E highly crosslinked UHMWPE against virgin UHMWPE, therefore the conclusions made regarding vitamin E and its effect on the wear of UHMWPE cannot be made. It is probable that the reduction in the wear factor observed in the previous study was due to the high levels of crosslinking rather than the presence of vitamin E (Micheli et al., 2012). The present study showed that under normal conditions (non-aged), vitamin E had no significant effect on the wear of UHMWPE in a pin-on-plate wear test.

The addition of vitamin E has previously been shown to maintain the mechanical properties of highly crosslinked UHMWPE following accelerated aging. The study by Kurtz et al., (2009) showed that after two or four weeks of accelerated, vitamin E enhanced UHMWPE at a dose of 500 ppm maintained the baseline mechanical properties of the material (Kurtz et al., 2009). The addition of vitamin E to UHMWPE has also been shown to improve fatigue crack propagation resistance following accelerated aging (Oral et al., 2008). These studies highlight that following accelerated aging; vitamin E may have a significant effect on the wear of the material compared to highly crosslinked and remelted UHMWPE. This is an area where further study would be beneficial to the understanding of the effect of vitamin E on the wear of UHMWPE.

One of the alternative antioxidants being considered for use in UHMWPE is the hindered phenol pentaerythritol tetrakis. Hindered phenols have been shown to be effective antioxidants due to the four phenol groups the molecule possesses. The first hindered phenol UHMWPE for orthopaedic use has been developed by DePuy Synthes, with the materials termed AOX™. This crosslinked AOX™ material (1020 AOX 8), along with a non-crosslinked AOX™ material (1020 AOX) and virgin material (1020 Virgin) were also tested using the six station pin-on-plate wear simulator. The addition of the hindered phenol antioxidant (AOX™) also had no significant effect on the wear factor of UHMWPE compared to GUR1020 Virgin UHMWPE. There was a lower mean wear factor for AOX™ enhanced UHMWPE compared to 1020 Virgin UHMWPE, and then a further reduction in the wear factor

with the addition of 8MRad gamma irradiation; however these reductions were not statistically significant (ANOVA; $p > 0.05$).

The wear factor of the GUR1020 Virgin UHMWPE was significantly lower than the mean wear factor for the GUR1050 Virgin UHMWPE material (ANOVA, $p < 0.05$). This was surprising given the lack of crosslinking in both materials. The main difference between these two materials is the resin used, and the average molecular weights of the materials. The GUR1050 resin has a higher average molecular weight ($7.3 \times 10^6 \text{ g.ml}^{-1}$) compared to the GUR1020 resin ($4.4 \times 10^6 \text{ g.ml}^{-1}$) (Tipper et al., 2005). These differences were not expected to generate a significant difference in the wear factor, and a previous study by Tipper et al., showed no significant difference in the wear rates of GUR1050 and GUR1020 Virgin UHMWPE when using a hip simulator (Tipper et al., 2005). Further investigation into the reasons for this difference is required to better understand the properties of these UHMWPE materials.

Wear Particle Characterisation

Serum lubricant from the six station pin-on-plate wear tests was collected to allow for the isolation and characterisation of wear debris generated during these tests. A previous study by Liu (2012) used a filtration sequence of 10 μm , 1 μm , and 0.015 μm to successfully isolate wear particles to be imaged using high resolution FEGSEM followed by characterisation using image analysis software. This method successfully characterised the wear debris sample generated on the six station pin-on-plate wear rig, and for that reason the same method was used in this study.

For each material, three serum lubricant samples were isolated using the methods outlined in section 2.3.1. This involved the use of 12M KOH to digest the protein present in the sample. Following this, 2:1 chloroform: methanol was used for lipid extraction from the sample, and protein precipitation. Finally, ethanol was used for further lipid extraction, while also precipitating and removing a large quantity of salts from the sample. Particle samples were then sequentially filtered through a sequence of filters consisting of 10 μm , 1.0 μm , and 0.015 μm pore-sized filters. These filters were then imaged using a FEGSEM at a range of magnifications. This method successfully produced high quality images of UHMWPE wear debris on the

filters, where the lack of protein or salt contamination on the filters allowed for clear images of particles, making the particle analysis process more accurate.

Wear particle characterisation was performed to compare to frequency and volume size distribution of wear particles, and to identify if the addition of an antioxidant and high levels of crosslinking affected the size distribution of the wear debris. The sizing and analysis of wear particles was done manually, and this allowed for UHMWPE wear particles to be identified according to their recognisable shape and appearance when imaging using SEM. Attempts have been made to use automated particle analysis, however amongst the pores and various contaminants on the filters this was never performed accurately enough by the computer, and manual analysis was continued. Wear debris from 1050 Virgin was compared to wear debris from 1050 Vit E 10. There was no significant difference in the size distribution of wear particles from both materials. The majority of wear particles generated from both materials were within the submicron categories of $<0.1 \mu\text{m}$ and $0.1\text{-}1.0 \mu\text{m}$. However, when analysing the volume of particles produced, both materials generated the vast majority of the total volume of particles in the $1.0\text{-}10 \mu\text{m}$ size range. This difference highlights the importance of considering the volume of wear debris rather than the number of wear particles. This result appeared to show the addition of crosslinking and vitamin E enhancement had no significant effect on the size distribution of wear particles generated against a smooth CoCr counterface.

Throughout the isolation and characterisation of 1050 HXL UHMWPE wear particles, limitations and difficulties arose. One of the limitations with isolating wear particles from serum lubricant samples used in the six station pin-on-plate wear tests is the limited volume of wear debris to work with. This became apparent when problems arose with the isolation and subsequent imaging of 1050 HXL wear particles. On two occasions, the $1.0 \mu\text{m}$ filter had high levels of contamination present, and this made identifying and sizing UHMWPE wear particles very difficult. This meant the author was not able to obtain even one full set of images to present a size distribution for one sample. Furthermore, when analysing a second sample of 1050 HXL UHMWPE wear debris, technical problems occurred with the FEGSEM. This subsequently meant that the complete lubricant sample for the 1050 HXL material was diminished during the unsuccessful isolation/imaging procedure. A future study would repeat this experiment and include this vital, clinically relevant

material for a more complete set of results, and adding more confidence to any conclusions made regarding the effect of crosslinking and vitamin E addition on the particle size distribution of UHMWPE.

This study also compared the wear particle distribution from 1020 Virgin and 1020 AOX 8. Once again there was no significant difference in the frequency or volume size distribution of wear debris between these materials. For both these GUR1020 materials, the majority of the wear particles were produced in the 0.1-1.0 μm size range. However, as with the GUR1050 materials, the mode size range for the volume size distribution was the 1.0-10 μm size range.

In this case, a further limitation prevented a full range of GUR1020 materials to be processed. A material that would have made the particle size distribution analysis more complete, in addition to the wear testing section of this chapter, would have been a highly crosslinked (8 MRad) non-antioxidant GUR1020 UHMWPE material. This would have filled the gap between 1020 Virgin and 1020 AOX 8 UHMWPE in both the wear test and particle analysis. However, this study was unable to source such a material. In addition, due to time constraints, it would have been difficult to include this extra material in the time provided for the study. As with the GUR1050 material, future work should aim to include this material in the GUR1020 studies, to provide a more complete matrix of materials.

A previous study investigating the wear particle size distribution of GUR1050 virgin UHMWPE, along with GUR1050 UHMWPE crosslinked with 5MRad or 10MRad irradiation was conducted by Ingram *et al.* (2004). Against a smooth CoCr counterface, the authors observed no significant difference in the particle frequency or volume size distribution between the three materials. The mode size range observed for all three materials in terms of frequency of particles was the $<0.1 \mu\text{m}$ nanometre size range, contributing around 90% of the particles measured. In the present study, a similar result was observed for 1050 Vit E 10 UHMWPE wear debris, with the mode size range also $<0.1 \mu\text{m}$. The frequency size distribution for 1050 Virgin was different in the present study compared to the study by Ingram *et al.* In the present study, the 0.1-1.0 μm size range was the mode size range, while in the previous study, the $<0.1 \mu\text{m}$ size range was represented the mode size range.

This variation in the GUR1050 virgin size distribution could be attributed to the variation in methodology between the two studies. In the present study, following sequential filtration through 0.015 μm , 1.0 μm and 10 μm filter membranes, each section of filter was imaged at a range of magnifications, with three separate fields of view at each magnification, as described in the method developed by Richards (2008). For example, the section of filter imaged from the 1.0 μm filter membrane was imaged at magnifications of x1.5K, x5K, x10K, x20K, x30K, x40K, x65K, with three fields of view captured at each magnification. In comparison, the authors in the previous study filtered their lubricant through 0.1 μm , 1.0 μm and 10 μm filter membranes. The authors then quantified the wear particles on only the 0.1 μm and 1.0 μm filter membranes, excluding the 10 μm filter. Finally, only six SEM images were captured from each membrane filter; two images at 'low magnification' and four images at a higher magnification, in order to capture the nano-metre sized wear particles. The low number of images captured in the previous study, combined with the small range of magnifications used, could explain the conflicting results obtained between the two studies for GUR1050 virgin UHMWPE frequency size distribution.

When comparing the volume size distribution of GUR1050 virgin UHMWPE in the two studies, a similar result was obtained, with the mode size range determined as the 1.0-10 μm range in both studies. Variation was observed when analysing the other size ranges, however these differences could also be due to the variation in the methodology outlined previously. Despite these variations, the previous study does shed some light on a question that remained following the investigation in this section. While the present study was unable to compare highly crosslinked UHMWPE with the virgin material, the previous study showed no significant difference in the frequency or volume size distribution between virgin and highly crosslinked GUR1050 UHMWPE. Combined with the present study, these results would suggest that the addition of high levels of crosslinking, and/or the addition of vitamin E/hindered phenol as an antioxidant, have no significant effect on the frequency and volume size distribution of UHMWPE wear debris following wear testing against a smooth counterface.

The size of UHMWPE wear particles has been shown to be critical to the cellular response the particles stimulate *in vitro*. Particles in the size range of 0.1-1.0 μm have been shown to be the most biologically active, stimulating a significant

osteolytic cytokine response from macrophages (Ingham and Fisher, 2000, Ingram et al., 2004). A previous study by Liu (2012) showed a significant cytokine response from peripheral blood mononuclear cells was stimulated by 100 μm^3 of 0.1-0.6 μm sized UHMWPE particles per cell. No significant cytokine response was observed from cells incubated with particles within either the smaller ($<0.1 \mu\text{m}$) or larger ($>0.6\mu\text{m}$) size ranges. This showed the importance of particle size, in addition to the volume of particles, for stimulating a significant biological response. Linking this to the particle size distribution results in this section, the small percentage of the volume of particles in the biologically active size range (0.1-1.0 μm), typically around 30%, may be important when investigating the biological response of peripheral blood mononuclear cells to the complete size range of wear debris from each material. It may also be important when considering the total volume of wear debris required to stimulate a significant cytokine response from a cell sample.

3.5 Conclusion

No significant difference in the wear factor was observed between virgin UHMWPE and vitamin E enhanced UHMWPE. Highly crosslinked versions of these vitamin E and non-vitamin E materials also showed no significant difference in the wear factor. The addition of high levels of crosslinking significantly reduced the wear factor of UHMWPE compared to the non-crosslinked equivalents. The addition of the hindered phenol antioxidant to UHMWPE (AOXTM UHMWPE) had no significant effect on the wear factor of UHMWPE. No significant difference was observed for the particle size distribution of GUR1050 Virgin and GUR1050 Highly Crosslinked Vitamin E enhanced UHMWPE. The mode size of particles was the 0.1-1.0 μm size range for both these materials; however the mode size of particles in terms of volume was the 1.0-10 μm size range. No significant difference was observed for the particle size distribution of GUR1020 Virgin and GUR1020 Highly Crosslinked hindered phenol enhanced UHMWPE.

The addition of vitamin E had no significant effect on the wear of UHMWPE, or the particle size distribution of debris generated during wear tests. High levels of crosslinking improved the wear resistance of UHMWPE, even in the presence of vitamin E. Hindered phenol had no significant effect on the wear resistance of GUR1020 UHMWPE.

Chapter 4

The Biological Response of Peripheral Blood Mononuclear Cells to Antioxidant UHMWPE Wear Debris

4.1 Introduction

The biological response of macrophages to UHMWPE wear debris is one of the main factors responsible for osteolysis and aseptic loosening associated with metal-on-UHMWPE total hip replacement devices (Amstutz et al., 1992). The majority of total hip replacements still follow the Charnley principle of a metal femoral head articulating against an UHMWPE acetabular cup (National Joint Registry, 2013), and it is this coupling of materials that leads to the generation of UHMWPE wear debris and the downstream immune response to these wear particles that is associated with aseptic loosening. While huge progress has been made in improving the physical properties of UHMWPE; such as the introduction of high levels of crosslinking which improves wear resistance (Galvin et al., 2006), thinner cups to facilitate larger femoral heads (Kelly et al., 2010), and heat treatments which quench free radicals and improve oxidative stability (Medel et al., 2007, Ferroni and Quaglini, 2010), no deliberate advances have been made to reduce the innate immune response to wear particles that leads to osteolysis and aseptic loosening.

The introduction of vitamin E as an antioxidant is the most recent major advance in UHMWPE technology for total joint replacements, with the intention of quenching the free radicals generated during irradiation crosslinking. An antioxidant like vitamin E therefore protects against oxidation, while simultaneously negating the need for post-irradiation heat treatments that have been shown to be detrimental to the mechanical properties of UHMWPE (Oral et al., 2005, Wang, 2006, Muratoglu, 2009). However, this mechanical improvement has the potential to also address the problem of particle-induced osteolysis. Vitamin E has well documented anti-inflammatory properties, and there is evidence to suggest that alpha tocopherol-treated macrophages demonstrate a reduction in the release of pro-inflammatory

cytokines such as interleukin-1 β , interleukin 6 and tumour necrosis factor – α (TNF- α) from macrophages (Singh and Jialal, 2004). The anti-inflammatory properties of vitamin E have also been demonstrated in the treatment of cardiovascular disease, such as atherosclerosis (Devaraj et al., 1996, Ricciarelli et al., 2000), and in treating rheumatoid arthritis through the uncoupling of joint destruction (De Bandt et al., 2002). Vitamin E is also the most potent lipid soluble antioxidant present in plasma and lipoproteins (Singh and Jialal, 2004), and its lipid solubility makes it an attractive additive to a carbon-rich polymer like UHMWPE.

Previous studies have shown an osteolytic cytokine response from peripheral blood mononuclear cells (PBMNCs) to UHMWPE wear debris generated *in vitro* (Richards, 2008, Bladen et al., 2013). A study by Ingram et al. (2004) showed elevated TNF- α release from PBMNCs incubated with wear debris generated from GUR1050 virgin UHMWPE, and GUR1050 UHMWPE with 5 MRad or 10 MRad irradiation compared to the cells only control. The strongest TNF- α release was observed after 24 hours. Bladen *et al.* (2013) demonstrated a significantly elevated TNF- α , IL-1 β and IL-6 response from PBMNCs cultured with GUR1050 Virgin UHMWPE wear debris (non-crosslinked) at a dose of 100 μm^3 particles per cell, compared to the cell only negative control. These authors also demonstrated a significant reduction in cytokine release from PBMNCs stimulated with 100 μm^3 per cell vitamin E enhanced UHMWPE wear debris, with vitamin E doped at a dose of 3000 ppm. While this study showed a reduction in the osteolytic response with vitamin E enhanced UHMWPE, the experimental materials were not representative of the clinical situation. The addition of high levels of crosslinking to modern vitamin E enhanced materials leads to questions about whether vitamin E can leach from the crosslinked material or whether crosslinking causes grafting of vitamin E to the polymer, and also raises questions about the availability of vitamin E to cells. In addition, with vitamin E doping of UHMWPE at 1000 ppm in Europe and the USA, the former study clearly used a UHMWPE material with vitamin E doping at a much higher level which is not clinically relevant to antioxidant UHMWPE materials used in these regions.

The cell culture technique used most frequently for incubating PBMNCs with UHMWPE wear debris is the agarose gel technique, with two variations on this basic principle (Green et al., 1998, Liu, 2012). This is a cell culture technique designed to

provide a matrix for the PBMNCs in cell culture to come into contact with the buoyant UHMWPE wear particles that would normally float in suspension. A previous study by Green et al. (1998) used this technique to produce a 2D culture system, whereby the wear debris was added to the molten agarose gel in a 48 well plate. Immediately following this, the 48 well plate was centrifuged to produce a superficial layer of UHMWPE wear debris at the surface. An alternative technique was developed and used by Liu (2012) and Bladen et al. (2013), whereby no centrifuge step was carried out, meaning the UHMWPE wear debris was suspended throughout the agarose gel, producing a more 3D culture system. This then allowed the cells to be seeded onto this porous gel where the cells can penetrate and come into contact with the wear particles. In addition, with the omission of the centrifuge step from the technique, larger-well plates could be used. This was an important option when very low-wearing UHMWPE debris was being used, and a larger volume of lubricant was required to reach a required particle dose per cell within the agarose plug. A detailed description and rationale behind this technique is outlined in section 2.4.3. Previous studies have used this technique and have shown it to be an effective way of incubating PBMNCs with UHMWPE wear debris to determine the cell viability and cytokine response to wear debris (Liu, 2012, Bladen et al., 2013). While this technique relies on the penetration of PBMNCs into the gel, it is more reliable in producing a level surface to the gel, as the centrifuge step can produce an uneven surface, leading to an uneven distribution of PBMNCs as they settle on the gel. However, phagocytosis of nanometre and micrometre sized UHMWPE wear particles using this 3D technique has never been proven, and therefore there are questions regarding the mechanism behind the cytokine response to UHMWPE wear debris, for example whether phagocytosis is necessary for the increased levels of cytokine release in response to UHMWPE wear debris observed in previous studies.

The aim of the present study was to further develop the methodology for investigating the biological response to clinically relevant antioxidant highly crosslinked UHMWPE wear particles in terms of osteolytic cytokine release. The challenges faced in developing this experiment was the need to create an environment where the TNF- α release from PBMNCs in response to UHMWPE wear debris observed in previous studies was repeated in this study, but in a 3D culture environment and using wear debris 'as-generated'. Following this

development of the methodology, the aim was to investigate the effect of clinically relevant antioxidant wear debris on TNF- α production by PBMNCs.

The present study tested aseptic wear debris from a highly crosslinked (10 MRad) GUR1050 UHMWPE (1050 HXL) as a representative of the highly crosslinked bearing material commonly used today, and tested aseptic wear debris from a highly crosslinked (10 MRad) vitamin E enhanced GUR1050 UHMWPE and a highly crosslinked (8MRad) hindered phenol (AOXTM) enhanced GUR1020 UHMWPE as antioxidant materials. The vitamin E enhanced material was very close to the specification of the vitamin E enhanced material available clinically (Biomet[®] E1[®] – GUR1050, highly crosslinked, vitamin E enhanced 1000 ppm), while the hindered phenol (AOXTM) enhanced material is a novel clinical material provided by DePuy Synthes (AOXTM UHMWPE with CovernoxTM antioxidant). Virgin GUR1050 and GUR 1020 UHMWPEs were used as control materials and to stimulate cells in early experiments.

Wear particles were generated from all materials using the aseptic single station pin-on-plate wear simulator, using a serum lubricant of 25% (v/v) bovine serum in RPMI 1640 medium. This simulator has been shown to successfully produce clinically relevant wear debris in a sterile environment (Ingram et al., 2004). Pins were weighed before and after the test to determine the volume of wear generated during the test, and hence the mass of sterile wear debris produced in the serum lubricant sample. Pins were articulated against rough high-carbon CoCr counterfaces to produce a large volume of wear debris in a reduced time frame.

Wear particles were then incubated with PBMNCs isolated from healthy human donors to investigate the uptake of UHMWPE wear particles by PBMNCs using confocal microscopy. The assay was then used to determine the effect of each UHMWPE material on cell viability, and to determine the TNF- α release over a 24 hour incubation time period. The methods for the particle: cell culture experiments are outlined in section 2.4.

Experimental Rationale

The rationale behind this section of the study was to replicate the clinical situation of the biological response to wear debris generated from antioxidant UHMWPE materials *in vivo*. A previous study by Liu (2012) demonstrated a significantly

elevated TNF- α response from PBMNCs to a fractionated sample of GUR1050 Virgin UHMWPE wear debris in the 0.1-0.6 μm size range. Wear particles in the other size ranges did not stimulate a significant TNF- α response. This highlighted the importance of particle size for the stimulation of macrophages by UHMWPE wear debris. However, the former study did not demonstrate the clinical situation where the full size range of wear particles would be generated and encountered by macrophages in the surrounding tissue. In addition, the particles generated by Liu (2012) were generated on the six station pin-on-plate wear simulator, with no serum proteins present in the lubricant. Serum lubricant was added to the particle sample prior to incubation with cells, however the particles generated in the present study used 25% (v/v) bovine serum throughout wear tests and particle generation.

The present study investigated the biological response to the full size range of wear particles generated using the single station pin-on-plate wear simulator. This gave a representative size distribution of particles that would be generated *in vivo*, to then allow for this particle cell environment to be replicated *in vitro* (Tipper et al., 2000).





In order to replicate the significant TNF- α release demonstrated in previous studies, several method development steps were taken in the present study to produce an environment whereby the full size range of UHMWPE wear debris ‘as generated’ would stimulate significant TNF- α release. Following this development, a comparison between antioxidant and non-antioxidant UHMWPE could be made. In addition to changing aspects of the protocol such as cell seeding density, agarose gel concentration and particle concentration, the U937 cell line was also used as an alternative to PBMNCs in order to remove the variation often seen between human donors.

4.2 Materials and Methods

4.2.1 Materials

For the cell culture experiments, four UHMWPE materials were tested and these are listed in Table 4.1. The materials were chosen to allow investigation of the effect of highly crosslinked antioxidant UHMWPE wear particles on the biological response of macrophages, in comparison to non-antioxidant highly crosslinked UHMWPE. The materials GUR1050 Virgin, GUR1050 HXL and GUR1050 Vit E 10 were used throughout the experiment and development of the experiment. Following successful method development, GUR1020 AOX 8 was then included in the study.

Table 4.1 – UHMWPE materials used in the cell culture experiments. Details of the full name of each material, the resin type, the gamma irradiation dose, the antioxidant used, the supplier, the abbreviation used through the study, and the colour key used throughout this chapter for each material.

Name	Resin	Gamma Irradiation Dose	Antioxidant	Supplier	Abbreviation	Colour Key
1050 Virgin	GUR1050	0 MRad	none	DePuy Synthes®	1050 Virgin	
1050 Highly Crosslinked UHMWPE	GUR1050	10 MRad	none	DePuy Synthes®	1050 HXL	
1050 Vitamin E enhanced UHMWPE + 10 MRad irradiation	GUR1050	10 MRad	Vitamin E	MediTech® Medical Polymers	1050 Vit E 10	
1020 Hindered Phenol enhanced UHMWPE + 8 MRad irradiation	GUR1020	8 MRad	Hindered Phenol	DePuy Synthes®	1020 AOX 8	

4.2.2 Methods

4.2.2.1 Generation of UHMWPE Wear Particles using the Aseptic Single Station Pin-on-Plate Wear Simulator

Wear particles were generated from each material listed in Table 4.1 using the aseptic single station pin-on-plate wear simulator, against a rough (R_a 0.07-0.09 μm) high carbon (0.27% w/v) CoCr alloy counterface. The lubricant was comprised of RPMI 1640 medium with 25% (v/v) bovine serum described in section 2.2.6. The assembly of the single station pin-on-plate wear simulator is outlined in section 2.2.7. A 2 ml sample of lubricant was collected and plated onto microbial growth plates each day of the wear test, to ensure no bacterial or fungal contamination was present, as described in section 2.2.7.5. Serum lubricants which remained sterile throughout the wear test were collected and stored at -20°C until required for cell culture experiments. Pins were weighed before and after the wear test, and the wear was measured to determine the mass of UHMWPE wear debris in the final lubricant sample, as described in section 2.4.3.1.

4.2.2.2 Endotoxin testing of the Serum Lubricant

The endotoxin levels in each serum lubricant sample were determined prior to their use in cell culture experiments. The methods for this test are outlined in section 2.4.2.2. Sample lubricants were sonicated for 40 min at 37°C , after which the samples were diluted 1:100 using LAL reagent water. The endotoxin levels in each sample lubricant from a 4 day test using the single station pin-on-plate simulator were determined using a standard curve of known endotoxin concentrations. The percentage product recovery in each sample was also determined using a sample spiked with a known concentration of endotoxin.

4.2.2.3 Culture of PBMNCs with Fluorescein-Labelled UHMWPE Wear Particles for Analysis of Particle Uptake using Confocal Microscopy

Cell culture experiments incubating PBMNCs isolated from human donor blood with fluorescently labelled UHMWPE wear particles were performed in order to visualise the uptake of UHMWPE wear particles by macrophages, and to confirm whether

phagocytosis occurs when using the agarose gel cell culture technique. Peripheral blood mononuclear cells were isolated from healthy human donors as described in section 2.4.4 and cells were incubated with micrometre sized (1- 10 μm) or nanometre sized (0.015- 0.1 μm) particles separately using the agarose gel technique. The microscope slide-cell culture apparatus described in section 2.4.7.4 (Figure 2.10) was used to allow for imaging using the confocal microscope. Cells were incubated with fluorescein labelled 1050 HXL UHMWPE wear particles for 48 hours at 37°C in 5% (v/v) CO₂ in air. Cells were seeded at a density of 2×10^5 cells per well, with a particle concentration of 100 μm^3 per cell. Throughout the incubation, the level of culture medium was checked and if necessary, was topped up with RPMI 1640 Culture medium to maintain a meniscus of medium above the top of the well. Following the 48 hour incubation, the culture medium was aspirated carefully, ensuring the cells were not disturbed. The cells were gently washed twice with 100 μl DPBS, after which, 100 μl Hoechst (5 $\mu\text{g}\cdot\text{ml}^{-1}$) was added to each well and incubated for 10 min at 37°C. Following this incubation, the Hoechst was aspirated from the well, and the top layers of tape were removed, to reveal a flatter well containing just the agarose gel. A volume of 100 μl RPMI Transport Medium was added to each well, and a sterile glass coverslip was applied.

A Zeiss LSM510 Confocal laser scanning upright microscope was used to determine the presence of UHMWPE wear particles in PBMNCs. Channels for DAPI and FITC were used to image the nucleus and green fluorescently labelled particles respectively, in addition to bright field microscopy. Where particles were identified inside a cell nucleus, a Z-stack of images was taken to determine that the particle was indeed inside the cell and not above or behind the cell nucleus. Images were captured and overlaid using Zen 2009 (Carl Zeiss).

4.2.2.4 Culture of PBMNCs with UHMWPE Wear Particles

Cell culture experiments were performed to determine the biological response of PBMNCs to highly crosslinked antioxidant UHMWPE wear particles. Tumour necrosis factor α has been shown to be an important cytokine in osteolysis, and is found in high levels around an osteolytic implant (Ingham et al., 2000). For this reason, TNF- α was used as a marker for the osteolytic response from PBMNCs.

Peripheral blood mononuclear cells were isolated from healthy human donors as described in section 2.4.4, and incubated with the complete size range (as generated) of wear particles for 24 hours at 37°C (5% (v/v) CO₂ in air). Due to the low density of the UHMWPE particles, particle: cell culture experiments used the agarose gel technique, as described in section 2.4.2, to ensure the cells were able to come into contact with the buoyant particles. The calculations for the dosing of UHMWPE particles are described in section 2.4.3.1. Polystyrene Fluospheres[®] (0.2 µm in size) were used as a positive control for particle uptake, dosed at a concentration of 100 µm³ per cell. Fluospheres have previously been shown to stimulate TNF-α release from PBMNCs (Liu, 2012). Lipopolysaccharide (LPS) (200 ng/ml) was also included as an additional positive control for TNF-α response. After 24 hours incubation, the supernatant was collected as described in section 2.4.5, and the ATP Lite cell viability assay was performed as outlined in section 2.4.5.1, to determine if the wear particles had any effect on cell viability. An ELISA for TNF-α was performed on the supernatant as described in section 2.4.5.2, to determine TNF-α release from PBMNCs in response to UHMWPE particles.

4.2.2.5 Culture of U937 Cell Line with UHMWPE Wear Particles

The U937 cell line was used in this study as a cell type that would remove donor variation as a factor in the cellular response to wear debris. The U937 cell line is a human cell type established from a histiocytic lymphoma, displaying monocytic characteristics. Stimulation with phorbol-12-myristate-13-acetate (PMA) causes the differentiation of U937 cells into macrophage cells, making it an ideal cell type to use as an alternative to PBMNCs isolated from human blood.

Cells were resurrected and split using the standard cell culture methods outlined in section 2.4.6.1. A sufficient cell population was maintained to provide enough cells for cell culture experiments.

4.2.2.5.1 Differentiation of U937 Cells

In order to stimulate the U937 cells to become macrophages, cells were incubated in RPMI 1640 culture medium as described in section 2.4.1.2, with the addition of 10

ng.ml⁻¹ phorbol 12-myristate 13-acetate (PMA). Cells were treated with PMA over a 24 hour period and then incubated with non-PMA standard culture medium for a further 24 hours prior to incubation with UHMWPE particle treatments, as described in section 2.4.6.2.

4.2.2.5.2 Harvesting and Culture of U937 Cells with UHMWPE Wear Debris

Following differentiation of U937 cells, cells were harvested from the flasks using 3 ml Trypsin-EDTA, and isolated to provide a known cell number in RPMI 1640 culture medium, as described in section 2.4.6.3. The Trypan blue assay was used to determine the number of viable cells in the sample, as described in section 2.4.4.1. Cells were then seeded onto the UHMWPE-containing agarose gels and incubated for 24 hours at 37°C, after which the cell viability was determined and the supernatant collected for TNF- α analysis, using the methods described in section 2.4.5.

4.3 Results

4.3.1. Generation of Clinically Relevant UHMWPE Wear Particles using the Aseptic Single Station Pin-on-Plate Wear Simulator – Test A

Using the aseptic single station pin-on-plate wear simulator, clinically relevant wear particles of each UHMWPE material listed in Table 4.1 were generated in a lubricant comprised of RPMI 1640 medium with 25% (v/v) bovine serum, and using rough (R_a 0.07-0.09 μ m) counterfaces, as described in section 2.2. The simulator was run for four days for each material, and these four-day wear tests were referred to as Test A throughout this chapter. From each material, a volume of 20 ml of lubricant was collected aseptically from the bath at the end of each wear test. The materials tested in Test A and the particle concentrations in the lubricants from each material are shown in Table 4.2. From these serum lubricants, particles were dosed at a concentration of 100 μ m³ per cell in the particle: cell incubations.

The rationale behind using rough plates to generate sterile wear debris was that there would be an increase in the volume of wear generated over four days compared to wear debris generated against a smooth counterface over the same period of time. This increase in wear is demonstrated in Figure 4.1. Using the six station pin-on-plate wear simulator and the methods outlined in section 2.1, 1050 Virgin UHMWPE was tested against smooth (R_a <0.01 μ m) and rough (R_a 0.07-0.09 μ m) CoCr counterfaces over a two-week long wear test (n=4). The wear factor for 1050 Virgin against a rough CoCr counterface was double the wear factor of 1050 Virgin against the smooth CoCr counterface. There was a significant increase in the wear factor for the 1050 Virgin material against the rough counterface compared to 1050 Virgin material against the smooth counterface (ANOVA; p <0.05).

To ensure the frequency and volume size distribution of the wear debris generated against the rough CoCr counterface was not significantly different to the clinically relevant wear debris generated against the smooth CoCr counterface, a sample of 1050 Virgin UHMWPE wear debris generated in the six station wear simulator against rough plates was isolated and characterised using the particle characterisation method described in section 2.3. The particle characterisation results were then compared to the size and frequency size distribution of 1050 Virgin UHMWPE wear

debris generated against a smooth CoCr counterface. The frequency and volume distribution of these two wear debris samples are shown in Figure 4.2.

There were no significant differences in the frequency or volume distributions of the 1050 Virgin UHMWPE particles generated against the rough counterface compared to 1050 Virgin UHMWPE particles generated against the smooth counterface (ANOVA; $p < 0.05$). The wear debris generated against a rough plate showed a mode size frequency in the $< 0.1 \mu\text{m}$ size range, followed by around 40% of wear particles comprised of particles in the $0.1\text{-}1.0 \mu\text{m}$ size range. The size distribution according to % volume was very closely matched to wear debris generated against a smooth counterface, with the mode of the volume distribution in the $1.0\text{-}10 \mu\text{m}$ size range. Since there was no significant difference between particles generated against the two different counterface finishes, this confirmed that a rough counterface was suitable for use for the generation of a large volume of clinically relevant UHMWPE wear particles.

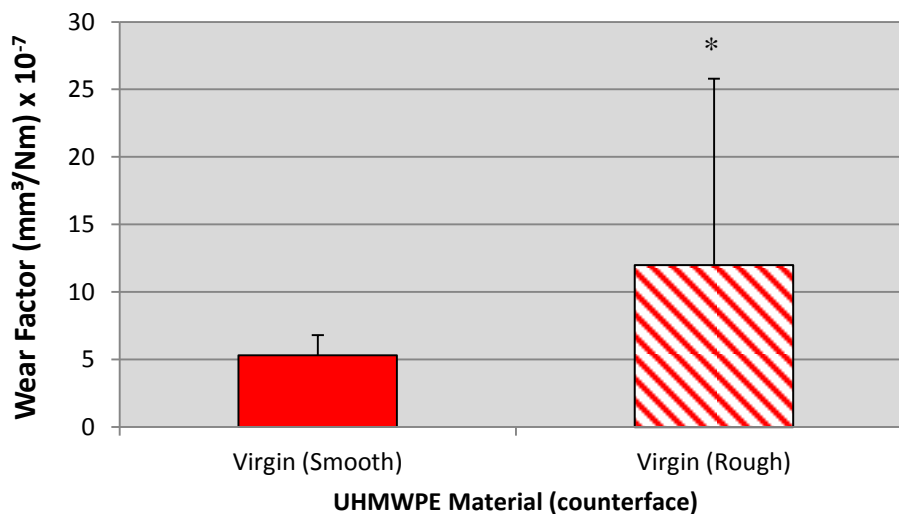


Figure 4.1 – Mean wear factors for 1050 Virgin UHMWPE against smooth ($R_a < 0.01 \mu\text{m}$) and rough ($R_a 0.07\text{-}0.09 \mu\text{m}$) CoCr alloy counterfaces. Wear tests were carried out using the six station pin-on-plate wear simulator for 2 weeks, achieving a minimum of 500,000 cycles. Wear tests used a stroke length of 28 mm at 1 Hz with a 160N load and used a lubricant of 25% (v/v) bovine serum supplemented with 0.3% (w/v) sodium azide. Error bars show the 95% confidence level, $n=3$. * indicates a statistically significant increase in the wear factor compared to the virgin (smooth) wear test (ANOVA; $p < 0.05$).

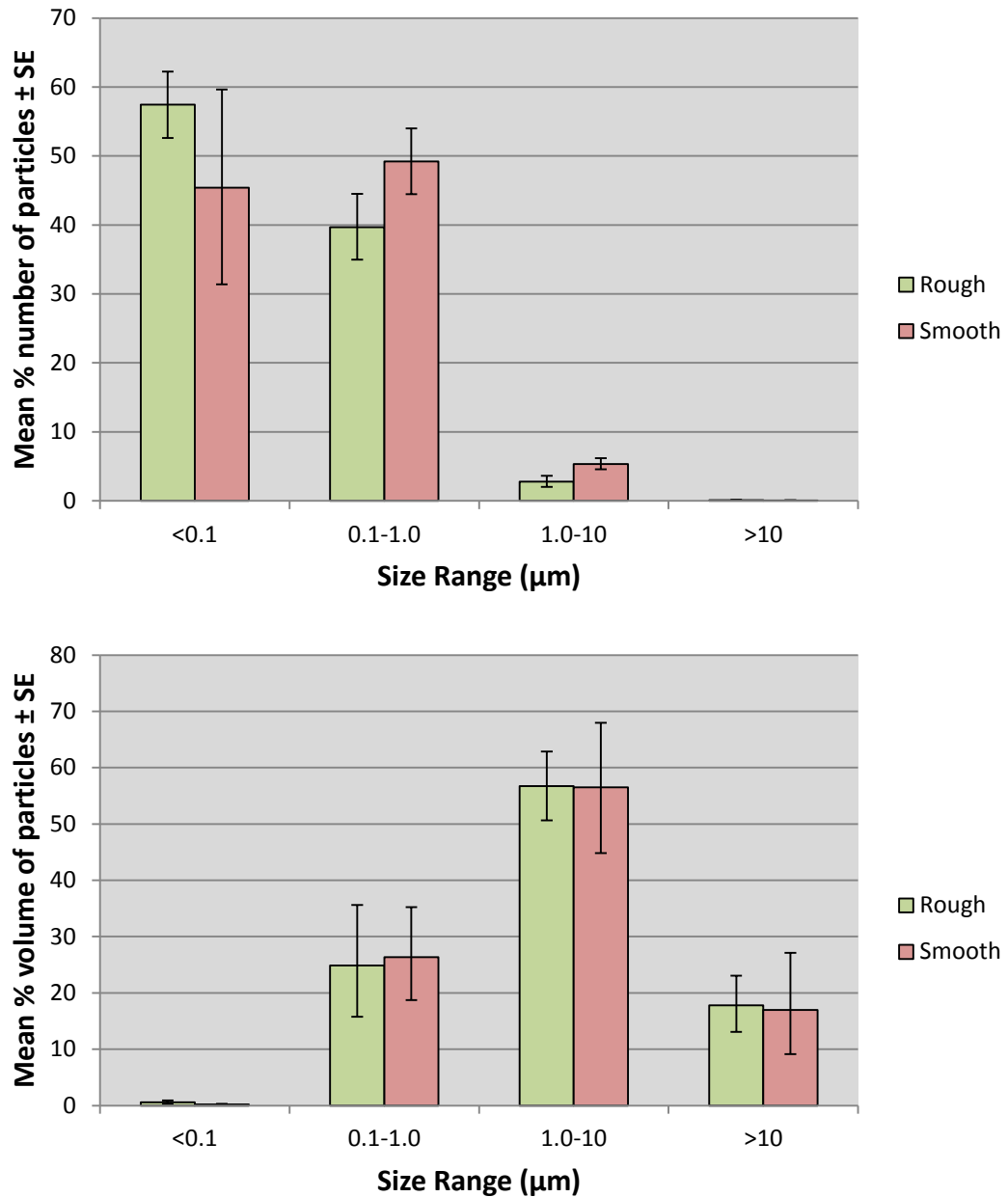





Figure 4.2 – A) The mean percentage number and B) the mean percentage volume size distribution of GUR1050 Virgin UHMWPE wear debris generated on the six station pin-on-plate simulator against either a smooth ($R_a < 0.01 \mu\text{m}$) CoCr alloy counterface, or a rough ($R_a 0.07\text{-}0.09 \mu\text{m}$) CoCr alloy counterface for 500,000 cycles. The wear simulator used a stroke length of 28 mm, with a load of 160 N at a frequency of 1 Hz. UHMWPE pins had a contact face of 10 mm and wear tests lubricants were 25% (v/v) bovine serum supplemented with 0.3% (w/v) sodium azide, for a minimum of 500,000 cycles. Error bars show the standard error, $n=4$.

Table 4.2 – The concentration of UHMWPE wear debris in serum lubricant samples collected from the aseptic single station pin-on-plate wear simulator during Test A. The colour key indicates the colour used to represent each UHMWPE material throughout this chapter.

Name	Resin	Conc. of UHMWPE Wear Debris ($\mu\text{g/ml}$)	Colour Key
1050 Virgin	GUR1050	45	
1050 HXL	GUR1050	71	
1050 Vit E 10	GUR1050	92.5	

4.3.1.1 Determination of the Endotoxin Levels in Serum Lubricants

The levels of endotoxin present in the sterile serum lubricant samples from the single station pin-on-plate wear simulator were detected using the LAL endotoxin assay. The detailed methods for this assay are described in section 2.4.2. The lubricant samples were sonicated for 40 min at 37°C, after which each sample was diluted 1:100 in LAL reagent water.

The endotoxin levels in each serum lubricant sample are shown in Table 4.3. The endotoxin levels of all three samples were below the range of the control standard endotoxin, and were therefore presented as $<0.005 \text{ EU.ml}^{-1}$. This result was below the accepted value of $<5 \text{ EU.ml}^{-1}$, as specified by the pharmaceutical industry for injectable pharmaceuticals (FDA, Regulatory Affairs, 1985). The positive product control percentage retrieval was within the 50-200% range, which indicated that the endotoxin levels detected in the serum lubricant samples were valid results. These results showed that using the single station pin-on-plate wear simulator under aseptic conditions allowed for the generation of sterile, endotoxin free wear debris in 25% (v/v) bovine serum lubricant.

Table 4.3 – Levels of endotoxin present in the lubricant samples generated in 25% (v/v) bovine serum lubricants using the single station pin-on-plate simulator (Test A).

UHMWPE Material	PPC% Recovery	Endotoxin (EU.ml⁻¹)
1050 Virgin	120%	<0.005
1050 HXL	120%	<0.005
1050 Vit E 10	102%	<0.005

Note – The positive product control (PPC%) was the sample which was spiked with a known concentration of endotoxin. The recovery of endotoxin was required to be equal to the known concentration, within 50-200% range, to be considered free of significant interference.

4.3.2 Uptake of UHMWPE Wear Particles by PBMNCs in the Agarose Gel Cell Culture Technique

The agarose gel cell culture technique is used to provide a matrix structure for cells to come into contact with UHMWPE wear debris. This method is an important protocol for the culture of PBMNCs with UHMWPE wear particles. Traditional direct culture does not allow contact between the cells and particles, due to the high buoyancy of the UHMWPE wear particles. However, prior to using the agarose gel technique to determine the cytokine response of PBMNCs to UHMWPE wear debris, it was deemed necessary to validate that this technique allowed for the contact and phagocytosis of UHMWPE wear particles by PBMNCs.

Using confocal microscopy, and the methods outlined in section 2.4.7, PBMNCs were incubated with fluorescein labelled 1050 HXL UHMWPE wear particles using the agarose gel technique, and imaged using confocal microscopy. The aim of this section was to visualise particles phagocytosed by PBMNCs, and therefore confirm that this technique facilitates the phagocytosis of UHMWPE wear particles *in vitro*.

Uptake of 0.04 μm sized Fluospheres

The initial experiments aimed to investigate the uptake of 0.04 μm Fluospheres by PBMNCs over a 48 hour incubation period. Fluospheres have previously been shown to be a good model particle to stimulate a significant cytokine response from PBMNCs (Liu, 2012). The confocal microscopy images for Fluospheres cultured with PBMNCs are shown in Figure 4.3. Fluospheres emitted bright green fluorescence under the confocal microscope when the FITC channel was selected. In Figure 4.3.1, a single monocyte can be seen, as indicated by the deep blue nucleus in image A. Image C (FITC) shows the presence of 40nm Fluospheres inside the cell. The overlay of DAPI, Bright field and FITC shows the localisation of Fluospheres inside the cell, focused around the edge of the nucleus. The images in Figure 4.3.2 show the localisation of Fluospheres inside the cells, around the edge of the nucleus. Each cell shows some internalisation of particles, indicating the agarose gel technique facilitated the uptake of 0.04 μm Fluospheres.

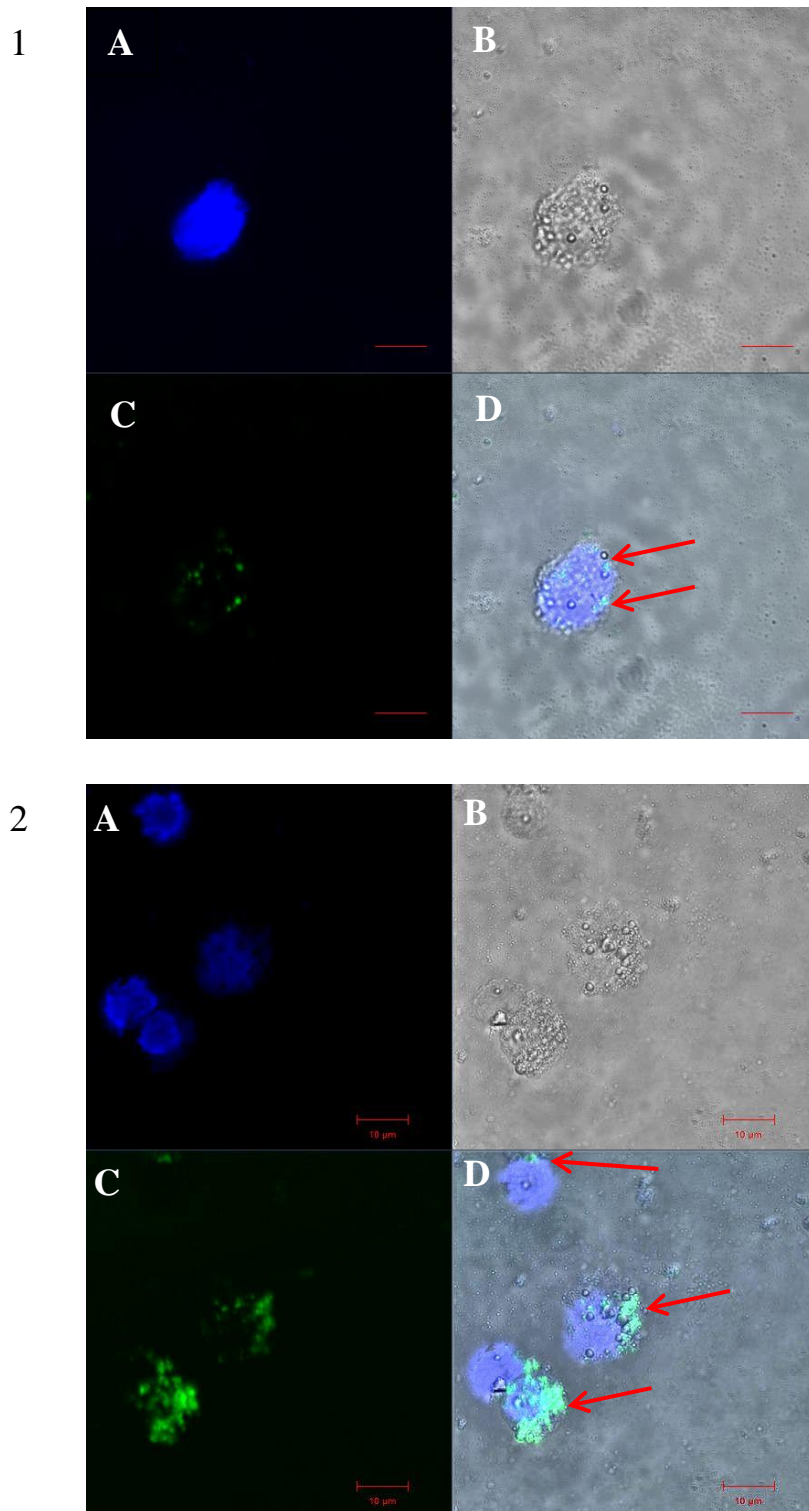


Figure 4.3 – Two fields of view of the visualisation of 0.04 μm Fluospheres internalised by PBMNCs. Confocal images show a single section through the agarose gel. A) Blue signals represent the cell nucleus stained with Hoechst 33342, B) Bright field microscopy showing the outline of the cell, C) Green signals represent 0.04 μm Fluospheres, D) Overlay. Arrows indicate the localisation of Fluospheres in the cytoplasm. Size bar indicates 10 μm .

Uptake of Micrometre sized UHMWPE Wear Particles

Using the methods outlined in section 2.4.7.2 for the fractionation of UHMWPE wear debris, a micrometre sized (1-10 μm) sample of 1050 HXL UHMWPE wear debris was incubated with PBMNCs for 48 hours at 37°C in 5% CO₂ (v/v) in air, using the agarose gel technique and the microscope slide-cell culture apparatus outlined in section 2.4.7.4. The experiment was performed as outlined for the uptake of 0.04 μm Fluospheres, with the only exception the use of micrometre sized UHMWPE wear debris.

The internalisation of micrometre sized UHMWPE wear particles is shown in Figure 4.4.1. In one of the cells, indicated by the red arrow in the FITC and overlay images, the internalisation of micrometre sized 1050 HXL wear particles can be observed. These wear particles appear to be outside of the cell nuclei and inside the cell cytoplasm. There also appears to be aggregation of wear particles once they are internalised. Two cells that have internalised UHMWPE wear particles are shown in Figure 4.4.2. The cell on the left of the image shows a faint green ring of particles around the nucleus, demonstrating the uptake of wear particles externally to the nucleus. The cell on the right of the image shows several larger particles inside the cell. The distribution of micrometre wear particles inside the cells was similar to the distribution of Fluospheres in Figure 4.3.

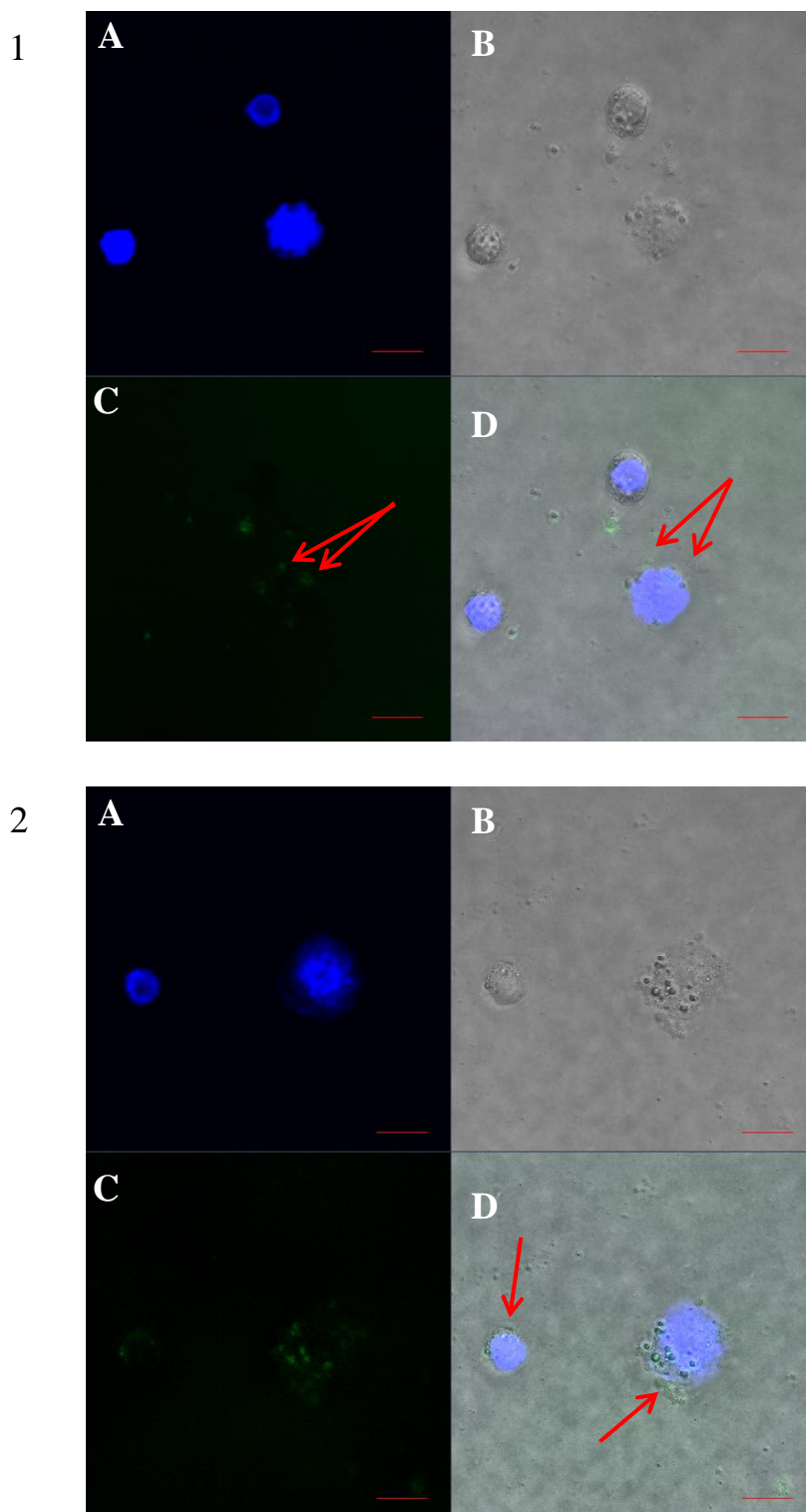


Figure 4.4 –Two fields of view of the visualisation of micrometre sized 1050 HXL UHMWPE wear particles internalised by PBMNCs. Confocal images show a single section through the agarose gel. A) Blue signals represent the cell nucleus stained with Hoechst 33342, B) Bright field microscopy showing the outline of the cell, C) Green signals represent Fluorescein labelled UHMWPE wear particles, D) Overlay. Arrows indicate the localisation of Fluospheres in the cytoplasm. Size bar indicates 10 μm.

Uptake of Nanometre sized UHMWPE Wear Particles

Using the methods outlined in section 2.4.7.2 for the fractionation of UHMWPE wear debris, a nanometre sized (0.015-0.1 μm) sample of 1050 HXL UHMWPE wear debris was incubated with PBMNCs using the agarose gel technique and the microscope slide-cell culture apparatus outlined in section 2.4.7.4. The experiment was performed as outlined for the uptake of 0.04 μm Fluospheres and micrometre sized UHMWPE wear debris, with the only difference being the use of nanometre sized UHMWPE wear debris in the agarose gels.

The internalisation of nanometre sized 1050 HXL UHMWPE wear particles is shown in Figure 4.5. These wear particles were much smaller than the particles used in the study up to this point, and were therefore observed as a diffuse green fluorescence rather than as defined particles. The uptake of nanometre sized UHMWPE wear particles in two cells shown is shown in Figure 4.5.1. The cell indicated by the red arrows showed internalisation of nanometre sized wear particles, and localisation outside the nucleus as previously observed. There were small aggregates of wear particles inside the cell cytoplasm, indicated by the red arrows. The other two cells in the image, indicated by the yellow arrows, also showed faint diffuse green fluorescence outside the nucleus, indicating the uptake of nanometre sized UHMWPE wear particles. The internalisation of nanometre sized wear particles is shown in both cells in Figure 4.5.2, although the fluorescence intensity was much weaker than observed in Figure 4.5.1. The cell at the top appears to show a clump of nanometre sized wear particles inside the cell, although further outside the nucleus than previously seen (red arrow). In the cell at the bottom of the image, the faint presence of fluorescent particles was observed (yellow arrow), which is expected following the uptake of such small wear particles. The porous structure of the agarose gel can be seen in Figure 4.5 in the bright field image, appearing as small dark dots.

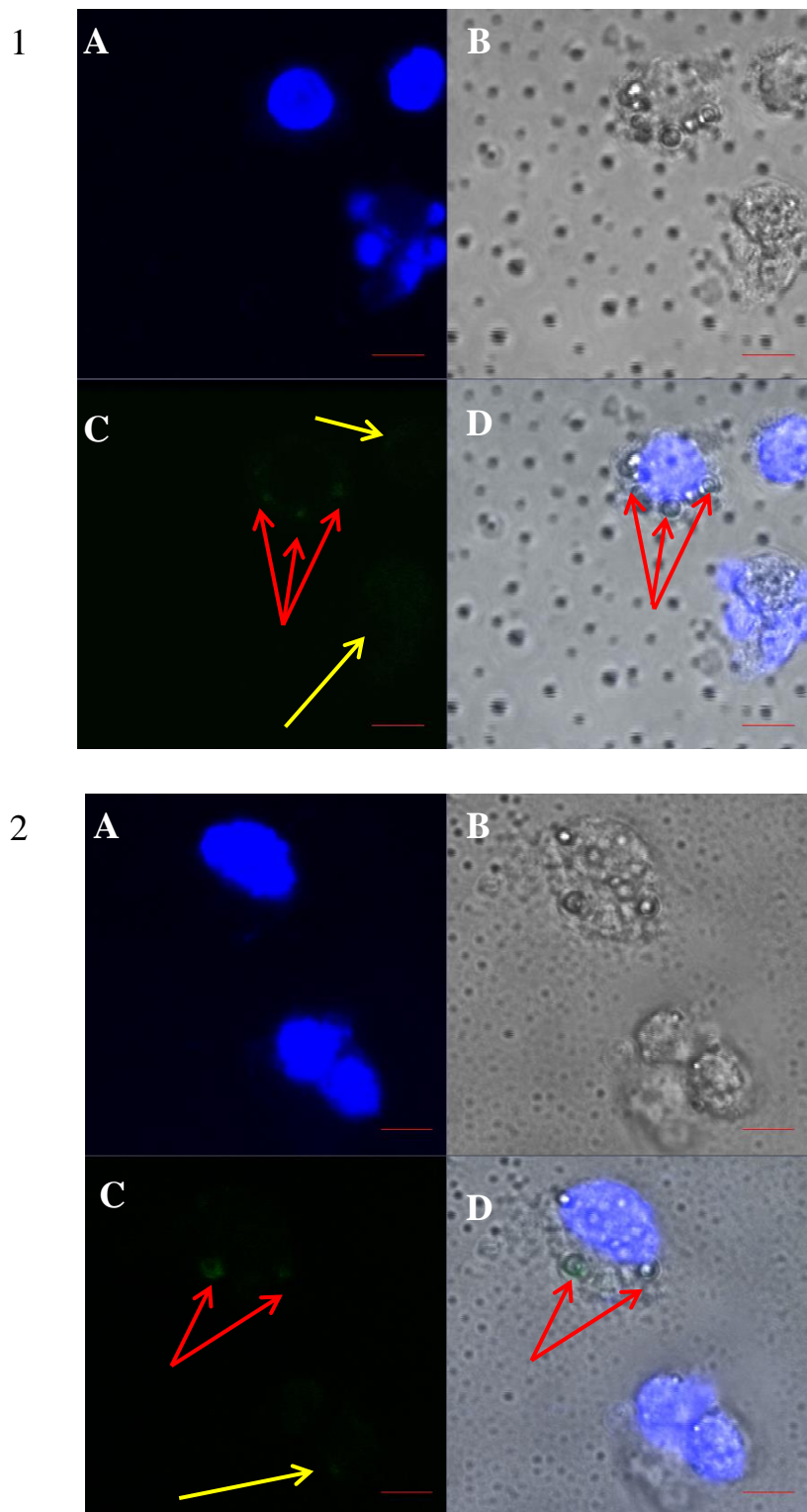


Figure 4.5 – Two fields of view of the visualisation of nanometre sized 1050 HXL UHMWPE wear particles internalised by PBMNCs. Confocal images show a single section through the agarose gel. A) Blue signals represent the cell nucleus stained with Hoechst 33342, B) Bright field microscopy showing the outline of the cell, C) Green signals represent fluorescein labelled UHMWPE wear particles, D) Overlay. Arrows indicate the internalisation of UHMWPE wear particles. Size bar indicates 10 μm .

Summary

These insightful experiments using fluorescently labelled UHMWPE wear particles incubated with PBMNCs were able to determine that cells were able to internalise UHMWPE wear particles when incubated together using the agarose gel technique. When incubated with 0.04 μm Fluospheres, micrometre and nanometre size UHMWPE 1050 HXL wear particles, PBMNCs internalised these particles, and localisation was commonly observed inside the cell cytoplasm, outside of the nucleus. These experiments validated the use of the agarose gel technique in order to provide a matrix to allow PBMNCs to come into contact with particles, but also to phagocytose them. Following this result, the agarose gel technique could be used with extra confidence for subsequent experiments investigating the effect of wear debris from the different UHMWPEs on the cell viability and TNF- α release from PBMNCs.

4.3.3. Development of the Method for Assessment of the Effects of UHMWPE Wear Particles on TNF- α Production in PBMNCs - Test A

The aim of this section of the study was to develop the methodology used to determine the osteolytic cytokine release from PBMNCs in response to both vitamin E and non-vitamin E enhanced highly crosslinked UHMWPE particles. Peripheral blood mononuclear cells isolated from healthy human volunteers were cultured with wear debris for 24 hours. The cell viability and the TNF- α release from PBMNCs in response to the different UHMWPE wear particles was determined.

The agarose gel technique, as described in section 2.4.3, was used throughout this section, unless stated otherwise. This methodology allowed the buoyant UHMWPE wear particles to be kept in suspension enabling the PBMNCs to come into contact with particles when the cells were seeded on top of the particle-containing gels. This therefore introduced an additional potential variable to the experiment in terms of the concentration and volume of the agarose gel. For that reason, the particle: cell culture assay required development in order to stimulate a cytokine response from the PBMNCs. The variables controlled and improved throughout this section

included the agarose gel concentration (v/v), the agarose gel volume, the particle concentration, the cell seeding concentration and the phagocytic fraction of the isolated peripheral blood cells.

The first part of this investigation determined the cytokine release from PBMNCs in response to stimulation with the materials listed in Table 4.1, under initial conditions used previously by Liu (2012) to determine whether these conditions were suitable for the present study. Under these conditions, Liu (2012) successfully stimulated a significantly elevated TNF- α release from PBMNCs incubated with UHMWPE wear particles fractionated into the size range of 0.1-0.6 μm at a dose of 100 μm^3 per cell. Due to the low concentration of UHMWPE wear debris in the lubricant samples generated in this study, the agarose gel plug was increased from 200 μl to a volume of 300 μl to provide a dose of 100 μm^3 particles per cell. A major difference between the present study and the study by Liu (2012) was the generation of UHMWPE wear debris, which was produced aseptically in a single station wear simulator a lubricant containing serum. Liu (2012) produced wear debris aseptically on a six station pin-on-plate wear simulator in a serum-free lubricant. The generation of wear debris by articulation in serum-containing lubricant is considered to be similar to the *in vivo* conditions and hence produces clinically relevant wear debris. The concentration of UHMWPE wear debris generated from each UHMWPE material is shown in Table 4.2, while the endotoxin levels in each sample are shown in Table 4.3. The initial conditions for the cell culture experiments for this section are outlined in Table 4.4.

Two different methods of aseptic particle generation were used in this study, with a four day test producing sample A, and the ten day test producing sample B. For this reason, the method of generation of lubricant sample (four (A) or ten (B) day) dictated the name of the test; either Test A or Test B. Throughout the method development section of the study, each experiment has been assigned under the name 'Test A', followed by the experiment number in the development section, as this section exclusively used wear debris generated in the four days; sample A. Where the study used wear debris generated over 10 days, the experiments were named Test B. Some method development used this B sample, and is therefore grouped within Test B. The investigatory section of this chapter exclusively used B sample wear debris therefore assigned the name Test B, with the relevant experiment number following that letter. For example the first method development experiment using a

lubricant sample generated in Test A was named *Test A:1*. In addition, for each condition (for example the conditions shown in Table 4.4 represent the initial conditions); the repeat experiments under those conditions are numbered starting from number 1 each time.

Table 4.4 – Cell culture conditions for the initial experiments investigating the biological response to antioxidant UHMWPE.

Cell number	1.125 x 10 ⁵ per well
Particle Concentration	100 μm ³ per cell
Agarose Gel Concentration	1 % (w/v)
Agarose Gel Volume	300 μl
Plate	48 well plate

4.3.3.1 TNF- α Release from PBMNCs Stimulated with Highly Crosslinked Vitamin E Enhanced UHMWPE Wear Debris under Initial Conditions

This aim of this section of the study was to determine TNF- α release from PBMNCs in response to the full size range of clinically relevant UHMWPE wear debris dosed at 100 μm³ particles per cell. Particle: cell incubations were conducted using the initial cell culture conditions outlined in Table 4.4. The cell viability of PBMNCs following incubation with the particle treatments and controls was determined using the ATP Lite assay (section 2.4.5.1), and an ELISA was conducted on the culture supernatants to determine the TNF- α release from cells over that period (section 2.4.5.2). The cellular response of PBMNCs to 1050 HXL UHMWPE wear debris was compared to the cellular response to 1050 Vit E 10 UHMWPE wear debris.

1. Biological Response of PBMNCs isolated from Donor 2 to 1050 Vit E 10 wear debris compared to 1050 HXL wear debris under initial cell culture conditions (Table 4.4) – Test A:1

Peripheral blood mononuclear cells isolated from Donor 2 were incubated with wear debris generated from 1050 HXL and 1050 Vit E 10 under the initial cell culture conditions successfully used by Liu (2012) and outlined in Table 4.4. The cell viability and TNF- α release from PBMNCs after 24 hours incubation with 100 μm^3 debris per cell is shown in Figure 4.6. None of the treatments had a significant effect on the cell viability of PBMNCs compared to the cells only negative control (ANOVA, $p > 0.05$). The positive control LPS treatment caused significant TNF- α release from PBMNCs compared to the cells only negative control (ANOVA; $p < 0.05$). Cells treated with 1050 HXL showed a higher mean TNF- α response compared to cells only and 1050 Vit E 10, however this increase was not significant.

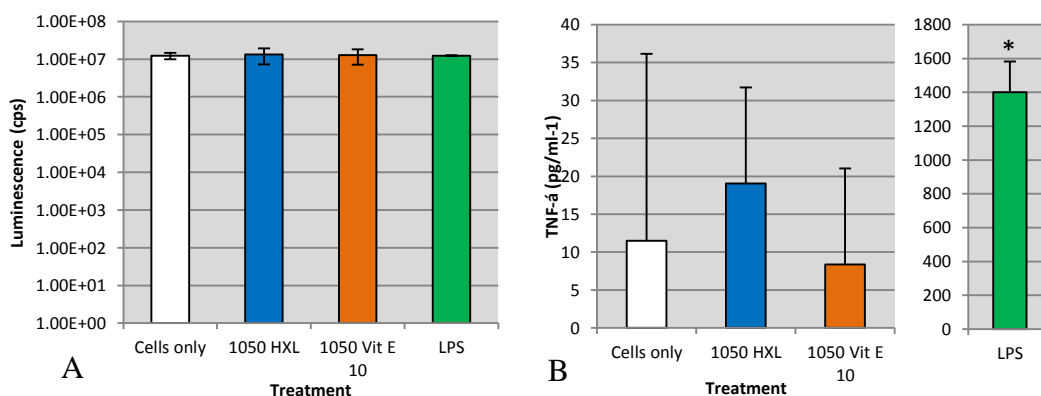


Figure 4.6 - A) Cell viability and B) TNF- α release from PBMNCs isolated from Donor 2 incubated with 1050 HXL and 1050 Vit E 10 UHMWPE wear debris at a concentration of 100 μm^3 debris per cell for 24 hours at 37°C in 5% (v/v) CO₂ in air. Cells were seeded at a density of 1.125 x 10⁵ cells per well. Cells only acted as the negative control, 200 ng/ml⁻¹ lipopolysaccharide acted as the positive control. * indicates statistically significant TNF- α release from PBMNCs compared to the cells only negative control (ANOVA, $p < 0.05$). Error bars show \pm the 95% confidence levels, n=4.

2. Biological Response of PBMCs isolated from Donor 12 to 1050 Vit E 10 wear debris and 1050 HXL wear debris under initial cell culture conditions (Table 4.4) – Test A:2

Peripheral blood mononuclear cells isolated from Donor 12 were incubated with wear debris generated from 1050 HXL and 1050 Vit E 10 under the initial cell culture conditions successfully used by Liu (2012) and outlined in Table 4.4. Cell viability and TNF- α release after 24 hours incubation are shown in Figure 4.7. None of the UHMWPE particle treatments had a significant effect on the cell viability of PBMCs compared to the cells only negative control (ANOVA, $p > 0.05$). The lipopolysaccharide treatment significantly reduced cell viability following the 24 hours incubation. The positive control LPS treatment caused significant TNF- α release from PBMCs compared to the cells only negative control (ANOVA; $p < 0.05$). However, neither of the UHMWPE particle treatments generated a significant TNF- α release compared to the cells only negative control (ANOVA; $p > 0.05$), indicating the absence of any biological response to these wear particles under the conditions applied.

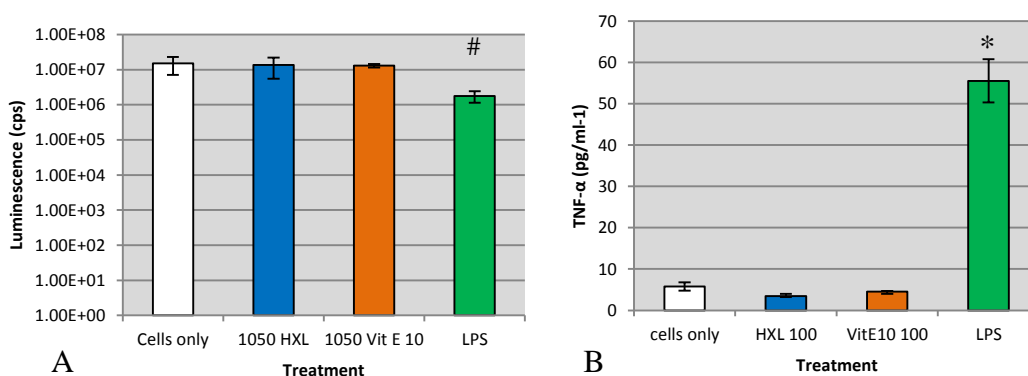


Figure 4.7 - A) Cell viability and B) TNF- α release from PBMCs isolated from Donor 12 incubated with 1050 HXL and 1050 Vit E 10 UHMWPE wear debris at a concentration of $100 \mu\text{m}^3$ debris per cell for 24 hours at 37°C in 5% (v/v) CO_2 in air. Cells were seeded at a density of 1.125×10^5 cells per well. Cells only acted as the negative control, 200 ng/ml^{-1} lipopolysaccharide acted as the positive control. # indicated a statistically significant reduction in cell viability compared to the cells only negative control. * indicates statistically significant TNF- α release from PBMCs compared to the cells only negative control (ANOVA, $p < 0.05$). Error bars show \pm the 95% confidence levels, $n=4$.

3. Biological Response of PBMCs isolated from Donor 13 to 1050 Vit E 10 wear debris compared to 1050 HXL wear debris under initial cell culture conditions (Table 4.4) – Test A:3

In the third experiment, 1050 Virgin wear debris was included as an additional material and the stimulation of TNF- α release from PBMCs was determined. The effects on cell viability and TNF- α release from PBMCs isolated from Donor 13 and incubated with 100 μm^3 wear debris per cell are shown in Figure 4.8. None of the treatments had a significant effect on cell viability. Peripheral blood mononuclear cells from Donor 13 released significantly elevated levels of TNF- α in response to LPS treatment, compared to the cells only negative control (Figure 4.8B). Cells treated with 1050 HXL wear debris elicited a higher mean level of TNF- α release compared to cells only and 1050 Vit E 10 treated cells, however this was not significantly different, and therefore not considered a significant biological response (ANOVA, $p > 0.05$). Cells treated with 1050 Virgin UHMWPE also showed no significant release of TNF- α compared to the cells only negative control.

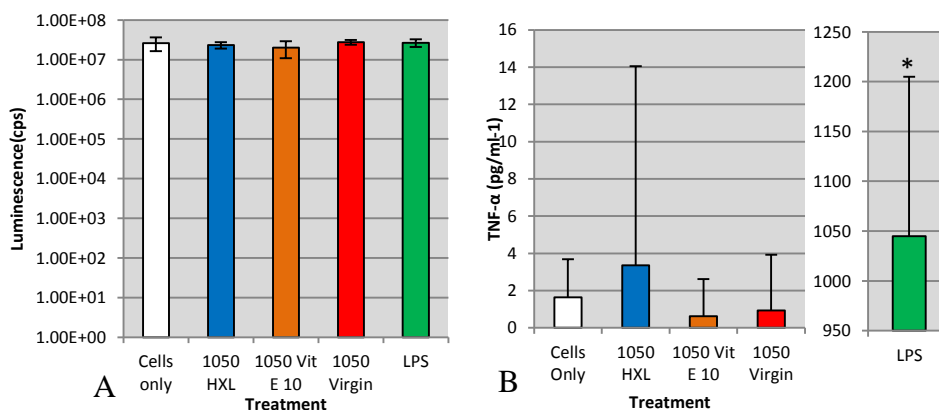


Figure 4.8 - A) Cell viability and B) TNF- α release from PBMCs isolated from Donor 13 incubated with 1050 HXL, 1050 Vit E 10 and 1050 Virgin UHMWPE wear debris at a concentration of 100 μm^3 debris per cell for 24 hours at 37°C in 5% (v/v) CO₂ in air. Cells were seeded at a density of 1.125 × 10⁵ cells per well. Cells only acted as the negative control, 200 ng/ml⁻¹ lipopolysaccharide acted as the positive control. * indicates statistically significant TNF- α release from PBMCs compared to the cells only negative control (ANOVA, $p < 0.05$). Error bars show \pm the 95% confidence levels, n=4.

4. Summary

The results presented from this set of initial experiments revealed that PBMNCs incubated with UHMWPE wear debris under the conditions outlined in Table 4.4 did not produce a significant response, in terms of TNF- α release compared to the cells only negative controls. Due to the number of potential variables in this experiment (e.g. cell seeding density, agarose concentration), there may have been several reasons for this lack of stimulation, and the experiment was subsequently developed to produce an environment where the UHMWPE wear debris produced a significant response from PBMNCs in a reproducible fashion. The first method development step was to determine the percentage agarose gel that would produce the optimal conditions for particle: cell interaction.

4.3.3.2 TNF- α Release from PBMNCs Stimulated with Highly Crosslinked Vitamin E Enhanced UHMWPE Wear Debris embedded in Different Concentrations of Agarose Gel

The first change to the cell culture conditions was to alter the agarose percentage concentration in the agarose plugs that contained the UHMWPE wear debris. The rationale behind this change was to potentially create a more porous medium by reducing the agarose concentration to allow for increased cell penetration. To test this hypothesis, particle: cell culture experiments were conducted treating PBMNCs with two test materials; 1050 HXL and 1050 Vit E 10 using 0.4% (w/v) agarose gels. The experiment also included 1050 Virgin wear debris in three different agarose concentrations; 1% (w/v), 0.4% (w/v), and a final test using no agarose. While investigating the effect of different agarose concentrations, the inclusion of an agarose-free well was used to determine the effect of the agarose on cells. A large volume of 1050 Virgin UHMWPE wear debris was produced using the single station wear simulator, and this allowed for these multiple experiments using this material, whereas the 1050 HXL and 1050 Vit E 10 were used more sparingly due to their lower wear and lower particle concentrations in these samples. An agarose volume of 300 μ l was maintained in these experiments, with additional RPMI 1640 transport medium used to dilute the agarose gel to the lower concentration of 0.4% (w/v). Where no agarose gel was used, the particles were added at a dose of 100 μ m³ wear

debris per cell, followed by the addition of cells, after which a volume of RPMI 1640 culture medium was added to bring the final volume to 1 ml per well as used previously, to ensure cells were cultured in the same volume of solution in all experiments.

1. Biological response of PBMNCs isolated from Donor 1 to 1050 Vit E 10 wear debris compared to 1050 HXL and 1050 Virgin wear debris using different agarose concentrations (Table 4.5) – Test A:4

In these experiments, the particle: cell culture experiment was repeated with 1050 HXL and 1050 Vit E 10 UHMWPE wear debris but using 0.4% (w/v) agarose gels instead of the 1% (w/v) gels used previously in section 4.3.2.1. In addition, 1050 Virgin UHMWPE wear debris was tested in 1% (w/v) and 0.4% (w/v) agarose, and also without agarose gel, in direct culture. The cell culture conditions are shown in Table 4.5. The aim of this section was to investigate the effect of changing the agarose concentration on the interaction of cells with wear particles and on the cellular response to the wear particles. The effect on cell viability and TNF- α release from PBMNCs isolated from Donor 1 incubated with 100 μm^3 wear particles per cell are shown in Figure 4.9. There was no significant effect of any of the treatments on cell viability (ANOVA, $p > 0.05$). There was a significantly elevated TNF- α release from PBMNCs treated with 200ng/ml⁻¹ LPS, however there was no significant TNF- α release in response to any of the UHMWPE particle treatments. The alteration of the agarose concentration had no significant effect on the cell viability or TNF- α response of PBMNCs treated with UHMWPE wear debris. Large error bars were observed for the mean TNF- α release of cells treated with each of the UHMWPE particle treatments..

Table 4.5 – Cell culture conditions for experiments investigating the biological response to antioxidant UHMWPE using different agarose concentrations

Cell number	1.125 x 10 ⁵ per well
Particle Concentration	100 μm ³ per cell
Agarose Gel Concentration	1 %, 0.4%, 0% (w/v)
Agarose Gel Volume	300 μl
Plate	48 well plate

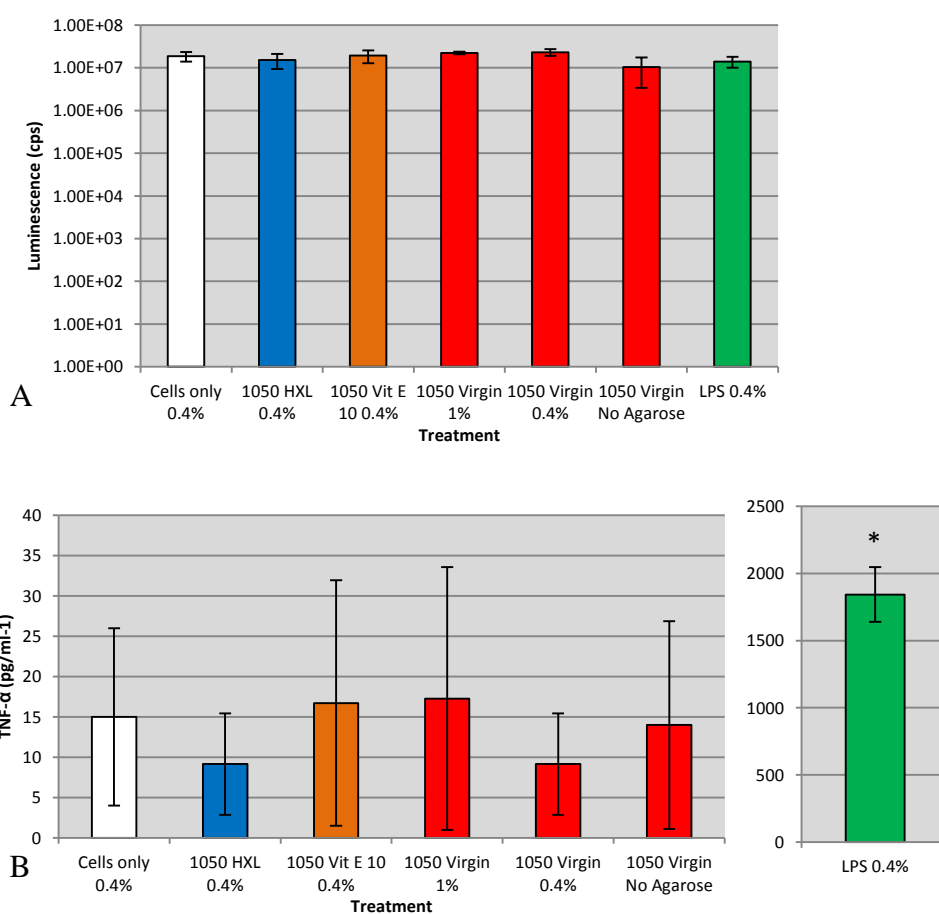


Figure 4.9 - A) Cell viability and B) TNF- α release from PBMCs isolated from Donor 1 incubated with 1050 HXL, 1050 Vit E 10 and 1050 Virgin UHMWPE wear debris at a concentration of 100 μm^3 wear debris per cell for 24 hours at 37°C in 5% (v/v) CO₂ in air. Cells were seeded at a density of 1.125 x 10⁵ cells per well. The agarose gel plugs were produced at a concentration of 0.4% (w/v) for each UHMWPE particle treatment, with an additional 1% (w/v) and no-agarose condition for 1050 Virgin treatments. Cells only acted as the negative control, 200 ng/ml⁻¹ lipopolysaccharide acted as the positive control. * indicates a statistically significant TNF- α response from PBMCs compared to cells only control (ANOVA, $p < 0.05$). Error bars show \pm the 95% confidence level, $n=4$.

2. Biological response of PBMNCs isolated from Donor 2 to 1050 Vit E 10 wear debris compared to 1050 HXL wear debris (no agarose) – Test A:5

A repeat experiment was carried out to determine the optimum agarose percentage concentration for the stimulation of PBMNCs with UHMWPE wear debris. Cells isolated from Donor 2 were seeded at a concentration of 1.125×10^5 , in a final volume of 1 ml RPMI 1640 culture medium with UHMWPE wear debris. The incubation was for 24 hours after which point the supernatant was carefully collected, so that the UHMWPE wear particles were not disturbed. The effect on cell viability and TNF- α release from PBMNCs isolated from Donor 2 and stimulated with 1050 HXL or 1050 Vit E 10 UHMWPE wear debris at a concentration of $100 \mu\text{m}^3$ per cell are shown in Figure 4.10.

In addition, this experiment included $0.2 \mu\text{m}$ polystyrene Fluospheres (FS) as a positive control at $100 \mu\text{m}^3$ per cell to determine TNF- α release. Fluospheres have previously been shown to stimulate TNF- α release from PBMNCs as a model particle (Liu, 2012).

There was no significant effect of any of the treatments on cell viability of PBMNCs (ANOVA; $p > 0.05$). The LPS positive control stimulated a significantly elevated level of TNF- α release from PBMNCs, compared to the cells only negative control (ANOVA; $p < 0.05$). None of the other treatments had a significant effect on TNF- α release. For this donor, the background cellular response was higher than in previous experiments with other donors, and also higher than when this donor (Donor 2) was used previously. The 1050 HXL treated cells produced a TNF- α response of 47 pg/ml^{-1} , a response that would have been considered high in previous experiments with a lower cells only negative control response. In comparison to the 1050 HXL treated cells, 1050 Vit E 10 treated cells produced lower levels of TNF- α . However, in comparison to the Fluosphere treated cells, the TNF- α response was generally low, indicating that removing the agarose gel technique had no beneficial effect on the stimulation of PBMNCs by UHMWPE wear debris.

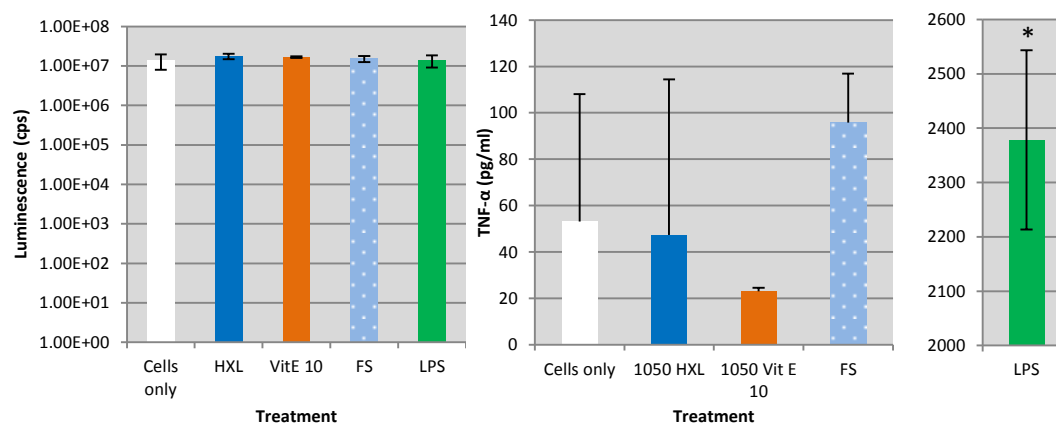


Figure 4.10 - A) Cell viability and B) TNF- α release from PBMNCs isolated from Donor 2 incubated with 1050 HXL and 1050 Vit E 10 UHMWPE wear debris at a concentration of $100 \mu\text{m}^3$ wear debris per cell for 24 hours at 37°C in 5% (v/v) CO_2 in air. Cells were seeded at a density of 1.125×10^5 cells per well. Particles and cells were incubated in RPMI 1640 culture medium using direct cell culture method. Cells only acted as the negative control, 200 ng/ml^{-1} lipopolysaccharide acted as the positive control along with $100 \mu\text{m}^3$ $0.2 \mu\text{m}$ Fluospheres. * indicates a statistically significant TNF- α response from PBMNCs compared to cells only control (ANOVA, $p < 0.05$). Error bars show \pm the 95% confidence level, $n=4$.

3. Summary

The change in agarose concentration had no significant effect on the cellular response to wear debris. There was no significant difference in the cell viability or the level of TNF- α release from cells incubated in 0.1% (w/v) or 0.4% (w/v) agarose gel, or from cells cultured directly with UHMWPE particles (agarose-free). As a result, particle: cell experiments from this point used 0.4% (w/v) agarose as it was believed that a more viscous agarose gel would maximise the movement of the buoyant UHMWPE particles to the surface of the gel before solidification.

4.3.3.3 TNF- α Release from PBMNCs Stimulated with Highly Crosslinked Vitamin E Enhanced UHMWPE Wear Debris - Altering the Cell Seeding Density

The density of cells incubated in each well was hypothesised to be an important part of the experimental procedure. For that reason, the next step was to alter the cell seeding density and phagocytic fraction to determine the ideal cell conditions for PBMNCs to be incubated and respond to UHMWPE wear debris.

The process for the isolation of peripheral blood mononuclear cells from human blood does not specifically isolate phagocytes but rather the white cell fraction, including lymphocytes, monocytes and macrophages. For that reason, the final cell seeding density of PBMNCs was determined as a fraction of the overall cell count. The process for calculating the final phagocytic cell count is described in section 2.4.4.1. The experiments performed previously (test A: 1 – A: 4) used a phagocytic fraction of 12% as the initial test phagocytic fraction, and a cell seeding density of 1.125×10^5 per well.

In addition, the following experiments incubated $0.2 \mu\text{m}$ polystyrene Fluospheres (FS) at $100 \mu\text{m}^3$ per cell as a positive particle control. Fluospheres have previously been shown to stimulate TNF- α release from PBMNCs and have been used as a model particle (Liu, 2012).

This aim of this section of experiments was to determine the effect of increasing the cell seeding density on the cell viability and TNF- α release from PBMNCs. Previous experiments had used 1.125×10^5 cells per well; here a density of 2×10^5 cells per well was tested with two donors. The first donor was Donor 7, followed by Donor 3. The cell culture conditions for this section are shown in Table 4.6.

One limitation when using primary cells isolated from blood from healthy human donors is the limitation on the total cell number, due to the finite number of cells available in the sample of blood used. Due to ethical reasons, only a small volume of blood could be taken from donors; usually around 28 ml. This limited the number of PBMNCs isolated, and subsequently only five-six treatments could be investigated with each sample at a cell seeding density of 2×10^5 .

Table 4.6 – Cell culture conditions for experiments investigating the biological response to antioxidant UHMWPE using an increased cell seeding density of 2×10^5 cells per well

Cell number	2×10^5 per well
Particle Concentration	$100 \mu\text{m}^3$ per cell
Agarose Gel Concentration	0.4% (w/v)
Agarose Gel Volume	300 μl
Plate	48 well plate

1. Biological response of PBMNCs isolated from Donor 7 to 1050 Vit E 10 wear debris compared to 1050 HXL wear debris with a higher cell seeding density of 2×10^5 cells per well – Test A:5

Cells isolated from Donor 7 were incubated with particles at a concentration of $100 \mu\text{m}^3$ per cell in 300 μl agarose (0.4% (w/v)) for 24 hours. The cell culture conditions are shown in Table 4.6, with the changes from the initial conditions being the increased cell seeding density of 2×10^5 per well, and the reduced agarose gel concentration of 0.4% (v/v). The effect on cell viability and TNF- α release of PBMNCs isolated from Donor 7 and incubated with $100 \mu\text{m}^3$ UHMWPE wear debris are shown in Figure 4.11. There was no significant effect of any of the treatments on cell viability compared to the cells only negative control. There was significantly elevated TNF- α release from cells treated with 200 ng/ml^{-1} LPS, and also from cells incubated with 0.2 μm Fluospheres. The mean TNF- α release from cells incubated with 1050 HXL was higher than from the cells only negative control and the 1050 Vit E 10 treated cells, however this was not statistically significant (ANOVA; $p > 0.05$).

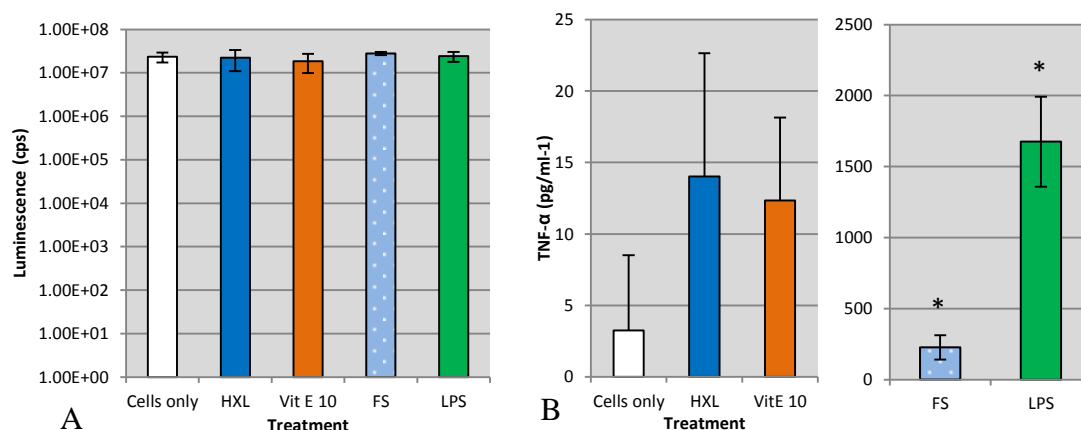


Figure 4.11 - A) Cell viability and B) TNF- α release from PBMNCs isolated from Donor 7 incubated at with 1050 HXL and 1050 Vit E 10 UHMWPE wear debris at a concentration of 100 μm^3 wear debris for 24 hours at 37°C in 5% (v/v) CO₂ in air. Cells were seeded at a density of 2×10^5 cells per well. Cells only acted as the negative control, 200 ng/ml⁻¹ lipopolysaccharide acted as the positive control, while 0.2 μm Fluospheres at a concentration of 100 μm^3 per cell acted as a model particle positive control. * indicates a statistically significant TNF- α response from PBMNCs compared to cells only control (ANOVA, $p < 0.05$). Error bars show \pm the 95% confidence level, $n=4$. Where only + error bars are shown, this is due to \pm error bars altering the scale of the graph to make it difficult to read.

2. Biological response of PBMNCs isolated from Donor 3 to 1050 Vit E 10 wear debris compared to 1050 HXL wear debris with a higher cell seeding density of 2×10^5 cells per well – Test A:6

A repeat experiment was carried out using the conditions outlined in test A: 5. In the previous test, neither 1050 HXL nor 1050 Vit E 10 UHMWPE debris treatments caused an increase in the TNF- α release from PBMNCs isolated from Donor 7. This experiment used cells isolated from Donor 3. The effect on cell viability and TNF- α release from PBMNCs isolated from Donor 3 and incubated with 100 μm^3 UHMWPE wear debris are shown in Figure 4.12. None of the treatments had any significant effect on the cell viability of PBMNCs isolated from Donor 3. There was significantly elevated TNF- α release from cells incubated with 200 ng/ml⁻¹ LPS, and also cells incubated with 0.2 μm Fluospheres, compared to the cells only negative control.

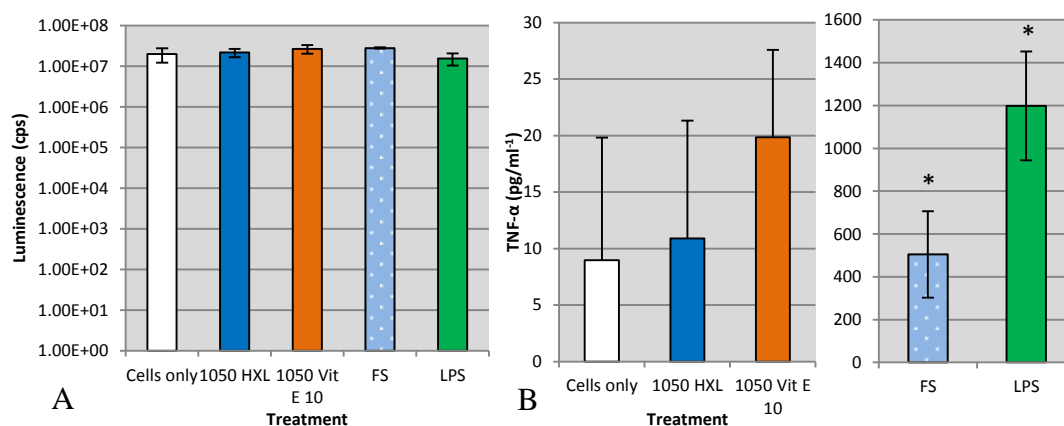


Figure 4.12 - A) Cell viability and B) TNF- α release from PBMNCs isolated from Donor 3 incubated with 1050 HXL, and 1050 Vit E 10 UHMWPE wear debris at a concentration of 100 μm^3 wear debris for 24 hours at 37°C in 5% (v/v) CO₂ in air. Cells were seeded at a density of 2×10^5 cells per well. Cells only acted as the negative control, 200 ng/ml⁻¹ lipopolysaccharide acted as the positive control, while 0.2 μm Fluospheres at a concentration of 100 μm^3 per cell acted as a model particle positive control. * indicates a statistically significant TNF- α response from PBMNCs compared to cells only control (ANOVA, $p < 0.05$). Error bars show \pm the 95% confidence level, $n=4$.

The increased cell seeding density had no negative effect on the cell viability or TNF- α release from PBMNCs in response to UHMWPE wear debris. While no significant release of TNF- α was observed from cells at a seeding density of 2×10^5 per well, the increased cell density provided a significant TNF- α response from cells incubated with 0.2 μm Fluospheres compared to the cells only control; a significant result not observed in the previous experiment with Fluospheres incubated with cells at a seeding density of 1.125×10^5 cells per well. This suggested a stronger cellular response was achieved at this cell seeding density, and therefore a density of 2×10^5 cells per well was used in all further experiments.

In an attempt to further develop the particle: cell experiment, a test was conducted investigating three different phagocytic fractions. The final cell seeding density remains at 2×10^5 cells per well, however the assumed fraction of cells that were phagocytes was adjusted.

3. Biological response of PBMNCs isolated from Donor 15 to 1050 HXL wear debris using different phagocytic fractions – Test A:7

To investigate the optimum phagocytic fraction to be used for this experiment, a test experiment was conducted using three different assumed phagocytic fractions of 12%, 6% and 3%. These fractions were chosen as a previous study showed that the fraction of phagocytes isolated from human blood was between 3-10%, using the latex bead assay (Liu, 2012). These experiments used a cell seeding density of 2×10^5 cells per well, in a 300 μ l agarose plug (0.4% (w/v)). Wear debris from 1050 HXL was the only UHMWPE treatment used in order to limit the treatment variables, while the assumed phagocytic fraction was adjusted. Wear debris derived from 1050 HXL was used at a concentration of 100 μ m³ per cell. The cells only negative and LPS positive controls used a phagocytic fraction of 12% due to the limit on cell number, and therefore the limit on the number of treatments in one experiment. The effect on cell viability and TNF- α release from PBMNCs isolated from Donor 15 and incubated with 100 μ m³ UHMWPE wear debris are shown in Figure 4.13.

None of the treatments had a significant effect on the cell viability of PBMNCs isolated from Donor 15, and there was no significant difference in the cell viability of the 1050 HXL treated cells at different phagocytic fractions compared to the cells only negative control. There was significantly elevated TNF- α release from cells incubated with 200 ng/ml⁻¹ LPS (ANOVA; $p < 0.05$). There was no significantly elevated TNF- α release from PBMNCs treated with 1050 HXL, indicating the change in phagocytic fraction had no effect on the cellular response to UHMWPE wear debris. However, cells seeded with a 6% assumed phagocytic fraction caused a higher mean TNF- α release than cells only negative control, with a large error bar. This increase was not significant however.

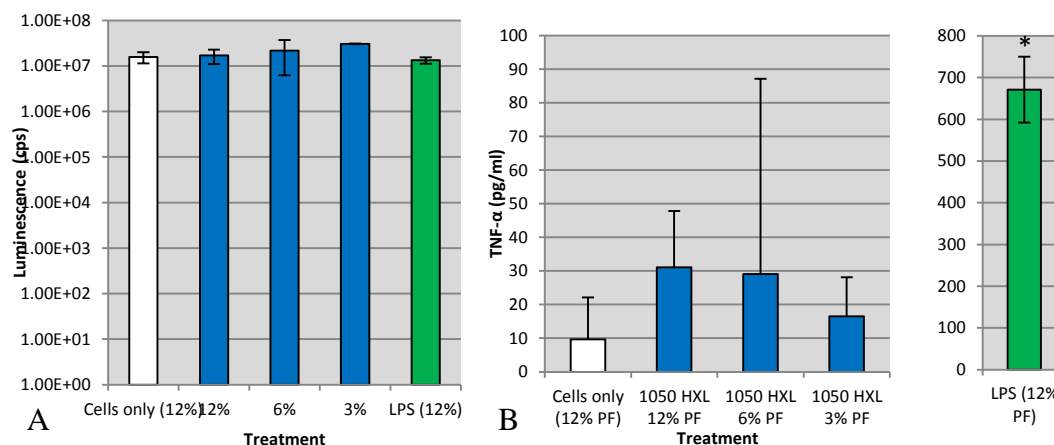


Figure 4.13 - A) Cell viability and B) TNF- α release from PBMNCs isolated from Donor 15 incubated with 1050 HXL UHMWPE wear debris at a concentration of 100 μm^3 wear debris for 24 hours at 37°C in 5% (v/v) CO₂ in air. Cells were seeded at a density of 2 x 10⁵ cells per well, using three different assumed phagocytic fractions (PF) of 12%, 6% and 3%. Cells only acted as the negative control, 200 ng/ml⁻¹ lipopolysaccharide acted as the positive control. * indicates a statistically significant TNF- α response from PBMNCs compared to cells only control (ANOVA, $p < 0.05$). Error bars show \pm the 95% confidence level, $n=4$.

4. Summary

Altering the assumed phagocytic fraction of cells isolated from Donor 15 had no significant effect on TNF- α release in response to 1050 HXL. The 6% phagocytic fraction test showed a mean TNF- α release very close to the TNF- α release from the 12% phagocytic fraction test. Using the previous 12% phagocytic fraction has so far not yielded significant TNF- α release, therefore to maximise cell usage, the subsequent particle: cell culture experiments used a 6% phagocytic fraction, and a cell seeding density of 2 x 10⁵ per well.

Throughout this section of the study, steps have been taken to alter the conditions of the particle: cell experiments in order to improve the stimulation of PBMNCs by UHMWPE wear debris at a dose of 100 μm^3 per cell. So far, no significantly elevated TNF- α release has been observed from PBMNCs incubated with UHMWPE wear debris, compared to the cells only negative control. At a cell seeding density of

2×10^5 , PBMNCs have shown a significant TNF- α response to $0.2\mu\text{m}$ Fluospheres at a dose of $100 \mu\text{m}^3$. Under all conditions, a significant TNF- α response has been observed from PBMNCs incubated with LPS at a concentration of 200 ng.ml^{-1} (ANOVA; $p < 0.05$).

Although several factors have been changed throughout this section, it was apparent that individual donor variation was an important factor when determining the response of primary cells isolated from human blood to UHMWPE wear particles. Some donors (e.g. Donors 8 and 15) showed slightly elevated TNF- α release in response to UHMWPE wear debris, while other donors showed almost no TNF- α release. At this stage, the present study therefore investigated the response of cells derived from a cell line, in order to eliminate the effects of donor variation. For the subsequent section of this study, cells derived from the U937 cell line were incubated with UHMWPE wear debris to determine the TNF- α response.

4.3.3.4 Cellular Response of U937 Cells to Vitamin E enhanced Highly Crosslinked UHMWPE Wear Debris

Donor variation was hypothesised to play an important role in TNF- α release from PBMNCs in response to UHMWPE wear debris. In a previous study, Liu (2012) showed certain donor PBMNCs responded to UHMWPE wear debris in the $0.1\text{-}0.6 \mu\text{m}$ size range with a significant TNF- α release compared to the cells only control; however this was not consistent across all donors. This variation was therefore thought to be an important factor in this study when using primary donor cells to determine the cellular response to non-fractionated antioxidant wear debris. For this reason, a cell line was used in order to remove donor variation as a factor from these experiments, while still providing a macrophage cell type to determine the cytokine response to UHMWPE wear debris.

The U937 cell line is a human cell line established from a histiocytic lymphoma and displays characteristics of monocytes. The cells differentiate following stimulation with phorbol 12-myristate 13-acetate (PMA) to form mature macrophages. For this reason this U937 cells were chosen as a cell type to use for the investigation of the TNF- α response to UHMWPE wear debris, without the factor of donor variation.

Cells from the U937 lineage were differentiated with $10\text{ng}\cdot\text{ml}^{-1}$ PMA for 24 hours and harvested as described in section 2.4.6.2 and 2.4.6.3, respectively. Differentiated cells were seeded with 1050 HXL and 1050 Vit E 10 UHMWPE wear debris using the agarose gel technique, as outlined in section 2.4.3.

1. Biological response of U937 macrophages to 1050 HXL, 1050 Vit E 10 and 1050 Virgin UHMWPE wear debris – Test A:8

Macrophages derived from U937 cells were seeded at a density of 2×10^5 per well, with a particle concentration of $100 \mu\text{m}^3$ per cell. Cells were incubated for 24 hours with 1050 HXL, 1050 Virgin and 1050 Vit E 10 UHMWPE wear debris, in addition to $0.2 \mu\text{m}$ Fluospheres and LPS as positive controls for TNF- α release. The lack of restriction on cell number allowed for more treatments in one experiment than was possible when using PBMNCs. Following seeding of cells, the experiment followed the same protocol as when using PBMNCs, including using the agarose gel technique, as outlined in section 2.4.5. The cell culture conditions are shown in Table 4.7.

Table 4.7 - Cell culture conditions for experiments investigating the biological response of U937 cells to antioxidant UHMWPE

Cell number	2×10^5 per well
Particle Concentration	$100 \mu\text{m}^3$ per cell
Agarose Gel Concentration	0.4% (w/v)
Agarose Gel Volume	300 μl
Plate	48 well plate

The effect on cell viability and TNF- α release from differentiated U937 cells following 24 hour incubation with $100 \mu\text{m}^3$ UHMWPE wear debris per cell are shown in Figure 4.14. None of the treatments had a significant effect on the cell viability after 24 hours. The LPS and Fluosphere treatments stimulated significantly elevated levels of TNF- α release compared to the cells only negative control. In addition, 1050 Virgin UHMWPE wear debris at $100 \mu\text{m}^3$ per cell stimulated

significantly elevated levels of TNF- α release from U937 cells compared to the cells only negative control (ANOVA; $p < 0.05$). The 1050 HXL UHMWPE particle treated cells did not show an increase in TNF- α release. The lack of TNF- α release compared to the cells only negative control was also the case in the 1050 Vit E 10 particle treated cells.

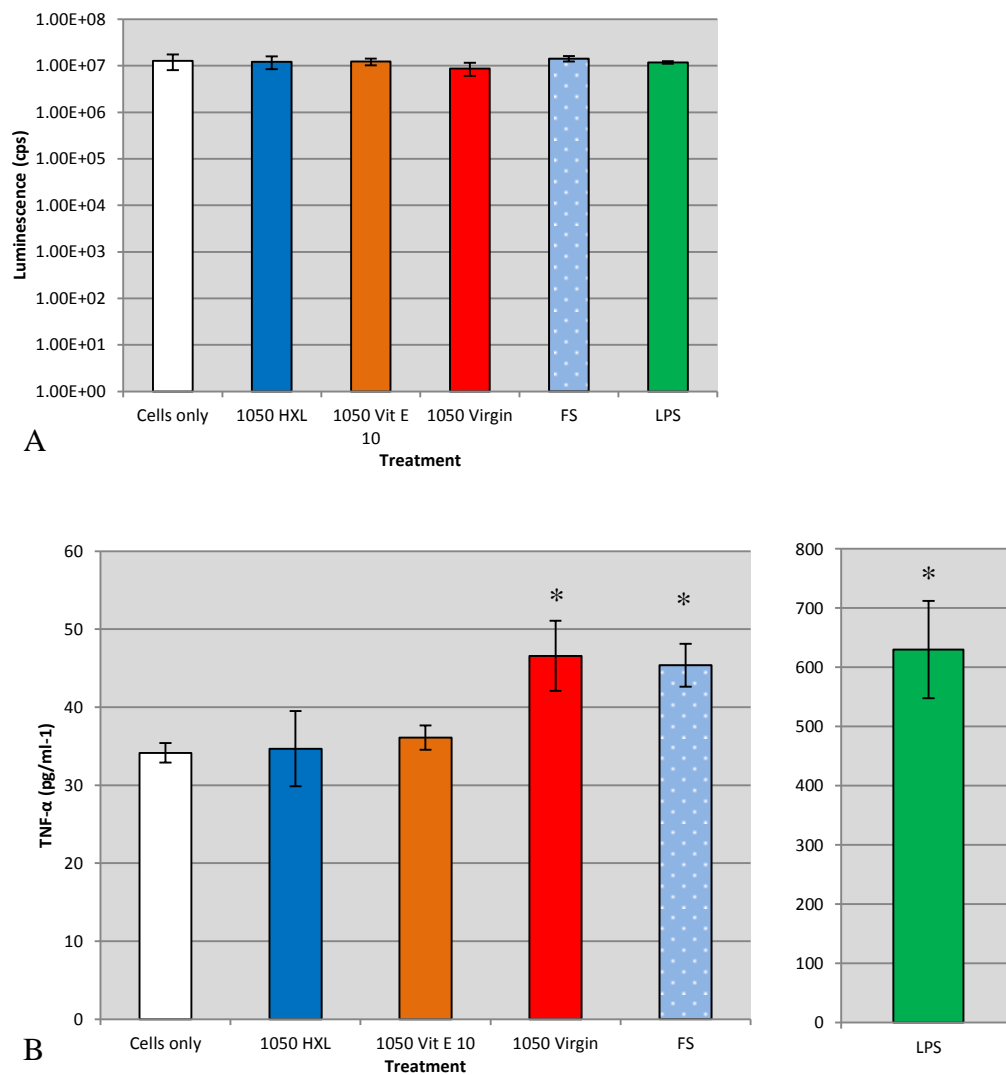


Figure 4.14 - A) Cell viability and B) TNF- α release from U937 derived macrophages incubated with 1050 HXL, 1050 Vit E 10 and 1050 Virgin UHMWPE wear debris at a concentration of $100 \mu\text{m}^3$ for 24 hours. Cells were seeded at a density of 2×10^5 cells per well with treatments using the agarose gel technique. Cells only acted as the negative control, 200 ng/ml^{-1} lipopolysaccharide acted as the positive control along with $100 \mu\text{m}^3$ $0.2 \mu\text{m}$ Fluospheres. * indicates a statistically significant TNF- α response from PBMNCs compared to cells only control (ANOVA, $p < 0.05$). Error bars show \pm the 95% confidence level, $n=4$.

2. Summary

So far in the method development section of this study, a significantly elevated TNF- α release has not been observed from PBMNCs in response to UHMWPE wear debris. Factors such as the cell seeding density, agarose gel concentration and phagocytic fraction have been altered during this section (Test A) to develop the conditions for the particle: cell culture, however no significant effect on the biological response to UHMWPE wear debris in PBMNCs has been observed.

This experiment then used U937 cells as an alternative source of macrophages, and demonstrated a significantly elevated level of TNF- α release from macrophages in response to 1050 Virgin UHMWPE wear debris. This was the first significant cytokine release from cells in response to UHMWPE wear debris in this study so far.

Throughout Test A, wear debris has been dosed at 100 μm^3 per cell in each experiment. However, it was hypothesised that this was an insufficient concentration to stimulate significant TNF- α release from PBMNCs. It was observed from the wear particle characterisation results shown in section 3.4.1.1 that only around 30% of wear particles for both 1050 Virgin and 1050 Vit E 10 fall within the range of 0.1-1.0 μm that is normally considered the most biologically active particles. The significant TNF- α stimulation achieved in a previous study by Liu (2012) was achieved by seeding PBMNCs with 100 μm^3 per cell of fractionated wear debris in the size range 0.1-0.6 μm . This method provided 100 μm^3 of particles, where 100% of the volume of the particles was within this biologically active size range. In comparison, in the present study, non-fractionated wear debris provided only 30-40% particles within this size range, therefore at a concentration of 100 μm^3 per cell, only 30 μm^3 of UHMWPE wear particles in the biologically active size range were available per cell. This reduction in the dose of critically sized UHMWPE particles was hypothesised to be a reason for the lack of TNF- α release from PBMNCs.

To dose UHMWPE wear debris at higher concentrations, a higher concentration of UHMWPE wear debris in the initial sterile lubricant sample was required. The difficulty with altering this is that the particle concentration achievable from a 4 day wear test is limited, as is the subsequent particle concentration available to dose in a 300 μl agarose plug. In order to generate a more concentrated sample of wear debris, a longer wear test was performed using the aseptic single station pin-on-plate wear

simulator. This longer wear test produced a more concentrated sample of UHMWPE wear debris, and cell culture experiments using this concentrated sample were subsequently named Test B.

4.3.4. Development of the Method for Assessment of the Effect of High Volume Concentrations of UHMWPE Wear Particles on TNF α Production in PBMNCs – Test B

The rationale behind increasing the concentration of the UHMWPE wear debris incubated with PBMNCs was two-fold. Firstly, during the method development of this experiment, investigating the effect of particle concentration on TNF- α response from PBMNCs was the final variable to be investigated. Secondly, as discussed in the previous section, only a small percentage of the 100 μm^3 of UHMWPE wear debris per cell is in the size range considered the most biologically active (0.1-1.0 μm). In order to dose the UHMWPE wear debris at a higher particle volume concentration, a more concentrated particle sample was required, and this was achieved by performing a longer wear test on the aseptic single station simulator. The difficulties with this longer aseptic wear test were maintaining the sterile environment for the extended time, and maintaining the running of the simulator throughout the extended period. Despite these difficulties, a longer wear test protocol was devised to provide a ‘super-concentrated’ sample of wear debris, generated over ten days instead of four.

4.3.4.1. Generation of Clinically Relevant UHMWPE Wear Particles using the Aseptic Single Station Pin-on-Plate Wear Simulator – Test B

Using the aseptic single station pin-on-plate wear simulator, clinically relevant wear particles of each UHMWPE material listed in Table 4.8 were generated in a lubricant comprised of RPMI 1640 medium with 25% (v/v) bovine serum, as described in section 2.2. The simulator was operated for ten days for each material, and these ten-day wear tests were categorised as Test B throughout this study. From each material, a volume of 20 ml of lubricant was collected from the bath under aseptic conditions at the end of a wear test. The materials tested in Test B and the particle concentrations of the lubricants from each material are shown in Table 4.9. For each material, there was approximately a five-fold increase in the volume of wear debris generated over a ten-day wear test compared to the traditional 4 day wear test.

Table 4.8 – UHMWPE materials used to generate super concentrated UHMWPE particle stocks. The full name of each material, the resin type, the gamma irradiation dose, the antioxidant used, the supplier, the abbreviation used through the study, and the colour key used throughout this chapter for each material are shown.







Name	Resin	Gamma Irradiation Dose	Antioxidant	Supplier	Abbreviation	Colour Key
1050 Highly Crosslinked UHMWPE	GUR1050	10 MRad	none	DePuy Synthes®	1050 HXL	
1050 Vitamin E enhanced UHMWPE + 10 MRad irradiation	GUR1050	10 MRad	Vitamin E 1000 ppm	MediTech® Medical Polymers	1050 Vit E 10	
1020 Hindered Phenol enhanced UHMWPE + 8 MRad irradiation	GUR1020	8 MRad	Hindered phenol	DePuy Synthes®	1020 AOX 8	

Table 4.9 – The concentration of UHMWPE wear debris in serum lubricant samples collected from the aseptic single station pin-on-plate wear simulator during Test B.

Name	Resin	Conc of UHMWPE Wear Debris (µg/ml)	Colour Key
1050 HXL	GUR1050	512	
1050 Vit E 10	GUR1050	431	
1020 AOX 8	GUR1020	835	

4.3.4.2 Determination of the Endotoxin Levels in each Serum Lubricant Sample

A new sample of UHMWPE wear debris from each material listed in Table 4.8 was generated using the single station pin-on-plate wear simulator under aseptic conditions. This additional test was conducted over 10 days, therefore increasing the risk of contamination. Throughout the test, the serum lubricant was tested for any microbial contamination, as outlined in section 2.2.7.5. In addition, to ensure the lubricant sample was also endotoxin free, the LAL endotoxin assay was performed to determine the levels of endotoxin present in each sample. Samples were tested using the method described in section 2.4.2. Samples were sonicated for 40 min at 37°C, after which each sample was diluted 100:1 in LAL reagent water.

Endotoxin levels present in the samples are shown in Table 4.10. The endotoxin levels of all the samples was below the accepted value of $<5 \text{ EU}\cdot\text{ml}^{-1}$, as specified by the pharmaceutical industry for injectable pharmaceuticals (FDA Regulatory Affairs, 1985). The positive product control percentage recovery was within the accepted range of 50-200%, indicating that the endotoxin levels detected in the samples were valid. These results showed that the longer 10 day test using the single station pin-on-plate wear simulator under aseptic conditions was suitable to produce sterile, endotoxin free UHMWPE wear debris samples.

Table 4.10 – Levels of endotoxin present in the lubricant samples generated in 25% (v/v) bovine serum lubricants using the single station pin-on-plate simulator (Test B).

UHMWPE Material	PPC% Recovery	Endotoxin ($\text{EU}\cdot\text{ml}^{-1}$)
1050 HXL	128%	0.017
1050 Vit E 10	156%	0.068
1020 AOX 8	120%	<0.005

Note – The positive product control (PPC%) was the sample which was spiked with a known concentration of endotoxin. The recovery of endotoxin was required to be equal to the known concentration, within 50-200% range, to be considered free of significant interference.

4.3.4.3 Cellular Response to High Volume Concentrations of Highly Crosslinked UHMWPE Wear Debris

The aim of this section of study was to further develop the methodology for determining the biological response of PBMNCs incubated with UHMWPE wear debris in terms of cell viability and TNF- α release after 24 hours. The agarose gel technique, as described in section 2.4.3, was used throughout this section as a matrix to suspend the buoyant UHMWPE wear particles and allow for contact between PBMNCs and wear debris. The developed cell culture conditions used in section 4.2.3.2 were used throughout this section, and these conditions are described in Table 4.11. Cells were isolated and seeded as described in section 2.4, with the only difference to the experiments in section 4.2.3.2 being a higher dose of UHMWPE wear debris in the 0.4% (w/v) agarose gels.

The first step in the development of the methodology using this lubricant sample was to determine the dose of UHMWPE wear debris (full size range) that would stimulate significant TNF- α release from PBMNCs compared to the cells only negative control. For this experiment, PBMNCs were seeded with 1050 HXL UHMWPE wear debris at doses of 100 μm^3 , 200 μm^3 and 600 μm^3 per cell. An intermediate dose of 400 μm^3 was planned, however the yield of mononuclear cells from the donor blood sample limited the number of treatments to five ($n = 4$). A cells only negative control was used, along with 200 ng/ml^{-1} LPS as a positive control. Cells were incubated for 24 hours in an incubator at 37°C in 5% (v/v) CO₂ in air. Cell culture conditions are shown in Table 4.11.

Table 4.11 –Cell culture conditions for experiments investigating the dose response PBMNCs to highly crosslinked UHMWPE

Cell number	2 x 10 ⁵ per well
Particle Concentration	100 μm ³ , 200 μm ³ , 600 μm ³ per cell
Agarose Gel Concentration	0.4% (w/v)
Agarose Gel Volume	300 μl
Plate	48 well plate

1. Biological Response of PBMNCs isolated from Donor 2 to 1050 HXL wear debris at different UHMWPE particle concentrations – Test B:1

Using the agarose gel technique, peripheral blood mononuclear cells isolated from Donor 2 were incubated with wear debris generated from 1050 HXL at different volume doses of particles per cell. The PBMNCs were treated with 100 μm³, 200 μm³ or 600 μm³ 1050 HXL wear debris per cell. The effect on cell viability and TNF-α release from PBMNCs isolated from Donor 2 following incubation with variable dose volume of 1050 HXL UHMWPE wear debris per cell at 37°C in 5% (v/v) CO₂ in air are shown in Figure 4.15. None of the UHMWPE or control treatments had a significant effect on the cell viability of PBMNCs compared to the cells only negative control. Significant elevated TNF-α release was produced by PBMNCs incubated with 200 μm³ and 600 μm³ 1050 HXL UHMWPE wear debris per cell, compared to the cells only negative control (ANOVA: p<0.05). A significantly elevated TNF-α release was also observed from cells incubated with the LPS positive control. Cells incubated with 100 μm³ 1050 HXL showed a higher mean TNF-α response compared to the cells only control; however this was not statistically significant.

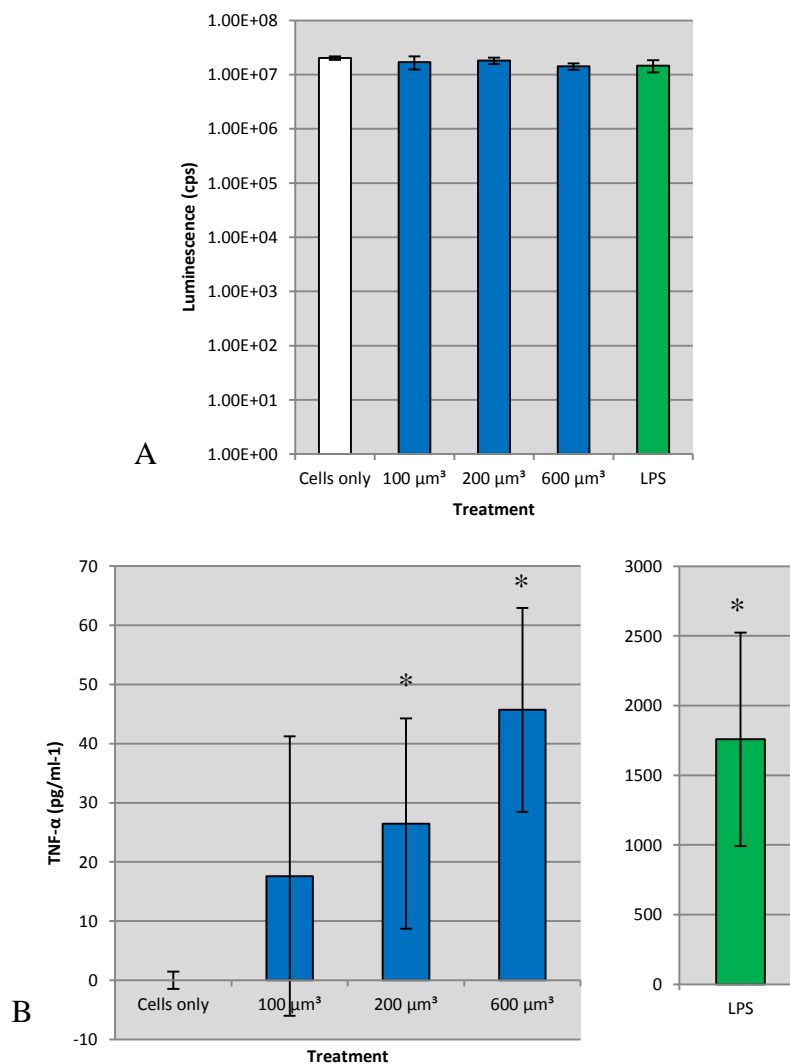


Figure 4.15 - A) Cell viability and B) TNF- α release from PBMNCs isolated from Donor 2 incubated with 1050 HXL UHMWPE wear debris at concentrations 100 μm^3 , 200 μm^3 and 600 μm^3 wear debris per cell for 24 hours at 37°C in 5% (v/v) CO₂ in air. Cells were seeded at a density of 2×10^5 cells per well with treatments using the agarose gel technique. Cells only acted as the negative control, 200 ng/ml⁻¹ lipopolysaccharide acted as the positive control. * indicates a statistically significant TNF- α response from PBMNCs compared to cells only negative control (ANOVA, $p < 0.05$). Error bars show \pm the 95% confidence level, $n=4$.

2. Biological Response of PBMNCs isolated from Donor 8 to 1050 HXL wear debris at different UHMWPE particle concentrations – Test B:2

A repeat experiment of test B:1 was conducted using an alternative donor. Peripheral blood mononuclear cells were isolated from blood from Donor 8 and incubated with 1050 HXL UHMWPE wear debris at concentrations of 100 μm^3 , 200 μm^3 and 600 μm^3 using the agarose gel technique. This test used the cell culture conditions described in Table 4.11. The effect on cell viability and TNF- α release from PBMNCs isolated from Donor 8 following incubation with variable dose volumes of 1050 HXL UHMWPE wear debris per cell at 37°C in 5% (v/v) CO₂ in air are shown in Figure 4.16. None of the treatments had a significant effect on the viability of PBMNCs compared to the cells only negative control. As with the previous test, significantly elevated levels of TNF- α release were observed from PBMNCs incubated with 200 μm^3 and 600 μm^3 1050 HXL UHMWPE wear debris, compared to the cells only control (ANOVA; $p < 0.05$). There was also significantly elevated TNF- α release from PBMNCs incubated with the LPS positive control.

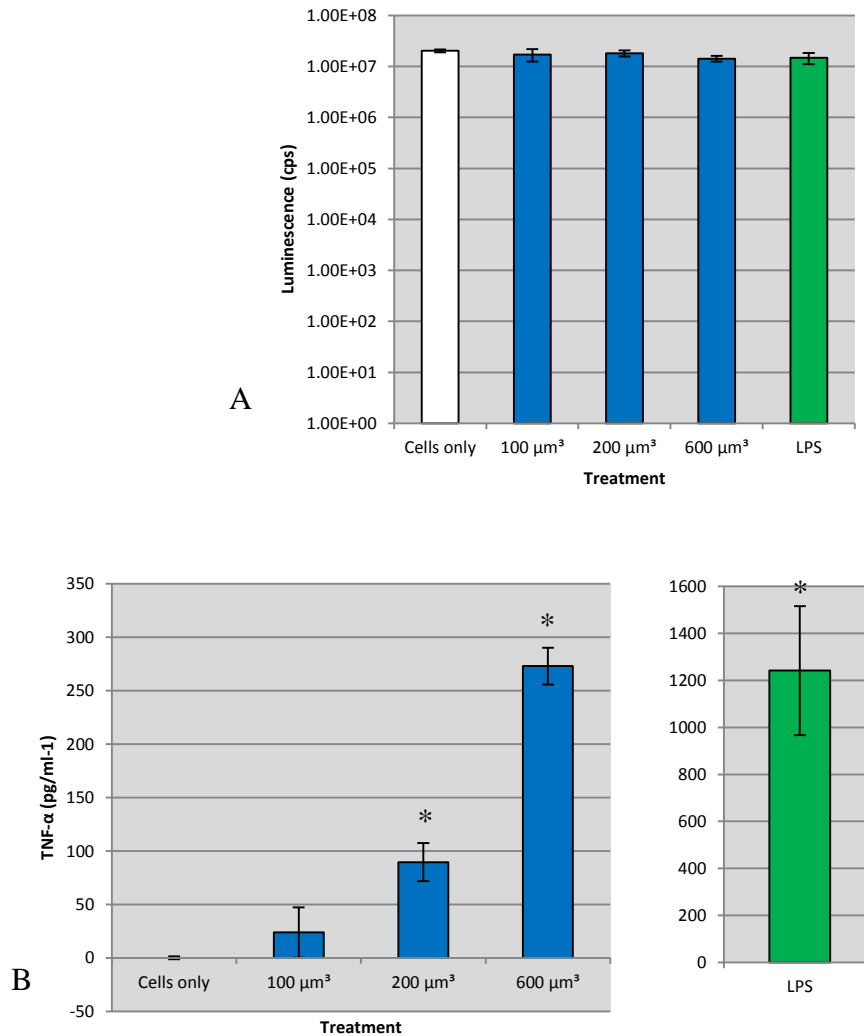


Figure 4.16 - A) Cell viability and B) TNF- α release from PBMNCs isolated from Donor 8 incubated with 1050 HXL UHMWPE wear debris at concentrations 100 μm^3 , 200 μm^3 and 600 μm^3 wear debris per cell for 24 hours at 37°C in 5% (v/v) CO₂. Cells were seeded at a density of 2×10^5 cells per well with treatments using the agarose gel technique. Cells only acted as the negative control, 200 ng/ml⁻¹ lipopolysaccharide acted as the positive control. * indicates a statistically significant TNF- α response from PBMNCs compared to cells only control (ANOVA, $p < 0.05$). Error bars show \pm the 95% confidence level, $n=4$.

3. Summary

Significantly elevated TNF- α release was observed when PBMNCs were incubated with 1050 HXL UHMWPE wear debris at 200 μm^3 and 600 μm^3 per cell, indicating that a higher concentration of wear debris per cell stimulated a significant cytokine response compared to the cells only negative control and 100 μm^3 per cell

treatments. This supports the hypothesis that a higher dose of particles within the 0.1-1.0 μm size range was important for a TNF- α response from PBMNCs.

Subsequently, higher volume doses of 1050 HXL and 1050 Vit E 10 were incubated with PBMNCs in order to investigate the biological response highly crosslinked antioxidant UHMWPE wear particles. Due to the low volume of 1050 Vit E 10 wear debris generated in the serum sample over ten days, the maximum particle concentration possible in a 300 μl agarose plug was 500 μm^3 wear debris per cell. This was therefore chosen as the particle concentration to compare these materials. Fluospheres (0.2 μm) were once again included as a positive control at 100 μm^3 per cell, along with 200 $\text{ng}\cdot\text{ml}^{-1}$ LPS. Cells were incubated for 24 hours using the cell culture conditions outlined in Table 4.10.

4.3.5 Investigating the Cellular Response to High Volume Concentrations of Vitamin E enhanced Highly Crosslinked UHMWPE and Highly Crosslinked UHMWPE Wear Debris

Following several steps of method development, this section of the study aimed to investigate the biological response of PBMCs to highly crosslinked UHMWPE wear debris compared to highly crosslinked vitamin E enhanced UHMWPE wear debris, in terms of TNF- α release from PBMC, and to determine the effect, if any, of vitamin E when present in highly crosslinked UHMWPE wear particles.

4.3.5.1 Cellular Response to Vitamin E enhanced Highly Crosslinked UHMWPE and Highly Crosslinked UHMWPE Wear Debris

Peripheral blood mononuclear cells were shown to produce significantly elevated levels of TNF- α release in response to 1050 UHMWPE wear debris at 200 μm^3 and 600 μm^3 per cell, compared to the cells only negative control. Using the experimental conditions developed in section 4.2.3.2, and the increased particle dose of 500 μm^3 per cell, the experiment was conducted to compare the cellular response to 1050 HXL and 1050 Vit E 10 UHMWPE wear debris. Cell culture conditions are shown in Table 4.12.

Table 4.12 –Cell culture conditions for experiments investigating the biological response of PBMCs to antioxidant UHMWPE

Cell number	2 x 10 ⁵ per well
Particle Concentration	500 μm^3 per cell
Agarose Gel Concentration	0.4% (w/v)
Agarose Gel Volume	300 μl
Plate	48 well plate

1. Biological Response of PBMNCs isolated from Donor 8 to 1050 HXL and 1050 Vit E 10 UHMWPE wear debris using improved conditions – Test B:3

Peripheral blood mononuclear cells were isolated from blood from Donor 8 and incubated with 1050 HXL and 1050 Vit E 10 UHMWPE wear debris at a concentration of 500 μm^3 per cell using the agarose gel technique. Fluospheres (0.2 μm) were included as a positive particle control at a dose of 100 μm^3 , along with 200 $\text{ng}\cdot\text{ml}^{-1}$ LPS. Cells were incubated for 24 hours at a seeding density of 2×10^5 cells per well. The effect on cell viability and TNF- α release from PBMNCs isolated from Donor 8 and incubated with 500 μm^3 wear debris per cell for 24 hours at 37°C in 5% (v/v) CO₂ in air are shown in Figure 4.17.

None of the treatments had a significant effect on the cell viability of PBMNCs following the 24 hour incubation. A significantly elevated level of TNF- α release was observed from PBMNCs incubated with 500 μm^3 1050 HXL UHMWPE wear debris compared to the cells only control (ANOVA: $p < 0.05$). In contrast, there was no significant increase in TNF- α release from PBMNCs incubated with 1050 Vit E 10 UHMWPE wear debris compared to cells only negative control. The level of TNF- α released from PBMNCs in response to 1050 Vit E 10 wear debris was significantly lower than that released from PBMNCs incubated with 1050 HXL wear debris. Cells incubated with 100 μm^3 Fluospheres produced a significant TNF- α response compared to cells only, along with the positive control of LPS treated cells (ANOVA: $p < 0.05$).

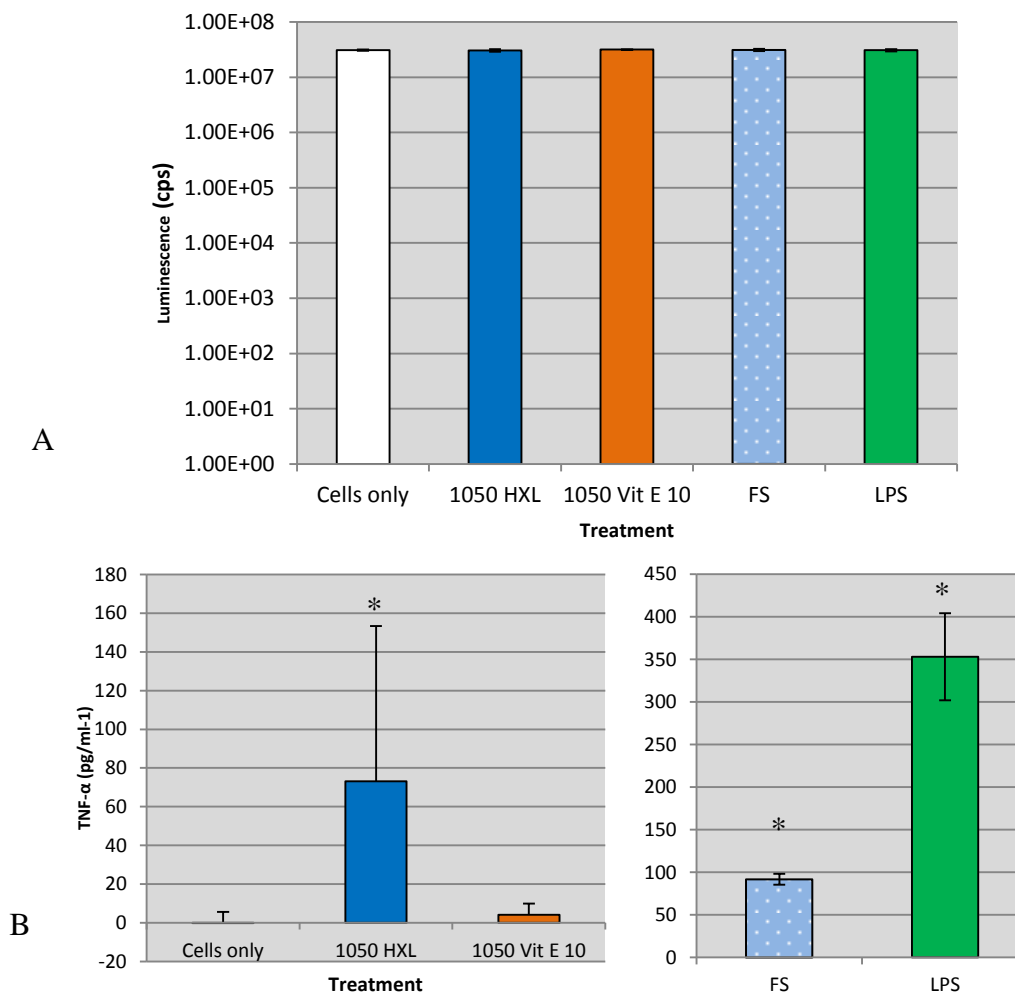


Figure 4.17 - A) Cell viability and B) TNF- α release from PBMCs isolated from Donor 8 incubated with 1050 HXL and 1050 Vit E 10 UHMWPE wear debris at a concentration of $500 \mu\text{m}^3$ wear debris per cell for 24 hours at 37°C in 5% (v/v) CO_2 . Cells were seeded at a density of 2×10^5 cells per well with treatments using the agarose gel technique. Cells only acted as the negative control, 200 ng/ml^{-1} lipopolysaccharide acted as the positive control along with $100 \mu\text{m}^3$ $0.2 \mu\text{m}$ Fluospheres. * indicates a statistically significant TNF- α response from PBMCs compared to cells only control (ANOVA, $p < 0.05$). Error bars show \pm the 95% confidence level, $n=4$. Only + error bars are shown where \pm error bars would change the scale of the graph, making the graph difficult to read.

This experiment was repeated using a different donor. Throughout this section of the study, it became apparent that certain donors responded to UHMWPE wear debris more aggressively than others. Donors 2, 8 and 15 produced a stronger TNF- α response to Fluospheres and subsequently to UHMWPE wear debris at doses above $200 \mu\text{m}^3$ per cell than any other donors used. For this reason, PBMCs isolated from

Donor 15 were used to compare the biological response of PBMNCs to 1050 HXL and 1050 Vit E 10 UHMWPE wear debris.

2. Biological Response of PBMNCs isolated from Donor 15 to 1050 HXL and 1050 Vit E 10 UHMWPE wear debris using improved conditions – Test B:4

Peripheral blood mononuclear cells were isolated from Donor 15 and incubated with UHMWPE wear debris using the agarose gel technique. As in test B:3, 1050 HXL and 1050 Vit E 10 were incubated at a concentration of 500 μm^3 per cell, with cells seeded at a density of 2×10^5 per well. Cells were incubated for 24 hours at 37°C in 5% (v/v) CO_2 , after which the cell viability and TNF- α release from PBMNCs was determined. Cells only acted as a negative control, while 0.2 μm Fluospheres at a dose of 100 μm^3 acted as a positive particle control, along with 200 $\text{ng}\cdot\text{ml}^{-1}$ LPS. . The effect on cell viability and TNF- α release from PBMNCs incubated with 500 μm^3 UHMWPE wear debris per cell for 24 hours at 37°C in 5% (v/v) CO_2 are shown in Figure 4.18.

None of the treatments had a significant effect on the cell viability of PBMNCs compared to the cells only control. Cells incubated with 1050 HXL UHMWPE wear debris produced significantly elevated TNF- α release compared to the cells only negative control (ANOVA: $p < 0.05$). In comparison, cells incubated with 1050 Vit E 10 UHMWPE wear debris did not show a significant increase in TNF- α release compared to the cells only negative control. The level of TNF- α produced by PBMNCs incubated with 1020 Vit E 10 wear debris was significantly lower than the level of TNF- α produced by PBMNCs incubated with the same volume of 1050 HXL wear debris, and comparable to the TNF- α release observed in the cells only negative control. Cells treated with 100 μm^3 per cell of 0.2 μm Fluospheres showed a significant TNF- α response compared to the cells only control, while LPS treated cells also showed a significant TNF- α response compared to the cells only negative control (ANOVA; $p < 0.05$).

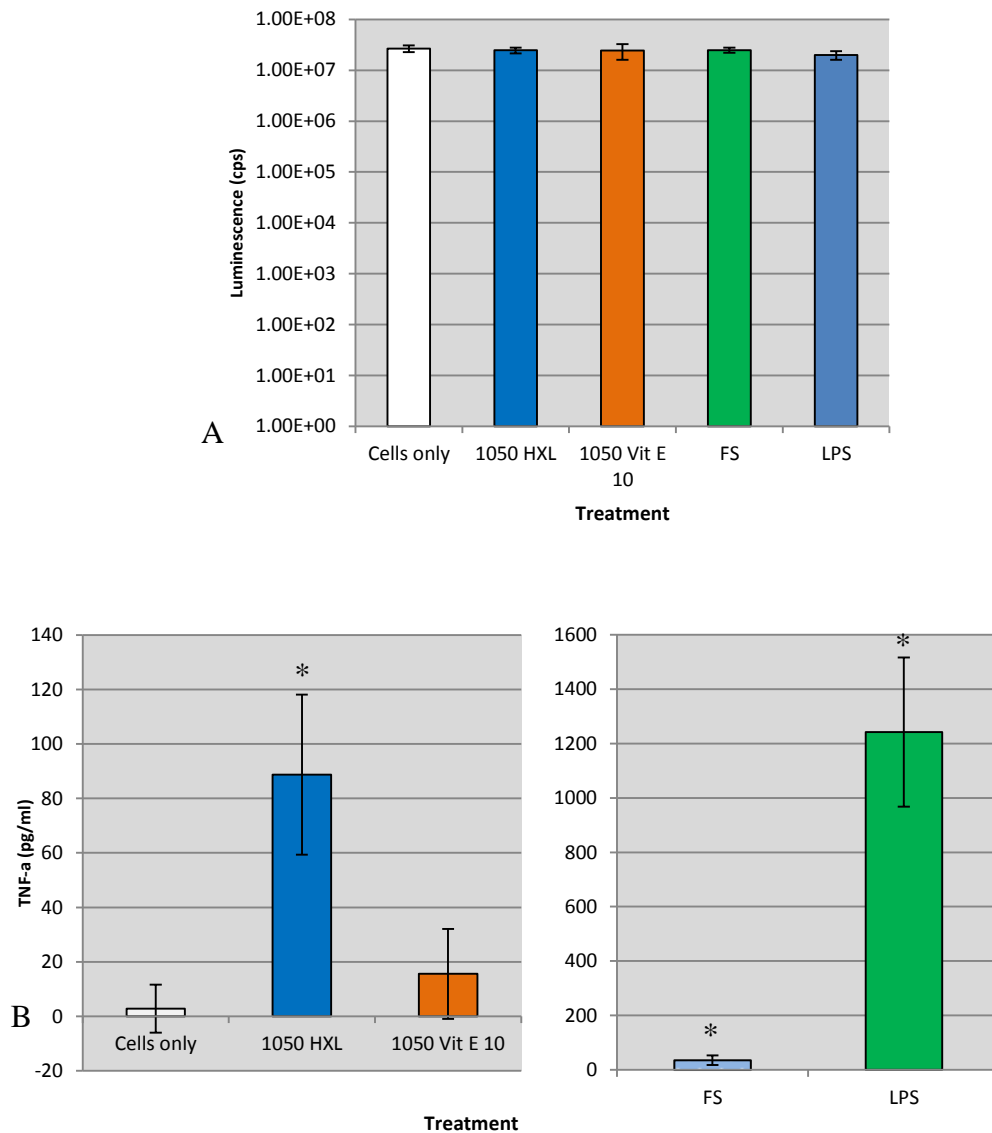


Figure 4.18 - A) Cell viability and B) TNF- α release from PBMNCs isolated from Donor 15 incubated with 1050 HXL and 1050 Vit E 10 UHMWPE wear debris at a concentration of $500 \mu\text{m}^3$ wear debris per cell for 24 hours at 37°C in 5% CO_2 (v/v) in air. Cells were seeded at a density of 2×10^5 cells per well with treatments using the agarose gel technique. Cells only acted as the negative control, 200 ng/ml^{-1} lipopolysaccharide acted as the positive control along with $100 \mu\text{m}^3$ $0.2 \mu\text{m}$ Fluospheres. * indicates a statistically significant TNF- α response from PBMNCs compared to cells only control (ANOVA, $p < 0.05$). Error bars show \pm the 95% confidence level, $n=4$.

3. Summary

Using cell culture conditions developed in this study, and seeding UHMWPE wear debris at a concentration of 500 μm^3 per cell, a significantly elevated level of TNF- α release was observed from PBMNCs incubated with 1050 HXL compared to the cells only negative control. In comparison, PBMNCs incubated with 1050 Vit E 10 at the same dose, and using the same conditions, produced a TNF- α release significantly lower than that observed in 1050 HXL treated cells. The TNF- α release from 1050 Vit E 10 treated cells was comparable to that observed in the cells only negative control. This result was observed with both Donor 8 and Donor 15; two of the donors that were considered to be responders to UHMWPE wear debris in terms of increased levels of TNF- α release. This result indicated that the presence of vitamin E in the highly crosslinked material had a significant effect on the TNF- α release from PBMNCs in response to wear debris at a dose of 500 μm^3 per cell.

Following the successful stimulation of PBMNCs, an additional material was included in the experiment. As an alternative to vitamin E enhanced highly crosslinked UHMWPE, a hindered phenol enhanced highly crosslinked UHMWPE was investigated to determine if this alternative antioxidant had any effect on the cellular response to UHMWPE wear debris at a concentration of 500 μm^3 per cell.

4.3.5.2 Cellular Response to Vitamin E enhanced Highly Crosslinked UHMWPE, Hindered Phenol enhanced Highly Crosslinked UHMWPE, and Highly Crosslinked UHMWPE Wear Debris

The previous section of the study showed that when seeded with 500 μm^3 UHMWPE wear debris per cell, PBMNCs produced a significantly elevated level of TNF- α release compared to the cells only negative control. This significant TNF- α release was not observed in PBMNCs incubated with 1050 Vit E UHMWPE wear debris at the same concentration, indicating that the presence of vitamin E had an effect on this response. Using the cell culture conditions described in Table 4.12, the novel highly crosslinked antioxidant material 1020 AOX 8 was included in the study to determine the cytokine response to wear debris from this material. The 1020 AOX 8 UHMWPE is enhanced with a hindered phenol antioxidant (pentaerythritol tetrakis),

and irradiated to a level of 8 MRad, therefore the material was considered highly crosslinked. Wear debris was generated from this material using the methods outlined in section 2.2, and the volume of wear debris generated is shown in Table 4.8.

1. Biological Response of PBMNCs isolated from Donor 8 to 1050 HXL, 1050 Vit E 10 and 1020 AOX 8 UHMWPE wear debris using improved conditions – Test B:5

Using the agarose gel technique, peripheral blood mononuclear cells isolated from Donor 8 were incubated with UHMWPE wear debris generated from 1050 HXL, 1050 Vit E 10 and 1020 AOX 8 at a particle concentration of 500 μm^3 per cell. Cells were incubated with particles for 24 hours, after which the cell viability and TNF- α response was determined. The effect on cell viability and TNF- α release from PBMNCs incubated with 500 μm^3 wear debris per cell for 24 hours at 37°C in 5% (v/v) CO₂ in air is shown in Figure 4.19. None of the UHMWPE treatments had a significant effect on the cell viability of PBMNCs compared to the cells only negative control. A significant TNF- α response was observed in PBMNCs incubated with both 1050 HXL and 1050 Vit E 10 UHMWPE wear debris treatments compared to the cells only control (ANOVA: $p < 0.05$). Cells incubated with 1050 HXL produced the strongest TNF- α response, with cells incubated with 1050 Vit E 10 producing a lower but significant TNF- α response compared to the cells only negative control (ANOVA; $p < 0.05$). Cells incubated with 1020 AOX 8 produced the lowest response out of the wear debris-treated cells, with a response not significantly elevated compared to the cells only control. A significant TNF- α response was also observed in the LPS positive control.

This was the only experiment that showed a significant response from cells incubated with 1050 Vit E 10. This response was lower than the 1050 HXL response, indicating vitamin E had an effect on the cytokine response. The 1020 AOX 8 treated cells produced a very low TNF- α response.

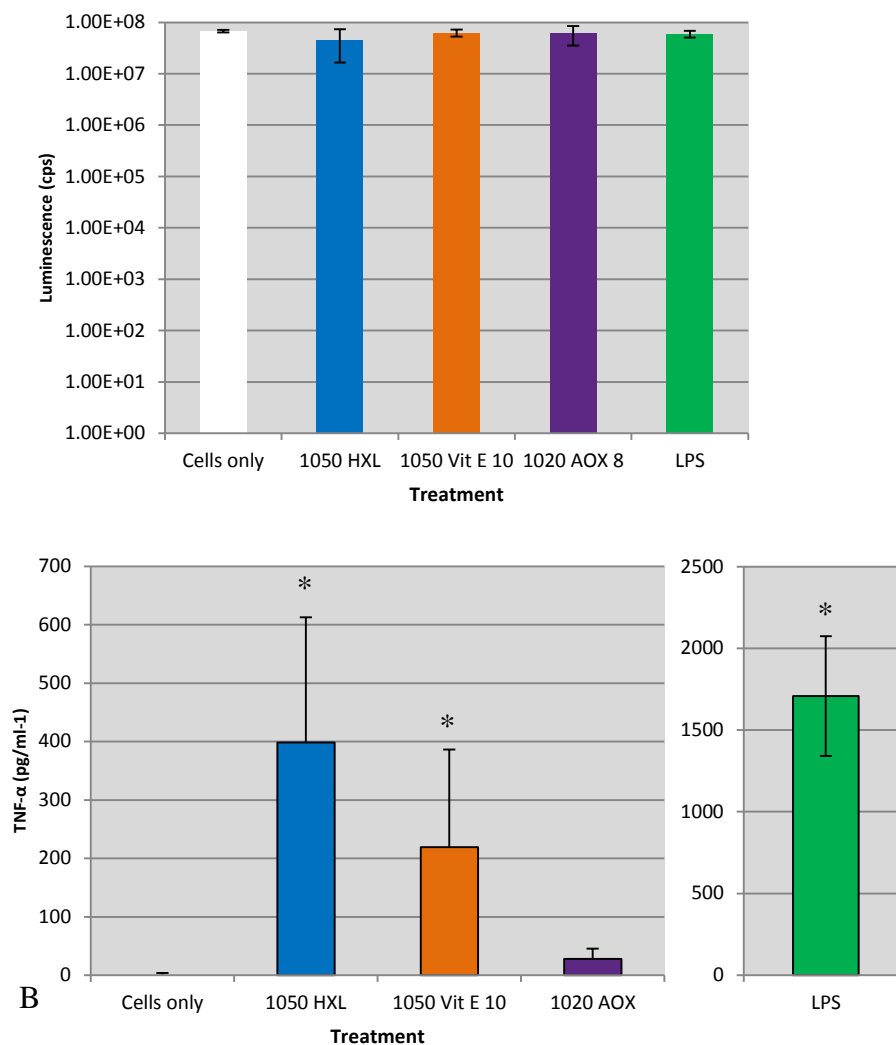


Figure 4.19 - A) Cell viability and B) TNF- α release from PBMCs isolated from Donor 8 incubated with 1050 HXL, 1050 Vit E 10 and 1020 AOX 8 UHMWPE wear debris at a concentration of 500 μm^3 wear debris per cell for 24 hours at 37°C in 5% (v/v) CO₂ in air. Cells were seeded at a density of 2×10^5 cells per well with treatments using the agarose gel technique. Cells only acted as the negative control, 200 ng/ml⁻¹ lipopolysaccharide acted as the positive control. * indicates a statistically significant TNF- α response from PBMCs compared to cells only control (ANOVA, $p < 0.05$). Error bars show \pm the 95% confidence level, apart from where + error bars are shown to maintain the scale of the graph, $n=4$.

4.4. Discussion

In this chapter, the cellular response to antioxidant UHMWPE wear debris in terms of the osteolytic cytokine response was determined. Previous studies have shown UHMWPE wear debris stimulated a significantly elevated TNF- α release from PBMNCs when they were incubated a dose of 100 μm^3 wear debris per cell (Richards, 2008, Liu, 2012). A separate study showed that non-crosslinked vitamin E enhanced UHMWPE particles reduced the release of TNF- α from PBMNCs incubated with 100 μm^3 UHMWPE wear debris compared to virgin UHMWPE wear debris (Bladen et al., 2011). However, up to this point no study has evaluated the cellular response to highly crosslinked vitamin E enhanced UHMWPE wear debris; the clinically relevant material. This chapter set out to determine the cellular responses to this material in comparison to clinically relevant non-antioxidant highly crosslinked UHMPWE wear debris. In addition, the cellular response to a novel antioxidant hindered phenol enhanced highly crosslinked UHMWPE material was determined, using the hindered phenol (pentaerythritol tetrakis) enhanced UHMWPE material from DePuy Synthes Joint Reconstruction®.

Firstly, confocal microscopy was used to determine if the agarose gel technique for the culture of PBMNCs with UHMWPE wear debris was indeed facilitating the contact and phagocytosis of wear particles. The agarose gel technique has been used previously by Liu (2012) and Bladen et al. (2013) to determine the cytokine release from PBMNCs in response to UHMWPE wear debris, however it had not been determined whether this technique allowed the uptake of wear particles. Using fluorescently labelled UHMWPE wear debris generated from the 1050 HXL material, wear particles in micrometre and nanometre size range were observed to be internalised in the PBMNCs, localising in the cytoplasm outside the nucleus. This validated that the agarose gel cell culture technique was facilitating the contact and internalisation of UHMWPE wear particles, and this technique was therefore subsequently used with confidence in the cellular response experiments that followed.

The agarose gel technique was used to determine the cell viability and TNF- α release from PBMNCs in response to highly crosslinked and antioxidant UHMPWE wear debris. Using the initial cell culture conditions used previously by Liu (2012; 1.125 x

10^5 cells per well, $100 \mu\text{m}^3$ wear debris per cell, 1% (w/v) agarose gel), no significant TNF- α release was observed from PBMNCs incubated with 1050 HXL, 1050 Vit E 10 or 1050 Virgin UHMWPE wear debris. The following experiments then investigated the effect of different agarose concentrations on the TNF- α response from PBMNCs. Using agarose concentrations of 1% and 0.4% (w/v), and also an agarose free test (direct cell culture), once again no significant TNF- α response was observed from PBMNCs incubated with 1050 HXL, 1050 Vit E 10 or 1050 Virgin UHMWPE wear debris. However, despite the change in agarose concentration having no significant effect on the TNF- α release from PBMNCs, a new agarose concentration of 0.4% (w/v) was carried forward to the subsequent experiments, due to the hypothesis that a more dilute gel would provide a better environment for particle: cell contact.

The next experiment investigated the effect of an increasing the cell seeding density on the biological response of PBMNCs to the UHMWPE treatments. Increasing the cell seeding density from 1.125×10^5 cells per well to 2×10^5 cells per well did not stimulate a significant TNF- α release from PBMNCs in response to the UHMWPE treatments. A significant response was seen, however, from PBMNCs incubated with $0.2 \mu\text{m}$ Fluospheres at a concentration of $100 \mu\text{m}^3$ per cell. This elevated TNF- α release did not occur with Fluospheres-treated cells at the lower cell seeding density, indicating an increased cell seeding density was beneficial for the experiment.

Following this method development step, and as a result of a variation that had been observed between donors, a U937 cell line was used. Macrophages derived from U937 cells were incubated with 1050 HXL, 1050 Vit E 10 and 1050 Virgin UHMWPE wear debris. Although the cells only negative control treatment produced a higher TNF- α release than previously seen, possibly due to the lingering effects of the PMA stimulation used to differentiate cells, significantly elevated TNF- α release was observed from cells incubated with 1050 Virgin UHMWPE wear debris at a dose of $100 \mu\text{m}^3$ per cell. This was the first time a significant TNF- α release was observed from macrophages incubated with a UHMWPE treatment in this study. While the use of U937 cells removed the possibility of donor variation, the use of a cell line did not represent the clinical situation as well as primary monocytes isolated from human blood. For that reason, the study continued developing the experiment using PBMNCs.

Up to this point, the development steps undertaken had revealed that when incubating the whole size range of wear debris 'as generated' using the 3D agarose technique used in this study, a particle concentration of 100 μm^3 wear debris per cell was not sufficient to stimulate a significant increase in TNF- α release from PBMNCs. A previous study by Ingram et al. (2004) demonstrated that using the 2D agarose culture technique, a UHMWPE particle concentration as low as 10 μm^3 (GUR1050 virgin; as generated) was sufficient to stimulate a significant TNF- α release from PBMNCs compared to a cells only control. The difference in results between the present study and previous study, while both using GUR1050 virgin and 10 MRad irradiation UHMWPE, could be due to the different agarose techniques used. The requirement for cells to penetrate the agarose in the 3D technique may increase the particle dose required to stimulate a given cell density.

In order to investigate the effect of higher doses of UHMWPE wear debris using the 3D agarose gel technique, the single station wear simulator was used to generate a 'super concentrated' UHMWPE wear debris sample. This provided the opportunity to seed cells with UHMWPE wear debris at a concentration up to five fold higher than previously used. Using the agarose gel technique for culturing cells with UHMWPE wear debris, it was determined that a particle volume concentration of greater than 200 μm^3 per cell of 1050 HXL wear debris was necessary to stimulate a significant TNF- α release from PBMNCs compared to the cells only negative control. This was thought to be due to the percentage of particles within the size range of 0.1-1.0 μm , which is thought to be the 'critical size range' for a biological response. Particle analysis in this study showed that only 30% of particles were generated in this size range when using wear debris across the full size range generated. This correlated with the findings of a previous study by Liu (2012), where a significant increase in TNF- α released from PBMNCs was only observed when incubated with 100 μm^3 0.1-0.6 μm sized UHMWPE wear debris per cell. These findings therefore indicate that a threshold of wear particles are required in this critical size range to stimulate significant cytokine release, and when using the full size range of wear debris, a volume of greater than 200 μm^3 per cell wear debris was required.

The development steps undertaken earlier in this study were to provide conditions that would best facilitate cellular interaction with UHMWPE wear debris. These

method development steps did not have a significant effect on the cellular response to UHMWPE wear debris. However, these steps were all carried out with wear debris at a concentration of $100 \mu\text{m}^3$ per cell; a concentration which was later found to be insufficient to stimulate elevated cytokine release from PBMNCs. With the knowledge that a higher concentration of UHMWPE wear debris was required to stimulate significant TNF- α release from PBMNCs, it would be beneficial to repeat these method development steps using the higher particle concentration to determine the truly optimal conditions for this experiment.

Eventually, the developed cell culture conditions were incorporated into the investigation of the cellular response to 1050 HXL and 1050 Vit E 10 UHMWPE wear debris. Incubating UHMWPE wear debris at a concentration of $500 \mu\text{m}^3$ per cell, and at a cell seeding density of 2×10^5 , a significant increase in TNF- α release was observed from PBMNCs incubated with 1050 HXL, compared to the cells only negative control. This TNF- α response was not observed with PBMNCs incubated with 1050 Vit E 10. There was a significant reduction in the TNF- α release from PBMNCs from two donors when incubated with 1050 Vit E 10 compared to 1050 HXL wear debris. This suggested the addition of vitamin E to highly crosslinked UHMWPE could be having an effect on the TNF- α release from PBMNCs, however further testing would be required to conclude this. Whether vitamin E is available to leach from the UHMWPE material, or even required to leach from the UHMWPE material to be available to cells, is a topic of great interest in this area of research. Mutual irradiation is technique commonly used to graft a monomer (for example vitamin E) to a polymer (e.g. UHMWPE) through the gamma irradiation of both compounds (as opposed to pre irradiation, where the polymer is irradiated prior to addition of the monomer). The mutual irradiation technique uses gamma irradiation in the presence of both monomer and polymer to create a free radical environment, whereby the co-polymerisation of these compounds then occurs (Bhattacharya and Misra, 2004). Despite the theory behind this process, the results of this study appear to suggest that vitamin E has biological effect when present in highly crosslinked UHMWPE. This is an area of the study where further research into the availability of vitamin E in highly crosslinked UHMWPE would be of great value. For example, investigating whether vitamin E can leach from the highly crosslinked material in

solution, or in the harsh environment of the cell lysosome following fusion with the phagosome would help add to the understanding of additives to UHMWPE in joint replacements.

Clinically, this reduction in TNF- α release could be beneficial to patients implanted with a vitamin E enhanced highly crosslinked UHMWPE acetabular cup. Mechanically, vitamin E addition has been shown to protect against oxidation *in vivo* and preserve the mechanical properties of UHMWPE. However by reducing the TNF- α response of PBMNCs incubated with wear debris, it could be hypothesised that vitamin E enhanced highly crosslinked UHMWPE wear debris may have an effect on the process of osteolysis. Osteolysis is dependent on the cytokine response of cells encountering UHMWPE wear debris; therefore a reduction in cytokine production could slow this osteolytic process and delay the onset of aseptic loosening. Eventually, vitamin E enhancement could result in a longer lasting hip replacement.

In addition to vitamin E enhanced highly crosslinked UHMWPE; a hindered phenol enhanced highly crosslinked UHMPWE (1020 AOX 8) was also incubated with PBMNCs using the improved cell culture conditions and higher particle volume concentrations. Hindered phenol enhanced UHMWPE is being developed as an alternative antioxidant material for use in joint replacement. Due to time restraints, only one experiment using 1020 AOX 8 was conducted, and with more time, this experiment would have been repeated with multiple donors and investigated further. Cells isolated from Donor 8 were incubated with 1050 HXL, 1050 Vit E 10 and 1020 AOX 8 at a dose of 500 μm^3 wear debris per cell. The 1050 HXL UHMWPE was shown to stimulate a significantly elevated TNF- α release from PBMNCs, along with PBMNCs incubated with 1050 Vit E 10, compared to the cells only negative control (ANOVA; $p < 0.05$). This was the first significant TNF- α release observed from cells incubated with 1050 Vit E 10, and once again shows the intra-donor variation. Alongside this, PBMNCs incubated with 1020 AOX 8 showed no elevation in TNF- α release compared to the cells only negative control. This result shows the hindered phenol material to also have some anti-inflammatory properties, therefore reducing the TNF- α release from PBMNCs. Further work is required, as the different resin of 1020 AOX 8 could also be a factor.

Another important finding in this chapter was the influence of donor variation, observed in the variable response of PBMNCs isolated from different donors to the UHMWPE and control treatments. While a significant increase in the TNF- α response to UHMWPE wear debris was observed from PBMNCs isolated just from two donors, the non-responsive donors also showed variation in the strength of the TNF- α response to 200 ng.ml⁻¹ lipopolysaccharide and 100 μm^3 per cell of 0.2 μm Fluospheres. For example, comparing the response of Donors 7 and 3 in tests A:5 and A:6 respectively, there was a difference in the level of TNF- α release from PBMNCs in response to 100 μm^3 per cell of 0.2 μm Fluospheres, and also to the LPS positive control. Under the same cell culture conditions (100 μm^3 per cell UHMWPE wear debris, 0.4% (v/v) agarose gel, 2×10^5 cells per well), Donor 7 produced a TNF- α response of around 250 pg/ml, while Donor 3 produced a TNF- α response of around 500 pg/ml. However, looking at the TNF- α release in response to 200 ng/ml LPS, Donor 7 produced a TNF- α response of over 1600 pg/ml, while Donor 3 produced 1200 pg/ml TNF- α . This highlights the varying cell response to the different kinds of stimulants. The positive particle control (FS) produced an increased TNF- α release in one donor, while the positive LPS control produced an increased TNF- α release in the other donor.

Variations and single nucleotide polymorphisms have been investigated to determine the reason for differences in the TNF- α response from human donors. For example, one study identified a G-to-A single nucleotide polymorphism 308 nucleotides upstream from the initiator site for the TNF- α promoter gene to be associated with elevated TNF- α release, and subsequently an increased risk of autoimmune disorders such as diabetes mellitus type 1 (Abraham and Kroeger, 1999). While this polymorphism is associated with disease and not necessarily the cause of TNF- α variation in this study, it highlights the potential for genetic variation to affect the TNF- α response in humans, as displayed in this study. The heterogeneity in the TNF- α response across donors has also been found to be stimulus and cell-type specific (Longo et al., 2012, Mueller et al., 2012). Donor variation is potentially important in the clinical setting, as some donors may respond with a stronger cytokine response to UHMWPE wear debris than others, therefore making these donors more susceptible to osteolysis and aseptic loosening.

In addition to inter-donor variation, intra-donor variation was also observed. Intra-donor variation was the variation in the response from the same donor at different times. For example, Donor 8 produced a significantly elevated TNF- α release to 500 μm^3 per cell of 1050 HXL wear debris consistently. However, this response to the wear debris varied at different times of the experiment. Test B:5 showed unusually high levels of TNF- α release from PBMNCs isolated from Donor 8 incubated with 1050 Vit E 10. This was a much higher level of TNF- α release in response to 1050 Vit E 10 wear debris compared to the response previously observed in test B:3 with the same donor under the same conditions.

4.5 Conclusions

In two donors, Vitamin E enhanced highly crosslinked UHMWPE wear debris caused a reduction in the levels of TNF- α release from PBMNCs compared to PBMNCs incubated with non-antioxidant highly crosslinked UHMWPE wear debris. Highly crosslinked UHMWPE stimulated a significant TNF- α response compared to cells only, however on two occasions, vitamin E enhanced highly crosslinked UHMWPE wear debris did not stimulate this TNF- α response, with a cellular response comparable to the cells only control. These results were variable, however they suggested that vitamin E is available to cells to exert its anti-inflammatory properties despite it being contained in a highly crosslinked polymer. Hindered phenol enhanced highly crosslinked UHMWPE wear debris also caused a significant reduction in TNF- α from PBMNCs incubated with this material compared to cells incubated with non-antioxidant highly crosslinked UHMWPE. It was also determined that a seeding density of over 200 μm^3 UHMWPE wear debris per cell was required to stimulate a significant TNF- α response from PBMNCs. This suggested that there existed the possibility of a volume threshold of UHMWPE particles required to stimulate an osteolytic cytokine response. Finally, inter- and intra-donor variation was observed, highlighting the importance of patient variation and the application of UHMWPE as a bearing material in hip replacements.

Chapter 5

The Production of Reactive Oxygen Species in Peripheral Blood Mononuclear Cells in Response to UHMWPE Wear Particles

5.1 Introduction

The results from the cell culture experiments in chapter 4 were variable, possibly due to the nature of using human donor cells, however the results suggested vitamin E enhanced highly crosslinked UHMWPE wear debris at a dose of 500 μm^3 per cell produced significantly lower levels of TNF- α release from PBMNCs compared to highly crosslinked UHMWPE wear debris at the same dose. Release of TNF- α in response to vitamin E enhanced highly crosslinked UHMWPE wear debris was in some cases comparable to the response observed in the cells only negative control, indicating vitamin E had an effect on the cells that resulted in a reduction in the level of TNF- α release. It was also determined that there was a minimum volume threshold required to produce a significantly elevated TNF- α release from PBMNCs when using the 3D agarose gel technique described previously. This threshold was found to be equivalent to a volume greater than 200 μm^3 of wear debris per cell.

Another aspect of the cellular responses to UHMWPE wear debris that has generated interest is oxidative stress as a result of phagocytosis of wear debris, and more specifically the production of reactive oxygen species following stimulation of cells by UHMWPE wear debris. Reactive oxygen species are reactive molecules that contain oxygen, for example hydrogen peroxide, and are produced following the reduction of oxygen to a superoxide molecule (O_2^-) (Murphy, 2009). Production of ROS in cells results in the alteration of cell membrane lipids, proteins and nucleic acids, and is an important cellular process for redox signalling, apoptosis and general cell signalling, while also causing oxidative stress in cells (Balaban et al., 2005). Phagocytosis of cobalt chrome nanometre-sized wear particles rapidly induces the production of reactive oxygen species in fibroblasts, indicating a phagocytosis mediated response. A more prolonged, MitoQ sensitive reactive oxygen species

response has also been observed (24h), indicating mitochondrial involvement in the response (Raghunathan et al., 2013). While this doesn't directly relate to the phagocytosis of UHMWPE wear debris, it does build intrigue as to whether the internalisation of UHMWPE particles could produce the same oxidative stress situation in cells. A previous study by Bladen *et al.* (2010) showed both UHMWPE and CoCr wear particles at doses of 100 μm^3 and 50 μm^3 per cell, respectively, induced oxidative stress in PBMNCs. The study showed an increase in the production of reactive oxygen species following incubation with these particles, and the authors hypothesised that the oxidative stress observed following UHMWPE wear particle treatment was not due to DNA damage, unlike the metal particle-induced oxidative stress (Bladen et al., 2010). This study investigated the effect of virgin UHMWPE, a material that is rarely used clinically today. With the introduction of antioxidant UHMWPEs, the present study investigated whether the presence of an antioxidant compound in UHMWPE could have a significant effect on the oxidative stress in cells after stimulation with UHMWPE wear debris treatment.

The antioxidant properties of vitamin E are very well documented. It is the structure of alpha tocopherol (vitamin E) that gives the compound its antioxidant properties, with the hydroxyl group on the aromatic ring able to donate a hydrogen atom to a radical species, therefore breaking the chain of oxidation (Diplock, 1983, Sheppard et al., 1993). The rationale behind the addition of vitamin E to highly crosslinked UHMWPE was to reduce the free radical burden after irradiation, and protect against oxidation in the polymer. It is hypothesised that this antioxidant activity could also act at a cellular level, potentially reducing the presence of reactive oxygen species and therefore protecting the cell against oxidative stress.

The antioxidant properties of vitamin E have been shown to have an effect at a cellular level, and these effects have been positively associated with the treatment several diseases where the mechanism of disease is due to oxidative stress and inflammation. For example, vitamin E administered intravenously has been shown to interrupt joint destruction in rheumatoid arthritis; a disease where reactive oxygen species are thought to play an important role (De Bandt et al., 2002). Vitamin E has also been shown to have a beneficial effect in atherosclerosis; a condition where plaques build up on the inside of arterial walls. The oxidation of lipoproteins is an

important mechanism that contributes to the development of this disease, and it is this process that vitamin E is able to disrupt due to its potent antioxidant and anti-inflammatory properties (Osterud and Bjorklid, 2003, Singh and Jialal, 2004, Singh et al., 2005).

Another aspect to consider is that the release of TNF- α following internalisation of wear debris may lead to the production of reactive oxygen species, therefore oxidative stress could also be a result of TNF- α release. Reactive oxygen species have been postulated to be produced following TNF- α stimulation as part of the signalling cascade associated with TNF- α release, however the mechanisms are poorly understood (Woo et al., 2000). The previous chapter showed that the presence of vitamin E in highly crosslinked UHMWPE wear debris might lead to a lower level of TNF- α release from PBMNCs. It is postulated this anti-inflammatory effect may subsequently lead to a reduction in reactive oxygen species, whilst also stabilising any radical-containing reactive oxygen species that are produced.

The aim of this chapter was to investigate the effect of highly crosslinked UHMWPE wear debris on the production of ROS in PBMNCs, and also to determine whether the presence of vitamin E in highly crosslinked UHMWPE had any effect on the production of ROS in PBMNCs. This was achieved by generating clinically relevant UHMWPE wear debris aseptically using a single station pin-on-plate wear simulator. Using both highly crosslinked UHMWPE and vitamin E enhanced highly crosslinked UHMWPE wear debris; PBMNCs were incubated with wear debris on serum-coated glass coverslips which allowed imaging of cells using a fluorescence microscope. Reactive oxygen species were detected using a kit with live PBMNCs. The Image-iT™ LIVE Green Reactive Oxygen Species detection kit was used, with the assay using 5-(and 6)-carboxy-2',7'-dichlorodihydrofluorescein diacetate (carboxy-H₂DCFDA) as the fluorogenic marker for accumulation of ROS in live cells. Generation of ROS is normal in live cells in an aerobic environment, however under conditions that induce oxidative stress, the production of ROS is increased. Cells were imaged using fluorescence microscopy, and the intensity of reactive oxygen species was then quantified using image analysis software that measured the grey scale intensity of the green fluorescent dye within cells.

5.2 Materials

Additional equipment and materials used in the assay for determination of reactive oxygen species are shown in Table 5.1.

Table 5.1 - Additional materials and reagents used for the investigation of the production of reactive oxygen species in PBMCs in response to UHMWPE wear debris.

Materials/ Regents	Supplier	Storage and Preparation
Image-iT™ LIVE Green ROS Detection Kit	Life Technologies - California, USA	Stored at 2-6°C, protected from light
Hoechst 33342, trihydrochloride, trihydrate	Life Technologies - California, USA	Aliquoted and stored at -20°C
Hanks Balanced Salt Solution (with Ca/Mg/phenol red)	Sigma Aldridge, St Louis, USA	Room temperature
6 well plates	Thermo-Scientific, Massachusetts, USA	N/A

5.3 Methods

5.3.1 Generation of UHMWPE Wear Particles using the Aseptic Single Station Pin-on-Plate Wear Simulator

For this section of the study, only two UHMWPE materials were tested with PBMCs to determine the production of ROS in response to the wear debris. These materials were GUR1050 highly crosslinked UHMWPE (1050 HXL) and GUR1050 Vitamin E enhanced highly crosslinked UHMWPE (1050 Vit E 10); the same UHMWPE materials used in chapter 4. . These materials are described in more detail in chapter 4; table 4.1. These materials were chosen in order to investigate the reactive oxygen species production in response to a clinically relevant highly crosslinked UHMWPE, and to determine if the presence of vitamin E in highly crosslinked UHMWPE had any effect.

A single station multidirectional pin-on-plate wear simulator was used to aseptically generate clinically relevant wear debris from these two materials. The rig components were sterilised as described in section 2.2.7.2. The assembly, running, and disassembly of the wear simulator was carried out using aseptic technique to

ensure sterility of the simulator and lubricant, as outlined in section 2.2.7. The wear tests were performed under the kinematics described previously, with a 28 mm stroke length and a rotation of $\pm 30^\circ$, under a load of 160N, at a reciprocating speed of 1 Hz. Tests were performed in RPMI 1640 medium supplemented with 25% (v/v) bovine serum, which is described in section 2.2.6. The serum lubricant was collected following completion of the ten day test using a sterile syringe and stored in a sterile glass universal. The sample was stored at -20°C until required. The levels of endotoxin in the sample were determined using the Limulus amoebocyte lysate (LAL) assay, as described in section 2.4.2.2. The UHMWPE pins used in the tests were weighed before and after the wear test, and the mass of wear debris generated from the pin was calculated. This calculation then provided an approximation of the wear debris in the serum lubricant sample which was used to calculate particle concentrations for particle: cell culture experiments.

5.3.2 Culture of PBMNCs with UHMWPE Wear Debris in Chamber Slides

In this section of the study, two UHMWPE materials were tested (1050 HXL and 1050 Vit E 10), and compared to the cells only negative control (no particle treatment). A positive control was included, which was provided in the ROS detection kit (*tert*-Butyl hydroperoxide (TBHP)).

The aim of these experiments was to determine the levels of reactive oxygen species produced in response to stimulation of PBMNCs with UHMWPE wear debris, through the visualisation of reactive oxygen species. Due to the difficulties experienced with labelling live cells with fluorescent dye in an agarose gel, in addition to the difficulties obtaining high quality images in a 3D culture system, these cell culture experiments did not use the agarose gel technique which has been used throughout this study. It was observed that in wear test lubricant samples containing UHMWPE wear debris, the wear debris appeared to sink in solution, which was in contrast with the theory that UHMWPE is less dense than water and therefore buoyant in solution. It was hypothesised that the presence of serum proteins on the wear particles may lead to the wear particles becoming less buoyant and therefore sinking in solution. For this reason, these experiments were performed

using a minimal volume of solution, ensuring the cells and UHMWPE wear debris came into contact and therefore provide an environment where the production of reactive oxygen species could be determined.

In order to culture PBMNCs with UHMWPE wear debris in a way that allowed for the imaging of cells using a fluorescence microscope, a novel technique for the seeding and incubation of PBMNCs with UHMWPE wear debris was developed. Initially, 16 well chamber slides with removable wells were used to incubate PBMNCs with UHMWPE wear debris, however the removal of the 16-well gasket proved difficult and often disrupted the cell monolayer on the slide. Therefore, the method was further developed. Rather than seeding the cells onto a 25 x 75 mm glass slide and using a coverslip, cells were instead seeded on to a coverslip, which could then be applied to a microscope slide following the incubation and staining. This provided a surface that the cells would attach to, and that was easier to manipulate than a 16-well chamber slide (prior to imaging).

Circular glass coverslips with a diameter of 16 mm were wrapped in aluminium foil and sterilised prior to use by heating at 190°C for 3 hours. To provide a surface that was favourable for attachment of cells, 16 mm diameter glass cover slips were incubated in 100% (v/v) bovine serum overnight at 4°C. The presence of serum proteins on the coverslip allowed for cell attachment. Following incubation in serum, the coverslips were placed at an angle around the edge of a sterile petri dish and dried in a class II cabinet for 30 min.

In order to create a well on each coverslip (which would be capable of containing cells, wear debris and culture medium) and prevent the initial cell culture solution from running off the coverslip, an agarose ring was applied around the edge of the circular coverslip. Agarose gel was prepared at a concentration of 2% (w/v) and sterilised in an autoclave at 121°C for 20 min, at 103 kPa, as described in section 2.4.1.3, and heated up in a microwave to provide agarose gel in liquid form. Using a 1000 µl pipette, agarose gel was carefully applied to the edge of the coverslip, leaving an area in the centre of the coverslip for cell culture, with an approximate diameter of 10 mm. When this initial agarose ring had set and become solid, a second layer of agarose gel was then applied on top of the first layer. This provided an adequate

agarose gel ring to contain the cell culture solution and UHMWPE wear debris. The coverslips were then ready for cell culture.

Using blood obtained from a healthy human donor, PBMNCs were isolated using the method outlined in section 2.4.4. Cells were then seeded onto the coverslip inside the agarose ring at a concentration of 1×10^5 cells per well. Following this step, UHMWPE wear debris was added to the cell culture at a concentration of $100 \mu\text{m}^3$ per cell. A volume of warmed RPMI 1640 culture medium was then added to the coverslip to provide a final volume of $200 \mu\text{l}$. This volume was sufficiently small enough to be contained within the agarose ring on the coverslip. Each coverslip was contained inside a well of a 6-well plate. Cells were then incubated for 4 hours at 37°C in 5% (v/v) CO_2 in air. This incubation step allowed the macrophages in the PBMNC sample to attach to the coverslip. Following this incubation, $1000 \mu\text{l}$ RPMI 1640 culture medium was added to each well of the 6-well plate that the coverslip was within, in order to fully submerge the coverslip. This larger volume of culture medium was deemed necessary to provide enough nutrition to the cells over the 48 hour incubation step. The culture medium was added carefully and slowly so as not to disrupt the attached cells and also to cause minimal disruption and dispersal of the UHMWPE wear debris that had settled on the coverslip.

Peripheral blood mononuclear cells were incubated with UHMWPE wear debris using the culture technique described above for a total of 48 hours at 37°C in 5% (v/v) CO_2 in air. Throughout this incubation, the 6-well plate housing the coverslips was handled very carefully so as not to disrupt the cells. The coverslips were routinely checked using a light microscope to ensure cell attachment, and halfway through the 48 hour incubation, a volume of $500 \mu\text{l}$ warmed RPMI 1640 culture medium was added to each well of the 6-well plate to compensate for evaporation of the media.

The positive control provided with the detection kit was TBHP, a known inducer of oxidative stress in cells. Ninety minutes prior to the end of 48 hour incubation, the cell culture medium was aspirated from the well containing the positive control coverslip. A volume of 2 ml $100 \mu\text{M}$ TBHP was added to the well, completely submerging the coverslip. Cells were then incubated for 90 min at 37°C in 5% (v/v) CO_2 in air.

5.3.3 Detection of Reactive Oxygen Species in PBMNCs using the Image-iT™ LIVE Detection Kit Following Incubation with UHMWPE Wear Debris

The Image-iT™ LIVE Green Reactive Oxygen Species (ROS) Detection kit provides the reagents for the detection of ROS in live cells. The key component of the assay is 5-(and 6-)-carboxy-2',7'-dichlorodihydrofluorescein diacetate (carboxy-H₂DCFDA), which acts as a fluorogenic marker for ROS. This non-fluorescent compound permeates the cells, and is deacetylated by cellular esterases. Reactive oxygen species present in the cell then oxidise the deacetylated compound, emitting bright green fluorescence which is detected using a fluorescence microscope.

Following the 48 hour incubation period of PBMNCs with wear debris, and after the 90 min positive control incubation, the RPMI 1640 culture medium within each well was carefully aspirated. Cells were washed once with 1000 µl warm HBSS, and the 6-well plate was gently tilted to ensure complete coverage of the coverslip. The HBSS solution was aspirated, and cells were covered with 200 µl of 25 µM carboxy-H₂DCFDA. Cells were incubated with this compound for 30 min at 37°C, protected from the light by wrapping the plates in aluminium foil.

Five minutes prior to the completion of this incubation, 2 µl of 100 µM Hoechst was added to the carboxy-H₂DCFDA: cell solution to provide a final concentration of 1 µM Hoechst. Upon completion of this incubation, coverslips were gently washed three times in warm HBSS. Following these washes, the agarose gel ring was carefully peeled away from the coverslip using sterile tweezers. The coverslips were then removed from the wells, inverted, and mounted onto 25 x 75 mm glass microscope slides using RPMI 1640 culture medium. The mounted coverslips were protected from light and imaged immediately.

5.3.4 Imaging and Quantification of Oxidative Stress in PBMNCs Using Fluorescence Microscopy

An upright fluorescent Zeiss Axio Imager 2 microscope was used to determine the presence of reactive oxygen species in PBMNCs following incubation with UHMWPE wear debris. Images were captured using the 20x and 63x (oil) lenses,

with quantification of 20x captured images only. DAPI and FITC channels were selected, which operated at wavelengths of 405 nm and 488 nm, respectively. These channels allowed imaging of the blue cell nuclei (DAPI) and the green fluorescent ROS (FITC). Images were extracted and overlay images were produced using ZEN 2009 software (Carl Zeiss Microscopy Ltd). Images were captured at random locations, and a minimum of four non-overlapping images from each treatment were captured for quantification (n=4). This number of images ensured over 100 cells per treatment were captured to then determine the mean ROS intensity for each treatment.

Images were analysed using Image J image analysis software. Analysis was focused on the FITC image, which showed the presence of reactive oxygen species. In order to quantify the intensity of green fluorescence in each cell, the image was converted to grey scale and a mean grey scale intensity value was obtained for each cell. The area to be measured for each cell was selected manually using the software, using the DAPI filter to indicate where the cell nucleus was located for each cell. This prevented analysis of any background green fluorescence that was not inside a cell. For each treatment, four images were analysed in order to capture a minimum of 100 cells. A mean intensity was determined for each image, and a final mean intensity was calculated from the four images to give an overall mean ROS intensity for each material. Values are shown as means \pm 95% confidence level and analysed using one-way ANOVA. Differences between the treatment groups and the negative control were determined by calculating the minimum significant difference (MSD) value ($p < 0.05$) using the Tukey-method (Sokal and Rohlf, 1981).

5.4. Results

5.4.1 Generation of Sterile UHMWPE Wear Debris

Two UHMWPE materials were selected to investigate the production of reactive oxygen species in PBMNCs in response to incubation with wear debris. The materials were vitamin E enhanced highly crosslinked UHMWPE (1050 Vit E 10) and highly crosslinked UHMWPE (1050 HXL). The samples of wear debris from each material were the same high concentration samples used in Test B in section 4.3.3, and the concentrations of wear debris generated are shown in Table 4.8. The endotoxin levels for these samples are shown in section 4.3.3.1. Throughout this section, three donors were used in total (Donors 8,11,15), due to these donors being considered responsive to UHMWPE. In section 5.4.2, only PBMNCs from Donor 15 were used to undertake the imaging of reactive oxygen species. PBMNCs from Donors 8 and 11 were used for the quantification of ROS production in PBMNCs. Due to ethical constraints on the time between blood donations; the present study was unable to include PBMNCs from Donor 15 in the quantification section of this study.

5.4.2 Visualisation of Reactive Oxygen Species Following Treatment with UHMWPE Wear Debris

Peripheral blood mononuclear cells were seeded at a density of 1×10^5 cells per well, with UHMWPE wear debris at a concentration of $100 \mu\text{m}^3$ per cell for 48 hours at 37°C in 5% (v/v) CO_2 in air. Cells were then stained for the presence of ROS, and the nucleus of the cells was stained with Hoechst.

Images presented in this section depict the blue Hoechst-labelled nuclei of PBMNCs along with green fluorescently labelled reactive oxygen species. The final image represents an overlay of these two channels (labelled overlay). The reactive oxygen species production in peripheral blood mononuclear cells isolated from Donor 15 following incubation with UHMWPE wear debris is shown in Figure 5.1-5.3. Higher magnification images of PBMNCs isolated from Donor 15 incubated with 1050 HXL and 1050 Vit E 10 are shown in Figure 5.4-5.5.

The cells only negative control is shown in Figure 5.1, where a large group of cell nuclei, stained blue by the Hoechst can be observed, indicating a large population of cells. While some traces of high intensity green fluorescence were observed in the fluorescence microscopy image, using the overlay it was determined that these areas were not within cells and were considered to be background fluorescence. Using the overlay image to indicate the cell locations, low levels of ROS were observed across the cell population, indicated by faint green spots. This indicated that ROS were produced by healthy functioning cells, or at least produced in response to the cell culture conditions, and was not an indication of severe oxidative stress in the cells.

In contrast, in PBMNCs incubated with 1050 HXL wear debris at a concentration of $100 \mu\text{m}^3$ per cell, bright, intense areas of green fluorescence were observed in the cytoplasm around the cell nuclei (Figure 5.2). This indicated the presence of high levels of ROS in cells, located outside the nucleus. These are believed to represent cells experiencing oxidative stress due to the high intensity of ROS production. The orange arrows show the clear localisation of ROS outside the cell nucleus but inside the cell cytoplasm, displayed as bright green rings around the nucleus (Figure 5.2).

In PBMNCs treated with 1050 Vit E 10 UHMWPE wear debris at a concentration of $100 \mu\text{m}^3$ per cell, only a faint green fluorescence was observed. While this fluorescence appeared brighter than that observed in the cells only negative control, it appeared much less intense than that observed in the HXL wear debris treated cells. This suggested that lower levels of ROS were produced in cells incubated with 1050 Vit E 10 wear debris compared to cells incubated with 1050 HXL wear debris not containing vitamin E.

Higher magnification images with a magnification of 63x (oil immersion) are shown in Figure 5.4 and 5.5. In PBMNCs incubated with 1050 HXL UHMWPE wear debris at a concentration of $100 \mu\text{m}^3$, localised areas of reactive oxygen species were observed in the cytoplasm of the cell, external to the cell nucleus (Figure 5.4). The orange arrow indicates a cell with a high intensity of ROS, clearly localised in the cytoplasm of the cell. In comparison, PBMNCs incubated with 1050 Vit E 10 UHMWPE wear debris at a concentration of $100 \mu\text{m}^3$ showed much less intense areas of ROS (Figure 5.5) The production of ROS in 1050 Vit E 10 wear debris treated cells was localised in the cytoplasm, however the levels of ROS were at a

lower intensity. These moderate levels of ROS production indicate a lower level of oxidative stress in the cell. The white arrow highlights a cell that appears to be undergoing mitosis, as indicated by its splitting nucleus.

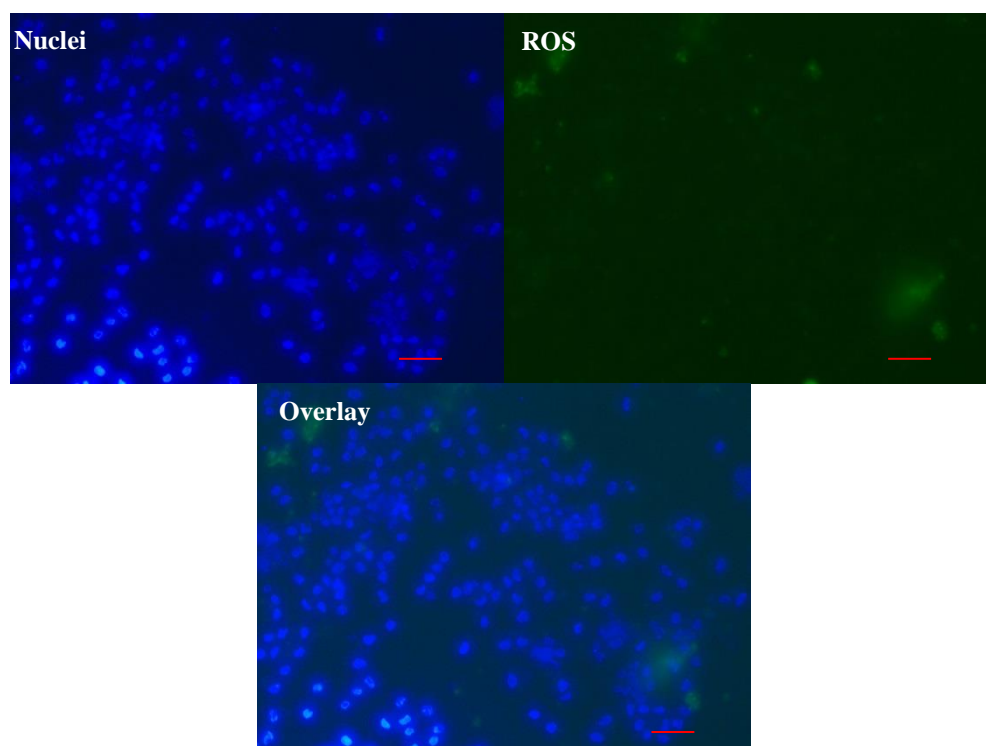


Figure 5.1 – Visualisation of the presence of ROS in PBMNCs (cells only negative control) following incubation for 48 hours at 37°C in 5% (v/v) CO₂. Blue signals represent cell nuclei stained with Hoechst, while green signals represent fluorescent ROS. Size bar: 20 µm, 20x Mag.

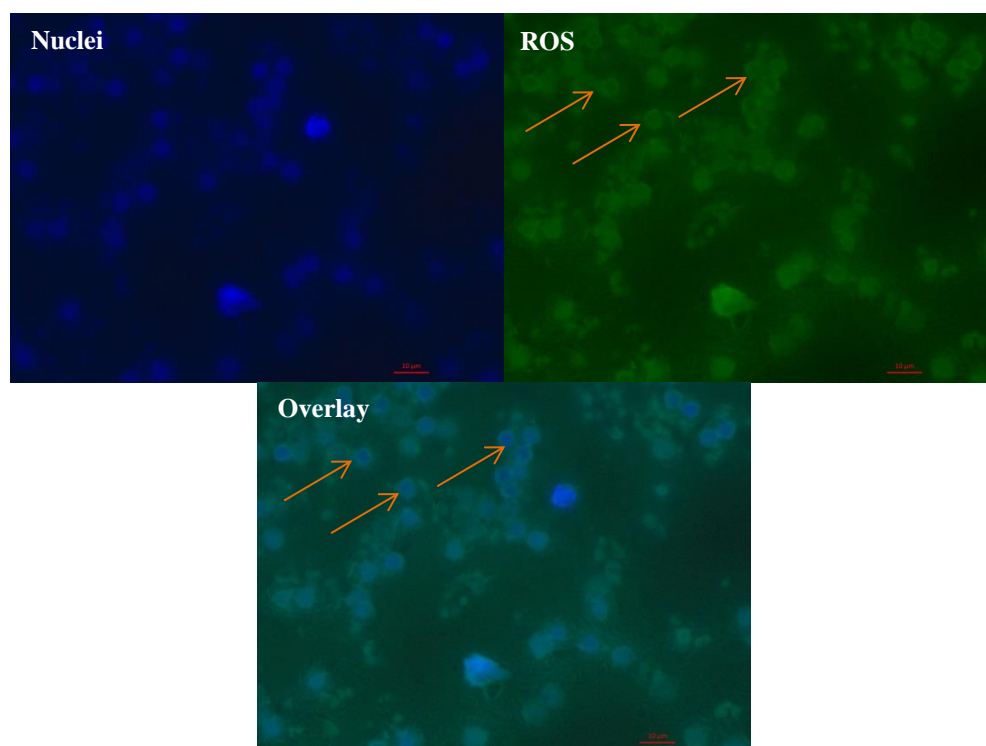


Figure 5.2– Visualisation of the presence of ROS in PBMCs following incubation with 1050 HXL UHMWPE wear debris at a concentration of $100 \mu\text{m}^3$ per cell, for 48 hours at 37°C in 5% (v/v) CO_2 . Blue signals represent nuclei stained with Hoechst, while green signals represent fluorescent ROS. Size bar: $10 \mu\text{m}$, 40x Mag.

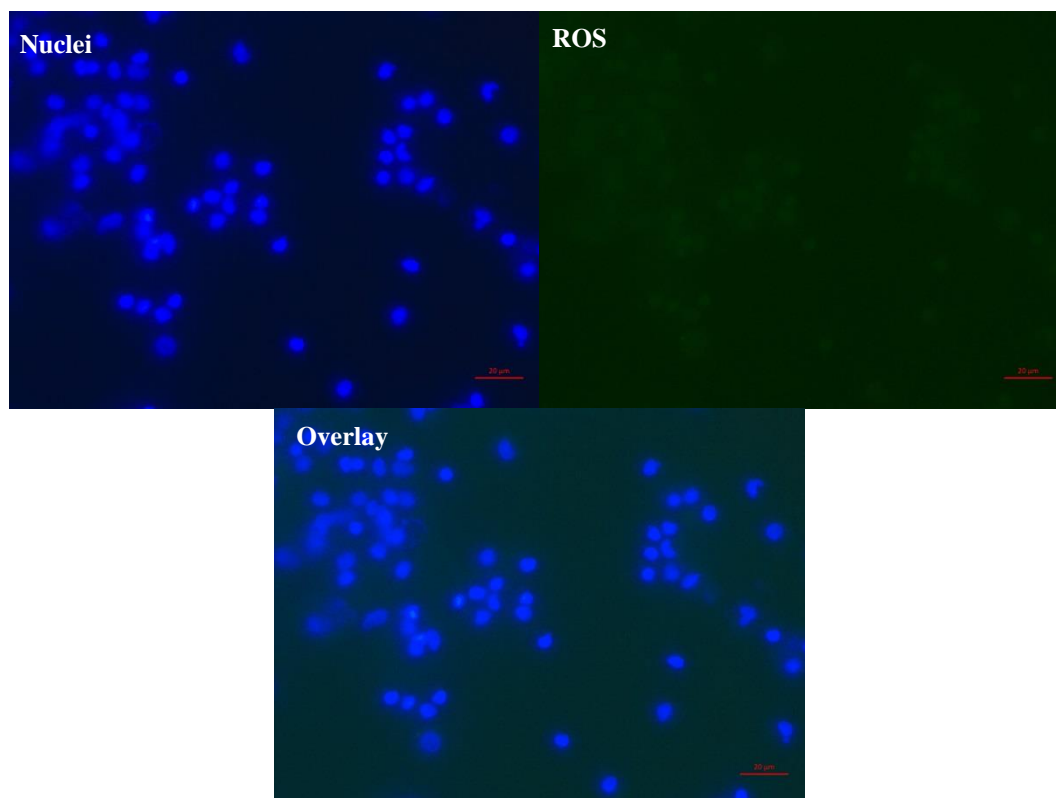


Figure 5.3– Visualisation of the presence of ROS in PBMCs following incubation with 1050 Vit E 10 UHMWPE wear debris at a concentration of $100 \mu\text{m}^3$ per cell, for 48 hours at 37°C in 5% (v/v) CO_2 . Blue signals represent nuclei stained with Hoechst, while green signals represent fluorescent ROS. Size bar: $10 \mu\text{m}$, 20x Mag.

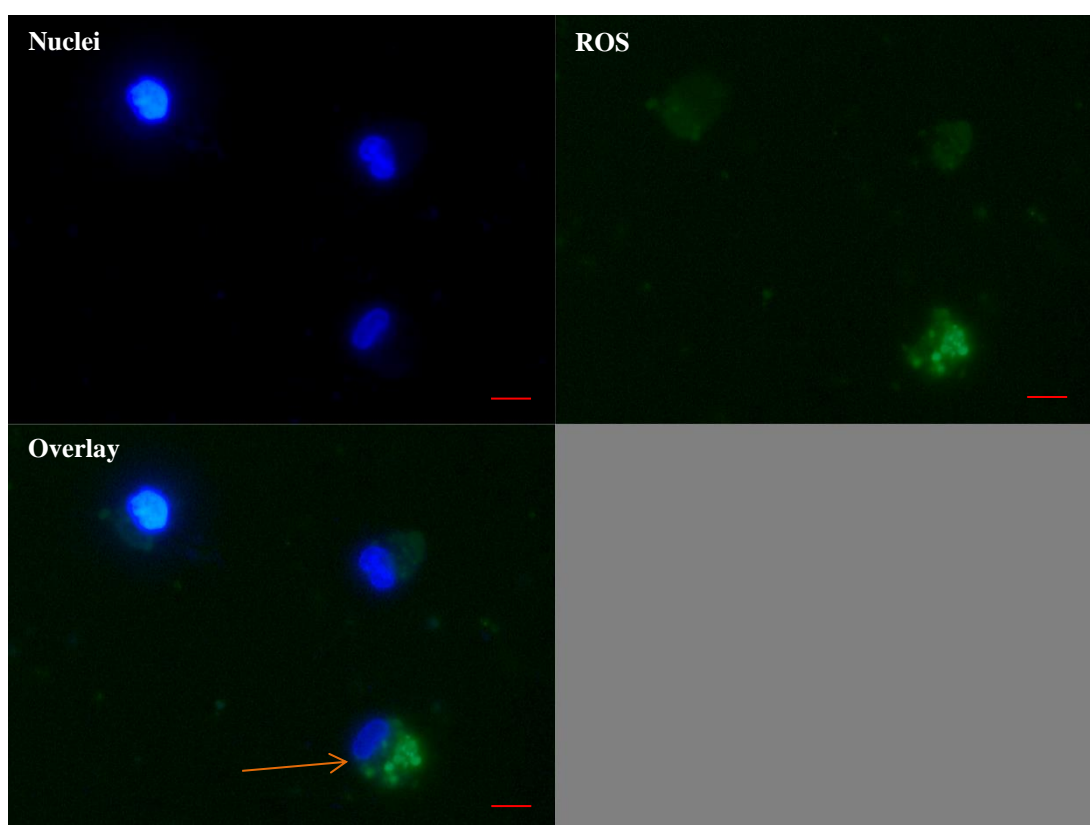
Higher Magnification Images

Figure 5.4 – Visualisation of the presence of ROS in PBMCs following incubation with 1050 HXL UHMWPE wear debris at a concentration of $100 \mu\text{m}^3$ per cell, over 48 hours at 37°C in 5% (v/v) CO_2 . Blue signals represent nuclei stained with Hoechst, while green signals represent fluorescent ROS. The orange arrow indicates a cell with intense oxidative stress. Size bar: $5 \mu\text{m}$, 63x (oil) Mag.

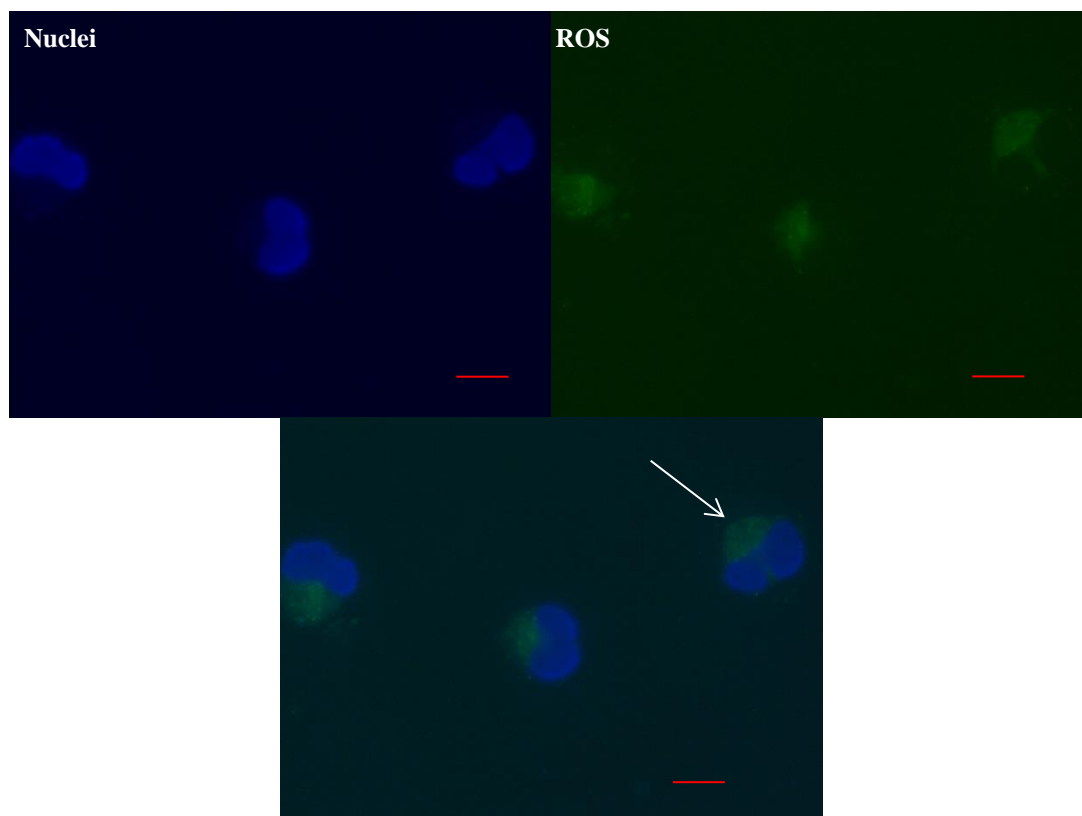


Figure 5.5 – Visualisation of the presence of ROS in PBMCs following incubation with 1050 Vit E 10 UHMWPE wear debris at a concentration of $100 \mu\text{m}^3$ per cell, for 48 hours at 37°C in 5% (v/v) CO_2 . Blue signals represent nuclei stained with Hoechst, while green signals represent fluorescent ROS. The white arrow shows a cell that appears to be undergoing cell division. Size bar: $5 \mu\text{m}$, 63x (oil) Mag.

While the images presented above are selected representative examples that illustrate the production of ROS in macrophages incubated with UHMWPE wear debris, this trend of intense levels of ROS in cells incubated with 1050 HXL UHMWPE wear debris, and lower levels of ROS in cells incubated with 1050 Vit E 10 UHMWPE wear debris was observed across the cell population in samples from three different healthy donors. As with $\text{TNF-}\alpha$ release in response to UHMWPE wear debris, the response to wear debris in terms of production of reactive oxygen specie was also variable. Reactive oxygen species intensity in PBMCs in response to UHMWPE wear debris was quantified in two donors (Donor 8 and Donor 11).

5.4.3 Quantification of ROS Intensity in PBMNCs Incubated with UHMWPE Wear Debris

From each sample, four images from each UHMWPE treatment were captured for analysis. Cells with no additional particles or agents acted as the negative control for oxidative stress, while 100 μM TBHP was used as the positive control. Quantification of green fluorescence intensity was carried out using Image J image analysis software, and the mean grey scale intensity was measured for each cell, where a mean intensity value was determined for each image, as described in section 5.4.3. Throughout these experiments, the positive control (TBHP) performed inconsistently. Despite this, the positive control has been included in the final mean intensity results from one donor, however no error bars are included as the TBHP only appeared to induce oxidative stress in one sample of cells. Despite this, an increase in production of ROS compared to the cells only negative control could still be determined

The mean intensity of ROS in PBMNCs isolated from Donor 8 and treated with UHMWPE wear debris at a concentration of 100 μm^3 per cell is shown in Figure 5.6. A significant increase in the mean intensity of ROS production was observed in PBMNCs incubated with 1050 HXL UHMWPE wear debris compared to the cells only negative control. In contrast, the mean intensity of ROS production in cells treated with 1050 Vit E 10 UHMWPE wear debris was significantly lower, with ROS intensity comparable to that recorded for the cells only negative control.

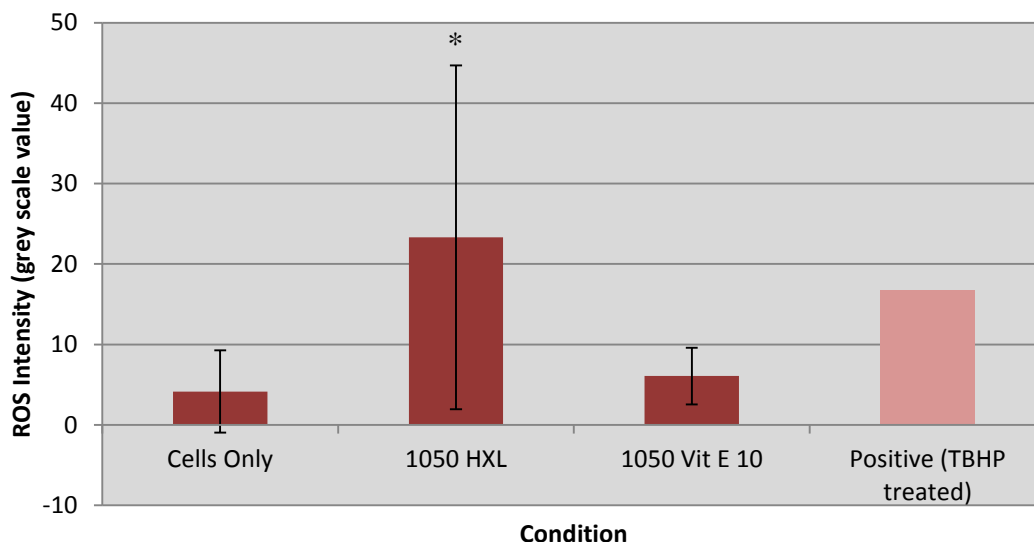


Figure 5.6 – Mean intensity of ROS in PBMCs isolated from Donor 8 treated with 1050 HXL UHMWPE wear debris at a concentration of $100 \mu\text{m}^3$ over 48 hours at 37°C in 5% (v/v) CO_2 in air. Mean ROS within each cell was determined from the grey scale value in each cell, calculated using Image J. A mean ROS intensity for each sample was determined. $100 \mu\text{M}$ TBHP was used as a positive control for ROS production in cells. Error bars show 95% confidence level; $n=4$. * indicates a significant increase in the mean ROS intensity in PBMCs compared to the cells only negative control (ANOVA; $p<0.05$).

The experiment to determine the intensity of reactive oxygen species production in PBMCs was repeated with Donor 11, and the mean ROS intensity is shown in Figure 5.7. A significant increase in the mean ROS intensity was observed in PBMCs incubated with 1050 HXL at a dose of $100 \mu\text{m}^3$, compared to the cell only negative control (ANOVA; $p<0.05$). In comparison, PBMCs incubated with 1050 Vit E 10 had a significantly lower mean ROS intensity compared to the 1050 HXL-treated cells. The mean ROS production in PBMCs treated with 1050 Vit E 10 was higher than the ROS production in the cells only negative control, however this was not a statistically significant difference.

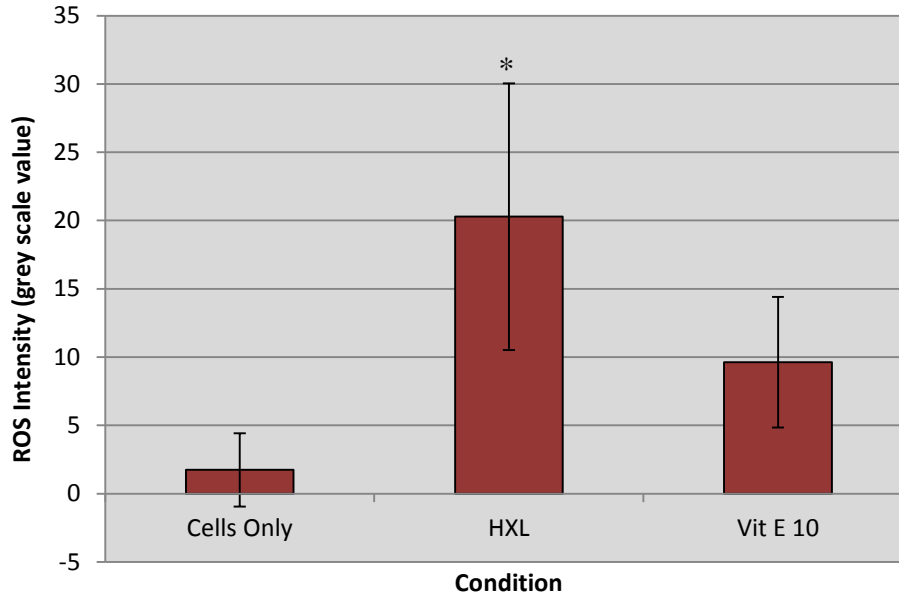


Figure 5.7 – Mean intensity of ROS in PBMNCs isolated from Donor 11 treated with 1050 Vit E 10 UHMWPE wear debris at a concentration of $100 \mu\text{m}^3$ over 48 hours at 37°C in 5% (v/v) CO_2 in air. Mean ROS within each cell was determined from the grey scale value in each cell, calculated using Image J. A mean ROS intensity for each sample was determined. Error bars show 95% confidence level; $n=4$. * indicates a significant increase in the mean ROS intensity in PBMNCs compared to the cells only negative control (ANOVA; $p<0.05$).

5.5 Discussion

Aerobic metabolism in mammalian cells is one of the most important processes that occur, with the generation of ATP being essential for the survival and proliferation of the cell. It is the energy within the electron transport chain that is harnessed to synthesise ATP, and at the end of this transport chain, molecular oxygen is reduced to form water as the end product. However, this final process is not completely efficient, and a proportion of molecular oxygen escapes reduction and is able to become partially reduced, forming reactive oxygen species. As a consequence, reactive oxygen species are produced in all healthy, metabolically active cells, with natural cellular antioxidants such as superoxide dismutase, glutathione, glutathione peroxidase and catalase present to deal with the natural production of reactive oxygen species and prevent cellular damage (Cerutti et al., 1994, Schumacker, 2006, Owusu-Ansah et al., 2008).

It is, however, the overproduction of reactive oxygen species that can be harmful to a cell, creating an environment of oxidative stress. Several diseases have been associated with the overproduction of reactive oxygen species and subsequent oxidative stress, such as some cancers, cardiovascular diseases (for example atherosclerosis), and emphysema (Schumacker, 2006, Owusu-Ansah et al., 2008). Oxidative stress in cells has been associated with the uptake of CoCr wear particles by macrophages and osteoblasts, with ions from this material interfering with the redox cycle in cells (Fleury et al., 2006). The way in which these metal ions could interfere with a chemical process such as the redox cycle is fairly well understood. In contrast, the effect of clinically relevant UHMWPE wear debris on the oxidative state of cells has not been widely investigated and hence is not well understood.

This study has demonstrated that PBMNCs successfully phagocytose both micrometre and nanometre sized UHMWPE wear debris. The phagocytosis of UHMWPE wear debris has also been demonstrated in a previous study by Liu (2012). Using this knowledge, a hypothesis could be generated that the intracellular response to UHMWPE wear debris following phagocytosis could cause a similar intracellular response to pathogens following phagocytosis of microbes. The production of microbicidal oxidants in response to phagocytosis of microbes has been demonstrated in macrophages, with the purpose theorised to be for the

destruction of phagocytosed pathogens (Babior, 2000). A similar oxidative response could therefore be hypothesised to occur following the phagocytosis of UHMWPE wear particles, and subsequently create an environment of oxidative stress in cells.

The only previous study investigating oxidative stress in response to UHMWPE wear debris was performed by Bladen *et al.* (2010). In this study, the authors showed that virgin UHMWPE wear debris at a dose of 100 μm^3 stimulated the production of reactive oxygen species in macrophages, compared to the background level of ROS production observed in cells only controls. While the previous study demonstrated an interesting result, this did not translate directly to the clinical situation, as virgin UHMWPE is rarely used as the bearing material in total hip replacements today. With the development of low wearing highly crosslinked UHMWPE bearing materials, it was necessary to investigate the production of ROS in response to clinically relevant highly crosslinked UHMWPE wear debris. In addition, antioxidant UHMWPE should also be investigated to determine if this UHMWPE material has an effect on the production of ROS and subsequent oxidative stress environment.

The present study used a fluorogenic marker to detect the presence of reactive oxygen species in PBMNCs after culture with UHMWPE wear debris. The marker used was 5-(and 6)-carboxy-2',7'-dichlorodihydrofluorescein diacetate (carboxy- H_2DCFDA). Upon permeation into the cell, this compound undergoes deacetylation by cellular esterases. This cleaved compound is then oxidised in the presence of reactive oxygen species, after which the reduced marker emits green fluorescence which was detected using the FITC channel of a fluorescence microscope. The intensity of green fluorescence within cells was attributed to the intensity of ROS production in the cell. Hoechst counterstain was also performed to allow imaging of the cell nuclei.

High quality images used in this chapter showing the production of ROS in cells are also available on the CD-ROM attached at the end of the thesis. These images show the presence of ROS in more detail and clearer than the printed images in this chapter.

Fluorescence microscopy images clearly showed the presence of a cell monolayer following 48 hours of incubation, identifiable by the presence of blue Hoechst-stained nuclei. Using this image to locate cells, low levels of fluorescence were observed in PBMNCs in the cells only negative control. This low level of green fluorescence was attributed to the production of ROS in metabolically active cells. In contrast to the cells only negative control, intense levels of green fluorescence were observed in cells treated with 1050 HXL UHMWPE wear debris at a concentration of 100 μm^3 per cell, indicating high levels of production of reactive oxygen species and oxidative stress. This oxidative stress was believed to be in response to HXL wear debris and the subsequent phagocytosis of these wear particles by the PBMNCs. Around 90% of ROS production occurs in the mitochondria in mammalian cells (Boveris and Chance, 1973), and the areas of intense ROS production were located outside of the nucleus. These intense areas of ROS were clearly shown on the overlay image as bright green rings around the nucleus of the cell. These images were similar to the images presented in a previous study by Bladen *et al* (2010) where the authors used the same method of ROS detection in PBMNCs in response to virgin UHMWPE wear debris.

Finally, PBMNCs were incubated with vitamin E enhanced highly crosslinked UHMWPE wear debris at a concentration of 100 μm^3 per cell. Low levels of green fluorescence were observed in cells, indicating low levels of ROS production. These levels of fluorescence appeared slightly more intense than in the cells only negative control, however no areas of intense fluorescence were observed in cells. This suggested that the presence of vitamin E in highly crosslinked UHMWPE wear debris led to lower levels of reactive oxygen species production in cells.

A closer, more detailed look at the levels of ROS production in PBMNCs incubated with 1050 HXL and 1050 Vit E 10 revealed that ROS were located outside of the cell nucleus in the cell cytoplasm. Reactive oxygen species production in PBMNCs incubated with 1050 HXL was intense, with punctate areas of ROS observed in some cells. These punctate areas may indicate that phagosomes containing UHMWPE wear particles fuse with lysosomes and could represent areas of accumulation of ROS, intended for the destruction of internalised pathogens. An alternative hypothesis is that these punctate areas of fluorescence were mitochondria; the organelle responsible for the vast majority of ROS production. In order to investigate

this further, a fluorescent marker for mitochondria could be included in these experiments, therefore enabling identification of this important organelle.

In an attempt to quantify the results from this assay to allow statistical analysis, the intensity of the green fluorescence was quantified using image analysis software, and this intensity was directly attributed to the intensity of ROS in cells. The image analysis software Image J was used to measure the average grey scale value of green fluorescence in each cell. The area of each cell was outlined manually using the location of the nucleus as a guide. A mean ROS intensity was determined for each image, where finally a mean ROS intensity was determined for each treatment.

This study, along with previous studies, has identified high levels of donor variation in terms of the biological response to UHMWPE wear particles (Matthews et al., 2000, Liu, 2012). In some experiments, no production of ROS was observed. This could be due to errors during the experimental procedure, or more likely due to certain donors not responding to UHMWPE wear debris, as has been demonstrated in the previous chapter in terms of TNF- α response to UHMWPE wear debris.

The mean ROS levels in PBMNCs isolated from Donor 8 and incubated with different UHMWPE wear debris treatments for 48 hours were significantly elevated compared to the cells only negative control (ANOVA, $p < 0.05$). This elevated level of ROS production in 1050 HXL-treated cells was also significantly greater than the level of ROS intensity in PBMNCs incubated with 1050 Vit E 10. With the addition of vitamin E to the highly crosslinked UHMWPE wear debris representing the only variable in between these materials, it could be concluded that the presence of vitamin E reduced the levels of ROS in cells.

A similar result was observed in PBMNCs isolated from Donor 11. A significantly elevated level of ROS intensity was observed in PBMNCs incubated with 1050 HXL UHMWPE wear debris compared to the cells only negative control and the 1050 Vit E UHMWPE wear debris treated PBMNCs (ANOVA, $p < 0.05$). Once again, the difference in ROS intensity between 1050 HXL treated cells and 1050 Vit E 10 treated cells was attributed to the presence of vitamin E in the highly crosslinked UHMWPE wear debris.

These results suggest that vitamin E could have an antioxidant effect intracellularly, and therefore quench the reactive oxygen species that are produced. In donating a hydrogen atom from the hydroxyl group on the aromatic ring of vitamin E, a radical species can then be reduced to form a stable molecule. This process could occur intracellularly, leading to reduced levels of ROS observed in PBMNCs. A study by Pathania *et al.* (1999) demonstrated that high doses of vitamin E supplementation to rats (250 mg.Kg) significantly reduced the production of ROS (H_2O_2 , O_2^-) in alveolar macrophages in response to lipopolysaccharide (LPS; 10 $\mu\text{g}.\text{ml}$) (Pathania *et al.*, 1999). While these were high doses relative to the size of the animal model, this study still demonstrated a reduced ROS response to LPS from primary macrophages pre-treated with vitamin E.

An area of debate relating to the activity of vitamin E in highly crosslinked UHMWPE exists, whereby the leaching of vitamin E from UHMWPE following crosslinking is questioned. Studies investigating the grafting of vitamin E to UHMWPE following gamma irradiation have shown that increasing irradiation of the polymer, and the subsequent increase crosslinking of UHMWPE reduces the rate of elution of vitamin E from the polymer (Oral *et al.*, 2013). This would suggest that in vitamin E enhanced highly crosslinked UHMWPE; vitamin E is not available outside the polymer as elution from the polymer does not occur. However, this study has shown that vitamin E enhanced highly crosslinked UHMWPE wear debris has altered the cytokine release and oxidative stress profiles in PBMNCs compared to the non-vitamin E highly crosslinked UHMWPE wear debris treated cells. It has not been shown that vitamin E elution from UHMWPE is necessary to elicit a biological effect. Through the production of micrometre and nanometre sized UHMWPE wear debris, where vitamin E is homogenous within the polymer, vitamin E may be available on the surface of these particles, where its antioxidant and anti-inflammatory properties can still be exerted.

Secondly, the very 'hostile' environment generated in the lysosomes of phagocytes may have the potential to encourage or cause leaching of vitamin E from the polymer. In previous experiments, boiling of the UHMWPE polymer in hexane has been used as a method for determination of the leaching of vitamin E, or lack of, from UHMWPE. Using this method, a previous study by Oral *et al.* (2013) showed a reduction in the elution of vitamin E from highly crosslinked UHMWPE following

crosslinking at elevated temperatures (Oral et al., 2013). Clinically, the bulk UHMWPE material in the form of the acetabular component will not encounter such harsh conditions as boiling in hexane, so it would be possible to conclude that vitamin E will not leach from the highly crosslinked bulk material. However, wear particles that have been phagocytosed and fused with the acidic, enzymatic lysosome may experience conditions that could lead to the elution of vitamin E. A lack of understanding about the availability of vitamin E in highly crosslinked UHMWPE is something that should stimulate future research, specifically the availability of vitamin E in clinically relevant wear particles as opposed to the thin sections used in previous studies (Oral et al., 2013). Research into this could lead to future advances in the area of antioxidant enhancement of UHMWPE for use in orthopaedics and other areas of medicine.

5.6 Conclusion

Highly crosslinked UHMWPE wear debris stimulated the production of oxidative stress in PBMNCs. In contrast, a significant reduction in the production of reactive oxygen species was observed in PBMNCs incubated with vitamin E enhanced highly crosslinked UHMWPE wear debris, indicating that vitamin E enhanced highly crosslinked UHMWPE had an antioxidant effect within cells, preventing the high levels of reactive oxygen species production observed in response to highly crosslinked UHMWPE wear debris.

Chapter 6

Discussion

Total hip replacements are considered one of the most successful surgical procedures in medicine, with over 76,000 primary hip replacements performed in the UK in 2013; and an estimated 1 million procedures performed worldwide (National Joint Registry, 2013, American Academy of Orthopaedic Surgeons, 2013). Total hip replacements are used to treat conditions that cause chronic pain and disability in the hip joint, such as osteoarthritis, rheumatoid arthritis, avascular necrosis, and following trauma to the hip. Total hip replacements successfully restore mobility and eliminate pain. An implant comprised of a metal femoral prosthesis articulating against an ultra-high molecular weight polyethylene (UHMWPE) acetabular cup is the most commonly used bearing, and is considered the gold standard for total hip arthroplasty (National Joint Registry, 2013).

With the success of this procedure, there has been a gradual increase in the number of procedures per year, and in addition to this, an increase in the number of younger, more active patients requiring a total hip replacement. The National Joint Registry 10th Annual Report for England and Wales revealed that around 20% of all primary hip replacement procedures were performed on patients under the age of 60 years of age. With an average life expectancy of 81 years in the UK (according to World Bank), this represents a group of patients that will require a total hip replacement for a minimum of 20 years if they are to avoid implant failure and revision surgery. A revision rate of around 2% after 10 years has been reported across the range of metal-on-UHMWPE total hip replacement devices, with this revision rate increasing after 10 years (National Joint Registry, 2013), and it is the need for long-lasting hip replacements that is driving the current research in total hip replacements.

One of the most crucial processes that occur in metal-on-UHMWPE hip replacements is the wear of the UHMWPE component; a normal process that occurs with the coupling of a hard-on-soft bearing. However, the wear of UHMWPE leads

to the generation of UHMWPE wear debris, and this UHMWPE wear debris stimulates macrophages in the tissues surrounding the implant, leading to an immune response involving the release of osteolytic cytokines such as TNF- α , IL-1 β and IL-6. This osteolytic immune response results in osteolysis around the implant, causing aseptic loosening and the subsequent failure of the joint replacement (Ingham and Fisher, 2000, Ingham et al., 2000).

Alternative bearing materials have been used in an attempt to create the ideal hip replacement. Metal-on-metal bearings have been used due to their low wearing and high hardness properties, and were thought to be ideal for younger, more active patients (Delaunay et al., 2008). However, with some metal-on-metal bearings, an increased rate of wear has been documented, alongside adverse tissue reactions and pseudotumours, believed to be stimulated by both nanometre-sized and micrometre-sized metal wear debris, in addition to the metal ions generated from the implant (Delaunay et al., 2008, Delaunay et al., 2010, Kwon et al., 2010). These problems have led to a steep decline in the use of metal-on-metal total hip replacements, while metal-on-UHMWPE has remained the bearing of choice (National Joint Registry, 2013).

A major advance in polymer technology for use in joint replacements was the introduction of high levels of irradiation to UHMWPE to increase the levels of crosslinking. This led to a significant improvement in the wear resistance of UHMWPE compared to non-crosslinked UHMWPE, and this improvement translated to an improved clinical bearing material (Rajadhyaksha et al., 2009, Galvin et al., 2006). Despite this improvement in the wear resistance observed with highly crosslinked UHMWPE, incidences of oxidation were reported. A consequence of high levels of irradiation energy is the generation of free radicals following scission of the carbon chains in polyethylene (Popoola et al., 2010). These free radicals are essential for the formation of crosslinks in the polymer. However, most free radicals do not reform but remain trapped in the polymer, and it is this free radical burden that can then cause oxidation of the polymer *in vivo*. Oxidation of UHMWPE reduces some mechanical properties, causing embrittlement of the polymer, and generally creates a material with less favourable properties for a bearing material in total joint replacement (Al-Ma'adeed et al., 2006).

Post-irradiation heat treatments of UHMWPE were implemented to quench the free radicals present and provide a stable polymer for implantation to the patient. However, these treatments were not completely effective. Remelting of UHMWPE provided sufficient energy for the radical species to recombine, therefore removing the free radical burden; however this process reduced some of the favourable mechanical properties of UHMWPE, such as fatigue crack propagation resistance (Oral et al., 2006b). Below-melt annealing was an alternative to remelting, and by not melting the polymer this process protected the mechanical properties of UHMWPE. However, this process was not successful in removing the free radical burden of the material, and oxidation could still occur (Wang, 2006). Alongside this mechanism of oxidation, an alternative mechanism of oxidation was believed to occur, which was independent of irradiation-induced radicals (Wannomae et al., 2006, Oral et al., 2010, Costa et al., 2001). This highlighted the importance of protecting the polymer against oxidation in order to achieve maximum performance from UHMWPE as a bearing material, and led to the introduction of an antioxidant compound into UHMWPE.

Vitamin E enhanced highly crosslinked UHMWPE was introduced as a clinical bearing material in total hip replacements in 2007, with manufacturers offering their own versions of this novel antioxidant bearing (E1[®] - Biomet; ECiMa[™] - Corin; Vivacit-E[®] - Zimmer). Vitamin E enhanced highly crosslinked UHMWPE has been shown to possess superior performance compared to remelted highly crosslinked UHMWPE in terms of its oxidative stability, with vitamin E enhanced UHMWPE showing improved wear resistance following two weeks accelerated aging, improved fatigue crack propagation resistance, and improved oxidative resistance (Oral et al., 2006b, Kurtz et al., 2009).

There has also been an increase in interest in alternative antioxidant UHMWPE materials for use in joint replacements. Some antioxidant compounds being researched for their use in UHMWPE include hindered phenols, polyphenols, nitroxides, lanthanides, and anthocyanins. While all these antioxidants have shown promising results *in vitro* in terms of their antioxidant properties in UHMWPE, a hindered phenol enhanced UHMWPE is the only alternative UHMWPE material currently available clinically (in the knee). AOX[®] UHMWPE, manufactured by DePuy Synthes Joint Reconstruction, uses a hindered phenol compound;

Pentaerythritol tetrakis. This is a compound with four phenol groups, and has been shown to be a potent antioxidant compound. This hindered phenol enhanced highly crosslinked UHMWPE has been shown to possess oxidative stability far superior to remelted highly crosslinked UHMWPE, along with comparable wear performance (King et al., 2009).

While the vast amount of literature on these antioxidant materials has focused on the mechanical performance and oxidative stability, there has been little research performed on the biological response to wear particles from these materials. When considering the importance of the immune response to UHMWPE wear debris in the failure mechanism of metal-on-UHMWPE joint replacements, it is surprising more focus is not placed on the biological response. Only one previous study investigated the cellular response to antioxidant wear debris, and this showed a significant reduction in osteolytic cytokine release from macrophages incubated with vitamin E enhanced UHMWPE compared to virgin UHMWPE (Bladen et al., 2013). The lack of crosslinking in these materials leaves a gap with respect to clinical relevance; with highly crosslinked UHMWPEs the most commonly used bearing materials in total hip replacements. However, this type of study, looking at clinically relevant wear debris, is important when predicting the biological response to wear debris at the site of the prosthesis.

Other studies have investigated the bone remodelling response to UHMWPE wear particles implanted under the skin of animal models, and shown vitamin E enhanced highly crosslinked UHMWPE wear particles stimulated significantly reduced levels of osteolysis compared to virgin UHMWPE (Bichara et al., 2013). While this study appears promising in terms of the performance of vitamin E enhanced highly crosslinked UHMWPE, it is important to point out that this material used post-irradiation diffusion of vitamin E, where the vitamin E may be available to elute from the material (Bichara et al., 2013). In addition, wear particles in the previous study were milled, as opposed to being generated aseptically using multidirectional articulation using kinematics associated with the hip joint. Clinically relevant wear particles have been shown to be critical to the subsequent biological response to UHMWPE wear debris, both in terms of their particle size distribution, and particle surface characteristics (Matthews et al., 2000b).

This study investigated the wear performance and biological response to antioxidant UHMWPEs. This involved wear testing of vitamin E enhanced highly crosslinked UHMWPE, hindered phenol enhanced highly crosslinked UHMWPE, along with experimental and clinical materials to determine the effect of antioxidant doping on the wear factor of UHMWPE. The study then went on to generate clinically relevant UHMWPE wear debris from the vitamin E enhanced and hindered phenol enhanced highly crosslinked UHMWPEs, in addition to non-antioxidant highly crosslinked UHMWPE, in order to determine the biological response of PBMNCs to wear particles from these materials. The use of clinically relevant UHMWPE wear debris is vitally important for evaluating the biological response to a UHMWPE material with confidence. The present study was able to use multidirectional articulation of clinical materials, under kinematics shown to be representative of the hip joint and in the presence of serum proteins to generate UHMWPE wear debris that could confidently be termed as clinically relevant.

In addition to determining the biological response to these UHMWPE materials, this clinically relevant wear debris was used to investigate the production of reactive oxygen species in cells following incubation with highly crosslinked UHMWPE wear debris, and investigate whether vitamin E enhancement had any effect on the production of reactive oxygen species and the subsequent oxidative stress in cells.

6.1. Pin on Plate Wear Testing of Antioxidant UHMWPE Materials With and Without Crosslinking

The first objective of the study was to conduct a wear test of nine UHMWPE materials to determine the wear factor of these materials, and determine the effect of crosslinking and antioxidant enhancement on the wear performance of UHMWPE. This section of the study used an accepted method of wear testing, using a six station simple configuration multidirectional pin-on-plate wear simulator. This method of wear testing has been used previously to determine the wear rate of UHMWPE materials against different counterface roughness conditions (Endo et al., 2001), in addition to determining the wear of UHMWPE under different kinematic conditions (Galvin et al., 2006). Different methods are available to determine the wear performance of materials in joint replacements, such as the hip joint simulator or pin-

on-disk rig. However, pin-on-plate wear testing was considered the most appropriate for this study due to its ability to compare the wear performance of each UHMWPE material in replicate, while also being a low-cost and non-time consuming method. Pin-on-plate wear tests allow for the wear of the UHMWPE component to be determined gravimetrically at the end of the wear test, generating data to determine a mean wear factor for each material tested. Wear tests in this study were performed by articulating a UHMWPE pin (10 mm contact face) against a smooth ($R_a \leq 0.01\mu\text{m}$) high carbon (0.27% w/w) CoCr counterface. Tests were performed using a lubricant of 25% (v/v) bovine serum supplemented with 0.03% (w/v) sodium azide, with a stroke length of 25 mm, rotation of $\pm 30^\circ$, under a load of 160N at a rate of 1 Hz. Wear tests were performed for a minimum of 500,000 cycles over the course of two weeks. These parameters have been used previously to replicate the forces and kinematics of the hip joint (Tipper et al., 2000, Galvin et al., 2006).

The nine UHMWPE materials tested in this section of the study were comprised of three non-antioxidant UHMWPEs (1050 Virgin, 1050 Marathon (5 MRad) and 1050 HXL (10 MRad)), three vitamin E enhanced UHMWPEs (1050 Vit E, 1050 Vit E 5 and 1050 Vit E 10), and three materials using a GUR1020 resin (1020 Virgin, 1020 AOX and 1020 AOX 8 (8 MRad)). This matrix of materials allowed for the comparison of crosslinked and non crosslinked UHMWPE, along with antioxidant and non-antioxidant UHMWPE at different levels of crosslinking.

The results from the wear tests indicated that with the GUR1050 UHMWPE materials, an increase in the level of crosslinking led to a significant reduction in the wear factor of UHMWPE. There was a significantly lower wear factor observed when 1050 HXL was compared to 1050 Virgin UHMWPE. Similarly, there was a significantly lower wear factor recorded for 1050 Vit E 10 compared to both 1050 Vit E and 1050 Vit E 5. Previous studies have demonstrated a significant reduction in the wear factor as a result of high levels of crosslinking, both in pin-on-plate wear tests and using hip joint simulators (Affatato et al., 2012, Jedenmalm et al., 2009, Galvin et al., 2006, Endo et al., 2002). However, few studies have clearly demonstrated the effects that vitamin E has on the wear of highly crosslinked UHMWPE.

A previous study by Oral *et al.* (2006) compared the wear performance of a vitamin E enhanced (diffused) highly crosslinked UHMWPE acetabular cup to a virgin UHMWPE acetabular cup using a hip simulator. As expected, the highly crosslinked vitamin E enhanced UHMWPE component had a significantly lower level of wear compared to the virgin UHMWPE component. However, the vitamin E enhanced component was also highly irradiated (10 MRad) and therefore a direct comparison is inappropriate (Oral *et al.*, 2006a). High levels of irradiation increase the levels of crosslinking in the material, improving the wear resistance of the polymer (Galvin *et al.*, 2006). A separate study tested the wear performance of virgin UHMWPE and vitamin E enhanced (blended) UHMWPE, with neither material crosslinked. In this study, there was no significant difference in the wear volume of the materials until 5 million cycles were reached, at which point the vitamin E enhanced UHMWPE had a significantly lower cumulative wear volume than the virgin UHMWPE (Teramura *et al.*, 2008). This brings up the possibility that there may be differences in performance between the virgin and antioxidant materials at higher numbers of cycles. This is an area where the present study could potentially be improved by increasing the duration of the tests.

In addition to the vitamin E enhanced highly crosslinked UHMWPE, an alternative antioxidant UHMWPE was also investigated in this study. Hindered phenols have recently been introduced into UHMWPE in the knee, and this hindered phenol enhanced UHMWPE material is being investigated for use in the hip. The material used in this study was the knee material, which was a GUR1020 highly crosslinked (8 MRad) UHMWPE material. Due to the difference in the resin of this material, GUR1020 virgin UHMWPE and GUR1020 AOX[™] (non-crosslinked) UHMWPE materials were also included in the wear tests. There was no significant difference in the mean wear factor of these materials, despite the addition of high levels of crosslinking (ANOVA, $p > 0.05$). With the addition of the hindered phenol antioxidant (AOX[™]), and the addition of crosslinking, the mean wear factor decreased, however this decrease was not statistically significant. This lack of a statistically significant result could be due to the large error bars observed with these three GUR1020 materials. These large error bars could be due to inconsistencies with the pin-on-plate wear simulator causing varying degrees of wear, or potentially contamination with fragments of metal debris generated from the wear simulator

machinery, which would act as third body particles and possibly increase the levels of UHMWPE wear in individual stations. Another possible reason for this lack of a reduction in the wear factor with increasing crosslinking was the fact that the mean wear factor for the GUR1020 Virgin UHMWPE material was also low compared to the GUR1050 Virgin UHMWPE material. A previous study showed comparable wear rates between GUR1050 and GUR1020 Virgin UHMWPE, which is in contrast with the results in this study (Tipper et al., 2005). This is an area where further testing would be beneficial, further investigating the difference in wear performance of these two resins. With the increase in the use of these AOXTM UHMWPE materials clinically; further research is required to evaluate the performance of these materials, using anatomical joint simulators to fully evaluate the performance of these materials *in vitro*.

6.2 Particle Characterisation of Antioxidant UHMWPE Materials With and Without Crosslinking

The second aim of this study was to determine the wear particle size distribution from a number of the nine materials in the study. The size distribution of wear debris generated from a UHMPWE material has been shown to be a crucial aspect of the biological response to the material. A study by Liu (2012) showed wear particles generated from virgin UHMWPE in the $<0.1\mu\text{m}$ and $>1.0\mu\text{m}$ size ranges, when dosed at $100\mu\text{m}^3$ per cell, did not stimulate a significant osteolytic cytokine response from PBMNCs following incubation. The only size range of UHMWPE wear particles to stimulate a statistically significant elevated release of TNF- α , when dosed at $100\mu\text{m}^3$ per cell, compared to the cells only negative control, was the 0.1-0.6 μm sized wear debris (Liu, 2012). This implicated that while the total volume of wear debris plays a part in stimulating a cellular response, the volume of this ‘critically sized’ wear debris is more important in generating a cellular response than the overall total volume, with this also being shown in previous studies (Howie, 1990, Howie et al., 1993, Revell et al., 1997, Green et al., 1998, Ingham and Fisher, 2000). For this reason, it is therefore vital to determine the frequency and volume distribution of wear particles generated from each material, and to determine whether

crosslinking and/or antioxidant enhancement has a significant effect on the wear particle size distribution.

In order to obtain high resolution images of the wear particles for sizing and analysis, serum lubricant samples were processed to remove proteins, lipids and salts from the sample, and lubricants were filtered through a series of three filters (10 μm , 1 μm and 0.015 μm). These filters were then imaged using a FEGSEM and particles were sized manually using image analysis software, after which the size distribution was plotted for comparison.

The frequency and volume distributions of wear debris from 1050 Virgin UHMWPE was compared to wear debris from 1050 Vit E 10 UHMWPE. There was no significant difference in the particle distribution between these two materials in terms of frequency and volume distribution. Both materials generated the majority of wear particles in the $<0.1 \mu\text{m}$ and $0.1\text{-}1.0 \mu\text{m}$ size ranges, however these two size ranges contributed a relatively small volume of the total wear volume produced; around 30%. For both materials, the mode size range in terms of volume of wear debris was the $1.0\text{-}10 \mu\text{m}$ size range. Focusing specifically on the critical $0.1\text{-}1.0$ size range, around 30% of the volume of wear debris was produced in this size range for both materials.

Unfortunately, analysis of the GUR1050 series of materials was not completed due to multiple problems regarding contamination of the filters, in addition to technical problems with the SEM on separate occasions. This left a gap in the data in what would have been a complete matrix of materials for analysing the effect of crosslinking, and vitamin E enhancement with crosslinking, on particle size distributions of UHMWPE. Despite this, no significant difference was observed in the frequency or volume distribution of 1050 virgin of 1050 Vit E 10. In future experiments, it would be necessary to analyse a complete matrix to confidently determine the effect of variables such as crosslinking and/or antioxidant enhancement on the particle size distribution.

The wear debris generated from two GUR1020 materials was also characterised. Using the same method, 1020 Virgin and 1020 AOX 8 UHMWPE wear debris was isolated and characterised to determine the volume and frequency distribution of the wear debris. No significant difference was determined between 1020 Virgin and

1020 AOX 8 in terms of both frequency and volume distribution. Unlike the GUR1050 materials, the mode size range in terms of particle numbers was the 0.1-1.0 μm size range. However, in terms of volume of the wear debris, the 1.0-10 μm size range was the mode size range. For the particle analysis of GUR1020 materials, there was no GUR1020 8MRad crosslinked UHMWPE material to include in this section of the study to complete the matrix of materials. The closest UHMWPE material available was XLK UHMWPE. This is a GUR1020 material irradiated to 5 MRad, and this difference in crosslinking was considered too large to be compared to the GUR1020 AOX 8 MRad UHMWPE material. However, as with the GUR1050 UHMWPE materials, no significant difference in the particle size distribution was observed.

This lack of variation in the particle size distribution of UHMWPE wear debris with different levels of crosslinking was also demonstrated in a previous study by Galvin (2003). Comparing GUR1050 Virgin, 5 MRad and 10 MRad UHMWPE wear debris generated on the six station pin-on-plate wear rig against a smooth counterface, the aforementioned study demonstrated no significant difference between the materials in terms of percentage frequency or volume distribution of wear particles (Galvin, 2003). A separate study characterising wear particles from a highly crosslinked UHMWPE and virgin UHMWPE generated on a hip simulator also showed no significant difference in the mode size range of wear particles in terms of frequency (Illgen et al., 2008). These previous studies support the findings of the present study, that crosslinking, antioxidant enhancement, or the combination of both treatments on UHMWPE, have no significant on the wear particle size distribution.

6.3 Biological Response of Peripheral Blood Mononuclear Cells to Antioxidant UHMWPE Wear Debris

Wear debris generated from UHMWPE in a metal-on-UHMWPE total hip replacement stimulates an immune response in the tissue surrounding the implant, leading to the resorption of bone around the prosthesis, and loosening of the implant. A cell culture technique which had previously been developed to incubate peripheral blood mononuclear cells isolated from blood with UHMWPE wear debris generated aseptically on a pin-on-plate wear simulator was used to investigate the cellular

response to antioxidant UHMWPEs compared to conventional UHMWPE. Wear particles generated from UHMWPE have a low density, and therefore are buoyant in solution, and when incubated with cells in 2D normal cell culture, the cells would adhere to the tissue culture plastic well and no contact would occur with the buoyant UHMWPE wear particles. To address this problem, a technique was developed by Green et al. (1998) which used an agarose gel to suspend the UHMWPE wear particles, and allow for the culture of PBMNCs on this gel. This initial technique involved mixing UHMWPE wear debris with molten 0.3% agarose gel in the wells of a 48 well plate and immediately centrifuging the 48 well plate. Upon the agarose gel cooling and solidifying, this technique produced a superficial layer of UHMWPE wear debris near the surface of the agarose gel, upon which the PBMNCs could then be seeded at a given density. This method was altered slightly in subsequent studies in that the concentration of agarose gel or cell seeding density was adjusted (Ingram et al., 2004, Richards, 2008).

Most recently, Liu (2012) modified this technique to produce a 3D culture system, whereby the centrifugation step was removed, meaning the UHMWPE wear debris was distributed throughout the agarose gel. This technique required the migration of PBMNCs into the agarose gel to contact the UHMWPE wear debris. For the present study, the agarose gel technique developed by Liu (2012) was used. The author of the present study had difficulty maintaining a level surface of the agarose gel when centrifugation of the cell culture plates was conducted; and found an uneven surface to cause uneven distribution of cells following seeding. In addition, the use of highly crosslinked UHMWPE in the present study, and the lower wear rates of these materials, meant a large volume of lubricant was required per well to achieve the minimum dose of UHMWPE wear debris per well. This therefore didn't allow for the use of a 48 well plate, as used previously by Green et al. (1998), and meant larger-well 24 well plates were required. This could have also contributed to the difficulties experienced when centrifuging the culture plates. For these reasons, the Liu (2012) agarose technique was used in this study. However, using this cell culture technique, there are several potential variables, such as cell seeding density, agarose gel volume and concentration, and particle concentration. As a result, different cell culture conditions were investigated to provide improved cell culture technique for this study.

In order to verify whether this 3D agarose cell culture technique facilitated the contact and phagocytosis of UHMWPE wear particles by PBMNCs, confocal microscopy was performed. Using fluorescently labelled UHMWPE wear particles in the micrometre or nanometre size range, the internalisation of UHMWPE wear particles in PBMNCs was observed. Wear particles were observed outside of the nucleus, as indicated by the green fluorescent particles being external to the blue Hoechst-stained nuclei of the cells. This confirmed that the agarose gel technique was not inhibiting the uptake of UHMWPE wear debris by PBMNCs, and added confidence to the previous studies that have drawn conclusions regarding the cellular response to UHMWPE using this technique, in addition to the present study.

As a result of the various method development steps taken, it was hypothesised that cell culture conditions comprising a low agarose gel concentration (0.4% (v/v)) were required to allow penetration of cells. It was also hypothesised, although not demonstrated, that a lower concentration of agarose gel, in addition to adding the UHMWPE wear particles to the gel at a slightly higher temperature (and therefore lower viscosity), allowed the buoyant particles to float towards the surface of the gel at a greater rate prior to the gel setting than using a lower temperature gel. The presence of a higher concentration of UHMWPE particles near the surface of gel was observed using the light microscope when checking the gels; however this was not quantified and presented in the results.

In order to generate clinically relevant UHMWPE wear particles, wear debris was generated using a serum-containing lubricant. A 25% (v/v) bovine serum lubricant supplemented with RPMI 1640 medium was used throughout the test, as it has previously been shown that the presence of serum proteins on the surface of the hydrophobic UHMWPE wear particles was required to stimulate a significant cytokine response in PBMNCs (Liu, 2012, Zolotarevova et al., 2010). The present study also generated sterile wear debris against a rough (R_a 0.7-0.9 μm) CoCr counterface in order to maximise the volume of wear debris generated in each test. The wear debris generated against a rough counterface was characterised to ensure the wear particle size distribution was not significantly different to the wear debris generated against smooth ($R_a \leq 0.01$) CoCr counterfaces, and to validate that the wear debris generated in this aseptic wear test was clinically relevant.

The most important finding during the method development of the agarose gel cell culture technique was the importance of the effect of UHMWPE particle concentration on the cellular response. With UHMWPE wear particles dosed at a concentration of $100 \mu\text{m}^3$ per cell, there was no significant TNF- α release observed from PBMNCs from any of the donors tested compared to the cells only negative control. Significantly elevated levels of TNF- α release were consistently observed from PBMNCs treated with the LPS positive control compared to the cells only negative control, along with lower yet still statistically significant elevated levels of TNF- α release from PBMNCs in response to 200 nm Fluospheres at a concentration of $100 \mu\text{m}^3$ per cell. The positive controls indicated that the cells were responding in terms the release of pro-inflammatory cytokines.

In a previous study by Liu (2012), it was demonstrated that the volume of UHMWPE wear debris within the critical size range was crucial to cytokine release after stimulation with wear debris. In the aforementioned study, wear particles in the 0.1-0.6 μm size range dosed at a concentration of $100 \mu\text{m}^3$ per cell promoted higher levels of cytokine release from PBMNCs, compared to nanometre sized ($<0.1 \mu\text{m}$) and larger micrometre sized (1.0-10 μm) wear particles. When comparing the dose of biologically active wear particles incubated with cells, the author of the present study noted a difference in terms of the dose per cell of wear particles within this critical size range. While the previous study was dosing $100 \mu\text{m}^3$ per cell of wear particles in the 0.1-0.6 μm size range, the present study had been dosing $100 \mu\text{m}^3$ per cell of the complete size range of wear debris. This equated to an actual dose of around $30 \mu\text{m}^3$ of biologically active wear debris per cell, significantly lower than the dose required to stimulate a cytokine response (Liu, 2012). As a result of this, the investigation was continued with UHMWPE wear debris at a higher concentration per cell.

As a result of the required higher dose of wear debris, it was necessary to produce new samples of wear debris with higher concentrations of UHMWPE particles. A 10 day wear test using the single station pin-on-plate wear simulator was conducted to generate a highly concentrated sample of wear debris from 1050 HXL, 1050 Vit E 10 and 1020 AOX 8 UHMWPE. Following incubation of PBMNCs with 1050 HXL at doses of $100 \mu\text{m}^3$, $200 \mu\text{m}^3$ and $600 \mu\text{m}^3$, a significant TNF- α response was observed from PBMNCs incubated with the new, higher doses of 1050 HXL UHMWPE wear debris at $200 \mu\text{m}^3$ and $600 \mu\text{m}^3$ per cell, compared to the cells only

negative control. This was the first instance of a significantly elevated TNF- α release from PBMNCs in response to UHMWPE HXL wear debris in the study so far, and this was observed in PBMNCs from two donors.

Following this, the TNF- α release in response to 1050 Vit E 10 and 1020 AOX 8 was also investigated at a concentration of 500 μm^3 per cell. This concentration of wear debris was chosen to provide the highest wear debris concentration possible from all three UHMWPE particle samples, at which point any significant differences in the biological responses could be determined. At a dose of 500 μm^3 per cell, 1050 HXL wear debris stimulated significantly elevated levels of TNF- α release from PBMNCs compared to the cells only control. In addition, a significantly reduced TNF- α release was observed in cells incubated with 1050 Vit E 10 and 1020 AOX 8 at the same concentration compared to cells incubated with 1050 HXL UHMWPE wear debris. This indicated that the presence of vitamin E or a hindered phenol antioxidant in highly crosslinked UHMWPE had a significant effect on the cytokine release from PBMNCs in response to UHMWPE wear debris. These results indicate that the presence of one of these antioxidant compounds in highly crosslinked UHMWPE could have an effect on the inflammatory pathways involved in osteolysis, potentially reducing osteolysis and improving the longevity of the implant.

There are few studies in the literature that have investigated the cellular response to antioxidant UHMWPE wear debris. A previous study by Bichara *et al* (2013) demonstrated a reduction in osteolysis of the calvaria following implantation with vitamin E enhanced highly crosslinked UHMWPE particles compared to implantation of virgin UHMWPE particles (Bichara *et al.*, 2013). However, the mentioned study used a vitamin E diffused material, as opposed to the present study which used a vitamin E blended material. This could have an effect on the biological response in terms of the availability of vitamin E to cells, although a study by Oral *et al* (2006) indicated that there was no loss of vitamin E from vitamin E enhanced (diffused) highly crosslinked UHMWPE sections following incubation in isopropanol (concentration not given) (Oral *et al.*, 2006c). The availability and potential leaching of vitamin E from highly crosslinked UHMWPE is an area where further research is required to provide a definitive answer to whether antioxidants can leach from the highly crosslinked material. Some studies have shown that

vitamin E does not leach from highly crosslinked UHMWPE sections, however the use of clinically relevant particles would provide a more accurate model to determine if there is any leaching of vitamin E, due to the hugely increased surface area of micrometre and nanometre sized particles compared to the 150 μm thick sections used in the previous studies (Oral et al., 2013). Despite this, the current study and the previous study by Bichara *et al.* (2013) both illustrate the anti-osteolytic potential of vitamin E enhanced highly crosslinked UHMWPE wear debris.

In a similar study, and using a similar animal model to investigate osteolysis potential of antioxidant UHMWPE, AOXTM UHMWPE (hindered phenol enhanced) particles were implanted under the skin of a mouse to come in contact with the calvaria. The study investigated the effect UHMWPE particles have on the osteogenic/osteolytic mechanisms of the bone, using Micro-CT at day 0 and day 10. The study used particles milled from either GUR1050 Marathon (5 MRad), GUR1020 XLK (5 MRad) and AOXTM (8 MRad) UHMWPE. The study showed a more osteogenic response from AOX UHMWPE treated sites, compared to XLK and Marathon treated mice. While other variables were present, such as particle size distribution and irradiation dose, the study implicated the presence of the hindered phenol antioxidant to the reduced osteolytic response compared to non-antioxidant UHMWPE. Once again, however, this study used milled UHMWPE particles; therefore the wear debris implanted was not clinically relevant. The importance of particle volume distribution, along with concentration, has been highlighted in the present study and previous studies, and for that reason the use of clinically relevant UHMWPE wear debris should try to be adopted in all studies investigating the biological response to UHMWPE wear particles.

Finally, this part of the study demonstrated the occurrence of donor variation, and specifically the heterogeneity of human individuals in terms of the biological response to UHMWPE wear particles. There were several incidences of variation between the TNF- α response to UHMWPE wear particles from different donors of the PBMCs. This has been observed in previous studies investigating the cellular response to UHMWPE wear particles (Matthews et al., 2000a, Liu, 2012). Specifically in the present study, only two donors produced a significant elevation in the levels of TNF- α in response to 1050 HXL UHMWPE wear debris. Despite the lack of a significant TNF- α response to the same treatment in other donors, there

were areas of variation between the non-responders in terms of the TNF- α response to the LPS and Fluosphere positive controls.

This is an occurrence that relates to the clinical situation, in that it could be hypothesised that some individuals with a metal-on-UHMWPE hip replacement would respond more aggressively to UHMWPE wear debris in terms of TNF- α release. A study by Wilkinson *et al.* (2003) investigated whether the carriage of a TNF- α allele could lead to an increased TNF- α response to UHMWPE, and subsequent increased risk of osteolysis following implantation of a metal-on-UHMWPE prosthesis. The authors found that a variation at the -238A position in the TNF- α gene promoter region had a prevalence of 17.3% in the group of patients who had a history of osteolysis following a total hip replacement. This was in comparison to a prevalence of 8.8% in the background population. The study also showed an increase in prevalence (20.5%) in patients with more widespread osteolysis (Wilkinson *et al.*, 2003). This study shows the importance of genetic factors in the biological response to UHMWPE wear debris, and specifically highlighted the importance of the -238 allele on the TNF- α gene promoter region.

For this reason, further research should be carried out into donor variation in terms of the immune response to UHMWPE wear debris, whereby individuals who appear to produce a particularly ‘aggressive’ response (like donor 8 and 15 in this study) would be advised to have an alternative bearing implanted, such as a ceramic material.

6.4 The Production of Reactive Oxygen Species in Peripheral Blood Mononuclear Cells in Response to UHMWPE Wear Particles

The production of reactive oxygen species and subsequent oxidative stress in cells is an important process in terms of cell signalling, and cell survival. The link between oxidative stress in PBMNCs following phagocytosis of UHMWPE wear debris has been suggested, but has not been demonstrated in terms of the current clinical UHMWPE materials today; highly crosslinked UHMWPE and antioxidant highly crosslinked UHMPWE (Bladen *et al.*, 2010).

The present study demonstrated that there was a significant increase in the levels of reactive oxygen species in cells following incubation with highly crosslinked UHMWPE wear debris at a dose of $100 \mu\text{m}^3$ per cell. The intensity of reactive oxygen species appeared to be very high in some cells, and this is believed to correlate to an environment of oxidative stress in cells. In contrast, the production of reactive oxygen species in response to vitamin E enhanced highly crosslinked UHMWPE wear debris was significantly lower than in response to highly crosslinked UHMWPE wear debris. This indicated that the presence of vitamin E in the highly crosslinked UHMWPE particles had an effect on the presence of reactive oxygen species in cells.

The exact mechanism by which this reduction in oxidative stress occurs was not deduced in this study, and this is an obvious area for further research. Two possible hypotheses relate to the antioxidant and anti-inflammatory properties of vitamin E. It could be that the antioxidant action of vitamin E is quenching the radical species that would normally be produced in response to the UHMWPE wear debris, therefore reducing the overall burden of reactive oxygen species. Alternatively, the anti-inflammatory properties of vitamin E could be reducing the production of reactive oxygen species. A study by Pathania *et al* (1999) showed vitamin E supplementation reduced the production of reactive oxygen species in rat macrophages in response to LPS and proinflammatory cytokines such as TNF- α and IL-6. This study failed to identify in which way vitamin E is reducing the burden of reactive oxygen species, and the author of the present study has failed to identify a study outlining this mechanism (Pathania *et al.*, 1999). Research into the exact mechanism by which vitamin E is able to reduce the free radical production in macrophages would be valuable in terms of producing a bearing material from which wear particles with a reduced inflammatory potential are produced.

6.5 Future Work

In the present study, it was demonstrated that using a 3D agarose gel technique, 1050 HXL UHMPWE wear debris at a concentration of $500 \mu\text{m}^3$ per cell stimulated significant release of TNF- α from PBMNCs compared to the cells only negative control, and that significantly lower TNF- α release was demonstrated in response to

1050 Vit E 10 UHMWPE wear debris. Due to time constraints during the method development of these experiments, there was insufficient time to then investigate the release of other cytokines in response to the wear debris from these materials. Previous studies have shown UHMWPE wear debris to stimulate the release of TNF- α from PBMNCs, along with IL-1 β , IL-6 and IL-8 (Green et al., 1998, Liu, 2012, Bladen et al., 2013), and this is an area where it would be obvious to include other cytokines. While it has been shown that vitamin E enhanced highly crosslinked UHMWPE wear debris produces lower TNF- α release than highly crosslinked UHMWPE wear debris, a more complex picture for osteolytic cytokine release would be beneficial.

A second area for future work directly related to the present study is to continue to investigate the cellular responses to AOX enhanced UHMWPE wear debris. Due to time constraints, one complete experiment was performed to investigate the biological response to wear debris from this novel material. Further repeats are required with additional donors for this novel material, in order to add confidence to the findings of this study that AOX enhanced highly crosslinked UHMWPE produced a lower TNF- α response than non-antioxidant highly crosslinked UHMWPE wear debris. The AOX enhanced UHMWPE material could also be included in the oxidative stress investigation in to determine if hindered phenol UHMWPE wear debris has a significant effect on the production of reactive oxygen species and subsequent oxidative stress in PBMNCs.

When considering the previous work conducted using the agarose gel technique, it would be of interest to repeat this work using the 2D agarose gel technique outlined by Green et al. (1998). The major difference between this initial technique and the technique used in the present study is the use of centrifugation of the gel by Green et al. (1998) to produce a superficial layer of UHMWPE wear debris, and therefore a 2D layer culture system. The previous technique demonstrated the stimulation of TNF- α release from PBMNCs at UHMWPE doses as low as 10 μm^3 per cell. The difficulty in using the previous technique with the highly crosslinked, low wearing materials used in this study is being able to accommodate the required doses of UHMWPE wear debris in the smaller wells of the 48 well plates. Given the buoyancy of UHMWPE, it is hypothesised that it would be difficult to concentrate the wear debris through centrifugation while still being able to accurately dose the

wear debris. None the less, it would be of interest to use the original 2D technique at lower particle concentrations to determine any significant TNF- α release from PBMNCs in these conditions.

One area where there is potential for a large body of research is the investigation of the cellular pathways that occur in response to UHMWPE wear debris. Numerous studies, including the present study, have demonstrated the cytokine response from PBMNCs in response to a range of clinical UHMWPE materials (virgin, different resins, highly crosslinked, and antioxidant). However, the cellular mechanisms that occur prior to these cytokine responses are not well understood. Future research in this area should bridge the knowledge gap between the UHMWPE particle being phagocytosed by the macrophage, and the resultant release of cytokines. This would help in the understanding of the osteolysis process and could contribute to further improvements to attenuate this process and increase the longevity of UHMWPE bearings.

Part of this cellular pathway has been demonstrated by Liu (2012) in a previous study, where the author showed both clathrin-mediated endocytosis and caveolae-mediated endocytosis occurred during the uptake of UHMWPE wear particles, however this study was not able to show any specificity of uptake pathways for certain sizes of UHMWPE particles due to issues with separating nano- and micrometre-sized UHMWPE wear particles. It would also be valuable to image the uptake of UHMWPE cells in real time to determine the transport of wear debris once internalised by the cell. This would involve real time confocal imaging as performed in the present study. This could potentially be extended to determine a more precise location of the UHMWPE wear debris in the cell by labelling particular organelles, such as the early endosome, late endosome and lysosome, in addition to determining the proteins associated with these organelles during the phagocytosis of UHMWPE wear debris (Garin et al., 2001, Ip et al., 2010).

This future experiment should include both antioxidant and non-antioxidant UHMWPE wear debris in order to determine the way in which antioxidant compounds such as vitamin E and pentaerythritol tetrakis (hindered phenol) reduce the osteolytic response when incorporated in UHMWPE, as shown in this study. Future work could also investigate the expression of certain genes in response to

UHMWPE wear debris, through determining the mRNA expressed following phagocytosis. This would allow for the investigation into certain cellular pathways and determine their expression following UHMWPE wear debris incubation.

In addition to the investigations into the cellular response to UHMWPE wear debris, future studies could continue to investigate the biological response to UHMWPE in animal models. Previous studies have investigated the bone resorbing potential of UHMWPE particles and sections using microCT-scanning to determine osteolysis following implantation of UHMWPE particles under the skin of the calvarium in a mouse model (Wolf et al., 2006, Bichara et al., 2013). However, to date, no studies have conducted this experiment using clinically relevant UHMWPE wear debris generated using multidirectional wear simulators. The inclusion of clinically relevant wear debris, as used in the present study, would make this experiment a much more clinically relevant model for determining the osteolytic potential of an UHMWPE material. Furthermore, in addition to using microCT analysis to determine osteolysis/osteogenesis in response to UHMWPE wear debris, histological analysis of the particle treated tissue and immunohistochemistry to determine the cytokine response to the wear debris would enable a greater understanding of the biological mechanisms that occur in response to antioxidant UHMWPE wear debris *in vivo*.

6.6 Conclusion

This study determined that vitamin E enhancement had no significant effect on the wear performance of highly UHMWPE, whether crosslinked or non- crosslinked. It was also determined that hindered phenol enhancement had no significant effect on wear under the same parameters. The level of crosslinking was the only factor to affect the wear performance of UHMWPE, with increasing levels of crosslinking producing significantly lower levels of wear from UHMWPE. The addition of antioxidant enhancement with high levels of crosslinking had no significant effect on the wear particle size distribution of UHMWPE.

The study also determined that there was a threshold volume of wear debris required to stimulate significant TNF- α release from PBMNCs. Using wear debris comprised of the whole size range, a minimum volume of 200 μm^3 per cell of GUR1050 highly crosslinked UHMWPE wear debris was required to stimulate significant TNF- α release from PBMNCs.

Using the 3D agarose cell culture technique, wear debris from vitamin E enhanced highly crosslinked UHMWPE was shown to produce significantly lower levels of TNF- α release from PBMNCs compared to wear debris from highly crosslinked UHMWPE. This significant reduction in the TNF- α release compared to highly crosslinked UHMWPE wear debris treated cells was also observed in PBMNCs incubated with debris from hindered phenol enhanced highly crosslinked UHMWPE (AOXTM). These results suggested that the presence of an antioxidant in highly crosslinked UHMWPE reduces the osteolytic response to wear debris. However, the significant TNF- α release in response to UHMWPE wear debris was only observed in PBMNCs from two donors. This therefore requires additional research with multiple responsive donors.

Finally, this study demonstrated that reactive oxygen species production and oxidative stress stimulated in macrophages by highly crosslinked UHMWPE wear debris was significantly reduced when vitamin E was present in the highly crosslinked UHMWPE wear debris. This suggested that the presence of vitamin E had an antioxidant effect on the cells, therefore reducing the levels of reactive oxygen species.

From a clinical point of view, these findings indicate that antioxidant UHMWPE for use in total hip replacements could improve the lifetime of the prosthesis by being low wearing and producing low volumes of wear debris that produce a reduced osteolytic response compared to non-antioxidant UHMWPE.

References

- ABRAHAM, L. J. & KROEGER, K. M. 1999. Impact of the -308 TNF promoter polymorphism on the transcriptional regulation of the TNF gene: relevance to disease. *J Leukoc Biol*, 66, 562-6.
- ABT, B., ALTEKRUSE, M. & BRINCKMANN, P. 1981. [Stress on the articular surface of the hip joint in persons with idiopathic coxarthrosis and healthy adults (author's transl)]. *Z Orthop Ihre Grenzgeb*, 119, 382-6.
- ABU-AMER, Y., DARWECH, I. & CLOHISY, J. C. 2007. Aseptic loosening of total joint replacements: mechanisms underlying osteolysis and potential therapies. *Arthritis Res Ther*, 9 Suppl 1, S6.
- AFFATATO, S., SPINELLI, M., ZAVALLONI, M., MAZZEGA-FABBRO, C. & VICECONTI, M. 2008. Tribology and total hip joint replacement: current concepts in mechanical simulation. *Med Eng Phys*, 30, 1305-17.
- AL-HAJJAR, M., LESLIE, I. J., TIPPER, J., WILLIAMS, S., FISHER, J. & JENNINGS, L. M. 2010. Effect of cup inclination angle during microseparation and rim loading on the wear of BIOLOX(R) delta ceramic-on-ceramic total hip replacement. *J Biomed Mater Res B Appl Biomater*, 95, 263-8.
- AL-MA'ADEED, M. A., AL-QARADAWI, I. Y., MADI, N. & AL-THANI, N. J. 2006. The effect of gamma irradiation and shelf aging in air on the oxidation of ultra-high molecular weight polyethylene. *Applied Surface Science*, 252, 3316.
- ALAM, T. M., CELINA, M., COLLIER, J. P., CURRIER, B. H., CURRIER, J. H., JACKSON, S. K., KUETHE, D. O. & TIMMINS, G. S. 2004. γ -irradiation of ultrahigh-molecular-weight polyethylene: Electron paramagnetic resonance and nuclear magnetic resonance spectroscopy and imaging studies of the mechanism of subsurface oxidation. *J Polym Sci: Part A Polym Chem* 42, 5929-59.
- AMERICAN ACADEMY OF ORTHOPAEDIC SURGEONS 2013. Total Hip Replacement. <http://orthoinfo.aaos.org/topic.cfm?topic=a00377>.
- ANDERSON, L. C. & BLAKE, D. J. 1994. The anatomy and biomechanics of the hip joint. *J Back Musculoskelet Rehabil*, 4, 145-53.
- ARTHRITISUK. 2011-2012. Annual Report. <http://www.arthritisresearchuk.org/about-us/annual-report-and-accounts.aspx>.
- ASPENBERG, P. & HERBERTSSON, P. 1996. Periprosthetic bone resorption. Particles versus movement. *J Bone Joint Surg Br*, 78, 641-6.

- ATHRITISRESEARCHUK 2011.
http://www.arthritisresearchuk.org/research/data_on_arthritis/data_on_oa.aspx.
- ATWOOD, S. A., VAN CITTERS, D. W., FURMANSKI, J., RIES, M. D. & PRUITT, L. A. 2010. Oxidative Stability and Fatigue Behaviour of Below-melt Annealed and Remelted Cross-linked UHMWPE. Transactions of the 56th Orthopaedic Research Society, New Orleans, USA.
- BARBOUR, P. S., STONE, M. H. & FISHER, J. 1999. A study of the wear resistance of three types of clinically applied UHMWPE for total replacement hip prostheses. *Biomaterials*, 20, 2101-6.
- BAXTER, R. M., STEINBECK, M. J., TIPPER, J. L., PARVIZI, J., MARCOLONGO, M. & KURTZ, S. M. 2009. Comparison of periprosthetic tissue digestion methods for ultra-high molecular weight polyethylene wear debris extraction. *J Biomed Mater Res B Appl Biomater*, 91, 409-18.
- BAYKAL, D., SISKEY, R. S., HAIDER, H., SAIKKO, V., AHLROOS, T. & KURTZ, S. M. 2014. Advances in tribological testing of artificial joint biomaterials using multidirectional pin-on-disk testers. *Journal of the mechanical behavior of biomedical materials*, 31, 117-34.
- BHATT, H. & GOSWAMI, T. 2008. Implant wear mechanisms--basic approach. *Biomed Mater*, 3, 042001.
- BHOSALE, A. M. & RICHARDSON, J. B. 2008. Articular cartilage: structure, injuries and review of management. *Br Med Bull*, 87, 77-95.
- BICHARA, D. A., MALCHAU, E., HYLLEHOLT, N., CAKMAK, S. & MURATOGLU, O. K. 2013. Particles from vitamin-E-diffused highly cross-linked UHMWPE induce less osteolysis compared to virgin highly cross-linked UHMWPE in a murine calvarial bone model. Proceedings of the 6th UHMWPE International Meeting - Turin.
- BLADEN, C. L., TERAMURA, S., RUSSELL, S. L., FUJIWARA, K., FISHER, J., INGHAM, E., TOMITA, N. & TIPPER, J. L. 2013a. Analysis of wear, wear particles, and reduced inflammatory potential of vitamin E ultrahigh-molecular-weight polyethylene for use in total joint replacement. *Journal of Biomedical Materials Research Part B: Applied Biomaterials*, 101B, 458-466.
- BLADEN, C. L., TZU-YIN, L., FISHER, J. & TIPPER, J. L. 2013b. In vitro analysis of the cytotoxic and anti-inflammatory effects of antioxidant compounds used as additives in ultra high-molecular weight polyethylene in total joint replacement components. *J Biomed Mater Res B Appl Biomater*, 101, 407-13.

- BOREK, C., ONG, A., MASON, H., DONAHUE, L. & BIAGLOW, J. E. 1986. Selenium and vitamin E inhibit radiogenic and chemically induced transformation in vitro via different mechanisms. *Proc Natl Acad Sci U S A*, 83, 1490-4.
- BOUTIN, P., CHRISTEL, P., DORLOT, J. M., MEUNIER, A., DE ROQUANCOURT, A., BLANQUAERT, D., HERMAN, S., SEDEL, L. & WITVOET, J. 1988. The use of dense alumina-alumina ceramic combination in total hip replacement. *J Biomed Mater Res*, 22, 1203-32.
- BRADFORD, L., BAKER, D. A., GRAHAM, J., CHAWAN, A., RIES, M. D. & PRUITT, L. A. 2004. Wear and surface cracking in early retrieved highly cross-linked polyethylene acetabular liners. *J Bone Joint Surg Am*, 86-A, 1271-82.
- BRAGDON, C. R., O'CONNOR, D. O., LOWENSTEIN, J. D., JASTY, M. & SYNIUTA, W. D. 1996. The importance of multidirectional motion on the wear of polyethylene. *Proc Inst Mech Eng H*, 210, 157-65.
- BROWN, C., WILLIAMS, S., TIPPER, J. L., FISHER, J. & INGHAM, E. 2007. Characterisation of wear particles produced by metal on metal and ceramic on metal hip prostheses under standard and microseparation simulation. *J Mater Sci Mater Med*, 18, 819-27.
- BUCKWALTER, J. A., KUETTNER, K. E. & THONAR, E. N. 1985. Age related changes in articular cartilage proteoglycans: Electromicroscopic studies. *J Orthop Res*, 3, 251-7.
- BUCKWALTER, J. A. & MANKIN, H. J. 1998. Articular cartilage: degeneration and osteoarthritis, repair, regeneration, and transplantation. *Instr Course Lect*, 47, 487-504.
- BUCKWALTER, J. A., MANKIN, H. J. & GRODZINSKY, A. J. 2005. Articular cartilage and osteoarthritis. *Instr Course Lect*, 54, 465-80.
- CAMPBELL, P., EBRAMZADEH, E., NELSON, S., TAKAMURA, K., DE SMET, K. & AMSTUTZ, H. C. 2010. Histological features of pseudotumor-like tissues from metal-on-metal hips. *Clin Orthop Relat Res*, 468, 2321-7.
- CAMPBELL, P., SHEN, F. W. & MCKELLOP, H. 2004. Biologic and tribologic considerations of alternative bearing surfaces. *Clin Orthop Relat Res*, 98-111.
- CHARNLEY, J. 1973. *Arthroplasty of the Hip: A New Operation**. *Clinical Orthopaedics and Related Research*, 95, 4-8.
- CHARNLEY, J. & HALLEY, D. K. 1975. Rate of wear in total hip replacement. *Clin Orthop Relat Res*, 170-9.

- CHIBA, J., RUBASH, H. E., KIM, K. J. & IWAKI, Y. 1994. The characterization of cytokines in the interface tissue obtained from failed cementless total hip arthroplasty with and without femoral osteolysis. *Clin Orthop Relat Res*, 304-12.
- CHO, H. J., WEI, W. J., KAO, H. C. & CHENG, C. K. 2004. Wear behaviour of UHMWPE sliding on artificial hip arthroplasty materials. *Mater, Chem, Phys*, 88, 9-16.
- CLARKE, I. C., GOOD, V., WILLIAMS, P., SCHROEDER, D., ANISSIAN, L., STARK, A., OONISHI, H., SCHULDIES, J. & GUSTAFSON, G. 2000. Ultra-low wear rates for rigid-on-rigid bearings in total hip replacements. *Proc Inst Mech Eng H*, 214, 331-47.
- COSTA, L., BRACCO, P., DEL PREVER, E. B., LUDA, M. P. & TROSSARELLI, L. 2001. Analysis of products diffused into UHMWPE prosthetic components in vivo. *Biomaterials*, 22, 307-15.
- COSTA, L., LUDA, M. P., TROSSARELLI, L., BRACH DEL PREVER, E. M., CROVA, M. & GALLINARO, P. 1998. Oxidation in orthopaedic UHMWPE sterilized by gamma-radiation and ethylene oxide. *Biomaterials*, 19, 659-68.
- CRAWFORD, R. W. & MURRAY, D. W. 1997. Total hip replacement: indications for surgery and risk factors for failure. *Ann Rheum Dis*, 56, 455-7.
- CURRIER, B. H., CURRIER, J. H., COLLIER, J. P., MAYOR, M. B. & VAN CITTERS, D. W. 2010. In vivo oxidation of highly cross-linked UHMWPE bearings. *Transactions of the 55th Orthopaedic Research Society*, New Orleans, USA.
- DANIEL, M., IGLIC, A. & KRALJ-IGLIC, V. 2005. The shape of acetabular cartilage optimizes hip contact stress distribution. *J Anat*, 207, 85-91.
- DE BANDT, M., GROSSIN, M., DRISS, F., PINCEMAIL, J., BABIN-CHEVAYE, C. & PASQUIER, C. 2002. Vitamin E uncouples joint destruction and clinical inflammation in a transgenic mouse model of rheumatoid arthritis. *Arthritis Rheum*, 46, 522-32.
- DEKKER, K., B, B., VAN DER WOODE. L, H., V & BIJLSMA. J, W., J 1992. Pain and Disability in Osteoarthritis: A Review of Biobehavioural Mechanisms. *Journal of Behavioural Medicine*, 15.
- DELAUNAY, C., PETIT, I., LEARMONTH, I. D., OGER, P. & VENDITTOLI, P. A. 2010. Metal-on-metal bearings total hip arthroplasty: The cobalt and chromium ions release concern. *Orthop Traumatol Surg Res*.

- DEVARAJ, S., LI, D. & JIALAL, I. 1996. The effects of alpha tocopherol supplementation on monocyte function. Decreased lipid oxidation, interleukin 1 beta secretion, and monocyte adhesion to endothelium. *J Clin Invest*, 98, 756-63.
- DHAOUADI, T., SFAR, I., ABELMOULA, L., JENDOUBI-AYED, S., AOUBADI, H., BEN ABDELLAH, T., AYED, K., ZOUARI, R. & GORGI, Y. 2007. Role of immune system, apoptosis and angiogenesis in pathogenesis of rheumatoid arthritis and joint destruction, a systematic review. *Tunis Med*, 85, 991-8.
- DIPLOCK, A. T. 1983. The role of vitamin E in biological membranes. *Ciba Found Symp*, 101, 45-55.
- DONALDSON, T., MASSIHI, A., BOWSER, J. & CLARKE, I. 2005. Co-Cr Head Roughness and its Effect on Wear of UHMWPE and XLPE Cups. *Bioceramics and Alternative Bearings in Joint Arthroplasty*. Steinkopff.
- DORR, L. D., WAN, Z., LONGJOHN, D. B., DUBOIS, B. & MURKEN, R. 2000. Total hip arthroplasty with use of the Metasul metal-on-metal articulation. Four to seven-year results. *J Bone Joint Surg Am*, 82, 789-98.
- DORR, L. D., WAN, Z., SHAHRDAR, C., SIRIANNI, L., BOUTARY, M. & YUN, A. 2005. Clinical performance of a Durasul highly cross-linked polyethylene acetabular liner for total hip arthroplasty at five years. *J Bone Joint Surg Am*, 87, 1816-21.
- DRAKE, R. L., VOGL, W. & MITCHELL, A. W. M. 2005. *Regional Anatomy - Transition from Abdomen and Pelvis to Lower Limb*. Grays Anatomy for Students Elsevier.
- DRUMMOND, J. C. & HOOVER, A. A. 1937. Studies on vitamin E (tocopherol). *Biochem J*, 31, 1852-60.
- DUPONT 1997. Synovial plicae of the knee: controversies and review. *CLin Sports Med*, 16, 87-122.
- EMERSON, O. H., EMERSON, G. A. & EVANS, H. M. 1936. The Isolation From Cottonseed Oil Of An Alcohol Resembling Alpha Tocopherol From Wheat Germ Oil. *Science*, 83, 421.
- ENDO, M. M., BARBOUR, P. S., BARTON, D. C., FISHER, J., TIPPER, J. L., INGHAM, E. & STONE, M. H. 2001. Comparative wear and wear debris under three different counterface conditions of crosslinked and non-crosslinked ultra high molecular weight polyethylene. *Biomed Mater Eng*, 11, 23-35.
- FELSON, D. T. & ZHANG, Y. 1998. An update on the epidemiology of knee and hip osteoarthritis with a view to prevention. *Arthritis Rheum*, 41, 1343-55.

- FIGGITT, M., NEWSON, R., LESLIE, I. J., FISHER, J., INGHAM, E. & CASE, C. P. 2010. The genotoxicity of physiological concentrations of chromium (Cr(III) and Cr(VI)) and cobalt (Co(II)): an in vitro study. *Mutat Res*, 688, 53-61.
- FISHER, J. & INGHAM, E. 2004. Wear Debris. *Encyclopedia of Biomaterials and Biomedical Engineering*, 1772 - 1779.
- FOURNIER, C. 2005. Where do T cells stand in rheumatoid arthritis? *Joint Bone Spine*, 72, 527-32.
- FUJITA, K., IWASAKI, M., OCHI, H., FUKUDA, T., MA, C., MIYAMOTO, T., TAKITANI, K., NEGISHI-KOGA, T., SUNAMURA, S., KODAMA, T., TAKAYANAGI, H., TAMAI, H., KATO, S., ARAI, H., SHINOMIYA, K., ITOH, H., OKAWA, A. & TAKEDA, S. 2012. Vitamin E decreases bone mass by stimulating osteoclast fusion. *Nature Medicine*, 18, 589-594.
- GALLO, J., KAMINEK, P., TICHA, V., RIHAKOVA, P. & DITMAR, R. 2002. Particle disease. A comprehensive theory of periprosthetic osteolysis: a review. *Biomed Pap Med Fac Univ Palacky Olomouc Czech Repub*, 146, 21-8.
- GALVIN, A., KANG, L., TIPPER, J., STONE, M., INGHAM, E., JIN, Z. & FISHER, J. 2006. Wear of crosslinked polyethylene under different tribological conditions. *J Mater Sci Mater Med*, 17, 235-43.
- GETGOOD, A., BHULLAR, T. P. S. & RUSHTON, N. 2009. Current concepts in articular cartilage repair. *Orthopaedics and Trauma*, 23, 189-200.
- GUILAK, F. 1995. Compression-induced changes in the shape and volume of the chondrocyte nucleus. *J Biomech*, 28, 1529-41.
- GIJSMAN, P., SMELT, H. J. & SCHUMANN, D. 2010. Hindered amine light stabilizers: An alternative for radiation cross-linked UHMwPE implants. *Biomaterials*, 31, 6685-91.
- GLYN-JONES, S., PANDIT, H., KWON, Y. M., DOLL, H., GILL, H. S. & MURRAY, D. W. 2009. Risk factors for inflammatory pseudotumour formation following hip resurfacing. *J Bone Joint Surg Br*, 91, 1566-74.
- GOMEZ-BARRENA, E., PUERTOLAS, J. A., MUNUERA, L. & KONTTINEN, Y. T. 2008. Update on UHMWPE research: from the bench to the bedside. *Acta Orthop*, 79, 832-40.
- GOMEZ, P. F. & MORCUENDE, J. A. 2005. Early attempts at hip arthroplasty--1700s to 1950s. *Iowa Orthop J*, 25, 25-9.
- GRAY, H. 1918. *Anatomy of the Human Body - Articulation of the Lower Extremity*. www.Bartleby.com/107.
- GREEN, J. M., HALLAB, N. J., LIAO, Y. S., NARAYAN, V. S., SCHWARZ, E. M. & XIE, C. 2013. Anti-oxidation treatment of ultra high molecular weight

polyethylene components to decrease periprosthetic osteolysis: evaluation of osteolytic and osteogenic properties of wear debris particles in a murine calvaria model. *Current Rheumatology Reports*, 15, 325.

GREEN, T. R., FISHER, J., STONE, M., WROBLEWSKI, B. M. & INGHAM, E. 1998. Polyethylene particles of a 'critical size' are necessary for the induction of cytokines by macrophages in vitro. *Biomaterials*, 19, 2297-2302.

GRUPP, T. M., MEISEL, H. J., COTTON, J. A., SCHWIESAU, J., FRITZ, B., BLOMER, W. & JANSSON, V. 2010. Alternative bearing materials for intervertebral disc arthroplasty. *Biomaterials*, 31, 523-31.

HALL, R. M., UNSWORTH, A., WROBLEWSKI, B. M. & BURGESS, I. C. 1994. Frictional characterisation of explanted Charnley hip prostheses. *Wear*, 175, 159.

HART, A. J., BUDDHDEV, P., WINSHIP, P., FARIA, N., POWELL, J. J. & SKINNER, J. A. 2008. Cup inclination angle of greater than 50 degrees increases whole blood concentrations of cobalt and chromium ions after metal-on-metal hip resurfacing. *Hip Int*, 18, 212-9.

HATFIELD, D. L. & GLADYSHEV, V. N. 2009. The Outcome of Selenium and Vitamin E Cancer Prevention Trial (SELECT) reveals the need for better understanding of selenium biology. *Mol Interv*, 9, 18-21.

HAYASE, Y., MUGURUMA, Y. & LEE, M. Y. 1997. Osteoclast development from hematopoietic stem cells: apparent divergence of the osteoclast lineage prior to macrophage commitment. *Exp Hematol*, 25, 19-25.

HILL, K. E., MONTINE, T. J., MOTLEY, A. K., LI, X., MAY, J. M. & BURK, R. F. 2003. Combined deficiency of vitamins E and C causes paralysis and death in guinea pigs. *Am J Clin Nutr*, 77, 1484-8.

HILL, K. E., MOTLEY, A. K., LI, X., MAY, J. M. & BURK, R. F. 2001. Combined selenium and vitamin E deficiency causes fatal myopathy in guinea pigs. *J Nutr*, 131, 1798-802.

HOOTMAN, J., BOLEN, J. & HELMICK, C. 2006. Prevalence of doctor-diagnosed arthritis and arthritis-attributable activity limitation - United States, 2003-2005. *MMWR*, 55, 1089-1092.

HOWIE, D. W. 1990. Tissue response in relation to type of wear particles around failed hip arthroplasties. *J Arthroplasty*, 5, 337-48.

HOWIE, D. W., HAYNES, D. R., ROGERS, S. D., MCGEE, M. A. & PEARCY, M. J. 1993. The response to particulate debris. *Orthop Clin North Am*, 24, 571-81.

HUKKANEN, M., CORBETT, S. A., BATTEN, J., KONTTINEN, Y. T., MCCARTHY, I. D., MACLOUF, J., SANTAVIRTA, S., HUGHES, S. P. &

- POLAK, J. M. 1997. Aseptic loosening of total hip replacement. Macrophage expression of inducible nitric oxide synthase and cyclo-oxygenase-2, together with peroxynitrite formation, as a possible mechanism for early prosthesis failure. *J Bone Joint Surg Br*, 79, 467-74.
- INGHAM, E. & FISHER, J. 2000. Biological reactions to wear debris in total joint replacement. *Proceedings of the Institution of Mechanical Engineers Part H-Journal of Engineering in Medicine*, 214, 21-37.
- INGHAM, E., GREEN, T. R., STONE, M. H., KOWALSKI, R., WATKINS, N. & FISHER, J. 2000. Production of TNF-alpha and bone resorbing activity by macrophages in response to different types of bone cement particles. *Biomaterials*, 21, 1005-13.
- INSTITUTE OF MEDICINE, F. A. N. B. 2000. *Dietary Reference Intakes: Vitamin C, Vitamin E, Selenium, and Carotenoids*. National Academy Press.
- ITO, H., MALONEY, C. M., CROWNINSHIELD, R. D., CLOHISY, J. C., MCDONALD, D. J. & MALONEY, W. J. 2010. In vivo femoral head damage and its effect on polyethylene wear. *J Arthroplasty*, 25, 302-8.
- JACOBS, J. J., SKIPOR, A. K., DOORN, P. F., CAMPBELL, P., SCHMALZRIED, T. P., BLACK, J. & AMSTUTZ, H. C. 1996. Cobalt and chromium concentrations in patients with metal on metal total hip replacements. *Clin Orthop Relat Res*, S256-63.
- JOHNSTONE, B., ALINI, M., CUCCHIARINI, M., DODGE, G. R., EGLIN, D., GUILAK, F., MADRY, H., MATA, A., MAUCK, R. L., SEMINO, C. E. & STODDART, M. J. 2013. Tissue engineering for articular cartilage repair--the state of the art. *Eur Cell Mater*, 25, 248-67.
- JOYCE, T. J. 2010. Wear testing of a DJOA finger prosthesis in vitro. *J Mater Sci Mater Med*, 21, 2337-43.
- JOYCE, T. J. & UNSWORTH, A. 2004. Wear studies of all UHMWPE couples under various bio-tribological conditions. *J Appl Biomater Biomech*, 2, 29-34.
- KANG, L., GALVIN, A. L., BROWN, T. D., FISHER, J. & JIN, Z. M. 2008. Wear simulation of ultra-high molecular weight polyethylene hip implants by incorporating the effects of cross-shear and contact pressure. *Proc Inst Mech Eng H*, 222, 1049-64.
- KARLSON, E. W., MANDL, L. A., AWEH, G. N., SANGHA, O., LIANG, M. H. & GRODSTEIN, F. 2003. Total hip replacement due to osteoarthritis: The importance of age, obesity, and other modifiable risk factors. *American Journal of Medicine*, 114, 93-98.

- KATZER, A., MARQUARDT, H., WESTENDORF, J., WENING, J. V. & VON FOERSTER, G. 2002. Polyetheretherketone--cytotoxicity and mutagenicity in vitro. *Biomaterials*, 23, 1749-59.
- KING, R. N., V. S. ERNSBERGER, C. HANES, M. 2010. Characterization of gamma-irradiated UHMWPE stabilized with a hindered-phenol antioxidant. *Transactions of the 56th Orthopaedic Research Society*, New Orleans, USA.
- KINOV, P., TZONCHEVA, A. & TIVCHEV, P. 2010. Evidence Linking Elevated Oxidative Stress And Aseptic Loosening Of Hip Arthroplasty. *Comptes Rendus De L Academie Bulgare Des Sciences*, 63, 1231-1238.
- KORDUBA, L. A. & WANG, A. 2011. The effect of cross-shear on the wear of virgin and highly-crosslinked polyethylene. *Wear*, 271, 1220-1223.
- KOVAL KJ, Z. J. 2000. Chapter 1 - Anatomy. *Hip Fractures, A practical guide to management*, 1-8.
- KOVAL, K. J. & ZUCKERMAN, J. D. 2000. Anatomy in. "Hip Fractures, A practical guide to management", 1-8.
- KRESS, A. M., SCHMIDT, R., HOLZWARTH, U., FORST, R. & MUELLER, L. A. 2010. Excellent results with cementless total hip arthroplasty and alumina-on-alumina pairing: minimum ten-year follow-up. *Int Orthop*.
- KURTZ, S. M. 2009a. In Vivo Oxidation of UHMWPE in. "UHMWPE Biomaterials Handbook" 2nd Edition, 325-339.
- KURTZ, S. M. 2009b. The origins of UHMWPE in total hip arthroplasty in. "UHMWPE Biomaterials Handbook", 31-41.
- KURTZ, S. M. 2009c. Packaging and Sterilization of UHMWPE in. "UHMWPE Biomaterials Handbook", 21-29.
- KURTZ, S. M. 2009d. A Primer on UHMWPE in. "UHMWPE Biomaterials Handbook" 2nd Edition, 1-6.
- KURTZ, S. M., MURATOGLU, O. K., EVANS, M. & EDIDIN, A. A. 1999. Advances in the processing, sterilization, and crosslinking of ultra-high molecular weight polyethylene for total joint arthroplasty. *Biomaterials*, 20, 1659-88.
- KURTZ, S. M. & ONG, K. 2009. Contemporary total hip arthroplasty: Hard on hard bearings and highly crosslinked UHMWPE in. "UHMWPE Biomaterials Handbook" 2nd Edition, 55-72.
- KWON, Y. M., GLYN-JONES, S., SIMPSON, D. J., KAMALI, A., MCLARDY-SMITH, P., GILL, H. S. & MURRAY, D. W. 2010. Analysis of wear of retrieved

metal-on-metal hip resurfacing implants revised due to pseudotumours. *J Bone Joint Surg Br*, 92, 356-61.

LANGTON, D. J., JAMESON, S. S., JOYCE, T. J., HALLAB, N. J., NATU, S. & NARGOL, A. V. F. 2010. Early failure of metal-on-metal bearings in hip resurfacing and large-diameter total hip replacement: A CONSEQUENCE OF EXCESS WEAR. *J Bone Joint Surg Br*, 92, 38-46.

LAURENT, P. M., GALLARDO, L. A., KUNZE, J. & WIMMER, M. A. 2010. Europium Stearate increases the oxidation resistance of UHMWPE Transactions of the 56th Orthopaedic Research Society, New

Orleans, USA.

LEARMONTH, I. D., YOUNG, C. & RORABECK, C. 2007. The operation of the century: total hip replacement. *Lancet*, 370, 1508-1519.

LI-WEBER, M., GIAISI, M., TREIBER, M. K. & KRAMMER, P. H. 2002. Vitamin E inhibits IL-4 gene expression in peripheral blood T cells. *Eur J Immunol*, 32, 2401-8.

LIU, A. 2012. Determination of the Biological Response and Cellular Uptake Mechanisms of Nanometre-sized UHMWPE Wear Particles from Total Hip Replacements. Ph.D. University of Leeds.

LODISH, H., BURK, A. & ZIPURSKY, S. L. 2000. 12.4. DNA Damage and Repair and Their Role in Carcinogenesis. *Molecular Cell Biology* 4th Edition.

LOMBARDI, A. V., JR., MALLORY, T. H., DENNIS, D. A., KOMISTEK, R. D., FADA, R. A. & NORTHCUT, E. J. 2000. An in vivo determination of total hip arthroplasty pistoning during activity. *J Arthroplasty*, 15, 702-9.

LORENZO, J. A., SOUSA, S. L., FONSECA, J. M., HOCK, J. M. & MEDLOCK, E. S. 1987. Colony-stimulating factors regulate the development of multinucleated osteoclasts from recently replicated cells in vitro. *J Clin Invest*, 80, 160-4.

MACHLIN, L. J., FILIPSKI, R., NELSON, J., HORN, L. R. & BRIN, M. 1977. Effects of a prolonged vitamin E deficiency in the rat. *J Nutr*, 107, 1200-8.

MACPHERSON, G. J. & BREUSCH, S. J. 2010. Metal-on-metal hip resurfacing: a critical review. *Arch Orthop Trauma Surg*.

MALCHAU, H., HERBERTS, P. & AHNFELT, L. 1993. Prognosis of total hip replacement in Sweden. Follow-up of 92,675 operations performed 1978-1990. *Acta Orthop Scand*, 64, 497-506.

MAQUET, P., G, J. 1985. Biomechanics of the Hip. Chapter 1 - Biomechanics of the Hip, 1-2.

MCCARTHY, M., BROWN, T. E. & SALEH, K. J. 2009. Etiology of Hip Arthritis in. "Arthritis & Arthroplasty: The Hip", 3-9.

MCCARTHY M, B. T., SALEH KJ 2009. Chapter 1 - Etiology of Hip Arthritis. Arthritis & Arthroplasty: The Hip, 3-9.

MCDEVITT, C. A. 1973. Biochemistry of articular cartilage. Nature of proteoglycans and collagen of articular cartilage and their role in ageing and in osteoarthritis. Ann Rheum Dis, 32, 364-78.

MCKEE, G. K. & CHEN, S. C. 1973. The statistics of the McKee-Farrar method of total hip replacement. Clin Orthop Relat Res, 26-33.

MCKEE, G. K. & WATSON-FARRAR, J. 1966. Replacement of arthritic hips by the McKee-Farrar prosthesis. J Bone Joint Surg Br, 48, 245-59.

MENDENHALL, S. 2008. Hospital resources and implant cost management - a 2007 update. Orthop Network News, 19, 13-19.

MHRA 2010. Medical Device Alert: ASR™ hip replacement implants manufactured by DePuy International Ltd

MOSELEY, J. B., O'MALLEY, K., PETERSEN, N. J., MENKE, T. J., BRODY, B. A., KUYKENDALL, D. H., HOLLINGSWORTH, J. C., ASHTON, C. M. & WRAY, N. P. 2002. A Controlled Trial of Arthroscopic Surgery for Osteoarthritis of the Knee. New England Journal of Medicine, 347, 81-88.

MULLINS, M. M., NORBURY, W., DOWELL, J. K. & HEYWOOD-WADDINGTON, M. 2007. Thirty-year results of a prospective study of Charnley total hip arthroplasty by the posterior approach. J Arthroplasty, 22, 833-9.

MURATOGLU, O. K. 2009. Highly crosslinked and melted UHMWPE in. "UHMWPE Biomaterials Handbook" 2nd Edition, 197-203.

MURATOGLU, O. K., BRAGDON, C. R., O'CONNOR, D. O., JASTY, M. & HARRIS, W. H. 2001. A novel method of cross-linking ultra-high-molecular-weight polyethylene to improve wear, reduce oxidation, and retain mechanical properties. Recipient of the 1999 HAP Paul Award. J Arthroplasty, 16, 149-60.

MURRAY, D. W. & RUSHTON, N. 1990. Macrophages stimulate bone resorption when they phagocytose particles. J Bone Joint Surg Br, 72, 988-92.

NARAYAN, V. S., KING, R., WARNER, D. & SHARP, M. 2010. Evaluation of antioxidant stabilized UHMWPE materials. Transactions of the 56th Orthopaedic Research Society, New

Orleans, USA.

- NATIONAL JOINT REGISTRY 2013. Patient Characteristics for Hip Revision Procedures in 2013. National Joint Registry 10th Annual Report, 81.
- NEUMANN, D. A. 1999. Joint deformity and dysfunction: a basic review of underlying mechanisms. *Arthritis Care Res*, 12, 139-51.
- NOAMAN, E., ZAHRAN, A. M., KAMAL, A. M. & OMRAN, M. F. 2002. Vitamin E and selenium administration as a modulator of antioxidant defense system: biochemical assessment and modification. *Biol Trace Elem Res*, 86, 55-64.
- ORAL, E., CHRISTENSEN, S. D., MALHI, A. S., WANNOMAE, K. K. & MURATOGLU, O. K. 2006. Wear resistance and mechanical properties of highly cross-linked, ultrahigh-molecular weight polyethylene doped with vitamin E. *J Arthroplasty*, 21, 580-91.
- ORAL, E., GHALI, B. W., NEILS, A. & MURATOGLU, O. K. 2012. A new mechanism of oxidation in ultrahigh molecular weight polyethylene caused by squalene absorption. *J Biomed Mater Res B Appl Biomater*, 100, 742-51.
- ORAL, E., GREENBAUM, E. S., MALHI, A. S., HARRIS, W. H. & MURATOGLU, O. K. 2005. Characterization of irradiated blends of alpha-tocopherol and UHMWPE. *Biomaterials*, 26, 6657-63.
- ORAL, E., WANNOMAE, K. K., HAWKINS, N., HARRIS, W. H. & MURATOGLU, O. K. 2004. [alpha]-Tocopherol-doped irradiated UHMWPE for high fatigue resistance and low wear. *Biomaterials*, 25, 5515.
- ORAL, E., WANNOMAE, K. K., ROWELL, S. L. & MURATOGLU, O. K. 2007. Diffusion of vitamin E in ultra-high molecular weight polyethylene. *Biomaterials*, 28, 5225-37.
- OSTERUD, B. & BJORKKLID, E. 2003. Role of monocytes in atherogenesis. *Physiol Rev*, 83, 1069-112.
- PANDIT, H., GLYN-JONES, S., MCLARDY-SMITH, P., GUNDLE, R., WHITWELL, D., GIBBONS, C. L., OSTLERE, S., ATHANASOU, N., GILL, H. S. & MURRAY, D. W. 2008. Pseudotumours associated with metal-on-metal hip resurfacings. *J Bone Joint Surg Br*, 90, 847-51.
- PARK, D. Y., MIN, B. H., KIM, D. W., SONG, B. R., KIM, M. & KIM, Y. J. 2013. Polyethylene wear particles play a role in development of osteoarthritis via detrimental effects on cartilage, meniscus, and synovium. *Osteoarthritis and Cartilage*.
- PAZZAGLIA, U. E., DELL'ORBO, C. & WILKINSON, M. J. 1987. The foreign body reaction in total hip arthroplasties. A correlated light-microscopy, SEM, and TEM study. *Arch Orthop Trauma Surg*, 106, 209-19.

PELLICCI, P. M., WILSON, P. D., SLEDGE, C. B., SALVATI, E. A., RANAWAT, C. S., POSS, R. & CALLAGHAN, J. J. 1985. Long-Term Results of Revision Total Hip-Replacement - a Follow-up Report. *Journal of Bone and Joint Surgery-American Volume*, 67A, 513-516.

QUINN, P. J. 2004. Is the distribution of alpha-tocopherol in membranes consistent with its putative functions? *Biochemistry (Mosc)*, 69, 58-66.

RAMAKRISHNAN, P., HECHT, B. A., PEDERSEN, D. R., LAVERY, M. R., MAYNARD, J., BUCKWALTER, J. A. & MARTIN, J. A. 2010. Oxidant Conditioning Protects Cartilage from Mechanically Induced Damage. *Journal Of Orthopaedic Research*, 28, 914-920.

REITER, E., JIANG, Q. & CHRISTEN, S. 2007. Anti-inflammatory properties of alpha- and gamma-tocopherol. *Mol Aspects Med*, 28, 668-91.

RICCIARELLI, R., TASINATO, A., CLEMENT, S., OZER, N. K., BOSCOBOINIK, D. & AZZI, A. 1998. alpha-Tocopherol specifically inactivates cellular protein kinase C alpha by changing its phosphorylation state. *Biochem J*, 334 (Pt 1), 243-9.

RICCIARELLI, R., ZINGG, J. M. & AZZI, A. 2000. Vitamin E reduces the uptake of oxidized LDL by inhibiting CD36 scavenger receptor expression in cultured aortic smooth muscle cells. *Circulation*, 102, 82-7.

ROCKWOOD, C. A., JR. & WIRTH, M. A. 2002. Observation on retrieved Hylamer glenoids in shoulder arthroplasty: problems associated with sterilization by gamma irradiation in air. *J Shoulder Elbow Surg*, 11, 191-7.

ROGERS, M., BLOM, A. W., BARNETT, A., KARANTANA, A. & BANNISTER, G. C. 2009. Revision for recurrent dislocation of Total Hip Replacement. *Hip International*, 19, 109-113.

ROSE, R. M., CIMINO, W. R., ELLIS, E. & CRUGNOLA, A. N. 1982. Exploratory investigations on the structure dependence of the wear resistance of polyethylene. *Wear*, 77, 89-104.

ROWELL, S. L., YABANNAVAR, P. & MURATOGLU, O. K. 2010. Oxidative stability of simulator tested acetabular liners after 7 years shelf-aging in air. *Transactions of the 56th Orthopaedic Research Society*, New

Orleans, USA.

SABOKBAR, A., FUJIKAWA, Y., NEALE, S., MURRAY, D. W. & ATHANASOU, N. A. 1997. Human arthroplasty derived macrophages differentiate into osteoclastic bone resorbing cells. *Annals Of The Rheumatic Diseases*, 56, 414-420.

- SAITO, S., ISHII, T., MORI, S., HOSAKA, K., OOTAKI, M. & TOKUHASHI, Y. 2010. Long-term results of metal-on-metal total hip arthroplasty. *Orthopedics*, 33.
- SANTAVIRTA, S., BOHLER, M., HARRIS, W. H., KONTTINEN, Y. T., LAPPALAINEN, R., MURATOGLU, O., RIEKER, C. & SALZER, M. 2003. Alternative materials to improve total hip replacement tribology. *Acta Orthop Scand*, 74, 380-8.
- SCHEINECKER, C., MARC, C. H., MD, MPH, ALAN, J. S., MD, FRCP, JOSEF, S. S., MD, MICHAEL, E. W., MD, MICHAEL, H. W. & MD 2009. *The Role of T Cells in Rheumatoid Arthritis*. Philadelphia: Mosby.
- SCHNEIDER, C. 2005. Chemistry and biology of vitamin E. *Mol Nutr Food Res*, 49, 7-30.
- SCHOLES, S. C., INMAN, I. A., UNSWORTH, A. & JONES, E. 2008. Tribological assessment of a flexible carbon-fibre-reinforced poly(ether-ether-ketone) acetabular cup articulating against an alumina femoral head. *Proc Inst Mech Eng H*, 222, 273-83.
- SCHOLES, S. C. & UNSWORTH, A. 2006. The effects of proteins on the friction and lubrication of artificial joints. *Proc Inst Mech Eng H*, 220, 687-93.
- SCHOLES, S. C., UNSWORTH, A. & GOLDSMITH, A. A. 2000. A frictional study of total hip joint replacements. *Phys Med Biol*, 45, 3721-35.
- SCHWARZ, E., BUKATA S, V., BENZ, E., ROSIER, R. N., PUZAS, J. E. & O'KEEFE, R., J. 1999. NF κ B and TNF- α are stimulated by titanium particles and are essential for in vivo bone resorption. In *Proceedings of the 45th annual Meeting of the Orthopaedic Research Society*, p305.
- SEED, S. M., DUNICAN, K. C. & LYNCH, A. M. 2009. Osteoarthritis: a review of treatment options. *Geriatrics*, 64, 20-9.
- SHEPPARD, A. J., PENNINGTON, J. A. & WEIHRAUCH, J. L. 1993. Analysis and distribution of vitamin E in vegetable oils and foods. *Vitamin E in health and disease*, 9-31.
- SHIH, J. C., JONAS, R. H. & SCOTT, M. L. 1977. Oxidative deterioration of the muscle proteins during nutritional muscular dystrophy in chicks. *J Nutr*, 107, 1786-91.
- SIEBER, H. P., RIEKER, C. B. & KOTTIG, P. 1999. Analysis of 118 second-generation metal-on-metal retrieved hip implants. *J Bone Joint Surg Br*, 81, 46-50.

- SOBIERAJ, M. C. & RIMNAC, C. M. 2009. Ultra high molecular weight polyethylene: mechanics, morphology, and clinical behavior. *J Mech Behav Biomed Mater*, 2, 433-43.
- SUTULA, L. C., COLLIER, J. P., SAUM, K. A., CURRIER, B. H., CURRIER, J. H., SANFORD, W. M., MAYOR, M. B., WOODING, R. E., SPERLING, D. K., WILLIAMS, I. R. & ET AL. 1995. The Otto Aufranc Award. Impact of gamma sterilization on clinical performance of polyethylene in the hip. *Clin Orthop Relat Res*, 28-40.
- TAI, Z., CHEN, Y., AN, Y., YAN, X. & XUE, Q. 2012. Tribological Behavior of UHMWPE Reinforced with Graphene Oxide Nanosheets. *Tribology Letters*, 46, 55-63.
- TATEIWA, T., CLARKE, I. C., WILLIAMS, P. A., GARINO, J., MANAKA, M., SHISHIDO, T., YAMAMOTO, K. & IMAKIIRE, A. 2008. Ceramic total hip arthroplasty in the United States: safety and risk issues revisited. *Am J Orthop (Belle Mead NJ)*, 37, E26-31.
- TERAMURA, S., RUSSEL, S., INGHAM, E., FISHER, J., TOMITA, N., FUJIWARA, K. & TIPPER, J. 2009. Reduced Biological Response to Wear Particles from UHMWPE containing Vitamin E.
- TERAMURA, S., SAKODA, H., TERAOKA, T., ENDO, M. M., FUJIWARA, K. & TOMITA, N. 2008. Reduction of wear volume from ultrahigh molecular weight polyethylene knee components by the addition of vitamin E. *J Orthop Res*, 26, 460-4.
- TIPPER, J. L., GALVIN, A. L., WILLIAMS, S., MCEWEN, H. M., STONE, M. H., INGHAM, E. & FISHER, J. 2006. Isolation and characterization of UHMWPE wear particles down to ten nanometers in size from in vitro hip and knee joint simulators. *J Biomed Mater Res A*, 78, 473-80.
- TIPPER, J. L., HATTON, A., NEVELOS, J. E., INGHAM, E., DOYLE, C., STREICHER, R., NEVELOS, A. B. & FISHER, J. 2002. Alumina-alumina artificial hip joints. Part II: characterisation of the wear debris from in vitro hip joint simulations. *Biomaterials*, 23, 3441-8.
- TIPPER, J. L., INGHAM, E., HAILEY, J. L., BESONG, A. A., FISHER, J., WROBLEWSKI, B. M. & STONE, M. H. 2000. Quantitative analysis of polyethylene wear debris, wear rate and head damage in retrieved Charnley hip prostheses. *J Mater Sci Mater Med*, 11, 117-24.
- TIPPER, J. L., INGHAM, E., JIN, Z. M. & FISHER, J. 2005. The science of metal-on-metal articulation. *Current Orthopaedics*, 19, 280-287.

- TIPPER, J. L., LIU, T.-Y. & BLADEN, C. L. 2011. Cytotoxicity of Anti-Oxidant Compounds in Human Macrophages Transactions of the 57th Orthopaedic Research Society, California, USA.
- TOLEDO-PEREYRA, L. H. 2004. John Charnley--father of modern total hip replacement. *J Invest Surg*, 17, 299-301.
- TOWHEED, T. E. & HOCHBERG, M. C. 1996. Health-related quality of life after total hip replacement. *Semin Arthritis Rheum*, 26, 483-91.
- TREUHAFT, P. S. & MCCARTY, D. J. 1971. Synovial fluid pH, lactate, oxygen and carbon dioxide partial pressure in various joint diseases. *Arthritis Rheum*, 14, 475-84.
- TURELL, M., WANG, A. & BELLARE, A. 2003. Quantification of the effect of cross-path motion on the wear rate of ultra-high molecular weight polyethylene. *Wear*, 255, 1034-1039.
- UTZSCHNEIDER, S., BECKER, F., GRUPP, T. M., SIEVERS, B., PAULUS, A., GOTTSCHALK, O. & JANSSON, V. 2010. Inflammatory response against different carbon fiber-reinforced PEEK wear particles compared with UHMWPE in vivo. *Acta Biomater*, 6, 4296-304.
- VISURI, T., PUKKALA, E., PAAVOLAINEN, P., PULKKINEN, P. & RISKKA, E. B. 1996. Cancer risk after metal on metal and polyethylene on metal total hip arthroplasty. *Clin Orthop Relat Res*, S280-9.
- VISURI, T. I., PUKKALA, E., PULKKINEN, P. & PAAVOLAINEN, P. 2006. Cancer incidence and causes of death among total hip replacement patients: a review based on Nordic cohorts with a special emphasis on metal-on-metal bearings. *Proc Inst Mech Eng H*, 220, 399-407.
- WALKER, P. S., BLUNN, G. W. & LILLEY, P. A. 1996. Wear testing of materials and surfaces for total knee replacement. *J Biomed Mater Res*, 33, 159-75.
- WANG, A. 2006. Wear, oxidation and mechanical properties of a sequentially irradiated and annealed UHMWPE in total joint replacement. *Journal of Physics D: Applied Physics*, 39, 3213.
- WANG, A., POLINENI, V. K., ESSNER, A., SOKOL, M., SUN, D. C., STARK, C. & DUMBLETON, J. H. 1997. The significance of nonlinear motion in the wear screening of orthopaedic implant materials. *American Society for Testing and Materials*, 2, 239-245.
- WANNOMAE, K. K., CHRISTENSEN, S. D., MICHELI, B. R., ROWELL, S. L., SCHROEDER, D. W. & MURATOGLU, O. K. 2010. Delamination and adhesive wear behavior of alpha-tocopherol-stabilized irradiated ultrahigh-molecular-weight polyethylene. *J Arthroplasty*, 25, 635-43.

- WEBER, B. G. 1996. Experience with the Metasul total hip bearing system. *Clin Orthop Relat Res*, S69-77.
- WILES, P. 1957. The surgery of the osteoarthritic hip. *Br J Surg*, 45, 488-97.
- WILLMANN, G. 1996. Development in medical-grade alumina during the past two decades. *Journal of Materials Processing Technology*, 56, 168.
- WINTER, M., GRISS, P., SCHELLER, G. & MOSER, T. 1992. Ten- to 14-year results of a ceramic hip prosthesis. *Clin Orthop Relat Res*, 73-80.
- WOLF, C., LEDERER, K., PFRAGNER, R., SCHAUENSTEIN, K., INGOLIC, E. & SIEGL, V. 2007. Biocompatibility of ultra-high molecular weight polyethylene (UHMW-PE) stabilized with alpha-tocopherol used for joint endoprostheses assessed in vitro. *J Mater Sci Mater Med*, 18, 1247-52.
- WROBLEWSKI, B. M., SINEY, P. D. & FLEMING, P. A. 2005. Low-friction arthroplasty of the hip using alumina ceramic and cross-linked polyethylene. A 17-year follow-up report. *J Bone Joint Surg Br*, 87, 1220-1.
- YAMAMOTO, K., CLARKE, I. C., MASAOKA, T., OONISHI, H., WILLIAMS, P. A., GOOD, V. D. & IMAKIIRE, A. 2001. Microwear phenomena of ultrahigh molecular weight polyethylene cups and debris morphology related to gamma radiation dose in simulator study. *J Biomed Mater Res*, 56, 65-73.
- YAMAMOTO, K., IMAKIIRE, A., MASAOKA, T., SHISHIDO, T., MIZOUE, T., CLARKE, I. C., SHOJI, H., KAWANABE, K. & TAMURA, J. 2003. Wear mode and wear mechanism of retrieved acetabular cups. *Int Orthop*, 27, 286-90.
- YUB, S. & DENISOV, E. T. 1974. Mechanism of the inhibiting activity of iminoxyl radicals during oxidation of polypropylene and polyethylene. *Vysokomol Soyed*, A14, 2313-2316.
- ZHANG, C., TANG, T., REN, W., ZHANG, X. & DAI, K. 2008. Influence of mouse genetic background on wear particle-induced in vivo inflammatory osteolysis. *Inflamm Res*, 57, 211-5.
- ABU-AMER, Y., DARWECH, I. & CLOHISY, J. C. 2007. Aseptic loosening of total joint replacements: mechanisms underlying osteolysis and potential therapies. *Arthritis Res Ther*, 9 Suppl 1, S6.
- AFFATATO, S., SPINELLI, M., ZAVALLONI, M., MAZZEGA-FABBRO, C. & VICECONTI, M. 2008. Tribology and total hip joint replacement: current concepts in mechanical simulation. *Med Eng Phys*, 30, 1305-17.

- AFFATATO, S., BRACCO, P., COSTA, L., VILLA, T., QUAGLINI, V. & TONI, A. 2012. In vitro wear performance of standard, crosslinked, and vitamin-E-blended UHMWPE. *J Biomed Mater Res A*, 100, 554-60.
- AL-HAJJAR, M., LESLIE, I. J., TIPPER, J., WILLIAMS, S., FISHER, J. & JENNINGS, L. M. 2010. Effect of cup inclination angle during microseparation and rim loading on the wear of BIOLOX(R) delta ceramic-on-ceramic total hip replacement. *J Biomed Mater Res B Appl Biomater*, 95, 263-8.
- AL-MA'ADEED, M. A., AL-QARADAWI, I. Y., MADI, N. & AL-THANI, N. J. 2006. The effect of gamma irradiation and shelf aging in air on the oxidation of ultra-high molecular weight polyethylene. *Applied Surface Science*, 252, 3316.
- ALAM, T. M., CELINA, M., COLLIER, J. P., CURRIER, B. H., CURRIER, J. H., JACKSON, S. K., KUETHE, D. O. & TIMMINS, G. S. 2004. γ -irradiation of ultrahigh-molecular-weight polyethylene: Electron paramagnetic resonance and nuclear magnetic resonance spectroscopy and imaging studies of the mechanism of subsurface oxidation. *J Polym Sci: Part A Polym Chem* 42, 5929-59.
- AMERICAN ACADEMY OF ORTHOPAEDIC SURGEONS 2013. Total Hip Replacement. <http://orthoinfo.aaos.org/topic.cfm?topic=a00377>.
- ANDERSON, L. C. & BLAKE, D. J. 1994. The anatomy and biomechanics of the hip joint. *J Back Musculoskelet Rehabil*, 4, 145-53. ARTHRITISUK. 2011-2012. Annual Report. <http://www.arthritisresearchuk.org/about-us/annual-report-and-accounts.aspx>.
- AMSTUTZ, H. C., CAMPBELL, P., KOSSOVSKY, N. & CLARKE, I. C. 1992. Mechanism and clinical significance of wear debris-induced osteolysis. *Clin Orthop Relat Res*, 7-18.
- ASPENBERG, P. & HERBERTSSON, P. 1996. Periprosthetic bone resorption. Particles versus movement. *J Bone Joint Surg Br*, 78, 641-6.
- ARTHRITIS RESEARCH UK 2011. http://www.arthritisresearchuk.org/research/data_on_arthritis/data_on_oa.aspx.
- ATWOOD, S. A., VAN CITTERS, D. W., FURMANSKI, J., RIES, M. D. & PRUITT, L. A. 2010. Oxidative Stability and Fatigue Behaviour of Below-melt Annealed and Remelted Cross-linked UHMWPE. Transactions of the 56th Orthopaedic Research Society, New Orleans, USA.
- BABIOR, B. M. 2000. Phagocytes and oxidative stress. *The American Journal of Medicine*, 109, 33-44.
- BAKER, D. A., BELLARE, A. & PRUITT, L. 2003. The effects of degree of crosslinking on the fatigue crack initiation and propagation resistance of orthopedic-grade polyethylene. *J Biomed Mater Res A*, 66, 146-54.

- BALABAN, R. S., NEMOTO, S. & FINKEL, T. 2005. Mitochondria, oxidants, and aging. *Cell*, 120, 483-95.
- BAXTER, R. M., STEINBECK, M. J., TIPPER, J. L., PARVIZI, J., MARCOLONGO, M. & KURTZ, S. M. 2009. Comparison of periprosthetic tissue digestion methods for ultra-high molecular weight polyethylene wear debris extraction. *J Biomed Mater Res B Appl Biomater*, 91, 409-18.
- BERTOLINI, D. R., NEDWIN, G. E., BRINGMAN, T. S., SMITH, D. D. & MUNDY, G. R. 1986. Stimulation of bone resorption and inhibition of bone formation in vitro by human tumour necrosis factors. *Nature*, 319, 516-8.
- BHATT, H. & GOSWAMI, T. 2008. Implant wear mechanisms--basic approach. *Biomed Mater*, 3, 042001.
- BHATTACHARYA, A. & MISRA, B. N. 2004. Grafting: a versatile means to modify polymers: Techniques, factors and applications. *Progress in Polymer Science*, 29, 767-814.
- BHOSALE, A. M. & RICHARDSON, J. B. 2008. Articular cartilage: structure, injuries and review of management. *Br Med Bull*, 87, 77-95.
- BICHARA, D. A., MALCHAU, E., HYLLEHOLT, N., CAKMAK, S. & MURATOGLU, O. K. 2013. Particles from vitamin-E-diffused highly cross-linked UHMWPE induce less osteolysis compared to virgin highly cross-linked UHMWPE in a murine calvarial bone model. *Proceedings of the 6th UHMWPE International Meeting - Turin*.
- BIOMET, C. A. 2011. <http://www.nomagicjusttechnology.com/biolox-delta.html>.
- BLADEN, C. L., FISHER, J., INGHAM, E. & TIPPER, J. 2011. The anti-inflammatory properties of Vitamin E significantly reduce TNF- α release from primary human monocytes after stimulation with UHMWPE wear particles. *Transactions of the 57th Orthopaedic Research Society, California, USA*.
- BLADEN, C. L., TERAMURA, S., RUSSELL, S. L., FUJIWARA, K., FISHER, J., INGHAM, E., TOMITA, N. & TIPPER, J. L. 2013. Analysis of wear, wear particles, and reduced inflammatory potential of vitamin E ultrahigh-molecular-weight polyethylene for use in total joint replacement. *Journal of Biomedical Materials Research Part B: Applied Biomaterials*, 101B, 458-466.
- BLADEN, C. L., BROWN, C., FISHER, J., INGHAM, E. & TIPPER, J. 2010. Oxidative Stress in Primary Human Monocytes Due to Exposure to Clinically Relevant UHMWPE and CoCr Wear Particles. *56th Annual Meeting of the Orthopaedic Research Society, New Orleans, USA*

- BOREK, C., ONG, A., MASON, H., DONAHUE, L. & BIAGLOW, J. E. 1986. Selenium and vitamin E inhibit radiogenic and chemically induced transformation in vitro via different mechanisms. *Proc Natl Acad Sci U S A*, 83, 1490-4.
- BOUTIN, P., CHRISTEL, P., DORLOT, J. M., MEUNIER, A., DE ROQUANCOURT, A., BLANQUAERT, D., HERMAN, S., SEDEL, L. & WITVOET, J. 1988. The use of dense alumina-alumina ceramic combination in total hip replacement. *J Biomed Mater Res*, 22, 1203-32.
- BOVERIS, A. & CHANCE, B. 1973. The mitochondrial generation of hydrogen peroxide. General properties and effect of hyperbaric oxygen. *Biochem J*, 134, 707-16.
- BRADFORD, L., BAKER, D. A., GRAHAM, J., CHAWAN, A., RIES, M. D. & PRUITT, L. A. 2004. Wear and surface cracking in early retrieved highly cross-linked polyethylene acetabular liners. *J Bone Joint Surg Am*, 86-A, 1271-82.
- BRAGDON, C. R., O'CONNOR, D. O., LOWENSTEIN, J. D., JASTY, M. & SYNIUTA, W. D. 1996. The importance of multidirectional motion on the wear of polyethylene. *Proc Inst Mech Eng H*, 210, 157-65.
- BROWN, C., WILLIAMS, S., TIPPER, J. L., FISHER, J. & INGHAM, E. 2007. Characterisation of wear particles produced by metal on metal and ceramic on metal hip prostheses under standard and microseparation simulation. *J Mater Sci Mater Med*
- BUCKWALTER, J. A., KUETTNER, K. E. & THONAR, E. N. 1985. Age related changes in articular cartilage proteoglycans: Electromicroscopic studies. *J Orthop Res*, 3, 251-7.
- BUCKWALTER, J. A. & MANKIN, H. J. 1998. Articular cartilage: degeneration and osteoarthritis, repair, regeneration, and transplantation. *Instr Course Lect*, 47, 487-504.
- BUCKWALTER, J. A., MANKIN, H. J. & GRODZINSKY, A. J. 2005. Articular cartilage and osteoarthritis. *Instr Course Lect*, 54, 465-80.
- CAMPBELL, P., EBRAMZADEH, E., NELSON, S., TAKAMURA, K., DE SMET, K. & AMSTUTZ, H. C. 2010. Histological features of pseudotumor-like tissues from metal-on-metal hips. *Clin Orthop Relat Res*, 468, 2321-7.
- CAMPBELL, P., SHEN, F. W. & MCKELLOP, H. 2004. Biologic and tribologic considerations of alternative bearing surfaces. *Clin Orthop Relat Res*, 98-111.
- CERUTTI, P., GHOSH, R., OYA, Y. & AMSTAD, P. 1994. The role of the cellular antioxidant defense in oxidant carcinogenesis. *Environ Health Perspect*, 102 Suppl 10, 123-9.

- CHARNLEY, J. 1973. Arthroplasty of the Hip: A New Operation*. *Clinical Orthopaedics and Related Research*, 95, 4-8.
- CHARNLEY, J. & HALLEY, D. K. 1975. Rate of wear in total hip replacement. *Clin Orthop Relat Res*, 170-9.
- CHIBA, J., RUBASH, H. E., KIM, K. J. & IWAKI, Y. 1994. The characterization of cytokines in the interface tissue obtained from failed cementless total hip arthroplasty with and without femoral osteolysis. *Clin Orthop Relat Res*, 304-12
- CHIESA, R., TANZI, M. C., ALFONSI, S., PARACCHINI, L., MOSCATELLI, M. & CIGADA, A. 2000. Enhanced wear performance of highly crosslinked UHMWPE for artificial joints. *J Biomed Mater Res*, 50, 381-7..
- CHO, H. J., WEI, W. J., KAO, H. C. & CHENG, C. K. 2004. Wear behaviour of UHMWPE sliding on artificial hip arthroplasty materials. *Mater, Chem, Phys*, 88, 9-16.
- CLARKE, I. C., GOOD, V., WILLIAMS, P., SCHROEDER, D., ANISSIAN, L., STARK, A., OONISHI, H., SCHULDIES, J. & GUSTAFSON, G. 2000. Ultra-low wear rates for rigid-on-rigid bearings in total hip replacements. *Proc Inst Mech Eng H*, 214, 331-47.
- COSTA, L., BRACCO, P., DEL PREVER, E. B., LUDA, M. P. & TROSSARELLI, L. 2001. Analysis of products diffused into UHMWPE prosthetic components in vivo. *Biomaterials*, 22, 307-15.
- COSTA, L., LUDA, M. P., TROSSARELLI, L., BRACH DEL PREVER, E. M., CROVA, M. & GALLINARO, P. 1998. Oxidation in orthopaedic UHMWPE sterilized by gamma-radiation and ethylene oxide. *Biomaterials*, 19, 659-68.
- CRAWFORD, R. W. & MURRAY, D. W. 1997. Total hip replacement: indications for surgery and risk factors for failure. *Ann Rheum Dis*, 56, 455-7.
- CURRIER, B. H., CURRIER, J. H., COLLIER, J. P., MAYOR, M. B. & VAN CITTERS, D. W. 2010. In vivo oxidation of highly cross-linked UHMWPE bearings. *Transactions of the 55th Orthopaedic Research Society, New Orleans, USA.*
- DE BANDT, M., GROSSIN, M., DRISS, F., PINCEMAIL, J., BABIN-CHEVAYE, C. & PASQUIER, C. 2002. Vitamin E uncouples joint destruction and clinical inflammation in a transgenic mouse model of rheumatoid arthritis. *Arthritis Rheum*, 46, 522-32.
- DEKKER, K., B, B., VAN DER WOODE. L, H., V & BIJLSMA. J, W., J 1992. Pain and Disability in Osteoarthritis: A Review of Biobehavioural Mechanisms. *Journal of Behavioural Medicine*, 15.

- DELAUNAY, C., PETIT, I., LEARMONTH, I. D., OGER, P. & VENDITTOLI, P. A. 2010. Metal-on-metal bearings total hip arthroplasty: The cobalt and chromium ions release concern. *Orthop Traumatol Surg Res*.
- DELAUNAY, C. P., BONNOMET, F., CLAVERT, P., LAFFARGUE, P. & MIGAUD, H. 2008. THA using metal-on-metal articulation in active patients younger than 50 years. *Clin Orthop Relat Res*, 466, 340-6.
- DEVARAJ, S., LI, D. & JIALAL, I. 1996. The effects of alpha tocopherol supplementation on monocyte function. Decreased lipid oxidation, interleukin 1 beta secretion, and monocyte adhesion to endothelium. *J Clin Invest*, 98, 756-63.
- DHAOUADI, T., SFAR, I., ABELMOULA, L., JENDOUBI-AYED, S., AOUADI, H., BEN ABDELLAH, T., AYED, K., ZOUARI, R. & GORGI, Y. 2007. Role of immune system, apoptosis and angiogenesis in pathogenesis of rheumatoid arthritis and joint destruction, a systematic review. *Tunis Med*, 85, 991-8.
- DIPLOCK, A. T. 1983. The role of vitamin E in biological membranes. *Ciba Found Symp*, 101, 45-55.
- DONALDSON, T., MASSIHI, A., BOWSHER, J. & CLARKE, I. 2005. Co-Cr Head Roughness and its Effect on Wear of UHMWPE and XLPE Cups. *Bioceramics and Alternative Bearings in Joint Arthroplasty*. Steinkopff.
- DORR, L. D., WAN, Z., LONGJOHN, D. B., DUBOIS, B. & MURKEN, R. 2000. Total hip arthroplasty with use of the Metasul metal-on-metal articulation. Four to seven-year results. *J Bone Joint Surg Am*, 82, 789-98.
- DORR, L. D., WAN, Z., SHAHRDAR, C., SIRIANNI, L., BOUTARY, M. & YUN, A. 2005. Clinical performance of a Durasul highly cross-linked polyethylene acetabular liner for total hip arthroplasty at five years. *J Bone Joint Surg Am*, 87, 1816-21.
- DRAKE, R. L., VOGL, W. & MITCHELL, A. W. M. 2005. *Regional Anatomy - Transition from Abdomen and Pelvis to Lower Limb*. Grays Anatomy for Students Elsevier.
- DRUMMOND, J. C. & HOOVER, A. A. 1937. Studies on vitamin E (tocopherol). *Biochem J*, 31, 1852-60.
- DUPONT 1997. Synovial plicae of the knee: controversies and review. *CLin Sports Med*, 16, 87-122.
- EBERHARDT, A., W., MCKEE, R., T., CUCKLER, J., M., PETERSON, D., W., BECK, P., R. & LEMONS, J., E. 2009. Surface Roughness of CoCr and ZrO2 Femoral Heads with Metal Transfer: A Retrieval and Wear Simulator Study. *International Journal of Biomaterials*, 2009.

- EMERSON, O. H., EMERSON, G. A. & EVANS, H. M. 1936. The Isolation From Cottonseed Oil Of An Alcohol Resembling Alpha Tocopherol From Wheat Germ Oil. *Science*, 83, 421.
- ENDO, M. M., BARBOUR, P. S., BARTON, D. C., FISHER, J., TIPPER, J. L., INGHAM, E. & STONE, M. H. 2001. Comparative wear and wear debris under three different counterface conditions of crosslinked and non-crosslinked ultra high molecular weight polyethylene. *Biomed Mater Eng*, 11, 23-35.
- ENDO, M., TIPPER, J. L., BARTON, D. C., STONE, M. H., INGHAM, E. & FISHER, J. 2002. Comparison of wear, wear debris and functional biological activity of moderately crosslinked and non-crosslinked polyethylenes in hip prostheses. *Proc Inst Mech Eng H*, 216, 111-22.
- FELSON, D. T. & ZHANG, Y. 1998. An update on the epidemiology of knee and hip osteoarthritis with a view to prevention. *Arthritis Rheum*, 41, 1343-55.
- FERRONI, D. & QUAGLINI, V. 2010. Thermal stabilization of highly crosslinked UHMWPE: a comparative study between annealed and remelted resins. *J Appl Biomater Biomech*, 8, 82-8.
- FIGGITT, M., NEWSON, R., LESLIE, I. J., FISHER, J., INGHAM, E. & CASE, C. P. 2010. The genotoxicity of physiological concentrations of chromium (Cr(III) and Cr(VI)) and cobalt (Co(II)): an in vitro study. *Mutat Res*, 688, 53-61.
- FISHER, J. & INGHAM, E. 2004. Wear Debris. *Encyclopedia of Biomaterials and Biomedical Engineering*, 1772 - 1779.
- FLEURY, C., PETIT, A., MWALE, F., ANTONIOU, J., ZUKOR, D. J., TABRIZIAN, M. & HUK, O. L. 2006. Effect of cobalt and chromium ions on human MG-63 osteoblasts in vitro: Morphology, cytotoxicity, and oxidative stress. *Biomaterials*, 27, 3351-3360.
- FOURNIER, C. 2005. Where do T cells stand in rheumatoid arthritis? *Joint Bone Spine*, 72, 527-32.
- FUJITA, K., IWASAKI, M., OCHI, H., FUKUDA, T., MA, C., MIYAMOTO, T., TAKITANI, K., NEGISHI-KOGA, T., SUNAMURA, S., KODAMA, T., TAKAYANAGI, H., TAMAI, H., KATO, S., ARAI, H., SHINOMIYA, K., ITOH, H., OKAWA, A. & TAKEDA, S. 2012. Vitamin E decreases bone mass by stimulating osteoclast fusion. *Nature Medicine*, 18, 589-594.
- GALLO, J., KAMINEK, P., TICHA, V., RIHAKOVA, P. & DITMAR, R. 2002. Particle disease. A comprehensive theory of periprosthetic osteolysis: a review. *Biomed Pap Med Fac Univ Palacky Olomouc Czech Repub*, 146, 21-8.

- GALVIN, A., KANG, L., TIPPER, J., STONE, M., INGHAM, E., JIN, Z. & FISHER, J. 2006. Wear of crosslinked polyethylene under different tribological conditions. *J Mater Sci Mater Med*, 17, 235-43.
- GALVIN, A. 2003. Interactive Influences of Crosslinking, Counterface Roughness and Kinematics on the Wear of Crosslinked UHMWPE. Ph.D. University of Leeds.
- GARIN, J., DIEZ, R., KIEFFER, S., DERMINE, J. F., DUCLOS, S., GAGNON, E., SADOUL, R., RONDEAU, C. & DESJARDINS, M. 2001. The phagosome proteome: insight into phagosome functions. *J Cell Biol*, 152, 165-80.
- GETGOOD, A., BHULLAR, T. P. S. & RUSHTON, N. 2009. Current concepts in articular cartilage repair. *Orthopaedics and Trauma*, 23, 189-200.
- GIJSMAN, P., SMELT, H. J. & SCHUMANN, D. 2010. Hindered amine light stabilizers: An alternative for radiation cross-linked UHMwPE implants. *Biomaterials*, 31, 6685-91.
- GLYN-JONES, S., PANDIT, H., KWON, Y. M., DOLL, H., GILL, H. S. & MURRAY, D. W. 2009. Risk factors for inflammatory pseudotumour formation following hip resurfacing. *J Bone Joint Surg Br*, 91, 1566-74.
- GOMEZ-BARRENA, E., PUERTOLAS, J. A., MUNUERA, L. & KONTTINEN, Y. T. 2008. Update on UHMWPE research: from the bench to the bedside. *Acta Orthop*, 79, 832-40.
- GOMEZ, P. F. & MORCUENDE, J. A. 2005. Early attempts at hip arthroplasty--1700s to 1950s. *Iowa Orthop J*, 25, 25-9.
- GRAY, H. 1918. *Anatomy of the Human Body - Articulation of the Lower Extremity*. www.Bartleby.com/107.
- GREEN, J. M., HALLAB, N. J., LIAO, Y. S., NARAYAN, V. S., SCHWARZ, E. M. & XIE, C. 2013. Anti-oxidation treatment of ultra high molecular weight polyethylene components to decrease periprosthetic osteolysis: evaluation of osteolytic and osteogenic properties of wear debris particles in a murine calvaria model. *Current Rheumatology Reports*, 15, 325.
- GREEN, T. R., FISHER, J., STONE, M., WROBLEWSKI, B. M. & INGHAM, E. 1998. Polyethylene particles of a 'critical size' are necessary for the induction of cytokines by macrophages in vitro. *Biomaterials*, 19, 2297-2302.
- GRUPP, T. M., MEISEL, H. J., COTTON, J. A., SCHWIESAU, J., FRITZ, B., BLOMER, W. & JANSSON, V. 2010. Alternative bearing materials for intervertebral disc arthroplasty. *Biomaterials*, 31, 523-31.
- HAIDER, H., WEISENBURGER, J. N., KURTZ, S. M., RIMNAC, C. M., FREEDMAN, J., SCHROEDER, D. W. & GARVIN, K. L. 2012. Does vitamin E-

stabilized ultrahigh-molecular-weight polyethylene address concerns of cross-linked polyethylene in total knee arthroplasty? *J Arthroplasty*, 27, 461-9.

HALL, R. M., UNSWORTH, A., WROBLEWSKI, B. M. & BURGESS, I. C. 1994. Frictional characterisation of explanted Charnley hip prostheses. *Wear*, 175, 159.

HART, A. J., BUDDHDEV, P., WINSHIP, P., FARIA, N., POWELL, J. J. & SKINNER, J. A. 2008. Cup inclination angle of greater than 50 degrees increases whole blood concentrations of cobalt and chromium ions after metal-on-metal hip resurfacing. *Hip Int*, 18, 212-9.

HATFIELD, D. L. & GLADYSHEV, V. N. 2009. The Outcome of Selenium and Vitamin E Cancer Prevention Trial (SELECT) reveals the need for better understanding of selenium biology. *Mol Interv*, 9, 18-21.

HAYASE, Y., MUGURUMA, Y. & LEE, M. Y. 1997. Osteoclast development from hematopoietic stem cells: apparent divergence of the osteoclast lineage prior to macrophage commitment. *Exp Hematol*, 25, 19-25.

HILL, K. E., MONTINE, T. J., MOTLEY, A. K., LI, X., MAY, J. M. & BURK, R. F. 2003. Combined deficiency of vitamins E and C causes paralysis and death in guinea pigs. *Am J Clin Nutr*, 77, 1484-8.

HILL, K. E., MOTLEY, A. K., LI, X., MAY, J. M. & BURK, R. F. 2001. Combined selenium and vitamin E deficiency causes fatal myopathy in guinea pigs. *J Nutr*, 131, 1798-802.

HOOTMAN, J., BOLEN, J. & HELMICK, C. 2006. Prevalence of doctor-diagnosed arthritis and arthritis-attributable activity limitation - United States, 2003-2005. *MMWR*, 55, 1089-1092.

HUKKANEN, M., CORBETT, S. A., BATTEN, J., KONTTINEN, Y. T., MCCARTHY, I. D., MACLOUF, J., SANTAVIRTA, S., HUGHES, S. P. & POLAK, J. M. 1997. Aseptic loosening of total hip replacement. Macrophage expression of inducible nitric oxide synthase and cyclo-oxygenase-2, together with peroxynitrite formation, as a possible mechanism for early prosthesis failure. *J Bone Joint Surg Br*, 79, 467-74.

ILLGEN, R. L., 2ND, FORSYTHE, T. M., PIKE, J. W., LAURENT, M. P. & BLANCHARD, C. R. 2008. Highly crosslinked vs conventional polyethylene particles--an in vitro comparison of biologic activities. *J Arthroplasty*, 23, 721-31.

INGHAM, E. & FISHER, J. 2000. Biological reactions to wear debris in total joint replacement. *Proceedings of the Institution of Mechanical Engineers Part H-Journal of Engineering in Medicine*, 214, 21-37.

INGHAM, E., GREEN, T. R., STONE, M. H., KOWALSKI, R., WATKINS, N. & FISHER, J. 2000. Production of TNF-alpha and bone resorbing activity by

macrophages in response to different types of bone cement particles. *Biomaterials*, 21, 1005-13.

INGRAM, J. H., STONE, M., FISHER, J. & INGHAM, E. 2004. The influence of molecular weight, crosslinking and counterface roughness on TNF-alpha production by macrophages in response to ultra high molecular weight polyethylene particles. *Biomaterials*, 25, 3511-22.

INSTITUTE OF MEDICINE, F. A. N. B. 2000. *Dietary Reference Intakes: Vitamin C, Vitamin E, Selenium, and Carotenoids*. National Academy Press.

IP, W. K., SOKOLOVSKA, A., CHARRIERE, G. M., BOYER, L., DEJARDIN, S., CAPPILLINO, M. P., YANTOSCA, L. M., TAKAHASHI, K., MOORE, K. J., LACY-HULBERT, A. & STUART, L. M. 2010. Phagocytosis and phagosome acidification are required for pathogen processing and MyD88-dependent responses to *Staphylococcus aureus*. *J Immunol*, 184, 7071-81.

ITO, H., MALONEY, C. M., CROWNINSHIELD, R. D., CLOHISY, J. C., MCDONALD, D. J. & MALONEY, W. J. 2010. In vivo femoral head damage and its effect on polyethylene wear. *J Arthroplasty*, 25, 302-8.

JACOBS, J. J., SKIPOR, A. K., DOORN, P. F., CAMPBELL, P., SCHMALZRIED, T. P., BLACK, J. & AMSTUTZ, H. C. 1996. Cobalt and chromium concentrations in patients with metal on metal total hip replacements. *Clin Orthop Relat Res*, S256-63.

JEDENMALM, A., AFFATATO, S., TADDEI, P., LEARDINI, W., GEDDE, U. W., FAGNANO, C. & VICECONTI, M. 2009. Effect of head surface roughness and sterilization on wear of UHMWPE acetabular cups. *J Biomed Mater Res A*, 90, 1032-42.

JOHNSTONE, B., ALINI, M., CUCCHIARINI, M., DODGE, G. R., EGLIN, D., GUILAK, F., MADRY, H., MATA, A., MAUCK, R. L., SEMINO, C. E. & STODDART, M. J. 2013. Tissue engineering for articular cartilage repair--the state of the art. *Eur Cell Mater*, 25, 248-67.

JOYCE, T. J. 2010. Wear testing of a DJOA finger prosthesis in vitro. *J Mater Sci Mater Med*, 21, 2337-43.

JOYCE, T. J. & UNSWORTH, A. 2004. Wear studies of all UHMWPE couples under various bio-tribological conditions. *J Appl Biomater Biomech*, 2, 29-34.

KANG, L., GALVIN, A. L., BROWN, T. D., FISHER, J. & JIN, Z. M. 2008. Wear simulation of ultra-high molecular weight polyethylene hip implants by incorporating the effects of cross-shear and contact pressure. *Proc Inst Mech Eng H*, 222, 1049-64.

- KARLSON, E. W., MANDL, L. A., AWEH, G. N., SANGHA, O., LIANG, M. H. & GRODSTEIN, F. 2003. Total hip replacement due to osteoarthritis: The importance of age, obesity, and other modifiable risk factors. *American Journal of Medicine*, 114, 93-98.
- KATZER, A., MARQUARDT, H., WESTENDORF, J., WENING, J. V. & VON FOERSTER, G. 2002. Polyetheretherketone--cytotoxicity and mutagenicity in vitro. *Biomaterials*, 23, 1749-59.
- KELLY, N. H., RAJADHYAKSHA, A. D., WRIGHT, T. M., MAHER, S. A. & WESTRICH, G. H. 2010. High stress conditions do not increase wear of thin highly crosslinked UHMWPE. *Clin Orthop Relat Res*, 468, 418-23.
- KING, R. N., V. S. ERNSBERGER, C. HANES, M. 2010. Characterization of gamma-irradiated UHMWPE stabilized with a hindered-phenol antioxidant. *Transactions of the 56th Orthopaedic Research Society, New Orleans, USA*.
- KINOV, P., TZONCHEVA, A. & TIVCHEV, P. 2010. Evidence Linking Elevated Oxidative Stress And Aseptic Loosening Of Hip Arthroplasty. *Comptes Rendus De L Academie Bulgare Des Sciences*, 63, 1231-1238.
- KOVAL KJ, Z. J. 2000. Chapter 1 - Anatomy. *Hip Fractures, A practical guide to management*, 1-8.
- KOVAL, K. J. & ZUCKERMAN, J. D. 2000. Anatomy in. "*Hip Fractures, A practical guide to management*", 1-8.
- KRESS, A. M., SCHMIDT, R., HOLZWARATH, U., FORST, R. & MUELLER, L. A. 2010. Excellent results with cementless total hip arthroplasty and alumina-on-alumina pairing: minimum ten-year follow-up. *Int Orthop*.
- KURTZ, S. M. 2009a. In Vivo Oxidation of UHMWPE in. "*UHMWPE Biomaterials Handbook*" 2nd Edition, 325-339.
- KURTZ, S. M. 2009b. The origins of UHMWPE in total hip arthroplasty in. "*UHMWPE Biomaterials Handbook*", 31-41.
- KURTZ, S. M. 2009c. Packaging and Sterilization of UHMWPE in. "*UHMWPE Biomaterials Handbook*", 21-29.
- KURTZ, S. M. 2009d. A Primer on UHMWPE in. "*UHMWPE Biomaterials Handbook*" 2nd Edition, 1-6.
- KURTZ, S. M., DUMBLETON, J., SISKEY, R. S., WANG, A. & MANLEY, M. 2009. Trace concentrations of vitamin E protect radiation crosslinked UHMWPE from oxidative degradation.

- KURTZ, S. M., MURATOGLU, O. K., EVANS, M. & EDIDIN, A. A. 1999. Advances in the processing, sterilization, and crosslinking of ultra-high molecular weight polyethylene for total joint arthroplasty. *Biomaterials*, 20, 1659-88.
- KURTZ, S. M. & ONG, K. 2009. Contemporary total hip arthroplasty: Hard on hard bearings and highly crosslinked UHMWPE in. "UHMWPE Biomaterials Handbook" 2nd Edition, 55-72.
- KWON, Y. M., GLYN-JONES, S., SIMPSON, D. J., KAMALI, A., MCLARDY-SMITH, P., GILL, H. S. & MURRAY, D. W. 2010. Analysis of wear of retrieved metal-on-metal hip resurfacing implants revised due to pseudotumours. *J Bone Joint Surg Br*, 92, 356-61.
- LANCASTER, J. G., DOWSON, D., ISAAC, G. H. & FISHER, J. 1997. The wear of ultra-high molecular weight polyethylene sliding on metallic and ceramic counterfaces representative of current femoral surfaces in joint replacement. *Proc Inst Mech Eng H*, 211, 17-24.
- LANGTON, D. J., JAMESON, S. S., JOYCE, T. J., HALLAB, N. J., NATU, S. & NARGOL, A. V. F. 2010. Early failure of metal-on-metal bearings in hip resurfacing and large-diameter total hip replacement: A CONSEQUENCE OF EXCESS WEAR. *J Bone Joint Surg Br*, 92, 38-46.
- LAURENT, P. M., GALLARDO, L. A., KUNZE, J. & WIMMER, M. A. 2010. Europium Stearate increases the oxidation resistance of UHMWPE Transactions of the 56th Orthopaedic Research Society, New Orleans, USA.
- LEARMONTH, I. D., YOUNG, C. & RORABECK, C. 2007. The operation of the century: total hip replacement. *Lancet*, 370, 1508-1519.
- LI-WEBER, M., GIAISI, M., TREIBER, M. K. & KRAMMER, P. H. 2002. Vitamin E inhibits IL-4 gene expression in peripheral blood T cells. *Eur J Immunol*, 32, 2401-8.
- LIU, A. 2012. Determination of the Biological Response and Cellular Uptake Mechanisms of Nanometre-sized UHMWPE Wear Particles from Total Hip Replacements. Ph.D. University of Leeds.
- LOMBARDI, A. V., JR., MALLORY, T. H., DENNIS, D. A., KOMISTEK, R. D., FADA, R. A. & NORTHCUT, E. J. 2000. An in vivo determination of total hip arthroplasty pistoning during activity. *J Arthroplasty*, 15, 702-9.
- LONGO, D., M., LOUIE, B. & CESANO, A. 2012. Inter-donor variation in cell subset specific immune signalling responses in healthy individuals. *Am J Clin Exp Immunol*, 1, 1-11.

- LORENZO, J. A., SOUSA, S. L., FONSECA, J. M., HOCK, J. M. & MEDLOCK, E. S. 1987. Colony-stimulating factors regulate the development of multinucleated osteoclasts from recently replicated cells in vitro. *J Clin Invest*, 80, 160-4.
- MACHLIN, L. J., FILIPSKI, R., NELSON, J., HORN, L. R. & BRIN, M. 1977. Effects of a prolonged vitamin E deficiency in the rat. *J Nutr*, 107, 1200-8.
- MACLENNAN, W. J. 1999. History of arthritis and bone rarefaction evidence from paleopathology onwards. *Scott Med J*, 44, 18-20.
- MACPHERSON, G. J. & BREUSCH, S. J. 2010. Metal-on-metal hip resurfacing: a critical review. *Arch Orthop Trauma Surg*.
- MALCHAU, H., HERBERTS, P. & AHNFELT, L. 1993. Prognosis of total hip replacement in Sweden. Follow-up of 92,675 operations performed 1978-1990. *Acta Orthop Scand*, 64, 497-506.
- MATTHEWS, J. B., GREEN, T. R., STONE, M. H., WROBLEWSKI, B. M., FISHER, J. & INGHAM, E. 2000. Comparison of the response of primary murine peritoneal macrophages and the U937 human histiocytic cell line to challenge with in vitro generated clinically relevant UHMWPE particles. *Bio-Medical Materials and Engineering*, 10, 229-240.
- MAQUET, P., G, J. 1985. Biomechanics of the Hip. Chapter 1 - Biomechanics of the Hip, 1-2. MCCARTHY, M., BROWN, T. E. & SALEH, K. J. 2009. Etiology of Hip Arthritis in. "Arthritis & Arthroplasty: The Hip", 3-9.
- MCCARTHY M, B. T., SALEH KJ 2009. Chapter 1 - Etiology of Hip Arthritis. *Arthritis & Arthroplasty: The Hip*, 3-9.
- MCDEVITT, C. A. 1973. Biochemistry of articular cartilage. Nature of proteoglycans and collagen of articular cartilage and their role in ageing and in osteoarthritis. *Ann Rheum Dis*, 32, 364-78.
- MCKEE, G. K. & CHEN, S. C. 1973. The statistics of the McKee-Farrar method of total hip replacement. *Clin Orthop Relat Res*, 26-33.
- MCKEE, G. K. & WATSON-FARRAR, J. 1966. Replacement of arthritic hips by the McKee-Farrar prosthesis. *J Bone Joint Surg Br*, 48, 245-59.
- MEDEL, F. J., PENA, P., CEGONINO, J., GOMEZ-BARRENA, E. & PUERTOLAS, J. A. 2007. Comparative fatigue behavior and toughness of remelted and annealed highly crosslinked polyethylenes. *J Biomed Mater Res B Appl Biomater*, 83, 380-90.
- MENDENHALL, S. 2008. Hospital resources and implant cost management - a 2007 update. *Orthop Network News*, 19, 13-19.

MHRA 2010. Medical Device Alert: ASR™ hip replacement implants manufactured by DePuy International Ltd

MICHELI, B. R., WANNOMAE, K. K., LOZYNSKY, A. J., CHRISTENSEN, S. D. & MURATOGLU, O. K. 2012. Knee simulator wear of vitamin E stabilized irradiated ultrahigh molecular weight polyethylene. *J Arthroplasty*, 27, 95-104.

MOSELEY, J. B., O'MALLEY, K., PETERSEN, N. J., MENKE, T. J., BRODY, B. A., KUYKENDALL, D. H., HOLLINGSWORTH, J. C., ASHTON, C. M. & WRAY, N. P. 2002. A Controlled Trial of Arthroscopic Surgery for Osteoarthritis of the Knee. *New England Journal of Medicine*, 347, 81-88.

MUELLER, S., C., MARZ, R., SCHMOLZ, M. & DREWELOW, B. 2012. Intraindividual long term stability and response corridors of cytokines in healthy volunteers detected by a standardised whole-blood culture system for bed-side application. *BMC Medical Research Methodology*, 12.

MULLINS, M. M., NORBURY, W., DOWELL, J. K. & HEYWOOD-WADDINGTON, M. 2007. Thirty-year results of a prospective study of Charnley total hip arthroplasty by the posterior approach. *J Arthroplasty*, 22, 833-9.

MURATOGLU, O. K. 2009. Highly crosslinked and melted UHMWPE in. "UHMWPE Biomaterials Handbook" 2nd Edition, 197-203.

MURATOGLU, O. K., BRAGDON, C. R., O'CONNOR, D. O., JASTY, M. & HARRIS, W. H. 2001. A novel method of cross-linking ultra-high-molecular-weight polyethylene to improve wear, reduce oxidation, and retain mechanical properties. Recipient of the 1999 HAP Paul Award. *J Arthroplasty*, 16, 149-60.

MURPHY, M. P. 2009. How mitochondria produce reactive oxygen species. *Biochem J.*, 417(Pt 1), 1-13.

MURRAY, D. W. & RUSHTON, N. 1990. Macrophages stimulate bone resorption when they phagocytose particles. *J Bone Joint Surg Br*, 72, 988-92.

NARAYAN, V. S. K., R. WARNER, D. SHARP, M. 2010. Evaluation of antioxidant stabilized UHMWPE materials. Transactions of the 56th Orthopaedic Research Society, New Orleans, USA.

NATIONAL JOINT REGISTRY 2013. Patient Characteristics for Hip Revision Procedures in 2013. National Joint Registry 10th Annual Report, 81.

NEUMANN, D. A. 1999. Joint deformity and dysfunction: a basic review of underlying mechanisms. *Arthritis Care Res*, 12, 139-51.

NOAMAN, E., ZAHRAN, A. M., KAMAL, A. M. & OMRAN, M. F. 2002. Vitamin E and selenium administration as a modulator of antioxidant defense system: biochemical assessment and modification. *Biol Trace Elem Res*, 86, 55-64.

- ORAL, E., CHRISTENSEN, S. D., MALHI, A. S., WANNOMAE, K. K. & MURATOGLU, O. K. 2006. Wear resistance and mechanical properties of highly cross-linked, ultrahigh-molecular weight polyethylene doped with vitamin E. *J Arthroplasty*, 21, 580-91.
- ORAL, E., MALHI, A. S. & MURATOGLU, O. K. 2006b. Mechanisms of decrease in fatigue crack propagation resistance in irradiated and melted UHMWPE. *Biomaterials*, 27, 917-25.
- ORAL, E., GHALI, B. W., NEILS, A. & MURATOGLU, O. K. 2012. A new mechanism of oxidation in ultrahigh molecular weight polyethylene caused by squalene absorption. *J Biomed Mater Res B Appl Biomater*, 100, 742-51.
- ORAL, E., GREENBAUM, E. S., MALHI, A. S., HARRIS, W. H. & MURATOGLU, O. K. 2005. Characterization of irradiated blends of alpha-tocopherol and UHMWPE. *Biomaterials*, 26, 6657-63.
- ORAL, E., MALHI, A. S., WANNOMAE, K. K. & MURATOGLU, O. K. 2008. Highly cross-linked ultrahigh molecular weight polyethylene with improved fatigue resistance for total joint arthroplasty: recipient of the 2006 Hap Paul Award. *J Arthroplasty*, 23, 1037-44.
- ORAL, E., NEILS, A. L., ROWELL, S. L., LOZYNSKY, A. J. & MURATOGLU, O. K. 2013. Increasing irradiation temperature maximizes vitamin E grafting and wear resistance of ultrahigh molecular weight polyethylene. *Journal of Biomedical Materials Research Part B: Applied Biomaterials*, 101B, 436-440.
- ORAL, E., WANNOMAE, K. K., HAWKINS, N., HARRIS, W. H. & MURATOGLU, O. K. 2004. [alpha]-Tocopherol-doped irradiated UHMWPE for high fatigue resistance and low wear. *Biomaterials*, 25, 5515.
- ORAL, E., WANNOMAE, K. K., ROWELL, S. L. & MURATOGLU, O. K. 2007. Diffusion of vitamin E in ultra-high molecular weight polyethylene. *Biomaterials*, 28, 5225-37.
- OSTERUD, B. & BJORKLID, E. 2003. Role of monocytes in atherogenesis. *Physiol Rev*, 83, 1069-112.
- OWUSU-ANSAH, E., YAVARI, A. & BANERJEE, U. 2008. A protocol for in vivo detection of reactive oxygen species.
- PANDIT, H., GLYN-JONES, S., MCLARDY-SMITH, P., GUNDLE, R., WHITWELL, D., GIBBONS, C. L., OSTLERE, S., ATHANASOU, N., GILL, H. S. & MURRAY, D. W. 2008. Pseudotumours associated with metal-on-metal hip resurfacings. *J Bone Joint Surg Br*, 90, 847-51.
- PARK, D. Y., MIN, B. H., KIM, D. W., SONG, B. R., KIM, M. & KIM, Y. J. 2013. Polyethylene wear particles play a role in development of osteoarthritis via

detrimental effects on cartilage, meniscus, and synovium. *Osteoarthritis and Cartilage*.

PATHANIA, V., SYAL, N., PATHAK, C. M. & KHANDUJA, K. L. 1999. Vitamin E suppresses the induction of reactive oxygen species release by lipopolysaccharide, interleukin-1beta and tumor necrosis factor-alpha in rat alveolar macrophages. *J Nutr Sci Vitaminol (Tokyo)*, 45, 675-86.

PAZZAGLIA, U. E., DELL'ORBO, C. & WILKINSON, M. J. 1987. The foreign body reaction in total hip arthroplasties. A correlated light-microscopy, SEM, and TEM study. *Arch Orthop Trauma Surg*, 106, 209-19.

PELLICCI, P. M., WILSON, P. D., SLEDGE, C. B., SALVATI, E. A., RANAWAT, C. S., POSS, R. & CALLAGHAN, J. J. 1985. Long-Term Results of Revision Total Hip-Replacement - a Follow-up Report. *Journal of Bone and Joint Surgery-American Volume*, 67A, 513-516.

POPOOLA, O. O., YAO, J. Q., JOHNSON, T. S. & BLANCHARD, C. R. 2010. Wear, delamination, and fatigue resistance of melt-annealed highly crosslinked UHMWPE cruciate-retaining knee inserts under activities of daily living. *J Orthop Res*, 28, 1120-6.

QUINN, P. J. 2004. Is the distribution of alpha-tocopherol in membranes consistent with its putative functions? *Biochemistry (Mosc)*, 69, 58-66.

RAGHUNATHAN, V. K., DEVEY, M., HAWKINS, S., HAILS, L., DAVIS, S. A., MANN, S., CHANG, I. T., INGHAM, E., MALHAS, A., VAUX, D. J., LANE, J. D. & CASE, C. P. 2013. Influence of particle size and reactive oxygen species on cobalt chrome nanoparticle-mediated genotoxicity. *Biomaterials*, 34, 3559-3570.

SCHUMACKER, P. T. 2006. Reactive oxygen species in cancer cells: Live by the sword, die by the sword. *Cancer Cell*, 10, 175-176.

RAJADHYAKSHA, A. D., BROTEA, C., CHEUNG, Y., KUHN, C., RAMAKRISHNAN, R. & ZELICOF, S. B. 2009. Five-year comparative study of highly cross-linked (crossfire) and traditional polyethylene. *J Arthroplasty*, 24, 161-7.

RAMAKRISHNAN, P., HECHT, B. A., PEDERSEN, D. R., LAVERY, M. R., MAYNARD, J., BUCKWALTER, J. A. & MARTIN, J. A. 2010. Oxidant Conditioning Protects Cartilage from Mechanically Induced Damage. *Journal Of Orthopaedic Research*, 28, 914-920.

REITER, E., JIANG, Q. & CHRISTEN, S. 2007. Anti-inflammatory properties of alpha- and gamma-tocopherol. *Mol Aspects Med*, 28, 668-91.

- RICCIARELLI, R., TASINATO, A., CLEMENT, S., OZER, N. K., BOSCOBOINIK, D. & AZZI, A. 1998. alpha-Tocopherol specifically inactivates cellular protein kinase C alpha by changing its phosphorylation state. *Biochem J*, 334 (Pt 1), 243-9.
- RICCIARELLI, R., ZINGG, J. M. & AZZI, A. 2000. Vitamin E reduces the uptake of oxidized LDL by inhibiting CD36 scavenger receptor expression in cultured aortic smooth muscle cells. *Circulation*, 102, 82-7.
- RICHARDS, L. 2008. The biological activity of nanometre sized polymer particles. . Ph.D. University of Leeds.
- ROCKWOOD, C. A., JR. & WIRTH, M. A. 2002. Observation on retrieved Hylamer glenoids in shoulder arthroplasty: problems associated with sterilization by gamma irradiation in air. *J Shoulder Elbow Surg*, 11, 191-7.
- ROGERS, M., BLOM, A. W., BARNETT, A., KARANTANA, A. & BANNISTER, G. C. 2009. Revision for recurrent dislocation of Total Hip Replacement. *Hip International*, 19, 109-113.
- ROWELL, S. L., YABANNAVAR, P. & MURATOGLU, O. K. 2010. Oxidative stability of simulator tested acetabular liners after 7 years shelf-aging in air. *Transactions of the 56th Orthopaedic Research Society*, New Orleans, USA.
- SABOKBAR, A., FUJIKAWA, Y., NEALE, S., MURRAY, D. W. & ATHANASOU, N. A. 1997. Human arthroplasty derived macrophages differentiate into osteoclastic bone resorbing cells. *Annals Of The Rheumatic Diseases*, 56, 414-420.
- SAITO, S., ISHII, T., MORI, S., HOSAKA, K., OOTAKI, M. & TOKUHASHI, Y. 2010. Long-term results of metasul metal-on-metal total hip arthroplasty. *Orthopedics*, 33.
- SANTAVIRTA, S., BOHLER, M., HARRIS, W. H., KONTTINEN, Y. T., LAPPALAINEN, R., MURATOGLU, O., RIEKER, C. & SALZER, M. 2003. Alternative materials to improve total hip replacement tribology. *Acta Orthop Scand*, 74, 380-8.
- SCHEINECKER, C., MARC, C. H., MD, MPH, ALAN, J. S., MD, FRCP, JOSEF, S. S., MD, MICHAEL, E. W., MD, MICHAEL, H. W. & MD 2009. *The Role of T Cells in Rheumatoid Arthritis*. *Rheumatoid Arthritis*. Philadelphia: Mosby.
- SCHNEIDER, C. 2005. Chemistry and biology of vitamin E. *Mol Nutr Food Res*, 49, 7-30.

- SCHOLES, S. C., INMAN, I. A., UNSWORTH, A. & JONES, E. 2008. Tribological assessment of a flexible carbon-fibre-reinforced poly(ether-ether-ketone) acetabular cup articulating against an alumina femoral head. *Proc Inst Mech Eng H*, 222, 273-83.
- SCHOLES, S. C. & UNSWORTH, A. 2006. The effects of proteins on the friction and lubrication of artificial joints. *Proc Inst Mech Eng H*, 220, 687-93.
- SCHOLES, S. C., UNSWORTH, A. & GOLDSMITH, A. A. 2000. A frictional study of total hip joint replacements. *Phys Med Biol*, 45, 3721-35.
- SCHWARZ, E., BUKATA S, V., BENZ, E., ROSIER, R. N., PUZAS, J. E. & O'KEEFE, R., J. 1999. NFkB and TNF-alpha are stimulated by titanium particles and are essential for in vivo bone resorption. In *Proceedings of the 45th annual Meeting of the Orthopaedic Research Society*, p305.
- SEED, S. M., DUNICAN, K. C. & LYNCH, A. M. 2009. Osteoarthritis: a review of treatment options. *Geriatrics*, 64, 20-9.
- SHEPPARD, A. J., PENNINGTON, J. A. & WEIHRAUCH, J. L. 1993. Analysis and distribution of vitamin E in vegetable oils and foods. *Vitamin E in health and disease*, 9-31.
- SHIH, J. C., JONAS, R. H. & SCOTT, M. L. 1977. Oxidative deterioration of the muscle proteins during nutritional muscular dystrophy in chicks. *J Nutr*, 107, 1786-91.
- SIEBER, H. P., RIEKER, C. B. & KOTTIG, P. 1999. Analysis of 118 second-generation metal-on-metal retrieved hip implants. *J Bone Joint Surg Br*, 81, 46-50.
- SINGH, U. & JIALAL, I. 2004. Anti-inflammatory effects of alpha-tocopherol. *Ann N Y Acad Sci*, 1031, 195-203.
- SINGH, U., DEVARAJ, S. & JIALAL, I. 2005. Vitamin E, oxidative stress, and inflammation. *Annu Rev Nutr*, 25, 151-74.
- SMITH, S. L., DOWSON, D. & GOLDSMITH, A. A. 2001. The effect of femoral head diameter upon lubrication and wear of metal-on-metal total hip replacements. *Proc Inst Mech Eng H*, 215, 161-70.
- SOBIERAJ, M. C. & RIMNAC, C. M. 2009. Ultra high molecular weight polyethylene: mechanics, morphology, and clinical behavior. *J Mech Behav Biomed Mater*, 2, 433-43.
- SOKAL, R. R. & ROHLF, J. F. 1981. *Biometry: The principles and practice of statistics in biological research*. In FREEMAN, W. H. (ed.) 2nd ed. San Francisco.

- SUTULA, L. C., COLLIER, J. P., SAUM, K. A., CURRIER, B. H., CURRIER, J. H., SANFORD, W. M., MAYOR, M. B., WOODING, R. E., SPERLING, D. K., WILLIAMS, I. R. & ET AL. 1995. The Otto Aufranc Award. Impact of gamma sterilization on clinical performance of polyethylene in the hip. *Clin Orthop Relat Res*, 28-40.
- TAI, Z., CHEN, Y., AN, Y., YAN, X. & XUE, Q. 2012. Tribological Behavior of UHMWPE Reinforced with Graphene Oxide Nanosheets. *Tribology Letters*, 46, 55-63.
- TATEIWA, T., CLARKE, I. C., WILLIAMS, P. A., GARINO, J., MANAKA, M., SHISHIDO, T., YAMAMOTO, K. & IMAKIIRE, A. 2008. Ceramic total hip arthroplasty in the United States: safety and risk issues revisited. *Am J Orthop (Belle Mead NJ)*, 37, E26-31.
- TERAMURA, S., RUSSEL, S., INGHAM, E., FISHER, J., TOMITA, N., FUJIWARA, K. & TIPPER, J. 2009. Reduced Biological Response to Wear Particles from UHMWPE containing Vitamin E.
- TERAMURA, S., SAKODA, H., TERAOKA, T., ENDO, M. M., FUJIWARA, K. & TOMITA, N. 2008. Reduction of wear volume from ultrahigh molecular weight polyethylene knee components by the addition of vitamin E. *J Orthop Res*, 26, 460-4.
- TIPPER, J. L., GALVIN, A. L., WILLIAMS, S., MCEWEN, H. M., STONE, M. H., INGHAM, E. & FISHER, J. 2006. Isolation and characterization of UHMWPE wear particles down to ten nanometers in size from in vitro hip and knee joint simulators. *J Biomed Mater Res A*, 78, 473-80.
- TIPPER, J. L., HATTON, A., NEVELOS, J. E., INGHAM, E., DOYLE, C., STREICHER, R., NEVELOS, A. B. & FISHER, J. 2002. Alumina-alumina artificial hip joints. Part II: characterisation of the wear debris from in vitro hip joint simulations. *Biomaterials*, 23, 3441-8.
- TIPPER, J. L., GALVIN, A., INGHAM, E. & FISHER, J. 2005. Comparison of the Wear, Wear Debris and Functional Biological Activity of Non-crosslinked and Crosslinked GUR 1020 and GUR 1050 Polyethylenes used in Total Hip Prostheses. *Trans. UHMWPE for arthroplasty: Degradation, stabilization, and crosslinking*, <http://www.uhmwpe.unito.it/>.
- TIPPER, J. L., INGHAM, E., HAILEY, J. L., BESONG, A. A., FISHER, J., WROBLEWSKI, B. M. & STONE, M. H. 2000. Quantitative analysis of polyethylene wear debris, wear rate and head damage in retrieved Charnley hip prostheses. *J Mater Sci Mater Med*, 11, 117-24.
- TIPPER, J. L., INGHAM, E., JIN, Z. M. & FISHER, J. 2005. The science of metal-on-metal articulation. *Current Orthopaedics*, 19, 280-287.

- TIPPER, J. L., LIU, T.-Y. & BLADEN, C. L. 2011. Cytotoxicity of Anti-Oxidant Compounds in Human Macrophages Transactions of the 57th Orthopaedic Research Society, California, USA.
- TOLEDO-PEREYRA, L. H. 2004. John Charnley--father of modern total hip replacement. *J Invest Surg*, 17, 299-301.
- TOWHEED, T. E. & HOCHBERG, M. C. 1996. Health-related quality of life after total hip replacement. *Semin Arthritis Rheum*, 26, 483-91.
- TREUHAFT, P. S. & MCCARTY, D. J. 1971. Synovial fluid pH, lactate, oxygen and carbon dioxide partial pressure in various joint diseases. *Arthritis Rheum*, 14, 475-84.
- UTZSCHNEIDER, S., BECKER, F., GRUPP, T. M., SIEVERS, B., PAULUS, A., GOTTSCHALK, O. & JANSSON, V. 2010. Inflammatory response against different carbon fiber-reinforced PEEK wear particles compared with UHMWPE in vivo. *Acta Biomater*, 6, 4296-304.
- VISURI, T., PUKKALA, E., PAAVOLAINEN, P., PULKKINEN, P. & RISKKA, E. B. 1996. Cancer risk after metal on metal and polyethylene on metal total hip arthroplasty. *Clin Orthop Relat Res*, S280-9.
- VISURI, T. I., PUKKALA, E., PULKKINEN, P. & PAAVOLAINEN, P. 2006. Cancer incidence and causes of death among total hip replacement patients: a review based on Nordic cohorts with a special emphasis on metal-on-metal bearings. *Proc Inst Mech Eng H*, 220, 399-407.
- WANG, A. 2006. Wear, oxidation and mechanical properties of a sequentially irradiated and annealed UHMWPE in total joint replacement. *Journal of Physics D: Applied Physics*, 39, 3213.
- WANNOMAE, K. K., CHRISTENSEN, S. D., MICHELI, B. R., ROWELL, S. L., SCHROEDER, D. W. & MURATOGLU, O. K. 2010. Delamination and adhesive wear behavior of alpha-tocopherol-stabilized irradiated ultrahigh-molecular-weight polyethylene. *J Arthroplasty*, 25, 635-43.
- WANNOMAE, K. K., BHATTACHARYYA, S., FREIBERG, A., ESTOK, D., HARRIS, W. H. & MURATOGLU, O. 2006. In vivo oxidation of retrieved cross-linked ultra-high-molecular-weight polyethylene acetabular components with residual free radicals. *J Arthroplasty*, 21, 1005-11.
- WEBER, B. G. 1996. Experience with the Metasul total hip bearing system. *Clin Orthop Relat Res*, S69-77.
- WILES, P. 1957. The surgery of the osteoarthritic hip. *Br J Surg*, 45, 488-97.

- WILKINSON, J. M., WILSON, A. G., STOCKLEY, I., SCOTT, I. R., MACDONALD, D. A., HAMER, A. J., DUFF, G. W. & EASTELL, R. 2003. Variation in the TNF gene promoter and risk of osteolysis after total hip arthroplasty. *J Bone Miner Res*, 18, 1995-2001.
- WILLMANN, G. 1996. Development in medical-grade alumina during the past two decades. *Journal of Materials Processing Technology*, 56, 168.
- WINTER, M., GRISS, P., SCHELLER, G. & MOSER, T. 1992. Ten- to 14-year results of a ceramic hip prosthesis. *Clin Orthop Relat Res*, 73-80.
- WOLF, C., LEDERER, K., PFRAGNER, R., SCHAUENSTEIN, K., INGOLIC, E. & SIEGL, V. 2007. Biocompatibility of ultra-high molecular weight polyethylene (UHMW-PE) stabilized with alpha-tocopherol used for joint endoprostheses assessed in vitro. *J Mater Sci Mater Med*, 18, 1247-52.
- WOLF, C., LEDERER, K., BERGMEISTER, H., LOSERT, U. & BOCK, P. 2006. Animal experiments with ultra-high molecular weight polyethylene (UHMW-PE) stabilised with alpha-tocopherol used for articulating surfaces in joint endoprostheses. *J Mater Sci Mater Med*, 17, 1341-7.
- WOO, C. H., EOM, Y. W., YOO, M. H., YOU, H. J., HAN, H. J., SONG, W. K., YOO, Y. J., CHUN, J. S. & KIM, J. H. 2000. Tumor necrosis factor-alpha generates reactive oxygen species via a cytosolic phospholipase A2-linked cascade. *J Biol Chem*, 275, 32357-62.
- WROBLEWSKI, B. M., SINEY, P. D. & FLEMING, P. A. 2005. Low-friction arthroplasty of the hip using alumina ceramic and cross-linked polyethylene. A 17-year follow-up report. *J Bone Joint Surg Br*, 87, 1220-1.
- YAMAMOTO, K., CLARKE, I. C., MASAOKA, T., OONISHI, H., WILLIAMS, P. A., GOOD, V. D. & IMAKIIRE, A. 2001. Microwear phenomena of ultrahigh molecular weight polyethylene cups and debris morphology related to gamma radiation dose in simulator study. *J Biomed Mater Res*, 56, 65-73.
- YAMAMOTO, K., IMAKIIRE, A., MASAOKA, T., SHISHIDO, T., MIZOUE, T., CLARKE, I. C., SHOJI, H., KAWANABE, K. & TAMURA, J. 2003. Wear mode and wear mechanism of retrieved acetabular cups. *Int Orthop*, 27, 286-90.
- YOSHIDA, H., FAUST, A., WILCKENS, J., KITAGAWA, M., FETTO, J. & CHAO, E. Y. 2006. Three-dimensional dynamic hip contact area and pressure distribution during activities of daily living. *J Biomech*, 39, 1996-2004.
- YUB, S. & DENISOV, E. T. 1974. Mechanism of the inhibiting activity of iminoxyl radicals during oxidation of polypropylene and polyethylene. *Vysokomol Soyed*, A14, 2313-2316.

ZHANG, C., TANG, T., REN, W., ZHANG, X. & DAI, K. 2008. Influence of mouse genetic background on wear particle-induced in vivo inflammatory osteolysis. *Inflamm Res*, 57, 211-5.

ZOLOTAREVOVA, E., HUDECEK, J., SPUNDOVA, M. & ENTLICHER, G. 2010. Binding of proteins to ultra high molecular weight polyethylene wear particles as a possible mechanism of macrophage and lymphocyte activation. *J Biomed Mater Res A*, 95, 950-5.

Appendix A

General Materials

General chemicals and reagents used in this study are shown in Table A- 1.

Table A-1 – Chemicals and reagents used in this study

Chemical/ Regents	Supplier	Storage and Preparation
ATPlite™ ATP detection assay	PerkinElmer, Massachusetts, USA	Stored at 4°C
Bovine Serum Albumin (BSA)	Sigma-Aldrich Ltd, Dorset, UK	Stored at room temperature
Carbon Paste	Agar Scientific, Stanstead, Essex, UK	Stored in the solvent cupboard, at room temperature
Chloroform	Genta Medical, York, UK	Stored in the flammables cupboard, at room temperature
ELISA kit (TNF- α)	Diaclone, France	Stored at 4°C
Ethanol	VWR International, UK	Stored at room temperature
Fluospheres (200 nm, 40 nm)	Invitrogen Technologies Ltd, Paisley, UK	Aliquoted and stored at -20°C
Foetal Bovine Serum (FBS)	Bio-Whittaker, Lonza, Verviers,	Stored in the flammables cupboard, at room temperature
Household Detergent	Fairy liquid, Procter and Gamble, UK	Purchased at a concentration of 200 mM.ml ⁻¹ . Solution was then aliquoted and stored at -20°C
Image-iT™ LIVE green ROS detection kit	Invitrogen Technologies Ltd, Paisley, UK	Aliquoted and stored at -20°C
Isopropan-2-ol	Fisher Scientific, Loughborough, Leicestershire, UK	Stored at 4°C
L-Glutamine	Bio-Whittaker, Lonza, Verviers	Stored at room temperature
Lipopolysaccharide (LPS)	Sigma Aldrich Ltd, Dorset, UK	Stored at room temperature

Lymphoprep	Fresenius Kabi Norge AS for Axis-Shield PoC AS, Oslo, Norway	Stored in the chemicals cupboard, at room temperature
N-(2-hydroxyethyl)piperazine- N'-(2-ethanulfonic acid)(HEPES)	Bio- Whittaker, Lonza, Verviers, Belgium	Stored at room temperature
Potassium Hydroxide	Sigma Aldrich Ltd, Dorset, UK	Stored at room temperature
Rosslyn Park Memorial Institute (RPMI) 1640 medium	Bio- Whittaker, Lonza, Verviers, Belgium	Stored at 4°C
Silica Gel (0.7% w/v)	MERCK, Darmstadt, Germany	Stored at 4°C
Sodium Hypochlorite Solution	BDH Laboratory Supplies, Poole, UK	Purchased at a concentration of 1M. Stored at room temperature.
Sterile Water	Baxter Healthcare, UK	Stored at room temperature
Trigene	Scientific Laboratory Supplies Ltd, Nottingham, UK	Stored at room temperature
Trypan Blue (0.4% v.v)	Sigma Aldrich Ltd, Dorset, UK	Stored at room temperature
Trypsin 0.5% with EDTA	Sigma Aldrich Ltd, Dorset, UK	Stored at -20°C
Tween 20	Sigma Aldrich Ltd, Dorset, UK	Stored at 4°C. Substrate solution was aliquoted and stored at -20°C following reconstitution
Ultra pure low melting point agarose	Invitrogen Life Technologies Ltd, Paisley, UK	Stored at 4°C
Vaseline	Unilever PLC, UK	Reconstituted at stored at - 20°C
Virkon	Scientific Laboratory Supplies Ltd, Nottingham, UK	Stored at room temperature

The general equipment used in this study is shown in table A-2.

Table A-2 – General equipment used in this study

Equipment	Supplier
47 mm Glass Filtration Apparatus	Sartorius, Goettingen, Germany
6 station pin-on-plate wear rig	Built 'in house', School of Mechanical Engineering, University of Leeds, UK Stanley, Sheffield, UK
Adjustable wrench	A&D Instruments Ltd, Oxford, UK
Automatic Pipetter (Fastpette v-2)	Labnet International Inc, New Jersey, USA
Balance (0.01g accuracy)	Bassaire, Southampton, UK
Balance AT21 Comparator - accurate to 1µg	Mettler Toledo, Sartorius, Germany
Balance GX-2000 EC - accurate to 0.01g	Jencons PLC, East Grinstead, UK
Bassaire 06-HB laminar flow hood	Bassaire, Southampton, UK
Bench pump	Hotpoint, UK
Benchtop Centrifuge (Harrier)	MSE Scientific Instruments, West Sussex, UK
Bunsen Burner	Camlab, UK
Cell Culture Inverted Light Microscope (CK40)	Olympus Optical Company, London, UK
Class II Safety Cabinet (cell culture)	Heraeus, Hanau, Germany
Confocal Laser Scanning Upright Zeiss LSM510	Carl Zeiss Ltd, UK
Contacting Form Talysurf Profilometer	Taylor Hobson Ltd, Leicester, UK
Duran Glass bottles (2 L, 1 L, 500 ml, 100ml)	Sigma Aldrich Ltd, Dorset, UK
Electronic Repeating Pipette Autorep E	Mettler Toledo, Sartorius, Germany
FEGSEM LEO-1530	LEO Electron Microscopy Ltd, Cambridge, UK
Finnpipette for cell culture work (1000 µl, 200µl, 20µl)	Thermo Scientific, Massachusetts, USA

Freezer (-20°C)	Jensons Plc, East Grinstead, UK
Genlab Oven (hot air)	Genlab Limited, Cheshire, UK
Gilson Pipettes (1000 µl, 200µl, 20µl)	Gilson, WI, USA
Haemocytometer	Marienfeld, Germany
High Speed Sorvall SS-34 Evolution RC Centrifuge	Kendro Laboratory Products Limited, Herts, UK
Image Pro Plus Image Analysis Software version 4.5.1	Media Cybernetics, Maryland, USA
Incubator and CO ₂ Gas in Air (MCO-20AIC) 5% (v/v)	SANYA Biomedical Europe BV, UK
Infra red lamps	Infraphil, Phillips, Surrey, UK
Ion Streamer (Stat Attack 1B-8)	Amersham International Ltd, Buckinghamshire, UK
KIMCARE® Medical Wipes	Kimberley Clarke, Kent, UK
Magnetic Stirrer	Scientific Laboratory Supplies Ltd, Nottingham, UK
Mistral 3000E bench centrifuge	MSE Scientific Instruments, London, UK
pH meter (Jenway 3510)	VWR International Poole, UK
Refrigerator	Jencons Plc, East Grinstead, UK
Sonicator	Fisher Scientific, Loughborough, Leicestershire, UK
Spirit level	Camlab, UK
Sputter Coater (B7341) & film thickness monitor (B7348)	Agar Scientific Limited, Stanstead, Essex, UK
TopCount® (NXT) Dual Detector Luminometer	Perkin Elmer, Massachusetts, USA
Ultrasonic Water Bath	Grant Instruments Ltd, Herts, UK
Unstirred Water Bath (Clifton NE1-56)	Nickel Electro Ltd, UK
Upright Fluorescence Microscope (AX10)	Carl Zeiss Ltd, UK
Water Purifier (PureLab)	Triple Red Limited, Buckinghamshire, UK

The general consumables and plasticware used in this study are shown in table A-3.

Table A-3 – Consumables and plasticware used in this study

Item	Size	Supplier
Bijous	5 ml	Scientific Laboratory Supplies, Nottingham, UK
Cyclopore track etched membranes	10 μm , 1 μm , 0.1 μm , 0.015 μm	BD Plastipak, BD, New Jersey, USA
Disposable Combi Tips	12.5 ml, 10 ml, 5 ml	Eppendorf AG, Hamburg, Germany
Glass Cover Slips (circular)	22 mm	Menzel Gläser, Gerhard Menzel GmbH, Germany
Glass Slides	76 x 26 mm	Menzel Gläser, Gerhard Menzel GmbH, Germany
Lab-Tek Chamber Slide	16 well	Fisher Scientific Limited, Leicester, UK
Maxisorb™ Plate	96 well	Scientific Laboratory Supplies, Nottingham, UK
Microplate Adhesive Sealing Film	96 well	PerkinElmer, Berkshire, UK
Optiplate	96 well	PerkinElmer, Berkshire, UK
Parafilm	N/A	Pechiney Plastic Packaging Company, Chicago, USA
Petri Dishes	30 mm diameter	Bibby Sterilin, Staffordshire, UK
Serological Pipettes	25 ml, 10 ml, 5 ml, 2 ml	Sarstedt AG and Co, Numbrecht, Germany

Sterile Filter Pipette Tips (OneTip)	1000 ml, 200 ml, 20 ml, 2 ml	Starlab UK, Milton Keynes, UK
Sterile Pipette Tips	1000 ml, 200 ml, 20 ml, 2 ml	Starlab UK, Milton Keynes, UK
Sterile Plastic Syringes	50 ml, 10 ml, 5 ml, 2 ml, 1 ml	Scientific Laboratory Supplies, Nottingham, UK
Sterile Screw-lid container	250 ml, 150 ml, 60 ml	Thermo Scientific, Massachusetts, USA
Sterile Test Tubes	15 ml	Scientific Laboratory Supplies, Nottingham, UK
Universals	25 ml	Scientific Laboratory Supplies, Nottingham, UK
Well Plates, Flat Bottomed	48 well, 12 well, 6 well	Scientific Laboratory Supplies, Nottingham, UK

Appendix B

List of Presentations

Nic Gowland, Sophie Williams, John Fisher, Joanne L Tipper (2012). The Wear and Biological Activity of Antioxidant UHMPWE for use in Total Hip Replacements. 14th Annual White Rose Work in Progress Meeting, York, UK. Poster Presentation.

Nic Gowland, Sophie Williams, John Fisher, Joanne L Tipper (2013). The Wear of Crosslinked and Non-Crosslinked UHMWPE with and without Vitamin E. Orthopaedic Research Society (ORS) 2013 Annual Meeting, San Antonio, Texas, USA. Poster Presentation.

Nic Gowland, Sophie Williams, John Fisher, Joanne L Tipper (2014). The Wear and Biological Activity of Antioxidant UHMWPE in Total Hip Replacements. The 26th Annual Conference of the European Society for Biomaterials (ESB), Liverpool, UK. Oral Presentation.